

**A STUDY OF THE MOLECULAR INTERACTIONS BETWEEN KINESIN  
MOTOR PROTEINS AND THE TRAK FAMILY OF KINESIN ADAPTORS**

**Thomas Steven Randall**

A Thesis Submitted for the Degree of Doctor of Philosophy from the UCL  
School of Pharmacy

This thesis describes research conducted in the UCL School of Pharmacy between October 2008 and August 2012 under the supervision of Prof. F. Anne Stephenson and Dr Carolyn Moores. I certify that the research described is original and any parts of the work that have been conducted by collaboration are clearly indicated. I also certify that I have written all the text herein and have clearly indicated by suitable citation any part of this dissertation that has already appeared in publication.

Signature:

Date:

## ABSTRACT

Kinesins are motor proteins that have roles in cell division as well as the transport of various organelles and protein complex cargoes within cells. Kinesin-1 is considered the conventional motor protein and consists of three main isoforms, KIF5A, KIF5B and KIF5C. The family of Trafficking Kinesin proteins (TRAKs) bind to the cargo binding domain of kinesin-1 forming a link between the motor protein and their cargoes. The best characterised cargo transported by TRAKs is mitochondria.

To understand further the mode of association between kinesin and TRAKs, the aim of this study was to determine the structure of the C-terminal cargo binding domain of kinesin-1. Due to the known binding of TRAK2 with the kinesin-1 family it was hypothesized that TRAKs may stabilize the KIF5A cargo binding domain. Hence, the cDNA encoding the KIF5A cargo binding domain, KIF5A<sub>800-1032</sub>, and the cDNA encoding the kinesin interacting domain of TRAK2, i.e. TRAK2<sub>100-380</sub> were cloned into a bicistronic expression vector to result in epitope-tagged constructs. The expression of both proteins was characterized with respect to yield and solubilisation efficiency. TRAK2<sub>100-380</sub> was stabilized by KIF5A<sub>800-1032</sub>. Affinity chromatography of soluble extracts found that KIF5A<sub>800-1032</sub> and TRAK2<sub>100-380</sub> did co-purify indicating that they do associate. However, the yield was insufficient for further characterisation.

To determine the structure of the cargo binding domain of KIF5A several C-terminal constructs which varied in size and epitope tag location were generated. Bacterial growth and solubilisation conditions were optimized to maximize the yield of the various KIF5A cargo domain recombinant proteins. Each was purified by an appropriate affinity chromatography resin. Conditions were established to optimize the purity, yield, stability and aggregation state. One construct, KIF5A<sub>800-951</sub> was isolated to a sufficient yield and did not aggregate. Therefore, KIF5A<sub>800-951</sub> is a good candidate for further structural analysis.

To refine further the TRAK binding site within the cargo domain of kinesin-1 a series of rationally designed C-terminal truncations of KIF5A and KIF5C were generated and co-expressed with either TRAK1 or TRAK2 in mammalian cells. The binding of kinesin-1 truncations to the TRAKs was determined by co-immunoprecipitation assays followed by quantitative immunoblotting. Deletion of the distal 71 amino acids of KIF5A resulted in an increased co-immunoprecipitation of KIF5A with TRAK2. Three possible TRAK2 binding sites within the KIF5A and KIF5C cargo binding domains were found. Furthermore, differences were found between TRAK1 and TRAK2 in terms of their association sites with KIF5A.

Overall these studies yield new insights into kinesin/kinesin adaptor interactions which may impact in the future on a better understanding of neurodegenerative diseases such as hereditary spastic paraplegia and Charcot–Marie–Tooth disease which have both been linked to deficiencies in neuronal transport mechanisms of mitochondria.

## CONTENTS TABLE

<b>ABSTRACT .....</b>	<b>2</b>
<b>LIST OF ABBREVIATIONS .....</b>	<b>14</b>
<b>1.0 INTRODUCTON.....</b>	<b>19</b>
1.1 Transport in the central nervous system .....	20
1.1.1 Neuronal cytoskeleton .....	21
1.1.2 Motor proteins .....	22
1.2 The kinesin superfamily of motor proteins.....	23
1.2.1 Structure of kinesin .....	26
1.2.2 Kinesin-1 .....	29
1.2.2.1 Kinesin light chain .....	30
1.2.3 Kinesin-1 in the central nervous system .....	32
1.2.4 Transport of cargo via the cargo binding domain of kinesin-1 .....	34
1.2.4.1 Adaptor proteins that bind via the kinesin heavy chain.....	35
1.2.4.2 Adaptor proteins that bind kinesin light chain .....	37
1.3 The TRAK/Milton family of kinesin adaptor proteins .....	42
1.3.1 Mitochondria as a cargo for the TRAK/Milton adaptor protein family.....	45
1.3.2 Proteins interacting with the TRAK/Milton family of kinesin adaptors .....	47
1.4 The regulation of kinesin-1 transport of mitochondria in neuronal cells.....	51
1.5 Disease states associated with the malfunction of motor protein complexes in the CNS .....	55
1.6 Aims of this thesis .....	57
<b>2.0 MATERIALS AND METHODS.....</b>	<b>59</b>
2.1 MATERIALS .....	59
2.1.1 Recombinant clones .....	62
2.1.2 Antibodies.....	62
2.2 METHODS.....	64
2.2.1 Bacterial methods .....	64
2.2.1.1 Preparation of chemically competent bacterial cells ( <i>DH5<math>\alpha</math></i> or <i>BL21 DE3</i> codonplus) .....	64
2.2.1.2 Transformation of chemically competent bacterial cells.....	64
2.2.1.3 Glycerol stocks of transformed bacterial cells .....	65

2.2.2 Molecular cloning methods.....	65
2.2.2.1 Bacterial clone design .....	65
2.2.2.2 Mammalian clone design.....	66
2.2.2.3 Design of polymerase chain reaction (PCR) and nucleotide sequencing oligonucleotide primers.....	69
2.2.2.3.1 PCR cycles.....	69
2.2.2.4 Flat bed agarose gel electrophoresis for DNA analysis .....	70
2.2.2.5 Extraction of DNA fragments from agarose gels .....	71
2.2.2.6 Restriction endonuclease (R.E) digestion .....	71
2.2.2.7 Purification of PCR products.....	72
2.2.2.8 Dephosphorylation of vector.....	72
2.2.2.9 Ligation reactions.....	72
2.2.2.10 PCR screening of recombinants.....	73
2.2.2.11 Mini preparation of plasmid DNA.....	73
2.2.2.12 Maxi preparation of plasmid DNA .....	74
2.2.2.13 Ethanol precipitation of plasmid DNA .....	75
2.2.2.14 Deletion mutagenesis by overlap extension PCR.....	76
2.2.3 Bacterial protein expression.....	77
2.2.3.1 Protein extraction from <i>BL21 DE3 codonplus E.coli</i> cells .....	77
2.2.3.2 Bradford assay protein quantification .....	77
2.2.3.4 SDS-PAGE .....	78
2.2.3.4.1 Preparation of running gel .....	78
2.2.3.4.2 Preparation of stacking gel .....	78
2.2.3.4.3 Methanol/chloroform precipitation of protein samples .....	79
2.2.3.4.4 Preparation and electrophoresis of protein samples .....	79
2.2.3.5 Immunoblotting.....	80
2.2.3.5.1 Transfer of proteins to nitrocellulose membranes.....	80
2.2.3.5.2 Immunoblotting .....	81
2.2.3.5.3 Quantitative immunoblot analysis.....	82
2.2.4 Purification of bacterially expressed recombinant proteins.....	82
2.2.4.1 Purification of bacterially expressed His tagged protein using ProBond™ Ni <sup>2+</sup> chelating resin.....	82

2.2.4.2 Purification of bacterially expressed S tagged protein using S-protein agarose resin.....	83
2.2.4.3 Buffer exchange and concentration of bacterially expressed protein samples .....	83
2.2.4.4 Aggregation state testing.....	84
2.2.4.5 Size exclusion chromatography .....	84
2.2.4.6 Preparation of stable and polymerised microtubules.....	85
2.2.4.6.1 Microtubule binding co-sedimentation assay .....	85
2.2.5 Expression in mammalian cells.....	86
2.2.5.1 Culturing of human embryonic kidney 293 cells .....	86
2.2.5.2 Preparation of cell culture media .....	86
2.2.5.3 Storage of HEK 293 cells in liquid nitrogen.....	87
2.2.5.4 Reviving HEK 293 cell stocks from liquid nitrogen storage .....	87
2.2.5.5 Sub-culturing of HEK 293 cells .....	87
2.2.5.6 Transient transfection of HEK 293 cells by the calcium phosphate method .....	88
2.2.5.7 Preparation of transfected HEK 293 cell homogenates .....	89
2.2.5.8 Detergent solubilisation and co-immunoprecipitation of HEK 293 cell homogenates .....	89
<b>3.0 TOWARDS THE STRUCTURAL DETERMINATION OF A TRAK2/KIF5A TRAFFICKING COMPLEX .....</b>	<b>91</b>
3.1 RATIONALE .....	92
3.1.1 Aims of this chapter.....	94
3.2 RESULTS.....	95
3.2.1 Oligonucleotide primer design for the amplification of rat TRAK2 <sub>100-380</sub> .....	97
3.2.1.1 Preparation of the pETDUETTRAK2 <sub>100-380</sub> construct.....	101
3.2.2 Oligonucleotide primer design for the amplification of human KIF5A <sub>800-1032</sub> ..	104
3.2.2.1 Preparation of the pETDUETKIF5A <sub>800-1032</sub> construct.....	108
3.2.3 Preparation of the pETDUETTRAK2 <sub>100-380</sub> /KIF5A <sub>800-1032</sub> construct.....	111
3.2.4 Optimisation of TRAK2 <sub>100-380</sub> , KIF5A <sub>800-1032</sub> and TRAK2 <sub>100-380</sub> /KIF5A <sub>800-1032</sub> protein expression.....	113
3.2.5 Affinity tag purification of soluble TRAK2 <sub>100-380</sub> /KIF5A <sub>800-1032</sub> .....	124
3.3 DISCUSSION .....	133

3.3.1 Overall conclusions.....	136
<b>4.0 TOWARDS THE STRUCTURAL DETERMINATION OF THE KIF5A CARGO BINDING DOMAIN .....</b>	<b>137</b>
4.1 RATIONALE .....	138
4.1.1 Aims of this chapter.....	139
4.2 RESULTS.....	140
4.2.1 Assessment of KIF5A <sub>800-1032</sub> as a suitable recombinant protein for structural studies .....	141
4.2.2 Assessment of His-tagged KIF5A <sub>800-1032</sub> as a suitable recombinant protein for structural studies.....	142
4.2.3 Assessment of KIF5A <sub>820-1032</sub> , KIF5A <sub>800-951</sub> and KIF5A <sub>820-951</sub> as suitable recombinant proteins for structural studies .....	151
4.3 DISCUSSION .....	161
4.3.1 Overall conclusions.....	164
<b>5.0 THE ASSOCIATION BETWEEN THE TRAK AND KINESIN-1 FAMILIES; AN INVESTIGATION USING A CO-IMMUNOPRECIPITATION STRATEGY .....</b>	<b>165</b>
5.1 RATIONALE .....	166
5.1.1 Aims of this chapter.....	167
5.2 RESULTS.....	168
5.2.1 Does TRAK2 associate with the cargo binding domain of KIF5A?.....	169
5.2.2 Refinement of the TRAK2 binding site within the KIF5A cargo binding domain .....	174
5.2.3 Further refinement of amino acids 877-885 of KIF5A by truncation.....	179
5.2.4 Further refinement of amino acids 877-883 of KIF5A by deletion .....	184
5.2.5 Does KIF5C associate with TRAK2 using the same amino acid motif as KIF5A? .....	187
5.2.6 Does TRAK1 associate with KIF5A in a similar manner to TRAK2?.....	192
5.3 DISCUSSION.....	198
5.3.1 Overall conclusions.....	201
<b>6.0 GENERAL CONCLUSIONS AND FUTURE DIRECTIONS .....</b>	<b>203</b>
6.1 GENERAL CONCLUSIONS .....	204
6.2 FUTURE DIRECTIONS .....	206

## APPENDICES

<b>3.1</b> The vector maps for pETDUET1, pETTRAK2 <sub>100-380</sub> , pETKIF5A <sub>800-1032</sub> and pETTRAK2 <sub>100-380</sub> /KIF5A <sub>800-1032</sub> .....	224
<b>4.1</b> The vector maps for pETKIF5A <sub>800-951</sub> , pETKIF5A <sub>820-951</sub> and pETKIF5A <sub>820-1032</sub> .....	225
<b>4.2</b> The vector maps for pET151D-TOPO and pET151D-TOPOKIF5A <sub>800-1032</sub> .....	226
<b>5.1</b> The vector maps for pcDNAKIF5A, pcDNAKIF5A <sub>1-961</sub> , pcDNAKIF5A <sub>1-942</sub> and pcDNAKIF5A <sub>1-885</sub> .....	227
<b>5.2</b> The vector maps for pcDNAKIF5A <sub>1-883</sub> , pcDNAKIF5A <sub>1-881</sub> , pcDNAKIF5A <sub>1-879</sub> and pcDNAKIF5A <sub>1-879</sub> .....	228
<b>5.3</b> The vector maps for pcDNAKIF5A <sub>1-861</sub> , pcDNAKIF5A <sub>1-825</sub> and pcDNAKIF5A <sub>Δ877-883</sub> ..	229
<b>5.4</b> The vector maps for pcDNAKIF5C, pcDNAKIF5C <sub>1-889</sub> , pcDNAKIF5C <sub>1-881</sub> and pcDNAKIF5A <sub>1-828</sub> .....	230

## LIST OF FIGURES

<b>1.1</b>	A structure of a thirteen filament microtubule .....	22
<b>1.2</b>	A schematic of motor protein transport of cargo in a neuronal cell .....	23
<b>1.3</b>	A summary of the major mouse kinesins.....	25
<b>1.4</b>	A schematic representation of the kinesin-1 heterodimer molecular motor .....	27
<b>1.5</b>	Structure of dimeric kinesin-1 in a ribbon representation .....	29
<b>1.6</b>	Structure of the TPR domains of human KLC1 in a ribbon representation .....	31
<b>1.7</b>	A schematic representation of the TRAK/kinesin-1/Miro complex.....	46
<b>1.8</b>	A schematic of the full length TRAK2 protein .....	51
<b>1.9</b>	Schematic representations of the two contrasting mechanisms on the method of mitochondrial regulation by kinesin-1 .....	54
<b>2.1</b>	A summary of the overall cloning strategy .....	68
<b>2.2</b>	Schematic of deletion mutagenesis by overlap extension PCR. ....	76
<b>3.1</b>	Vector map of pETDUET1.....	95
<b>3.2</b>	The full amino acid sequence alignment of human KIF5A and KIF5C .....	96
<b>3.3</b>	Full nucleotide and amino acid sequence of rat TRAK2 .....	99
<b>3.4</b>	Flat bed agarose gel electrophoresis analysis of TRAK2 <sub>100-380</sub> nucleotide amplification by PCR .....	101
<b>3.5</b>	Analysis of putative pETTRAK2 <sub>100-380</sub> constructs by 1 % (w/v) flat bed agarose gel electrophoresis.....	103
<b>3.6</b>	Nucleotide sequencing results of the pETDUETTRAK2 <sub>100-380</sub> clone.....	103
<b>3.7</b>	The full nucleotide and amino acid sequence of human KIF5A.....	106
<b>3.8</b>	Flat bed agarose gel electrophoresis analysis of KIF5A <sub>800-1032</sub> nucleotide amplification by PCR .....	108
<b>3.9</b>	Analysis of putative pETDUETKIF5A <sub>800-1032</sub> constructs using a PCR screen by 1 % (w/v) flat bed agarose gel electrophoresis .....	110
<b>3.10</b>	Nucleotide sequencing results of the pETDUETKIF5A <sub>800-1032</sub> clone .....	111
<b>3.11</b>	Summary of the pETDUETTRAK2 <sub>100-380</sub> , pETDUETKIF5A <sub>800-1032</sub> and pETDUETTRAK2 <sub>100-380</sub> /KIF5A <sub>800-1032</sub> recombinant clones .....	112
<b>3.12</b>	Demonstration of the expression of TRAK2 <sub>100-380</sub> , KIF5A <sub>800-1032</sub> and TRAK2 <sub>100-380</sub> /KIF5A <sub>800-1032</sub> in <i>BL21 E.coli</i> cells.....	114
<b>3.13</b>	Demonstration of the expression of TRAK2 <sub>100-380</sub> , KIF5A <sub>800-1032</sub> and TRAK2 <sub>100-380</sub> /KIF5A <sub>800-1032</sub> in <i>BL21 E.coli</i> cells.....	115

<b>3.14</b> Demonstration of the expression of TRAK2 <sub>100-380</sub> , KIF5A <sub>800-1032</sub> and TRAK2 <sub>100-380</sub> /KIF5A <sub>800-1032</sub> in <i>BL21 E.coli</i> cells with 1 % w/v glucose supplemented LB media ....	117
<b>3.15</b> Demonstration of the optimised expression of TRAK2 <sub>100-380</sub> , KIF5A <sub>800-1032</sub> and TRAK2 <sub>100-380</sub> /KIF5A <sub>800-1032</sub> in <i>BL21 E.coli</i> cells .....	123
<b>3.16</b> Purification of TRAK2 <sub>100-380</sub> /KIF5A <sub>800-1032</sub> under native conditions using Ni <sup>2+</sup> affinity resin.....	125
<b>3.17</b> Assessment of the specific activity and purification factor after the purification of TRAK2 <sub>100-380</sub> /KIF5A <sub>800-1032</sub> under native conditions using Ni <sup>2+</sup> affinity resin .....	127
<b>3.18</b> Purification of TRAK2 <sub>100-380</sub> /KIF5A <sub>800-1032</sub> under denaturing conditions using Ni <sup>2+</sup> affinity resin .....	131
<b>4.1</b> Schematic representations of the recombinant tagged KIF5A cargo binding domain constructs.....	140
<b>4.2</b> Purification of KIF5A <sub>800-1032</sub> under native conditions using S-tag protein affinity resin .....	141
<b>4.3</b> Demonstration of the expression of KIF5A <sub>800-1032</sub> in <i>BL21 E.coli</i> cells.....	143
<b>4.4</b> Demonstration of the expression of KIF5A <sub>800-1032</sub> in <i>BL21 E.coli</i> cells.....	144
<b>4.5</b> Demonstration of the optimized expression of His-tagged KIF5A <sub>800-1032</sub> in <i>BL21 E.coli</i> cells.....	146
<b>4.6</b> Initial purification of His-tagged KIF5A <sub>800-1032</sub> under native conditions using Ni <sup>2+</sup> affinity resin .....	147
<b>4.7</b> Optimal purification of KIF5A <sub>800-1032</sub> under native conditions using Ni <sup>2+</sup> affinity resin.....	149
<b>4.8</b> Assessment of the aggregation state of KIF5A <sub>800-1032</sub> .....	150
<b>4.9</b> Demonstration of the expression of KIF5A <sub>820-1032</sub> , KIF5A <sub>800-951</sub> and KIF5A <sub>820-951</sub> in <i>BL21 E.coli</i> cells .....	152
<b>4.10</b> Demonstration of the expression of KIF5A <sub>820-1032</sub> , KIF5A <sub>800-951</sub> and KIF5A <sub>820-951</sub> in <i>BL21 E.coli</i> cells .....	153
<b>4.11</b> Purification of KIF5A <sub>820-1032</sub> , KIF5A <sub>800-951</sub> and KIF5A <sub>820-951</sub> under native conditions using Ni <sup>2+</sup> affinity resin.....	155
<b>4.12</b> Assessment of the aggregation state of KIF5A <sub>800-951</sub> .....	157
<b>4.13</b> Size exclusion chromatography analysis of affinity chromatography purified KIF5A <sub>800-951</sub> .....	158
<b>4.14</b> Microtubule binding assay showing the association of microtubules with	

KIF5A <sub>800-951</sub> .....	160
<b>5.1</b> Comparison of human KIF5A, KIF5B and KIF5C kinesin-1 sub-types .....	167
<b>5.2</b> A schematic representation of the co-immunoprecipitation experiments.....	168
<b>5.3</b> Schematic representations of recombinant tagged KIF5A, KIF5C, TRAK1 and TRAK2 .....	169
<b>5.4</b> Demonstration of the expression of TRAK2, KIF5A, KIF5A <sub>1-825</sub> and KIF5A <sub>1-961</sub> in HEK 293 cells.....	170
<b>5.5</b> Association of TRAK2 with KIF5A, KIF5A <sub>1-825</sub> and KIF5A <sub>1-961</sub> : demonstration by co- immunoprecipitation .....	171
<b>5.6</b> Histograms showing the expression levels of TRAK2 and KIF5A, KIF5A <sub>1-825</sub> and KIF5A <sub>1-961</sub> following co-expression .....	172
<b>5.7</b> Histograms showing the association of TRAK2 with KIF5A, KIF5A <sub>1-825</sub> and KIF5A <sub>1-961</sub> following co-immunoprecipitation .....	173
<b>5.8</b> Alignment of the kinesin-1 cargo binding domains .....	174
<b>5.9</b> Demonstration of the expression of KIF5A <sub>1-942</sub> , KIF5A <sub>1-909</sub> , KIF5A <sub>1-885</sub> , KIF5A <sub>1-877</sub> and KIF5A <sub>1-861</sub> in HEK 293 cells .....	175
<b>5.10</b> Association of TRAK2 with KIF5A, KIF5A <sub>1-942</sub> KIF5A <sub>1-909</sub> , KIF5A <sub>1-885</sub> , KIF5A <sub>1-877</sub> KIF5A <sub>1- 861</sub> and KIF5A <sub>1-825</sub> : demonstration by co-immunoprecipitation.....	176
<b>5.11</b> Histograms showing the expression levels of TRAK2 and KIF5A, KIF5A <sub>1-942</sub> , KIF5A <sub>1- 909</sub> , KIF5A <sub>1-885</sub> , KIF5A <sub>1-877</sub> , KIF5A <sub>1-861</sub> and KIF5A <sub>1-825</sub> following co-expression.....	177
<b>5.12</b> Histograms showing the association of TRAK2 with KIF5A, KIF5A <sub>1-942</sub> , KIF5A <sub>1-909</sub> , KIF5A <sub>1-885</sub> , KIF5A <sub>1-877</sub> , KIF5A <sub>1-861</sub> and KIF5A <sub>1-825</sub> following co-immunoprecipitation.....	178
<b>5.13</b> Amino acid regions responsible for the association of KIF5A with TRAK2 .....	179
<b>5.14</b> Demonstration of the expression of KIF5A <sub>1-883</sub> , KIF5A <sub>1-881</sub> and KIF5A <sub>1-879</sub> in HEK 293 cells.....	180
<b>5.15</b> Demonstration by immunoprecipitation the association of TRAK2 with KIF5A, KIF5A <sub>1-883</sub> , KIF5A <sub>1-881</sub> , KIF5A <sub>1-879</sub> and KIF5A <sub>1-825</sub> following their co-expression in HEK 293 cells.....	181
<b>5.16</b> Histograms showing the expression levels of TRAK2 and KIF5A, KIF5A <sub>1-883</sub> , KIF5A <sub>1- 881</sub> , KIF5A <sub>1-879</sub> and KIF5A <sub>1-825</sub> following co-expression.....	182
<b>5.17</b> Histograms showing the association of TRAK2 with KIF5A, KIF5A <sub>1-883</sub> , KIF5A <sub>1-881</sub> , KIF5A <sub>1-879</sub> and KIF5A <sub>1-825</sub> following co-immunoprecipitation .....	183
<b>5.18</b> Demonstration of the expression of KIF5A <sub>Δ877-883</sub> in HEK 293 cells.....	184

<b>5.19</b> Demonstration by immunoprecipitation the association of TRAK2 with KIF5A, KIF5A <sub>1-825</sub> and KIF5A <sub>Δ877-883</sub> following their co-expression in HEK 293 cells.....	185
<b>5.20</b> Histograms showing the expression levels of TRAK2 and KIF5A, KIF5A <sub>1-825</sub> and KIF5A <sub>Δ877-883</sub> following co-expression.....	186
<b>5.21</b> Histograms showing the association of TRAK2 with KIF5A, KIF5A <sub>1-825</sub> and KIF5A <sub>Δ877-883</sub> following co-immunoprecipitation .....	187
<b>5.22</b> Demonstration of the expression of KIF5C, KIF5C <sub>1-889</sub> , KIF5C <sub>1-881</sub> and KIF5C <sub>1-828</sub> in HEK 293 cells .....	188
<b>5.23</b> Association of TRAK2 with KIF5C, KIF5C <sub>1-889</sub> , KIF5C <sub>1-881</sub> and KIF5C <sub>1-828</sub> : demonstration by co-immunoprecipitation .....	189
<b>5.24</b> Histograms showing the expression levels of TRAK2 and KIF5C, KIF5C <sub>1-889</sub> , KIF5C <sub>1-881</sub> and KIF5C <sub>1-828</sub> following co-expression .....	190
<b>5.25</b> Histograms showing the association of TRAK2 with KIF5C, KIF5C <sub>1-889</sub> , KIF5C <sub>1-881</sub> and KIF5A <sub>1-828</sub> following co-immunoprecipitation .....	191
<b>5.26</b> Demonstration of the expression of TRAK1 in HEK 293 cells .....	193
<b>5.27</b> Association of TRAK1 with KIF5A, KIF5A <sub>1-961</sub> , KIF5A <sub>1-879</sub> , KIF5A <sub>1-877</sub> and KIF5A <sub>1-825</sub> : demonstration by co-immunoprecipitation .....	194
<b>5.28</b> Histograms showing the expression levels of TRAK1 and KIF5A, KIF5A <sub>1-961</sub> , KIF5A <sub>1-879</sub> , KIF5A <sub>1-877</sub> and KIF5A <sub>1-825</sub> following co-expression .....	195
<b>5.29</b> Histograms showing the association of TRAK1 with KIF5A, KIF5A <sub>1-961</sub> , KIF5A <sub>1-879</sub> , KIF5A <sub>1-877</sub> and KIF5A <sub>1-825</sub> following co-immunoprecipitation .....	196
<b>5.30</b> Comparison of human KIF5A, KIF5B and KIF5C kinesin-1 sub-types .....	197

## LIST OF TABLES

<b>1.1</b> A summary of all the known KHC cargo adaptor proteins .....	35
<b>1.2</b> A summary of KLC protein interactors.....	38
<b>1.3</b> The studied splice variants of TRAK1 and TRAK2.....	43
<b>1.4</b> A summary of the TRAK/Milton protein interactors .....	48
<b>2.1</b> A summary of oligonucleotide primer sequences used for the generation of bacterially expressed TRAK2 and KIF5A constructs .....	60
<b>2.2</b> A summary of oligonucleotide primer sequences used for the generation of mammalian expressed KIF5A and KIF5C constructs .....	61
<b>2.3</b> A summary of the oligonucleotide primers used for nucleotide sequencing .....	62
<b>2.4</b> A summary of the primary antibodies used for immunoblotting and immunoprecipitation experiments .....	63
<b>2.5</b> A summary of accession numbers of KIF5A, KIF5C and the TRAK family of proteins .....	63
<b>2.6</b> A summary of the bacterial expression constructs generated and used for the expression of recombinant TRAK2 and KIF5A.....	66
<b>2.7</b> A summary of the mammalian expression constructs generated and used for the expression of recombinant KIF5A, KIF5C, TRAK1 and TRAK2 .....	67
<b>3.1</b> Summary table of the ligation reactions used to create pETDUETTRAK2 <sub>100-380</sub> .....	102
<b>3.2</b> Summary table of the ligation reactions used to create pETDUETKIF5A <sub>800-1032</sub> .....	109
<b>3.3</b> A summary of growth conditions to establish optimal conditions for the expression and solubilisation of TRAK2 <sub>100-380</sub> .....	119
<b>3.4</b> A summary of growth conditions to establish optimal conditions for the expression and solubilisation of KIF5A <sub>800-1032</sub> .....	120
<b>3.5</b> A summary of growth conditions to establish optimal conditions for the expression and solubilisation of TRAK2 <sub>100-380</sub> /KIF5A <sub>800-1032</sub> .....	121
<b>3.6</b> A summary of growth conditions to establish optimal conditions for the expression and solubilisation of TRAK2 <sub>100-380</sub> /KIF5A <sub>800-1032</sub> .....	122
<b>3.7</b> Summary of the overall cloning, expression and expression optimisation for pETDUETTRAK2 <sub>100-380</sub> , pETDUETKIF5A <sub>800-1032</sub> and pETDUETTRAK2 <sub>100-380</sub> /KIF5A <sub>800-1032</sub>	124
<b>3.8</b> Table summarising the different conditions and affinity chromatography resins tested to purify the TRAK2 <sub>100-380</sub> /KIF5A <sub>800-1032</sub> co-complex .....	129

<b>4.1</b> A summary of growth conditions to establish optimal conditions for the expression and solubilisation of His-tagged KIF5A <sub>800-1032</sub> .....	145
<b>4.2</b> Summary of the overall cloning, expression and solubilisation optimisation for pETDUETKIF5A <sub>820-1032</sub> , pETDUETKIF5A <sub>800-951</sub> and pETDUETKIF5A <sub>820-951</sub> .....	154
<b>4.3</b> Summary of the overall cloning, expression, solubilisation optimisation, purification and aggregation testing for KIF5A <sub>800-1032</sub> , His-tagged KIF5A <sub>800-1032</sub> , KIF5A <sub>820-1032</sub> , KIF5A <sub>800-951</sub> and KIF5A <sub>820-951</sub> .....	157

## LIST OF ABBREVIATIONS

ADP – Adenine diphosphate

ALS – Amyotrophic lateral sclerosis

APP – Amyloid precursor protein

APS – Ammonium persulphate

bp – Base pairs

CO-IP – Co-immunoprecipitation

COS-7 - Kidney cells of the African Green Monkey

CRMP2 - Collapsin response mediator protein-2

DMSO – Dimethyl sulfoxide

DNA – Deoxyribonucleic acid

dNTP – Deoxynucleoside-5'-triphosphate

DTT – Dithiothreitol

*E.coli* - *Escherichia coli*

EDTA – Ethylenediaminetetraacetic acid

FBS – Fetal bovine serum

FMRP - Fragile X mental retardation protein

FRET - Fluorescence resonance energy transfer

G/C - Guanine/cysteine

GFP – Green fluorescent protein

GRIF-1 – GABA<sub>A</sub> receptor interacting factor-1

GRIP-1 - Glutamate receptor interacting protein

GTP – Guanosine triphosphate

HAP1 – Huntington associated protein 1

HBS – HEPES buffered saline

HEK 293 – Human embryonic kidney cells

HEPES - 4-(2-hydroxyethyl)-1-piperazineethanesulfonic acid

His - Histidine

HRP – Horseradish peroxidase

HSP – Hereditary spastic paraplegia

HUMMR - Hypoxia up-regulated mitochondrial movement regulator

IPTG – Isopropylthio- $\beta$ -D-galactosidase

JIP - JNK interacting protein

JNK - C-jun N-terminal kinase

Kb – Kilobase

KDa - Kilodalton

KHC – Kinesin heavy chain

Kidins 220 - Kinase-D-interacting substrate of 220 kDa

KIF – Kinesin superfamily

KIF5A – Kinesin-1 sub-type A

KIF5B – Kinesin-1 sub-type B

KIF5C - Kinesin-1 sub-type C

KLC – Kinesin light chain

LB – Lennox B broth

MAP – Microtubule associated protein

MCS – Multiple cloning site

MgADP – Magnesium adenosine diphosphate

$M_r$  – Molecular weight

mRNA – Messenger ribonucleic acid

NMR – Nuclear magnetic resonance

OD – Optical density

O-GlyNAc - N-Acetylglucosamine

OGT –  $\beta$ -O-linked N-Acetylglucosamine transferase

OIP106 – O-linked N-acetylglucosamine transferase interacting protein 106

Ori – Point of origin

PBS – Phosphate buffered saline

PC12 - Pheochromocytoma 12 cells

PCR – Polymerase chain reaction

Pink1 - PTEN induced putative kinase 1

SAP – Shrimp alkaline phosphatase

SDS – Sodium dodecyl sulphate

SDS-PAGE - Sodium dodecyl sulphate – polyacrylamide gel electrophoresis

shRNAi – Short hairpin ribonucleic acid interference

siRNA – Small interfering ribonucleic acid

SNAP23 - Synaptosome-associated protein of 23 kDa

SNAP25 - Synaptosome-associated protein of 25 kDa

TBE – Tris-borate-EDTA buffer

TE – Tris-EDTA

TEMED – N,N,N',N'-tetramethylethylene diamine

TPR - Tetratricopeptide repeat

TRAK1 - Trafficking protein, kinesin binding 1

TRAK2 - Trafficking protein, kinesin binding 2

Tris – Tris(hydroxymethyl)aminomethane

Triton® X-100 – 4-(1,1,3,3-tetramethylbutyl) phenyl-polyethylene glycol

Tween®-20 – Polyethylene glycol sorbitan monolaurate

β-ME – β mercaptoethanol

γTuRC - γ-Tubulin ring complex

## **ACKNOWLEDGEMENTS**

This PhD thesis would not have been possible without the support of many people. I wish to express my gratitude to my primary supervisor Prof. Anne Stephenson who was abundantly helpful and offered invaluable assistance, support and guidance. I also wish to express my gratitude to my secondary supervisor Dr Carolyn Moores whose knowledge, enthusiasm and assistance and has again proven invaluable.

I would like to thank members of the Stephenson laboratory, including Dr Sarah Cousins for her help in teaching me the techniques needed in the laboratory as well as for her advice, enthusiasm and insightful discussions, whether they were science related or not. I would also like to thank Dr Kieran Brickley for his insight and helpful discussions especially when first starting my PhD. I would also like to thank all of my friends and colleagues at UCL School of Pharmacy for their advice and support and for creating an enjoyable place to work.

I am very grateful to the Bloomsbury consortium for funding my studentship, which without, this PhD thesis would not have been possible.

Finally, I would like to thank my family as they have always supported me whatever I chose to do and cheered me up during tough times.

“If I have ever made any valuable discoveries, it has been owing more to patient attention than to any other talent.”

Isaac Newton

# **CHAPTER 1**

## **INTRODUCTION**

## **1.0 INTRODUCTON**

In all eukaryotic cells there is a constant movement of molecules, vesicles, protein complexes and organelles throughout the cytoplasm. Small molecules can move relatively easily throughout a cell over a short distance using simple diffusion. This is more difficult for larger cellular components such as vesicles, protein complexes and organelles. This is partly due to their large and bulky structure but also because the cell is crowded not allowing much free space for easy movement. Thus, motor proteins are necessary to facilitate movement and to direct these larger cellular components to their desired location within the cellular system. For example, the movement of mitochondria occurs due to the association of two proteins, the molecular motor kinesin-1 and the family of kinesin adaptor proteins - trafficking protein kinesin binding (TRAKs), along microtubules. It is the molecular mechanisms behind the interaction of kinesin-1 and TRAKs which will be addressed in this PhD thesis.

### **1.1 Transport in the central nervous system**

Intracellular transport is essential for correct cellular function and morphology. Most newly synthesised proteins are transported to various locations throughout the cell via a form of motor protein. The central nervous system (CNS) of vertebrates consists of the brain and spinal cord which help to coordinate movement and transmit signals via a network of neuronal cells. Due to the physical structure of neuronal cells the need for an effective transport mechanism is even more pronounced. Neurons are asymmetric, highly polarised cells that transmit and process information by electrical and chemical signalling. Signalling occurs via synapses that connect to each other to form neuronal networks. A typical neuron possesses a cell body, dendrites and a single axon. Dendrites are structures that protrude from the main cell body often branching multiple times giving rise to a complex "dendritic tree". The axon is a special cellular extension that extends from the main cell body and travels for a long distance, which can be as far as 1 m in humans (Goldberg, 2003). Correct maintenance of neuronal function requires the presence of vesicles, mitochondria and protein complexes in the axon and dendritic terminals. As these are generally synthesised in the main cell body, motor proteins are known to be responsible for the trafficking of cargo along the long length of both the dendrites and axon to the terminals (Miki *et*

*al.*, 2005; Hirokawa *et al.*, 2009; Hirokawa, 2011). Neuronal transport can occur in either an anterograde direction *i.e.* away from the main cell body towards the dendritic and axonal terminals, or in a retrograde direction *i.e.* towards the cell body from the dendritic and axonal terminals (Hirokawa *et al.*, 2009). The transport of vesicles, protein complexes and organelles is mediated via several motor proteins along the neuronal cytoskeleton.

### **1.1.1 Neuronal cytoskeleton**

The neuronal cytoskeleton is a dynamic structure present in the cytoplasm. It helps to protect and maintain the shape of neuronal cells and consists of three different structural microfilament complexes that interact with one another. These are actin microfilaments, neurofilaments and microtubules. Actin microfilaments are formed from 43 kDa actin monomers that arrange into fibrils of around 4 – 6 nm in diameter (Theriot, 1994). Actin microfilaments are found mostly at the periphery of the cell and, in the case of neurons, at the axon terminals and dendritic spines. Neurofilaments are intermediate filaments in neurons composed of three subunits; neurofilament heavy, medium and light subunits. They are used to help maintain structure within the axon and provide support for normal axonal radial growth (Siegel *et al.*, 1999). Microtubules consist of a core polymer structure made from 50 kDa tubulin subunits. The polymer is formed by heterodimers of  $\alpha$ - and  $\beta$ -tubulin making 13 helical rings. These can also exist as 12 and 14 helical rings which together form the long microtubules. The preferred end for addition of tubulin dimers, also known as the 'plus' end, is where the  $\beta$ -tubulin subunit is exposed. The opposite 'minus' end grows at a slower rate. The minus ends of microtubules are stabilised and nucleated by the  $\gamma$ -tubulin ring complex ( $\gamma$ TuRC) which effectively acts as a cap (Kollman *et al.*, 2011). Microtubules have many roles in neurons besides acting as the substrate for the transport of membrane-bound organelles. Microtubules are needed for the extension of neurites during development as well as their maintenance. Microtubules also help to retain the integrity and definition of intracellular compartments within the neuron (Siegel *et al.*, 1999). Microtubules are very dynamic structures and have the ability to alternate between states of polymerisation and depolymerisation.  $\beta$ -tubulin subunits bind to guanosine triphosphate (GTP) and act as GTPases. The presence of GTP and  $Mg^{2+}$  causes the microtubule to extend from the plus end forming a GTP cap which is progressively

hydrolysed by tubulin in turn providing protection from depolymerisation. It is only GDP-bound tubulin molecules that are able to depolymerise and once the GTP is hydrolysed the microtubule begins to depolymerise and shrink rapidly (Garnham and Roll-Mecak, 2012). The formation of microtubules from tubulin subunits is shown in Figure 1.1.

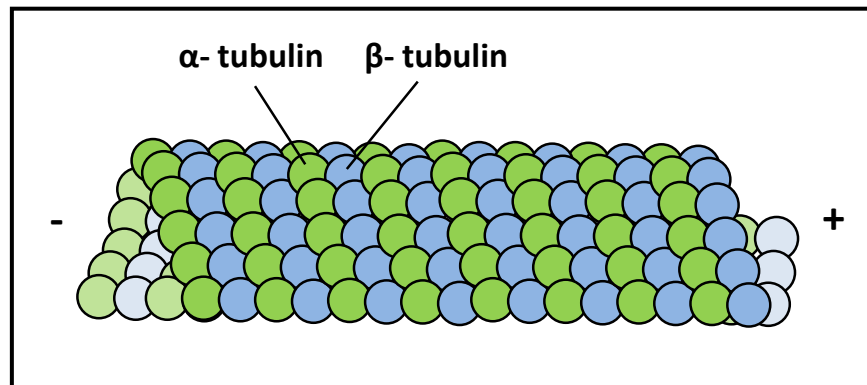


**Figure 1.1 A structure of a thirteen filament microtubule.**

Heterodimers of  $\alpha$ -tubulin and  $\beta$ -tubulin forming a microtubule structure.  $\alpha$ -tubulin is exposed at the minus end and  $\beta$ -tubulin at the plus end.

### 1.1.2 Motor proteins

Motor proteins are a class of molecular motors that are known to use the chemical energy taken from adenosine triphosphate (ATP) breakdown to fuel the force and motion needed to create movement along actin filaments and microtubule protein polymers (Cooke, 2001). These motor proteins can be divided into three protein superfamilies; myosin, dynein and kinesin. The myosin superfamily is responsible for force generation along actin polymers to create muscle movement as well as involvement in cytokinesis and short-range membrane/vesicle transport within cells (Hartman and Spudich, 2012). The dynein superfamily is responsible for movement of multiprotein complexes and organelles towards the designated minus ends of microtubules (Bowman, 2001). Dyneins are large protein complexes formed of two identical heavy chains that generate force movement along microtubules, two intermediate chains needed for binding to cargo, four light intermediate chains also needed for binding to cargo and several light chains which are again also thought to be involved in cargo binding (Kamal and Goldstein, 2002). Dynein is known to interact with dynactin which acts as a linker to help tether organelles during transport (Schroer, 2004). The kinesin superfamily is responsible for movement of multiprotein complexes

and organelles along microtubules (Bowman, 2001). The kinesin protein superfamily will be discussed in more detail in Section 1.2. An example schematic of both kinesin and dynein transport in a neuron is shown in Figure 1.2.

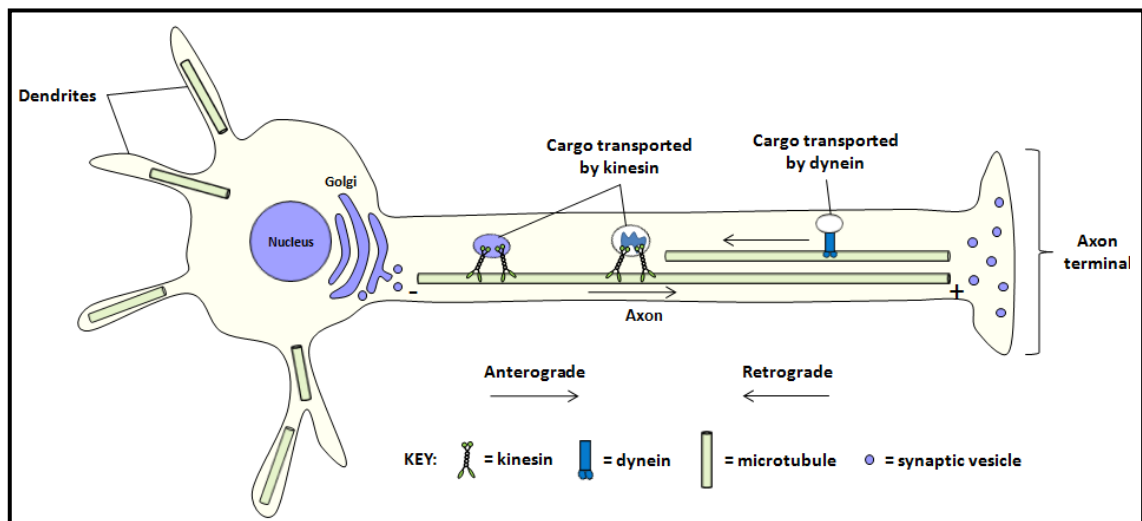


**Figure 1.2** A schematic of motor protein transport of cargo in a neuronal cell. Kinesin motor proteins are shown in green trafficking in an anterograde direction. The dynein motor protein is shown in blue trafficking cargo in a retrograde direction.

## 1.2 The kinesin superfamily of motor proteins

As mentioned in Section 1.1.2 kinesins are microtubule based molecular motors that transport cargoes such as organelles and protein complexes (Bowman, 2001; Hirokawa *et al.*, 2009). Kinesins have fundamental roles in the function, plasticity, morphogenesis and the survival of cells by helping to transport cargoes throughout the cellular system (Hirokawa *et al.*, 2010). Generally kinesins consist of a motor, neck linker, stalk and tail domain. The motor domain is known to utilise the energy from the binding and hydrolysis of ATP to create movement along microtubules. The stalk domain gives flexibility to the kinesin protein and the tail domain is known to recognise and bind to cargoes to be transported (Hirokawa *et al.*, 2010). The mammalian kinesin superfamily (KIF) of motor proteins consists of 14 kinesins currently made up of 138 recognised mammalian family members (Miki *et al.*, 2005). A summary of the major mammalian KIFs found in mouse is shown in Figure 1.3. Initially the naming of the kinesin proteins was based upon several differing criteria including the functional characteristic, the position of the motor domain or the evolutionary origin of the motor protein. To simplify the system, Lawrence *et al.* (2004) introduced the characterisation of 14 kinesin family members to ease the confusion brought about

by many years of inconsistent naming and organisation of the kinesin proteins. This new system groups kinesins according to their phylogenetic analysis.

KIFs generally comprise three major groups depending on the position of the motor domain. These include N-terminal motor domain kinesins (N-KIFs), middle motor domain kinesins (M-KIFs) and C-terminal motor domain kinesins (C-KIFs) (Hirokawa and Takemura, 2005). N-KIFs generally move towards the microtubule plus end in an anterograde direction while C-KIFs move towards the microtubule minus end in a retrograde direction. Both N-KIFs and C-KIFs are composed of a motor domain, a stalk domain and a tail region known as the cargo binding domain. Whereas M-KIFs possess a motor domain yet lack the long flexible stalk domain exhibited by both N-KIFs and C-KIFs (Ovechkina and Wordeman, 2003). It is also unclear if M-KIFs possess a tail domain in a similar manner to both N-KIFs and C-KIFs. The amino acid sequence encoding the motor domain is highly conserved across the 14 types of KIFs (Hirokawa and Takemura, 2005). Comparatively, the rest of the kinesin protein has evolved and adapted to target different cargoes for transport whilst conserving the basic means of propulsion along the microtubule (Vale and Fletterick, 1997). An example of kinesin binding to cargo includes the kinesin-3 family member KIF16B and its interaction with fibroblast growth factor receptor vesicles (Ueno *et al.*, 2010). The binding of cargoes to the tail domain is not always direct and can be mediated by a variety of adaptor proteins over the entirety of the different N-KIFs and C-KIFs (Hirokawa *et al.*, 2009a). For example, the kinesin-2 family member, KIF17, is capable of transporting the *N*-methyl-D-aspartate (NMDA) receptor subunit NR2B-containing receptor vesicles present in dendrites of neuronal cells via several adaptor proteins including Lin10, Lin2 and Lin7 (Setou *et al.*, 2000; Guillaud *et al.*, 2003). The kinesin-3 family member KIF13A is known to bind vesicles containing the mannose-6-phosphate receptor (M6PR) via the adaptor protein AP-1 (Nakagawa *et al.*, 2000). The variety of adaptor proteins known to bind to kinesin-1 will be discussed in further detail in Section 1.2.2.

Nearly all KIFs are responsible for transporting some form of cargo for example, proteins or organelles. However, there are other roles than can be played by some KIFs. These include the members of the kinesin-8, kinesin-13 and kinesin-14 families which can depolymerise microtubules in an ATP-dependent manner. The need for kinesin motor proteins to depolymerise microtubules is thought either to deconstruct

microtubules at certain cellular locations or to help enable the coupling of microtubule depolymerisation to the movement of the cellular cargo (Moore *et al.*, 2006). Most kinesin molecules form a dimeric structure consisting of two kinesin proteins interacting together via the stalk domain. However, the kinesin-3 family member, KIF1A, is unique in that it is a monomeric motor (Okada *et al.*, 1995). The kinesin-2 family members KIF3A, KIF3B and kinesin associated protein 3 (KAP3) are known to together form a tetrameric kinesin protein (Mueller *et al.*, 2005). Also two KIF heavy chains of the kinesin-1 family are known to form a heterodimer with two kinesin light chain (KLC) proteins (Gauger and Goldstein, 1993). The kinesin-5 family are tetrameric kinesins with two motor domains on each side of the tetramer. This in turn allows kinesin-5 to simultaneously bind and walk along two antiparallel microtubules assisting to slide the microtubules apart in centrosome separation during cell division (Tanenbaum and Medema, 2010). A summary of the major mammalian KIFs found in mouse is shown in Figure 1.3.

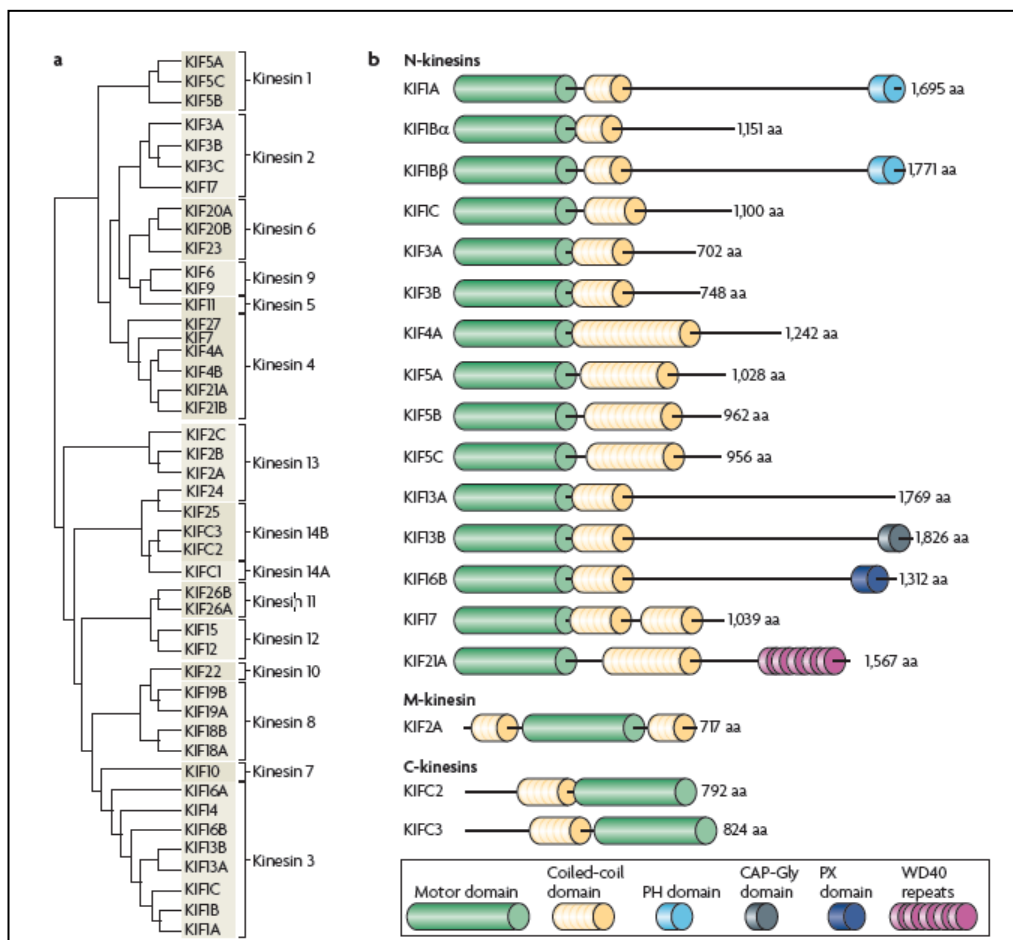


**Figure 1.3 A summary of the major mouse kinesins.**

**a** = Phylogenetic tree of the 45 kinesin superfamily genes in the mouse genome. **b** = Schematic structures of the major mouse kinesins. Reproduced with permission from Hirokawa *et al.* (2009).

The importance of several kinesin sub-types in the CNS has been demonstrated by utilising knock-out studies in murine models. Deletion of the ubiquitous kinesin-1 subtype, KIF5B, in rat models resulted in neonatal death of pups before birth (Tanaka *et al.*, 1998). KIF5A knock-out mice also resulted in the neonatal death of pups before birth (Xia *et al.*, 2003). Yet mice lacking the KIF5C gene survived yielding viable and normal sized mice, albeit with a notably smaller brain mass of approximately 5 % (Kanai *et al.*, 2000). In the same study by Kanai *et al.* reported that there was a relative loss of motor neurons compared to sensory neurons in these KIF5C mutant mice. The role of the kinesin-1 family in the CNS will be discussed in more detail in Section 1.2.3. Deletion of KIF3A in knock-out mice models also demonstrated neonatal death (Takeda *et al.*, 1999). KIF1B knock-out mice survived birth but died within 30 min. The KIF1B knock-out mouse brains were reduced ~ 10 % in size and the organisation and development of the brain stem nuclei, hippocampus and commissural fibres were significantly affected (Zhao *et al.*, 2001). KIF2A knock-out mice also managed to survive birth but died within a day of being born (Homma *et al.*, 2003). Conversely, KIFC2 mutant mice were viable and reproduced normally after demonstrating normal development (Yang *et al.*, 2001).

### **1.2.1 Structure of kinesin**

The structure of kinesin in its entirety has not yet been solved, although the structure of the motor domain has been solved for many different kinesins, including the kinesin-1, kinesin-2, kinesin-3, kinesin-5, kinesin-10, kinesin-13 and kinesin-14 families (Hirokawa *et al.*, 2009). However the most well studied has been that of kinesin-1. Previous work by Kull *et al.* (1996) successfully resolved the structure of the motor domain of the human kinesin-1 sub-type KIF5B to a 1.8 Å resolution by X-ray crystallography. This was carried out using amino acids 7-325 of KIF5B in complex with its magnesium adenosine diphosphate (MgADP) ligand in a ratio of 1:1. Kozielski *et al.* (1997) resolved the motor and stalk domains of KIF5B from rat in its native dimeric form to a resolution of 3 Å. This study showed that the two dimeric KHC motor domains share a similar conformation to one another. The crystal structure also showed the neck region to be a coiled-coil domain (Kozielski *et al.*, 1997). The structure of the kinesin-1 motor domain is shown in Figure 1.5.

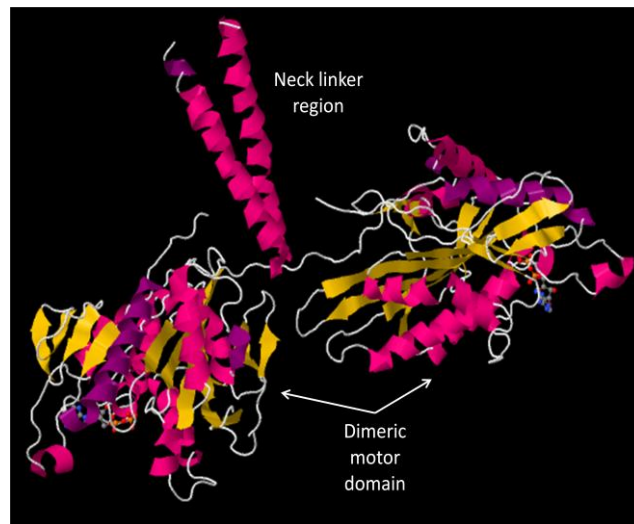


**Figure 1.5 Structure of dimeric kinesin-1 in a ribbon representation.**

$\alpha$ -Helices are highlighted in pink and purple,  $\beta$ -sheets are highlighted in yellow and loops in grey. The image was adapted from Jmol, an open-source Java viewer for chemical structures in 3D ([www.jmol.org](http://www.jmol.org)). Data of the crystal structure was obtained from Kozielski *et al.* (1997).

The success in determining a crystal structure of the kinesin-1 motor domain, as well as studies utilising electron paramagnetic resonance, fluorescence resonance energy transfer (FRET), pre-steady state kinetics and cryo-electron microscopy experiments led to the elucidation of the function and mechanism of kinesin-1 movement along microtubules (Rice *et al.*, 1999). Movement of kinesin-1 occurs by a process known as the “hand-over-hand” model. In this model, every ATP molecule hydrolysed in the ATP binding site of a trailing motor domain head is forced from the energy released to overtake the “partner head” in front. This action propagates, in effect, to create movement along the microtubule (Asbury, 2003; Yildiz *et al.*, 2003; Shao and Gao, 2005). Due to the alternating biochemistry of the ATP binding site of each motor domain, at least one motor domain remains bound to the microtubule in turn helping to facilitate the stepping action known as processivity (Howard *et al.*, 1999). Each KHC motor domain will bind a tubulin heterodimer present on the microtubule and for every movement of the motor domain, the kinesin protein will travel 8 nm along the microtubule (Song and Mandelkow, 1993; Hua *et al.*, 1997). Switch regions have been identified in the motor domain and are known to be responsible for changing conformation depending on whether the nucleotide binding site is occupied. These switch regions aid in the binding and attachment of the motor domains to microtubules (Kull *et al.*, 1996). Due to the high amino acid sequence homology between the motor domains of KIFs, this hand-over-hand method can be used as a

template to explain the movement along microtubules for nearly every dimeric KIF protein. As previously described, KIF1A (kinesin-3 family) is known to be monomeric (Okada *et al.*, 1995). Interestingly KIF1A has also been shown to move directionally along the length of microtubules (Okada *et al.*, 1999). Hence, the hand-over-hand model does not explain the ability of KIF1A to create movement along microtubules. Studies by Okada *et al.* (2000) have demonstrated that an interaction of the negatively charged C-terminal hook of tubulin and the positively charged K-loop of KIF1A enables the one-dimensional diffusion of KIF1A to the next tubulin binding site in turn allowing for progressive movement. Other N-KIFs, such as the kinesin-5 family members, show both the ability to carry out hand-over-hand and diffusive movement along microtubules (Kapitein *et al.*, 2008). M-KIFs are also known to use a diffusive method to create movement along the microtubule, where at the ends of microtubules M-KIFs are known to cause microtubule depolymerisation (Helenius *et al.*, 2006). Relatively little is known about the exact mechanism of C-KIF motility, although it is known that the two heavy chains dimerise using a different mechanism compared to N-KIF and M-KIF. C-KIFs also lack the neck linker domain hence it is unlikely that they move in a similar manner. Thus, kinesins move by at least two known and differing conserved mechanisms rather than by mechanisms that are unique to each kinesin molecule (Endow, 1999; Hirokawa *et al.*, 2009a).

The neck linker domain is highly conserved among kinesin sub-families. Within N-KIFs, the neck linker domain is approximately 10 amino acids in length and is present just above the motor domain. The neck linker domain is known to amplify the conformational changes in the motor domain and is essential for the generation of movement along microtubules (Rice *et al.*, 1999; Case *et al.*, 2000). The stalk domain that follows the neck linker domain in nearly all kinesin family members consists of some form of a coiled-coil domain. In the case of kinesin-1 two coiled-coil regions in the stalk domain are known to interact to form the dimeric protein. The formation of the dimer is needed to create processive movement of kinesin along the microtubule using the hand-over-hand method mentioned previously (Hancock and Howard, 1998; Hackney, 2007). The stalk domain is known to give flexibility to the kinesin protein and hinge domains present within the stalk domain are responsible for allowing the kinesin molecule to change conformation (Gutierrez-Medina *et al.*, 2009). Structural

information regarding the conformation of the hinge domains in mammalian kinesins is relatively unknown, although analysis of a synthetic peptide of the hinge domain of rat kinesin-1 has indicated that it consists of short non-helical secondary domains that break the stalk domains coiled-coil structure (Seeberger *et al.*, 2000). In the *Drosophila* kinesin-1, there are two known hinge domains, termed hinge 1 and hinge 2. Hinge 1 contains several proline and glycine residues which are known to give flexibility. The stalk domain is further interrupted by hinge 2 whose role has been linked to the ability of the dimeric kinesin-1 to fold back on itself (Hirokawa *et al.*, 1989; Hackney *et al.*, 1992; Gutierrez-Medina *et al.*, 2009). Analysis of the hinge 1 region of fungal kinesin-1 has also demonstrated its importance for the efficient activity of the motor domain (Grummt *et al.*, 1998). Little is known regarding the structure of the cargo binding domain of kinesin. The divergence of this domain makes it difficult to compare across all kinesin sub-families. This may be due, as mentioned previously, to a number of cargoes that can bind the cargo binding domain either directly or indirectly in order to facilitate transport throughout the cell.

### 1.2.2 Kinesin-1

Kinesin-1 also known as “conventional kinesin” was the first of the kinesins to be identified and was originally isolated from the axon of squid and bovine brain (Brady, 1985; Vale *et al.*, 1985). Human kinesin-1 is a protein heterotetramer consisting of two kinesin heavy chains (KHCs) and two KLCs. A schematic representation of the kinesin-1 heterodimer is shown in Figure 1.4.

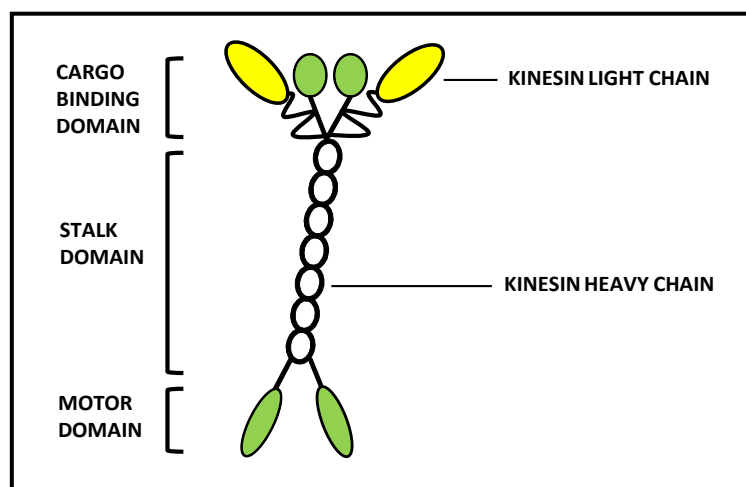


**Figure 1.4** A schematic representation of the kinesin-1 heterotetramer molecular motor. The kinesin heavy chain is shown in green and the kinesin light chain is shown in yellow.

Each KHC has a molecular weight of ~ 120 kDa and contains a globular head region also known as the motor domain which is responsible for force generation along the microtubule (Section 1.2.1; Yang *et al.*, 1989). This motor domain is connected to a long central coiled stalk domain via a neck-linker region which in turn ends in a tail region known as the cargo binding domain. The two central stalks intertwine to form a dimer via a coiled-coil domain giving flexibility to the kinesin protein. There are three kinesin-1 heavy chain family members - KIF5A, KIF5B and KIF5C (Lawrence *et al.*, 2000). The two KLCs each have a molecular weight of ~ 64 kDa and bind to each of the KHCs acting as an alternative platform for the binding of specific cargo (Cyr *et al.*, 1991). Four isoforms of KLC exist in humans. These include KLC1, KLC2, KLC3 and KLC4. Despite this interaction not all kinesin-1 proteins exist as heterotetramers with only approximately 50 % of dimeric kinesin-1 known to associate with KLCs at any one time (Kanai *et al.*, 2000; DeLuca *et al.*, 2001; Palacios and Johnston, 2002; Gyeova *et al.*, 2004). Yet KLCs are important components of kinesin-1 as loss of KLC function leads to progressive lethargy, crawling defects and paralysis followed by death at the end of the second larval instar stage of development in *Drosophila* knock-out mutants (Gindhart *et al.*, 1998). KLC1 knock-out mouse models also resulted in smaller animals with pronounced motor disabilities (Rahman *et al.*, 1999). Immunofluorescence studies of sensory and motor neuron cells in the same KLC1 mutants also revealed abnormal accumulations of KIF5A and KIF5B. (Rahman *et al.*, 1999).

### **1.2.2.1 Kinesin light chain**

The KLCs have only been seen to bind KHC as a homodimer meaning that only identical KLCs can bind the dimeric KHC at any one time (Gyeova *et al.*, 2004). The KLC binding site has been mapped to amino acids 771-813 of KIF5B. Within this KHC region are four highly conserved heptad repeats present at amino acids 775-802 which are predicted to form a tight alpha-helical coiled-coil interaction with the heptad repeat-containing N-terminus of the KLC, in particular the amino acid region KLC 106-152 (Diefenbach *et al.*, 1998). The C-terminal tail domains of KLCs include several tetratricopeptide repeats (TPRs). These 34 amino acid TPRs are known to mediate protein-protein interactions and are involved in the binding of KLC to several cargoes. (Gyeova *et al.*, 2004; Adio *et al.*, 2006). The TPR domains within the various KLC isoforms are almost

identical and therefore KLC1 and KLC2, the most studied KLC sub-types, are thought to interact with cargo in a similar manner (Rahman *et al.*, 1998). The binding of KLCs to their cargoes will be explained in more detail in Section 1.2.4.1. Work by Zhu *et al.* (2012) has successfully resolved the structure of the TPR domains of both KLC1 and KLC2 to a 1.9 Å resolution by X-ray crystallography. This was carried out using amino acids KLC1 228-495 and KLC2 217-480. This study hypothesised that the six TPR repeats of KLC1 can form two polar patches within its groove to interact with negatively charged and aromatic residues of various cargo proteins. The structure of the TPR domain of KLC1 is shown in Figure 1.6. In contrast to the similarity in the TPR domains there is considerable variability in the C-terminal region of the KLCs (McCart *et al.*, 2003; Wozniak and Allan, 2006). The binding of cargo to kinesin-1 via KLCs is discussed in further detail in Section 1.3.2.2.

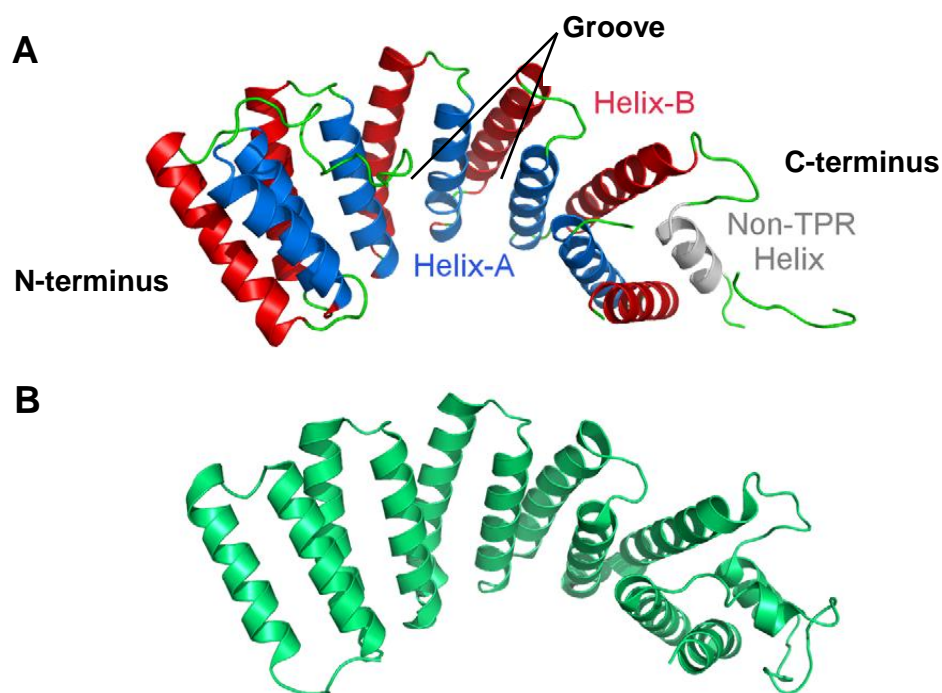


**Figure 1.6 Structure of the TPR domains of human KLC1 in a ribbon representation.**

**A** = TPR domain of KLC1 with the outer loop  $\alpha$ -helices highlighted in red, inner loop  $\alpha$ -helices highlighted in blue, the non-TPR domain highlighted in grey and loops highlighted in green. The groove which is known to interact with cargo proteins is also highlighted and the N-terminus and C-terminus of the protein fragment indicated. **B** = TPR domain of KLC2. The figure was adapted from Zhu *et al.* (2012).

### 1.2.3 Kinesin-1 in the central nervous system

As discussed in Section 1.2 kinesin-1 is essential for the correct function and survival of pups in murine models. All three of the kinesin-1 sub-types are found in neurons however they differ with respect to their localisation. KIF5A is distributed evenly throughout the nervous system (Reid *et al.*, 2002). KIF5B is known as a ubiquitous kinesin-1 since it is found in nearly all cell types including neurons. More specifically in neuronal cells, the highest concentration of KIF5B is found in glial cells and in axon-elongating neurons such as the mossy fibres found in the cerebellum and the olfactory primary neurons involved in smell (Kanai *et al.*, 2000). KIF5C is found in the retina and spinal cord where it is mainly located in motor neurons (Schafer *et al.*, 2009; Kanai *et al.*, 2000). Both the KLC1 and KLC2 isoforms are also highly expressed in neurons. They are found in the olfactory bulb, hippocampus, dentate gyrus and in the granular layer of the cerebellum. KLC1 has also been shown to have a uniform distribution throughout mouse brain. In the peripheral nervous system KLC1 is found only in axons whereas KLC2 is found in axons and Schwann cells (Rahman *et al.*, 1998).

Kinesin-1 is responsible for transporting cargo throughout neuronal cells. The majority of cargo transported by kinesin-1 occurs in the axon, although some cargoes such as  $\alpha$ -amino-3-hydroxy-5-methyl-4-isoxazolepropionic acid (AMPA) receptor GluA2 subunits (GluR2), huntington and mRNA containing complexes are transported by kinesin-1 in the dendrites of neuronal cells (Setou *et al.*, 2002; Kanai *et al.*, 2004; Twelvetrees *et al.*, 2010). There are two kinds of axonal transport: fast transport and slow transport. In axons, vesicles move quickly at approximately 50–400 mm/day, while soluble proteins are known to move more slowly at approximately 2-8 mm/day (Roy *et al.*, 2008; Hirokawa, 2011). Kinesin-1 is capable of transporting cargos using both fast and slow transport. The slow transport of cytoplasmic proteins by kinesin-1 is essential for neuronal homeostasis. Slow transport depends on the interaction between the DnaJ-like domain in the TPRs of KLCs and heat-shock cognate protein of 70 kDa (Hsc70) which helps to mediate the interaction between cytoplasmic proteins and kinesin-1. This DnaJ-like domain can bind to membranous organelles. The competitive inhibition of this Dna-J like domain was shown to disrupt cytoplasmic protein transport and increase the transport of membranous organelles in squid axons (Terada *et al.*, 2010). This indicates that this DnaJ-like domain might function as a switch between slow and

fast transport involving Hsc70. Transgenic mice over-expressing a dominant-negative form of this DnaJ-like domain exhibited delayed slow transport, accelerated fast transport and the disruption of optic axons. (Terada *et al.*, 2010).

Kinesin-1 has been shown to have the ability to distinguish between different microtubule populations (Cai *et al.*, 2009). Kinesin-1 will associate with microtubules with post-translational modifications of tubulin that indicate a more stable form of microtubule. An acetylated form of  $\alpha$ -tubulin has been shown to help in the promotion of binding of kinesin-1 to microtubules (Reed *et al.*, 2006). Whereas the deetyrosination of  $\alpha$ -tubulin leads to kinesin-1 being directed down axons (Konishi *et al.*, 2009). Also the motor domain of KIF5B has been shown to preferentially localise to the tips of axons as opposed to dendrites in cultures of hippocampal mouse neurons. When these hippocampal mouse neurons are treated with a low concentration of paclitaxel, a microtubule stabiliser, axonal microtubules lose their polar characteristics and the KIF5B motor domain localises in both the axon and dendrites (Nakata and Hirokawa, 2003). However, a previous study by Dotti and Banker (1991) found that the distribution of both acetylated or tyrosinated tubulins are not found in greater quantity in axons compared to dendrites. Hence, this work shows no definitive answer as to how kinesin-1 can selectively differentiate between microtubules present in either the axon or dendrites within a neuron (Hirokawa *et al.*, 2010). Microtubule associated proteins (MAPs) such as MAP2c and tau help to regulate the stability and organisation of the microtubule network (Vershinin *et al.*, 2007), but the presence of these MAPs on microtubules is known to interfere with the movement of motor proteins such as kinesins. Work by Marx *et al.* (2005) has demonstrated that the binding regions of MAPs, such as tau, to the tubulin subunits of microtubules overlap with the binding of the KHC motor domain. The number of kinesin-1 motors attached to mitochondria at any one time are estimated to be anywhere between 2 and 200 (Gross *et al.*, 2007). This may explain how the dissociation of kinesin-1 from the microtubules by various MAP proteins does not prevent the disruption of cargo transport as other microtubule bound kinesins helping to transport the same cargo could help to retain movement along the microtubule network.

#### 1.2.4 Transport of cargo via the cargo binding domain of kinesin-1

The binding to and movement along the microtubule via the kinesin motor domain has been well characterised over the majority of the KIFs. However, the way in which kinesin-1 initially binds the cargo to be transported and how this is regulated is only now beginning to be understood. It is known that a variety of adaptor proteins can help to associate some cargoes to various KIFs. Proteins that interact with kinesin-1 can be divided into two main categories; those that interact with KHC and those that interact with KLC. Proteins that are known to interact with either the KHC or KLC are explained in Section 1.2.4.1 and Section 1.2.4.2 respectively. However, some cargoes do not require adaptor proteins in order to mediate binding to kinesin-1 and can instead bind directly. One such cargo is p180, a ribosome receptor. Yeast two-hybrid assays demonstrated the ability of KIF5B 867-907 to bind 1293-1413 of p180. These known interacting regions of both KIF5B and p180 are made up of mostly heptad repeats which indicate that this protein interaction is mediated via a coiled-coil interaction. (Diefenbach *et al.*, 2004).

The Ran-binding protein 2 (RanBP2) is a large scaffold protein involved in a wide range of cellular functions including the movement of proteins between the nuclear and cytoplasm compartments of the cell. RanBP2 is known to associate directly both *in vitro* and *in vivo* with KIF5B and KIF5C but not KIF5A. This interaction demonstrated that RanBP2 could interact with the C-terminal amino acids 527–936 of KIF5B (Cai *et al.*, 2001; Cho *et al.*, 2007).

Interestingly herpes simplex virus (HSV), known for the ability to remain dormant in sensory ganglion neurons (Kramer *et al.*, 2003), can associate with the KHC of KIF5B. This interaction was demonstrated after *in vitro* binding assays showed that the interaction of HSV with the C-terminus of KIF5B was direct. HSV infection occurs at the nerve terminus where replication of HSV then manifests in the nucleus and new viruses are transported back to the synapse (Diefenbach *et al.*, 2002; Gindhart, 2006).

The potential cargoes of both KLCs and KHCs can bind simultaneously on the kinesin-1 protein (Huang *et al.*, 1999; Diefenbach *et al.*, 2002). An exception to this is the mitochondrial adaptor protein, Milton, which is known to compete with the KLCs for binding to the same KHC domain (Glater *et al.*, 2006; Wozniak and Allan, 2006).

### 1.2.4.1 Adaptor proteins that bind via the kinesin heavy chain

There are several known kinesin adaptor proteins that are responsible for mediating the binding of cargo to KHC. A summary of all the current known KHC adaptor proteins and their cargo are shown in Table 1.1.

Adaptor protein	KHC cargo	Methods used to ascertain the interaction between the cargo domain of KHC and the adaptor protein	Region of KHC interaction	References
<b>GRIP-1</b> (753-987 to KHC)	GluR2 (subunit of AMPA receptors)	Co-immunoprecipitation assays and co-localisation studies	KIF5A KIF5B KIF5C (807-934)	Setou <i>et al.</i> , 2002
<b>Syntabulin</b>	Syntaxin-1, mitochondria	Co-immunoprecipitation assays and co-localisation studies	KIF5B	Su <i>et al.</i> , 2004; Cai <i>et al.</i> , 2005; Cai <i>et al.</i> , 2007
<b>SNAP23</b> (1-85 to KIF5B)	Membrane protein containing vesicles	Yeast two-hybrid and <i>in vitro</i> pull-down assays	KIF5B (814-907)	Diefenbach <i>et al.</i> , 2002
<b>SNAP25</b> (1-85 to KIF5B)	Membrane protein containing vesicles	Yeast two-hybrid and <i>in vitro</i> pull-down assays	KIF5B (814-907)	Diefenbach <i>et al.</i> , 2002
<b>UNC-76</b> ( <i>Drosophila</i> ) FEZ1 is the mammalian homologue	Thought to be protein kinase C (PKC)	Yeast two-hybrid and co-purification assays	<i>Drosophila</i> KHC (850-975)	Gindhart <i>et al.</i> , 2003
<b>FEZ1</b> (mammalian homologue to UNC-76)	Syntaxin 1 and Munc19 (synaptic vesicle exocytosis proteins) also mitochondria	<i>In vivo</i> pull-down assay, co-immunoprecipitation	Rat KIF5B	Fujita <i>et al.</i> , 2007; Chua <i>et al.</i> , 2012
<b>TRAK1</b> (TRAK/Milton family member)	Mitochondria, K <sup>+</sup> channel and GABA <sub>A</sub> receptor $\beta$ 2 subunit	Yeast two-hybrid and co-immunoprecipitation assays, co-localisation studies	KIF5A KIF5B KIF5C (827-957)	Brickley <i>et al.</i> , 2005; Smith <i>et al.</i> , 2006; Brickley and Stephenson, 2011.
<b>TRAK2</b> (TRAK/Milton family member)	Mitochondria, K <sup>+</sup> channel and GABA <sub>A</sub> receptor $\beta$ 2 subunit	Yeast two-hybrid and co-immunoprecipitation assays, co-localisation studies	KIF5A KIF5B KIF5C (827-957)	Brickley <i>et al.</i> , 2005; Smith <i>et al.</i> , 2006; Brickley and Stephenson, 2011.
<b>Milton</b> (TRAK/Milton family member) ( <i>Drosophila</i> ) (810-891 interacts with Miro) (1-450 interacts with KIF5B)	Mitochondria	Co-immunoprecipitation assays and co-localisation studies	KIF5B (810-891)	Stowers <i>et al.</i> , 2002; Glater <i>et al.</i> , 2006

**Table 1.1 A summary of all the known KHC cargo adaptor proteins.**

The table demonstrates the known interacting domains of the relevant protein interactions and the experiments used to demonstrate their interaction.

One such adaptor protein is glutamate receptor interacting protein (GRIP-1). GRIP-1 is an adaptor protein for GluR2, a subunit of excitatory AMPA type glutamate receptors. Antibodies directed against all the kinesin-1 subtypes co-immunoprecipitated GRIP1 from rat brain lysates. GRIP1, GluR2 and kinesin-1 have also been shown to co-localise within the dendrites and cell bodies of cultured hippocampal neurons and can also be co-immunoprecipitated from vesicle fractions (Setou *et al.*, 2002).

Syntabulin is an adaptor protein known to mediate the transport of syntaxin-1, a transmembrane protein responsible for vesicular fusion. The KHC of KIF5B was shown to interact with syntabulin *in vitro* and both syntaxin-1 and KHC associate with syntabulin-linked membrane organelles that were isolated from rat brain homogenates (Su *et al.*, 2004). Small interfering ribonucleic acid (siRNA) knockdown of syntabulin in cultures of hippocampal neurons led to inhibition of syntaxin-1 attachment to microtubules as well as the decrease in distribution of syntaxin-1 in processes (Su *et al.*, 2004). Work by Cai *et al.*, (2007) demonstrated that the complex of syntaxin-1, syntabulin and KIF5B helps to mediate axonal transport components essential for presynaptic assembly. These components include active zone precursor carriers and Bassoon, a component of the presynaptic cytoskeleton (Dieck *et al.*, 1998). Syntabulin knock down in developing neurons delayed the appearance of synaptic activity and in mature neurons impaired synaptic transmission, including reducing basal activity and slowing recovery rates after depletion of synaptic vesicles. These defects have also been linked with the reduced transport of mitochondria in neuronal cells (Ma *et al.*, 2009). Synaptosome-associated protein of 25 kDa and synaptosome-associated protein of 23 kDa (SNAP25 and SNAP23) are thought to be important in forming a complex with syntaxin to help synaptic vesicle exocytosis (Lin and Scheller, 2000). The amino acids KIF5B 814-907 were shown to bind amino acids SNAP25 1-85 in yeast two-hybrid assays. The interaction of KIF5B with SNAP25 was further confirmed when an *in vitro* pull-down assay also demonstrated the ability of KIF5B 814–907 to bind both SNAP23 1-85 and SNAP25 1-85. Both KIF5B 814-907 and SNAP23/SNAP25 1-85 amino acid regions that are known to interact are composed almost entirely of heptad repeats suggesting the interaction between KIF5B and SNAP25 is that of a coiled-coil interaction (Setou *et al.*, 2002).

UNC-76 is a cytosolic protein known to help regulate the trafficking of vesicles in axons of *Drosophila*. Yeast two-hybrid analysis revealed that *Drosophila* KHC 850-975 interacted with UNC-76. This was further tested when co-purification experiments of bacterially expressed KHC and UNC-76 showed that a direct interaction occurred between the two proteins (Gindhart *et al.*, 2003). The same study also demonstrated that loss of UNC-76 function in *Drosophila* null mutants resulted in death between the second and third instar stage of development. Prior to death, immunostaining of *Drosophila* larvae with the synaptic vesicle precursor marker SYT showed that segmental nerves contain aggregates of SYT immunoreactivity, whereas control larvae showed a diffuse and punctate staining pattern (Gindhart *et al.*, 2003). This indicates that UNC-76 is essential for kinesin-1 transport in the *Drosophila* nervous system.

Other proteins known to associate with KHC are FEZ1 (mammalian homologue to UNC-76), Milton and the TRAKs (Fujita *et al.*, 2007; Stowers *et al.*, 2002; Beck *et al.*, 2002). The TRAK/Milton kinesin adaptor protein family, known to act as kinesin adaptors for the transport of mitochondria, will be discussed in more detail in Section 1.4.

#### **1.2.4.2 Adaptor proteins that bind kinesin light chain**

As mentioned previously the KLC1 isoform is highly expressed in neurons and can bind several proteins that are associated with neurodegeneration or axonal outgrowth. Several cargoes are transported by kinesin-1 courtesy of their binding via the KLCs. A summary of the known adaptor proteins and the cargo transported by KLCs are shown in Table 1.2.

Name of KLC interactor	KLC cargo	Methods used to ascertain the interaction between KLC and the adaptor protein	Region of KLC interaction	References
<b>JIP1</b> (307-700) <b>JIP2</b> <b>JIP3</b>	JNKs	Yeast two-hybrid, co-immunoprecipitations, co-localisation, dominant negative, <i>in vitro</i> motility assays	Rat KLC (TPR motif) Also KIF5C	Meyer <i>et al.</i> , 1999; Stockinger <i>et al.</i> , 2000; Verhey <i>et al.</i> , 2001; Horiuchi <i>et al.</i> , 2005; Sun <i>et al.</i> , 2011
<b>HAP1</b> (rat)	huntington	Yeast two-hybrid, pull-down, co-immunoprecipitations assays and co-localisation studies	Rat KLC2	McGuire <i>et al.</i> , 2006; Rong <i>et al.</i> , 2006; Ma <i>et al.</i> , 2011
<b>APP</b>	Vesicles containing APP, $\beta$ -secretase and presenilin-1	Co-immunoprecipitations, sucrose gradients, <i>in vitro</i> binding assays and APP knock-out mice	Mouse KLC1	Kamal <i>et al.</i> , 2000; Kamal <i>et al.</i> , 2001; Hirokawa and Takemura, 2003
<b>Calsyntenin-1</b> (mouse)	Neuronal vesicles and tubulovesicular organelles	Yeast two-hybrid, <i>in vivo</i> pull-down assays, co-immunoprecipitations assays and co-localisation studies	Mouse KLC1 (TPR domain), mouse KLC2	Konecna <i>et al.</i> , 2006; Vagnoni <i>et al.</i> , 2011
<b>TorsinA</b> (251-332)	Transmembrane proteins LAMP1 and LULL1	Yeast two-hybrid and co-localisation studies	KLC1 (209-547)	Kamm <i>et al.</i> , 2004
<b>CRMP-2</b>	Sra-1/WAVE1 complex as well as tubulin	Co-localisation studies, co-immunoprecipitation and <i>in vitro</i> pull-down assays	Mouse KLC1 (375-542)	Kimura <i>et al.</i> , 2005; Kawano <i>et al.</i> , 2005
<b>UNC-83</b> ( <i>C.elegans</i> )	Docking site for the outer nuclear membrane	Yeast two-hybrid, <i>in vitro</i> interaction assays	KLC2 (137-362). Also interacts with dynein	Meyerzon <i>et al.</i> , 2009; Fridolfsson <i>et al.</i> , 2010
<b>Hsc70</b>	Clathrin-coated vesicle containing cytoplasmic proteins. Also creatine kinase	Co-immunoprecipitations, dominant negative, KLC mutant mice	KLC1	Tsai <i>et al.</i> , 2000; Terada <i>et al.</i> , 2010
<b>FMRP</b> (386-585)	Ribonucleoprotein complexes	Co-immunoprecipitation assays	Mouse KLC	Dictenberg <i>et al.</i> , 2008
<b>Kidins 220</b> (rat) (kinase-D-interacting substrate of 220 kDa) (1361-1395 binds to KLC1)	No known cargo	Yeast two-hybrid, pull-down assays, co-immunoprecipitations and co-localisation studies	Rat KLC1 (83-296)	Bracale <i>et al.</i> , 2007

**Table 1.2 A summary of KLC protein interactors.**

The table demonstrates the known interacting domains of the relevant protein interactions and the experiments used to demonstrate their interaction.

One such cargo that binds to KLC is C-jun N-terminal kinases (JNKs) which are mitogen-activated protein kinases. These MAP kinases respond to stress stimuli and are known to be trafficked by a set of proteins called JNK interacting proteins (JIPs). Three proteins, JIP1, JIP2 and JIP3 were identified and are known to bind to the C-terminus of the KLCs acting as scaffolding proteins for the JNK pathway (Verhey *et al.*, 2001). The three JIP proteins were originally found to interact with the TPR domain of rat KLC1 in a yeast two-hybrid screen (Verhey *et al.*, 2001). More specifically JIP1 307-700 was shown to interact with the TPR domain of KLC after co-immunoprecipitation of transfected constructs in human embryonic kidney 293 (HEK 293) cells. Co-localisation of JIP-1 and KLC1 in cultured neuronal cells demonstrated the complex at the tips of neuronal processes, with dominant negative experiments leading to a disruption of this distribution (Verhey *et al.*, 2001). In addition, interestingly JIP3 has recently been shown to bind the KIF5C KHC. Using an *in vitro* motility assay it was demonstrated that JIP3 can activate KHC for microtubule-based transport and it also helps to promote efficient motility of KHC along microtubules. This in turn increases both processive run length and the velocity of KHC. Importantly, JIP3 binding to KHC is functional in neurons as mutated JIP3 that can bind KHC but not KLC are transported to axons and dendrites similarly to wild-type JIP3. JIPs have been shown to be essential for correct functioning of vesicle transport in axons, with mutated JIP-1 and JIP-3 genes in *Drosophila* and *C. elegans* models showing similar results to that of stopping general kinesin-1 movement (Horiuchi *et al.*, 2005). This work has helped to establish JIP3 as an adaptor for both KLC and KHC and it also indicates that JIP3 is a positive regulator of kinesin-1 motility in neuronal cells (Sun *et al.*, 2011). In addition, JIP-1 and JIP-2 have been found to interact with rhoGEF and with the cell surface receptor for Reelin, ApoER2 (Meyer *et al.*, 1999; Stockinger *et al.*, 2000).

Huntington-associated protein-1 (HAP-1) is a protein found predominantly in neurons. It is a 629 amino acid protein with two coiled-coil domains (Li *et al.*, 1995). The dysfunction of HAP-1 and its interacting protein partner huntington has been linked to Huntington's disease. HAP-1 has been shown to interact with rat KLC2 using yeast two-hybrid screens. This was also shown to occur *in vivo* after co-immunoprecipitation of KLC with HAP-1 from mouse brain hypothalamic tissue using antibodies directed to KLC (McGuire *et al.*, 2006). The same study also demonstrated that HAP-1 can co-localise

with kinesin-1 in pheochromocytoma 12 (PC12) cells, a cell line derived from rat adrenal medulla. HAP-1 was also enriched in the end processes of neurites in PC12 cells. siRNA knock-down of HAP-1 resulted in the reduction of neurite growth in PC12 cells (McGuire *et al.*, 2006). HAP-1 has also been shown to interact with dynactin p150, a member of the dynein family (Engelender *et al.*, 1997). The phosphorylation of HAP-1 at T598 was shown to be important in mediating the binding interaction between HAP-1 and both KLC2 and dynactin p150 (Rong *et al.*, 2006). Recent work by Ma *et al.* (2011) showed that the knock-down of KIF5A resulted in reduced levels of HAP-1. This work not only indicates that HAP-1 is being utilised as a cargo linker in bi-directional transport of its associated cargoes, but it is also associated with KLC via the KIF5A sub-type of kinesin-1.

KLC has been shown to interact with and transport amyloid precursor protein (APP). The cleavage of APP by  $\beta$  and  $\gamma$  secretase produces the pathogenic form of APP, amyloid  $\beta$ , known to cause the plaques that may be responsible for Alzheimer's disease (O'Brien and Wong, 2011). Experiments by Kamal *et al.* (2000) using co-immunoprecipitation assays, sucrose gradients and direct *in vitro* binding assays established that the 47 C-terminal amino acids, known to constitute the cytoplasmic domain of APP, interacted directly with the TPRs of mouse KLC1. The follow up study also showed that kinesin-1 is associated with axonally transported vesicles that contain APP and the transmembrane proteins involved in its proteolytic cleavage (Kamal *et al.*, 2001). Although it is worth noting that the work regarding the binding of APP to KLC has been refuted by several different laboratories (Lazarov *et al.*, 2005).

The type-1 membrane-spanning protein, calsyntenin-1, is also known to interact with KLC1. Calsyntenin-1 is involved in the transport of neuronal vesicles and tubulovesicular organelles. Yeast two-hybrid and GST pulldown assays demonstrated that two highly conserved segments in the cytoplasmic domain of mouse calsyntenin-1, amino acids 878-924, are known to mediate its binding to the TPR domain of KLC1 (Konecna *et al.*, 2006). Work by Vagnoni *et al.* (2011) further demonstrated the importance of the KLC1 S460 in the regulation and binding to calsyntenin-1. S460 residue is known to be phosphorylated and experiments to mimic the pre-phosphorylation state *i.e.* mutating the serine to an alanine, resulted in an increase in the co-immunoprecipitation of calsyntenin-1 with KLC1 after co-transfection in chinese

hamster ovary (CHO) cells. The identical experiment although this time mutating the S460 residue to aspartate to mimic a constant phosphorylation state resulted in a decrease in co-immunoprecipitation. The same study also showed that KLC1 S460 is targeted by extracellular-signal-regulated kinase (ERK) and KLC1 S460D decreased co-localisation with calyntenin-1 in the monkey kidney cell line, CV-1. These results indicate that the KLC1 S460 may be involved in regulating the binding to calyntenin-1 (Vagnoni *et al.*, 2011).

Fragile X mental retardation protein (FMRP) has been shown to be vital in the trafficking of various mRNA, including its own transcript, via the association with KLC. Altered expression of FMRP results in Fragile X syndrome, a highly prevalent form of inherited mental retardation which is thought to contribute to the spectrum of autism disorders (Schaeffer *et al.*, 2003). The association of KLC with FMRP was first shown after the C-terminal domain of FMRP, amino acids 386-585, co-immunoprecipitated KLC from co-transfected HEK 293 cells using antibodies directed towards the FLAG-tag present on FMRP (Dictenberg *et al.*, 2008).

Collapsin response mediator protein-2 (CRMP-2) has shown to be important in the trafficking of the Rac1-associated protein 1 (Sra-1)/WASP family verprolin-homologous protein 1 (WAVE1) complex, which is a regulator of the actin cytoskeleton (Kawano *et al.*, 2005). Mouse KLC1 was originally shown to co-immunoprecipitate with CRMP2 from solubilised rat brain lysate. In addition, punctate CRMP-2 immunoreactivities were seen to be co-localised with KLC in axonal shafts of primary rat hippocampal neurons (Kimura *et al.*, 2005). The same study by Kimura *et al.* (2005) also used *in vitro* binding assays utilising recombinant His-tagged CRMP-2 and with GST-tagged KLC1 to demonstrate that KLC1 168-542 is responsible for binding to CRMP-2. Work carried out by Kawano *et al.* (2005) further refined the CRMP-2 binding site of KLC1 using *in vitro* binding assays to demonstrate that KLC 375-542 is responsible for binding CRMP-2.

Nearly all of the proteins that associate with KLC discussed above have displayed the ability to bind with at least two of the KLC sub-types, typically KLC1 and KLC2. In the case of the protein TorsinA that is responsible for numerous functions within neuronal cells including cytoskeletal dynamics and neurotransmitter release (Chen *et al.*, 2010), it can only bind KLC1 and not KLC2. Initially, yeast two-hybrid experiments using the

amino acid region 251–332 of TorsinA as bait showed a positive interaction with that of KLC1. Co-immunoprecipitation of TorsinA from human hippocampal brain samples showed the presence of KLC1 but not KLC2 indicating an *in vivo* interaction of TorsinA with KLC1. These co-immunoprecipitation results demonstrating the interaction between KLC1 and TorsinA were further replicated using adult rat brain, rat primary cortical neurons and embryonic rat brain samples. TorsinA and kinesin-1 were also shown to co-localise to a high degree in rat primary cortical neurons in the cell body, neurite extensions and at the end of processes. Mutant TorsinA, which does not bind KLC1, is found accumulated in inclusions suggesting that the binding of TorsinA to KLC1 is required for proper trafficking of TorsinA within the neurons (Kamm *et al.*, 2004). The difference in binding properties between KLC1 and KLC2 is unexpected since their TPR domains, the putative binding site for these cargoes, share ~ 87 % amino acid sequence identity (Zhu *et al.*, 2012).

As discussed in Section 1.2.3, slow transport depends on the interaction between the DnaJ-like domain in the TPRs of KLCs and Hsc70 which helps to mediate the interaction between cytoplasmic proteins and kinesin-1. The interaction between KLC1 and Hsc70 was demonstrated when both anti-KLC1 and anti-Hsc70 antibodies successfully co-immunoprecipitated the KLC1/Hsc70 complex from the sciatic nerve axons of mouse (Terada *et al.*, 2010).

### **1.3 The TRAK/Milton family of kinesin adaptor proteins**

The family of trafficking kinesin proteins (TRAKs) are kinesin adaptor proteins. The TRAK family consists of TRAK1 and TRAK2 both of which are known to bind to the cargo binding domain of conventional kinesin-1 heavy chains forming a link between the motor protein and cargo (Brickley *et al.*, 2005; Smith *et al.*, 2006; Brickley and Stephenson, 2011). Human TRAK1 is 953 amino acids in length and has a calculated molecular weight of 105 kDa (Iyer *et al.*, 2003; Brickley *et al.*, 2005). TRAK1 is thought to possibly exist as several isoforms, including TRAK1 isoforms 1-5 (isoform 1 being full length TRAK1). However, the abundance as well as the tissue specificity of isoforms 2-5 is as yet unknown. Alternatively, the mouse TRAK1 is a predicted 939 amino acids in length and is known to exist as a second isoform, TRAK1 *hyrt*, which has a truncated C-terminal domain due to missing the final 16<sup>th</sup> exon resulting in TRAK1 1-824 (Gilbert *et*

*al.*, 2005). TRAK2 is 913 amino acids in length and has a calculated molecular weight of 102 kDa and is known to exist as three main isoforms, TRAK2-1a, TRAK2-1b and TRAK2-1c (Table 1.3). The entire TRAK2 gene contains 16 exons in total, with TRAK2-1b missing exons 15 and 16, and TRAK2-1c missing exon 15. The three TRAK2 isoforms are summarised in Table 1.3. TRAK1 is expressed in both excitable and non-excitable tissues (Iyer *et al.*, 2003), whereas TRAK2 has been reported to only be expressed in excitable tissue (Beck *et al.*, 2002). It is also thought that TRAK2 may exist as at least a dimer (Beck, M., Ojla, G., Stephenson, F.A., unpublished observations). However, it is currently unknown if the members of the TRAK/Milton family can hetero dimerise with one another.

TRAK isoform	Amino acid length	Missing TRAK domain	Tissue distribution	Reference
TRAK1 (Mouse)	939	-	Liver, kidney and CNS (including the cortex, hippocampus, thalamus, forebrain and midbrain)	Gilbert <i>et al.</i> , 2005
TRAK1 <i>hyrt</i> (Mouse)	824	824-939	Liver, kidney and CNS (including the cortex, hippocampus, thalamus, forebrain and midbrain)	Gilbert <i>et al.</i> , 2005
TRAK2-1a (Rat)	913	-	Cerebellum, forebrain, heart, skeletal muscle and testes	Beck <i>et al.</i> , 2002
TRAK2-1b (Rat)	672	673-913	Forebrain, heart and skeletal muscle	Beck <i>et al.</i> , 2002
TRAK2-1c (Rat)	848	620-688	Brain, heart, lung and smooth muscle tissue	Iyer <i>et al.</i> , 2003

**Table 1.3 The studied splice variants of TRAK1 and TRAK2.**

This table includes their amino acid length and distribution within tissue types.

Originally named GRIF-1 (gamma-aminobutyric acid type A (GABA<sub>A</sub>) receptor interacting factor-1), TRAK2 was initially discovered after a yeast two-hybrid screen of a rat brain complementary deoxyribonucleic acid (cDNA) library was used to search for proteins interacting with the intracellular loop of the GABA<sub>A</sub> receptor  $\beta$ 2 subunit. This interaction was confirmed using co-immunoprecipitation assays after co-transfection

of TRAK2 and GABA<sub>A</sub>  $\beta$ 2 constructs in HEK 293 cells (Beck *et al.*, 2002). Originally named OIP106 (O-linked N-acetylglucosamine (O-GlcNAc) transferase (OGT) interacting protein of 106 kDa), TRAK1 was initially shown to interact with OGT via a yeast two-hybrid screen (Beck *et al.*, 2002; Iyer *et al.*, 2003). Both TRAK1 and TRAK2 share an overall 60 % amino acid similarity with one another but share a 76 % amino acid similarity within their coiled-coil domains (Iyer *et al.*, 2003). Hence, both TRAK1 and TRAK2 were proposed to belong to the same family of coiled-coil proteins. Other proteins known to share sequence homology with the TRAK protein family are Milton and HAP1. TRAK2 shares a 47 % amino acid similarity with Milton, a *Drosophila* protein. It is thought that Milton is the species homologue to both TRAK1 and TRAK2 (Stowers *et al.*, 2002). HAP1 shares a 56 % amino acid similarity when compared to the coiled-coil region of TRAK2. HAP-1 is known to interact with both the KLC of kinesin-1 and with dynactin/p150<sup>Glued</sup>, a protein known to associate with dynein (Engelender *et al.*, 1997; McGuire *et al.*, 2006; Section 1.2.4.1). HAP1 is also known to transport brain-derived neurotrophic factor (BDNF) (Wu *et al.*, 2010). Hence, it is possible that HAP1 may also be a member of the TRAK adaptor protein family.

Previous experiments to identify the binding domain of kinesin-1 to the TRAK family of adaptor proteins utilised KIF5C as the model system. Initially KIF5C was divided into two main regions. These regions were amino acids 1-335 and 336-957. KIF5C 1-335 corresponded to the motor domain and KIF5C 336-957 included the non-motor domain. KIF5C 336-957 was shown using yeast two-hybrid interaction assays, co-immunoprecipitation experiments and FRET studies to interact with TRAK2. Whereas yeast two-hybrid interaction assays and co-immunoprecipitation experiments using KIF5C 1-335 showed no interaction with TRAK2 (Smith *et al.*, 2006). FRET experiments utilising TRAK1 have also concluded that the non-motor domain of KIF5C is responsible for correct interaction (Brickley *et al.*, 2011). Further work divided the KIF5C non-motor domain into three regions; these were amino acids 336-542, 593-804 and 827-957. Again using yeast two-hybrid interaction assays and co-immunoprecipitation experiments it was shown that amino acids 827-957 of KIF5C interact with TRAK2 while 336-542 and 593-804 do not. Conversely the amino acids 124-283 of TRAK2 but not TRAK1 were found to associate with the cargo binding domain of KIF5C, amino acids 827-957 (Brickley *et al.*, 2005).

Work carried out by Smith *et al.* (2006) has demonstrated that there is no association between TRAK2 and KLC. This was shown using both yeast two-hybrid assays and co-immunoprecipitation of KLC and TRAK2 in mammalian cell lines. Experiments carried out by Glater *et al.* (2006) have demonstrated that the binding of Milton to kinesin-1 is also KLC independent. This was shown after a rat KLC1 clone was transfected into COS-7 cells (kidney cells of the African Green Monkey) both alone and in combination with KHC and Milton. In the absence of KLC, KHC is found co-localised to mitochondria. However, when Milton, KHC, and KLC were co-expressed, KLC was cytoplasmic and not located on the mitochondria. Therefore, KLC expression appeared to inhibit the recruitment of KHC to the mitochondria by Milton. Work in the same study also showed that via co-immunoprecipitation techniques KLC can in fact inhibit the binding of Milton to KHC. In *Drosophila* homogenates KLC was also not detected in co-immunoprecipitations of the Milton/KHC complex. (Glater *et al.*, 2006).

### **1.3.1 Mitochondria as a cargo for the TRAK/Milton adaptor protein family**

As previously mentioned in Section 1.3 both TRAK1 and TRAK2 are responsible for acting as kinesin adaptor proteins helping to mediate the interaction between the cargo to be transported and the KHC of kinesin-1. The most well established cargo known to be transported by that of the TRAK/Milton family are mitochondria. Miro1 and Miro2 are atypical Rho GTPases present on the outer membrane of mitochondria. Both Miro1 and Miro2 are known to bind the TRAK/Milton protein family acting as the receptor for mitochondrial trafficking (Fransson *et al.*, 2006; MacAskill *et al.*, 2009a; Wang and Schwarz, 2009). Both TRAK1 and TRAK2 have been shown to co-localise with mitochondria after co-expression in HEK 293 and COS-7 cells (Brickley *et al.*, 2005; Smith *et al.*, 2006). The co-expression of either TRAK1 or TRAK2 with KHC results in the localisation of mitochondria to the ends of cellular processes (Smith *et al.*, 2006). Both co-localisation studies and co-immunoprecipitation experiments have demonstrated the ability of either TRAK1 or TRAK2 to associate with both Miro1 and Miro2 (Fransson *et al.*, 2006; MacAskill *et al.*, 2009). The over-expression of Miro1 in cultures of hippocampal neuronal cells also showed an increased distribution of mitochondria at the ends of axonal processes as well as resulting in an increase in moving mitochondria in dendrites (MacAskill *et al.*, 2009a; MacAskill *et al.*, 2009). Inhibition of both TRAK1 and TRAK2 in primary neuronal cultures from the hippocampus of rats utilising both

short hairpin ribonucleic acid interference (shRNAi) and dominant negative gene silencing resulted in a decrease in axonal mitochondrial mobility (Brickley and Stephenson, 2011). The same study also highlighted differences between TRAK1 and TRAK2 regarding their individual contribution towards mitochondrial transport. Both the transfection of green fluorescent protein (GFP)-TRAK1 and GFP-TRAK2 were shown to rescue mitochondrial transport after TRAK1 shRNAi caused a decrease in mitochondrial mobility (Brickley and Stephenson, 2011). This work indicates a distinct mechanism for the transport of mitochondria in axons and the differing roles TRAK1 and TRAK2 may play. The theory of differing methods of mitochondrial transport was further highlighted when Macaskill *et al.* (2009a) demonstrated the ability of Miro to associate directly with all three kinesin-1 sub-types KIF5A, KIF5B and KIF5C using *in vitro* pulldown assays, implying that direct transport of mitochondria may occur. A schematic representation of the TRAK/kinesin-1/Miro complex is shown in Figure 1.7.

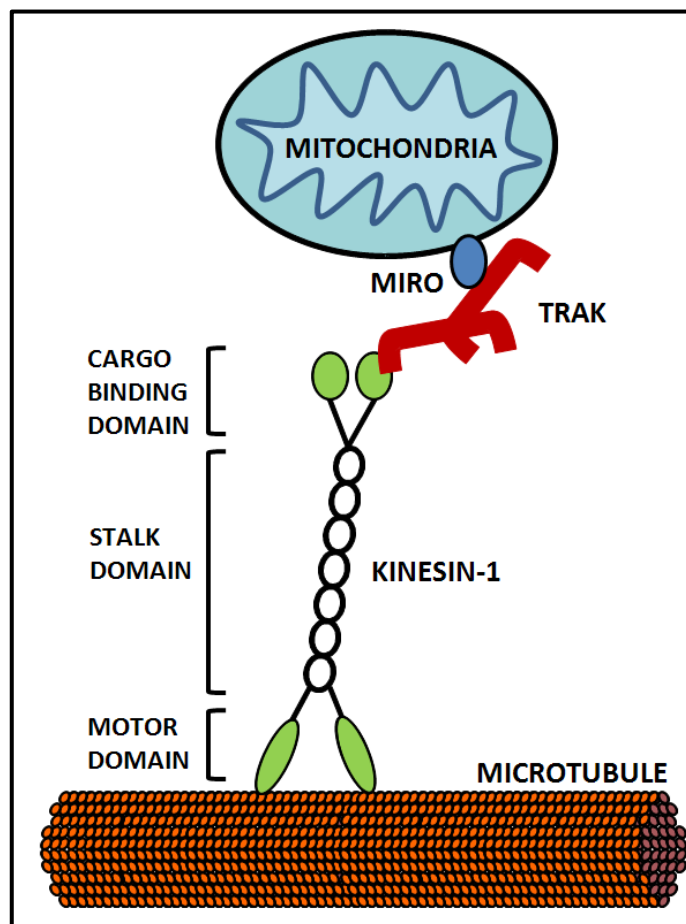


**Figure 1.7 A schematic representation of the TRAK/kinesin-1/Miro complex.**  
The KHC is shown in green, TRAK in red and Miro in blue. Figure adapted from Brickley *et al.* (2005).

Work by Misko *et al.* (2010) has also indicated other proteins, mitofusin 1 (Mfn1) and mitofusin 2 (Mfn2), that interact with the TRAKs and thus may be involved in the mitochondrial trafficking complex. Mfn1 and Mfn2 are dynamin family GTPases which are known to form a complex to tether mitochondrial membranes together and in turn help to facilitate mitochondrial fusion (Santel and Fuller, 2001). Co-immunoprecipitation experiments on exogenously expressed Mfn1 and Mfn2 in HEK 293 cells have demonstrated that Mfn2 and Mfn1 are both capable of interacting with Miro1, Miro2, TRAK1 or TRAK2 (Misko *et al.*, 2010). The same study also showed that neither Mfn1 nor Mfn2 can interact with KIF5C or KLC in co-immunoprecipitation experiments indicating that Mfn1 and Mfn2 are not involved in directly associating with kinesin-1. However the knockdown of Mfn2 in cultured rat dorsal root ganglion neurons produced mitochondrial transport deficits identical to the loss of Miro2, which includes increased pause time and slower movement velocities of mitochondria in both anterograde and retrograde directions. The work regarding the involvement of Mfn1 and Mfn2 in the mitochondrial trafficking complex is only preliminary but indicates that both Mfn2 and Miro2 proteins may be present to help mediate axonal mitochondrial transport (Misko *et al.*, 2010).

### **1.3.2 Proteins interacting with the TRAK/Milton family of kinesin adaptors**

As discussed in Section 1.3.1 the TRAK/Milton family of kinesin adaptors are responsible for binding to and transporting mitochondria. However, the TRAK/Milton family has also been shown to traffic a number of different cargoes. A summary of the known TRAK1, TRAK2 and Milton interacting proteins are shown in Table 1.4.

Name of protein interactor	Region of TRAK1, TRAK2 or Milton where it is known to interact	Methods used to ascertain this interaction	References
<b>Miro1</b> (476-750) <b>Miro2</b> (mitochondrial membrane proteins)	TRAK1 TRAK2	Transfected HEK 293 cells, co-immunoprecipitation assays	Fransson <i>et al.</i> , 2006
<b>KIF5A</b>	TRAK1 TRAK2 Milton	Transfected HEK 293 cells, co-immunoprecipitation assays	Brickley <i>et al.</i> , 2005
<b>KIF5B</b>	TRAK1 TRAK2 Milton	Transfected HEK 293 cells, co-immunoprecipitation assays	Brickley <i>et al.</i> , 2005
<b>KIF5C</b> (827-957)	TRAK1 TRAK2 (124-293) Milton	Transfected HEK 293 cells, co-immunoprecipitation assays	Brickley <i>et al.</i> , 2005
<b>Kir2.1</b> (180-428) (K <sup>+</sup> channel)	TRAK2 (1-497)	Yeast two-hybrid screen, co-immunoprecipitation assays	Grishin <i>et al.</i> , 2006
<b>GABA<sub>α</sub> receptor β2 subunit</b>	TRAK2 (124-293)	Yeast two-hybrid screen and co-immunoprecipitation assays	Beck <i>et al.</i> , 2002
<b>GABA<sub>α</sub> receptor α1 subunit</b>	TRAK1	Co-localisation studies and <i>in vivo</i> co-immunoprecipitation assays	Gilbert <i>et al.</i> , 2005
<b>OGT</b>	TRAK1 (639-859) TRAK2 (622-846)	Yeast two-hybrid screen, co-immunoprecipitation assays and co-localisation studies.	Iyer <i>et al.</i> , 2003; Brickley <i>et al.</i> , 2011.
<b>Hrs</b> (Hepatocyte growth factor-regulated tyrosine kinase substrate)	TRAK1 TRAK2 (359-507)	Yeast two-hybrid screen, co-immunoprecipitation and <i>in vitro</i> binding assays	Kirk <i>et al.</i> , 2006; Webber <i>et al.</i> , 2008
<b>Mfn1 and Mfn2</b> (mitochondrial membrane proteins)	TRAK1 TRAK2	Co-immunoprecipitation assays in HEK 293 cells	Misko <i>et al.</i> , 2010
<b>Pink1</b>	Milton	Co-immunoprecipitation assays in HEK 293 cells analysed via mass spectrometry	Weihofen <i>et al.</i> , 2009

**Table 1.4 A summary of the TRAK/Milton protein interactors.**

The table demonstrates the methods to ascertain the interactions and the amino acid regions responsible.

As discussed previously in Section 1.3 another protein that is known to interact with the TRAK family is OGT (Iyer *et al.*, 2003). OGT is a post-translational modification enzyme known to catalyse the addition and removal of N-acetylglucosamine (O-GlyNAc) moieties to the serine and threonine amino acid residues of nuclear and cytoplasmic proteins (Hart and Akimoto, 2009). This addition or removal of O-GlycNAc is a dynamic modification and can occur at a rapid rate. The formation of stable TRAK1 and TRAK2 complexes with OGT has been demonstrated *in vitro* and *in vivo* (Iyer *et al.*, 2003; Smith *et al.*, 2004; Brickley *et al.*, 2011). Further work by Brickley *et al.* (2011) showed that OGT co-associates with TRAK2/KIF5C after co-expression in HEK 293 cells. Co-immunoprecipitations of KIF5A from rat brain extract also demonstrated the presence of either TRAK1 or TRAK2 and OGT. Co-expression of OGT with either of the TRAK family members in COS-7 cells resulted in the co-localisation of protein with aggregated mitochondria as opposed to a diffuse cytosolic distribution of the TRAKs when expressed alone. The same study by Brickley *et al.* (2011) illustrated that S562 was O-glycosylated in TRAK2. The exact involvement of OGT in the TRAK/kinesin/mitochondrial trafficking complex is currently unclear, although it is possible to speculate that due to its role as a post-translational modification enzyme that OGT may be involved in the regulation of mitochondrial trafficking (Brickley *et al.*, 2011).

As discussed in Section 1.3, TRAK2 was discovered by virtue of its interaction with GABA<sub>A</sub> receptor  $\beta$ 2 subunit in a yeast two-hybrid screen (Beck *et al.*, 2002). The interaction of TRAK1 with GABA<sub>A</sub> receptor  $\alpha$ 1 subunit has also been demonstrated. Co-staining of both TRAK1 and GABA<sub>A</sub> receptor  $\alpha$ 1 using specific antibodies in mouse and spinal cord slices demonstrated positive co-immunofluorescence. Furthermore, when TRAK1 was immunoprecipitated from the detergent solubilised extracts of mouse brainstem and spinal cord samples using a specific TRAK1 antibody, GABA<sub>A</sub> receptor  $\alpha$ 1 was shown to successfully co-immunoprecipitate (Gilbert *et al.*, 2005). This evidence in conjunction with further work by Gilbert *et al.* (2005) demonstrating that a mutated TRAK1 protein lacking the C-terminal domain, found in *hyrt* mice, can also co-immunoprecipitate with GABA<sub>A</sub> receptor  $\alpha$ 1 indicates that TRAK1 1-824 is necessary for the interaction with GABA<sub>A</sub> receptor  $\alpha$ 1.

Yeast two-hybrid screens using the rat brain hippocampal/cortical cDNA library and utilising rat Hrs as bait resulted in TRAK2 199-507 showing a positive interaction. This interaction was confirmed when co-immunoprecipitation experiments using the cell lysate of TRAK2 and Hrs transfected HeLa cells indicated co-immunoprecipitation of TRAK2 and Hrs after using either TRAK2 or Hrs directed antibodies. Additionally, co-immunoprecipitation of endogenous TRAK2 and Hrs in PC12 cells also indicated the existence of the TRAK2/Hrs complex. This interaction was further confirmed *in vivo* when immunofluorescence studies in PC12 cells indicated significant co-localisation of TRAK2 and Hrs in early endosomes. Mapping studies of the Hrs binding site on TRAK2, again using a co-immunoprecipitation strategy, revealed that that TRAK2 359-507 is necessary for TRAK2/Hrs interaction (Kirk *et al.*, 2006). Interestingly, similar work by Webber *et al.* (2008), this time using TRAK1 demonstrated an interaction with Hrs. Both TRAK1 and Hrs were shown to specifically co-immunoprecipitate from TRAK1 and Hrs co-transfected HeLa cell lysates, in addition to the successful co-immunoprecipitation of TRAK1/Hrs from endogenously expressed TRAK1 and Hrs in HeLa cells. This study also showed that TRAK1 359-951 is essential for the interaction of TRAK1/Hrs as demonstrated by the presence of Hrs in pull-down assays of recombinant tagged TRAK1 359-951 protein. TRAK1 359-507 and TRAK2 359-507 share a 50 % amino acid similarity and both these regions have been shown to be important for the binding of TRAK1 and TRAK2 to Hrs. This may indicate a possible shared mechanism of interaction between TRAK1 and TRAK2 in binding to Hrs (Webber *et al.*, 2008).

The interaction of TRAK2 with the K<sup>+</sup> channel, Kir2.1, was initially discovered after a yeast two-hybrid screen of a human brain cDNA library demonstrated a positive interaction with that of TRAK2 (Grishin *et al.*, 2006). The interaction of Kir2.1 and TRAK2 was further demonstrated by co-immunoprecipitation assays using the lysates of Kir2.1 and TRAK2 co-transfected HEK 293 cells. The *in vivo* association of Kir2.1 and GRIF-1 was then demonstrated by co-immunoprecipitation from brain lysate. Microscopy analysis of immunolabelled surface GFP-Kir2.1 showed that transfection of TRAK2 in COS-7 and HEK 293 cells significantly increases the number of Kir2.1 channels in the plasma membrane. Furthermore yeast two-hybrid assays showed that TRAK2 1-497 interacts specifically with Kir2.1 180-428 (Grishin *et al.*, 2006). These results

indicate that TRAK2 binds to Kir2.1 and helps to facilitate the trafficking of Kir2.1 to the cell surface of neurons.

PTEN induced putative kinase 1 (Pink1), is a gene that encodes a serine/threonine protein kinase that localises to mitochondria (Weihofen *et al.*, 2008). It is thought to be involved in the kinesin-1, Milton and Miro complex since Weihofen *et al.* (2009) showed that over-expression of Miro1, Miro2 or Milton all increase the concentration of Pink1 in mitochondrial enriched sub-cellular fractions. These findings indicate a possible role for Pink1 in the transport of mitochondria by the TRAK/Milton family (Weihofen *et al.*, 2009; Wang *et al.*, 2011). A schematic of TRAK2 and the known interacting protein domains is shown in Figure 1.8.

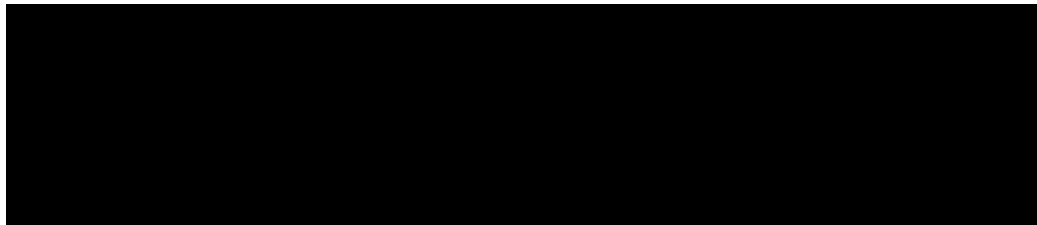


**Figure 1.8 A schematic of the full length TRAK2 protein.**

The Figure shows the predicted coiled-coil domains in black (amino acids 133-188 and 202-355) and the locations of where these known interacting proteins bind. Figure taken from the Stephenson laboratory.

#### **1.4 The regulation of kinesin-1 transport of mitochondria in neuronal cells**

The regulation of kinesin-1 cargo transport is critical in order to ensure the correct delivery of cargo, such as mitochondria, within the neuron. It is also necessary because a constantly active kinesin-1 complex would waste ATP and accumulate at the processes of axons. As explained in Section 1.2.4 the number of identified cargoes transported by kinesin-1 is increasing. However, the way in which the regulation of these cargoes occurs is not as well understood. There are several methods in which the transport of cargo by kinesin-1 may be regulated. These include the binding and release of cargo, autoinhibition, motor domain activation and the binding of the cargo binding domain to the microtubules (Verhey and Hammond, 2009).

There are two conflicting views of how kinesin-1 is thought to govern regulation of movement throughout the cell by utilising the binding relationship with its cargo. The first of which was put forward by Wang and Schwarz (2009) and uses the example of

mitochondrial transport. Miro proteins are present on the outer membrane of mitochondria and have two EF hand  $\text{Ca}^{2+}$ -binding domains. These EF hands consist of two alpha helices positioned roughly perpendicular to one another and are linked together by a short loop region that once bound to  $\text{Ca}^{2+}$  ions will undergo a conformational change (Nelson and Chazin, 1998). Wang and Schwarz (2009) demonstrate that the motor domain of kinesin-1 dissociates from the microtubule and interacts with Miro present on the outer membrane of the mitochondria in the presence of increased levels of  $\text{Ca}^{2+}$ . Endogenous mammalian KHC, Miro and Milton were successfully co-immunoprecipitated from HEK 293 cells, but in the absence of Milton, Miro was not sufficient to recruit KHC to the mitochondria in cultured neuronal cells. Transfected constructs of Miro which had been mutated to disrupt the EF hand domain saw normal distribution and transport of mitochondria in the axons of neuronal cultures which did not change with the increase in  $\text{Ca}^{2+}$ . However, movement of mitochondria using transfected non-mutated Miro constructs saw a decrease in bi-directional transport. The KHC/Milton/Miro complex was also shown to co-localise in neurons after transfection of either the wild-type or EF hand mutated Miro in conditions of both high and low  $\text{Ca}^{2+}$ , indicating that Miro remains in complex with KHC and Milton. This evidence in conjunction with further experiments from Wang and Schwarz (2009) indicating that the presence of  $\text{Ca}^{2+}$  causes the KHC to dissociate from microtubules and when a construct encoding only the motor domain of KHC was co-expressed with Miro they exhibited  $\text{Ca}^{2+}$ -dependent co-immunoprecipitation, shows that Miro might be able to interact with KHC in two ways. The first being that the tail of KHC is linked to Miro by Milton in a  $\text{Ca}^{2+}$ -independent manner and the second, that the motor domain can interact directly with Miro in the presence of  $\text{Ca}^{2+}$ . It is this conformational change in the EF hand domain of Miro via the binding of  $\text{Ca}^{2+}$  that is thought to be responsible for changing the binding properties of the motor domain such that the KHC motor domain binds to Miro instead of microtubules. This would keep the KHC/Milton/Miro trafficking complex intact while at the same time preventing transport of mitochondria as the complex is no longer bound to microtubules (Wang and Schwarz, 2009).

An alternative mechanism put forward by MacAskill *et al.* (2009a) is that mitochondria dissociate from kinesin-1 in the presence of elevating cytosolic  $\text{Ca}^{2+}$ . In the presence of

increased  $\text{Ca}^{2+}$ , GFP-Miro1 constructs expressed in neuronal cells showed almost complete inhibition of mitochondrial transport, whereas expression of the EF hand mutated Miro in the presence of increased  $\text{Ca}^{2+}$  did not affect mitochondrial transport. This concurs with the results seen in the study carried out by Wang and Schwarz (2009). In the absence of  $\text{Ca}^{2+}$  Miro1 was found to bind directly to each of the kinesin-1 sub-types, KIF5A, KIF5B and KIF5C by GST fused Miro1 pull-down assays but in the presence of  $\text{Ca}^{2+}$  the binding of Miro1 to kinesin-1 was inhibited (MacAskill *et al.*, 2009a). The binding interaction of TRAK2 and Miro1 remained intact after increasing  $\text{Ca}^{2+}$  implying that  $\text{Ca}^{2+}$  does not detach mitochondria from kinesin-1 motors by acting at the binding site between Miro1 and TRAK2 (MacAskill *et al.*, 2009a).

The way in which these two studies differ is in the proposed mechanism of kinesin-1 association with the trafficking complex, but they do both confirm the importance of  $\text{Ca}^{2+}$  as a method to pause mitochondrial trafficking in neurons. It is thought that when ATP concentrations are low,  $\text{Ca}^{2+}$  transport mechanisms are compromised and cytosolic  $\text{Ca}^{2+}$  increases. If moving mitochondria stop where  $\text{Ca}^{2+}$  is elevated they will be recruited to regions of low ATP and will remain until ATP concentrations are elevated thus decreasing levels of  $\text{Ca}^{2+}$  restarting the movement of mitochondria. This  $\text{Ca}^{2+}$  control mechanism is most likely used to help distribute mitochondria to where they are needed throughout the cell (Wang and Schwarz, 2009). The contrasting views on the method of mitochondrial regulation by kinesin-1 by both Wang and Schwarz, (2008) and MacAskill *et al.* (2009a) are summarised in Figure 1.9.

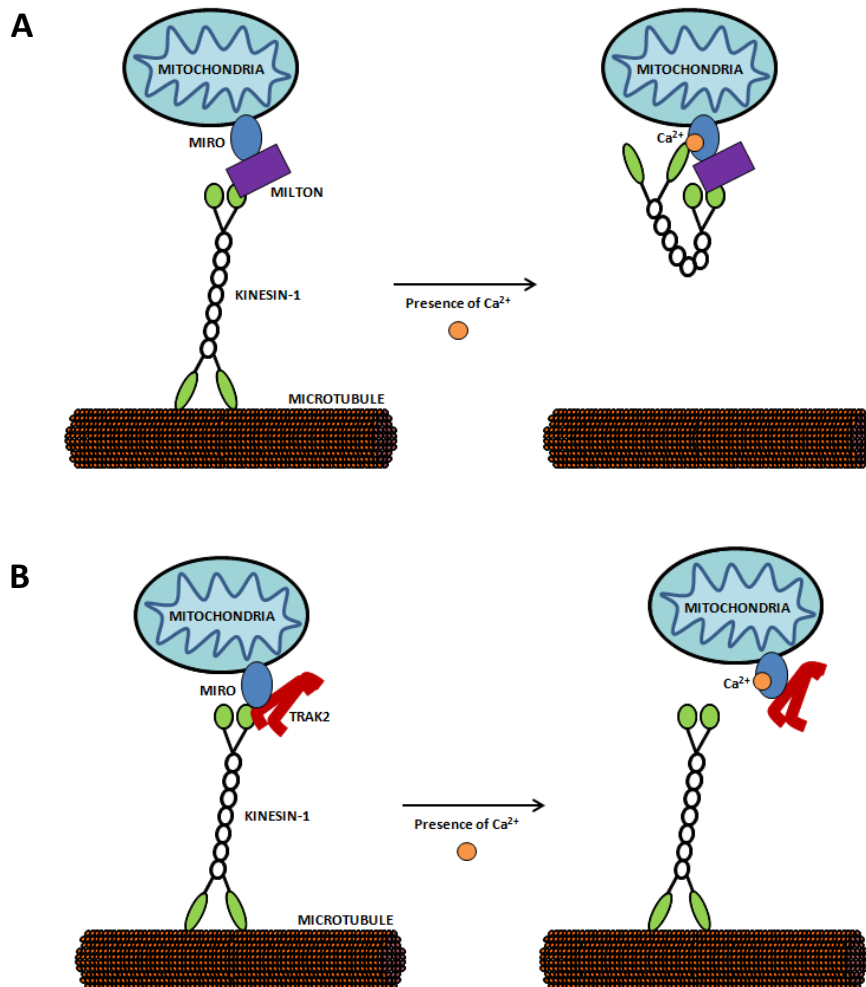


**Figure 1.9 Schematic representations of the two contrasting mechanisms on the method of mitochondrial regulation by kinesin-1.**

**A** = Schematic model of the means by which Ca<sup>2+</sup> interacts with Miro to regulate the motility of mitochondria (Wang and Schwarz, 2009). **B** = Schematic model of the means by which a rise of Ca<sup>2+</sup> dissociates Miro1 from kinesin-1 (MacAskill *et al.*, 2009a).

The regulation of mitochondrial transport by kinesin-1 could also be regulated, in part, by another mechanism. Under physiological conditions the kinesin-1 heterodimer exists in a folded compact conformation. This conformation is possible due to a conserved QIAK amino acid region present in the cargo binding domain that is known to interact with the motor and neck regions. Binding of the cargo binding domain to the tail domain of conventional *Drosophila* kinesin-1 was shown to stabilise the conformation with bound ADP and further slow the rate of ADP release from the motor domain. Only one KHC cargo binding domain molecule is required to prevent ATPase activity in the kinesin-1 dimer (Hackney *et al.*, 2009). This interaction can occur due to the flexibility of the kinesin-1 protein at the hinge regions of the stalk domain (Hackney and Stock, 2000; Hackney, 2007; Seeger and Rice, 2010). Kinesin-1 appears to

be turned off in the absence of cargo by a self-inhibition mechanism that depends on its tail and involves folding of the KHC dimer (Schnapp, 2003). Work by Friedman and Vale (1999) has demonstrated that mutating the hinge 1 domain of KIF5B leads to an inability of kinesin-1 to change to the folded conformation, resulting in a constant active state kinesin-1 protein. It is the ability of the hinge domain and its flexible properties that allows the conserved amino acid QIAK region in the cargo binding domain to come into contact with the motor domain, specifically the switch 1 domain, to prevent ADP release from the nucleotide binding pocket (Hackney and Stock, 2008; Kaan *et al.*, 2011). More recently it has also been demonstrated that amino acids 822-944 of KIF5B can interact with microtubules with a sub micromolar affinity using electrostatic forces to bind the acidic E-hook at the C-terminal end of tubulin (Seeger and Rice, 2010). Combined with the work by MacAskill *et al.* (2009a) indicating that the presence of  $\text{Ca}^{2+}$  will dissociate cargo and its adaptor protein complex from kinesin-1 entirely, this indicates that the now cargo free C-terminus of kinesin-1 may interact with the KHC dimer and/or the C-terminal end of tubulin to prevent movement along the microtubule. These steps may be in part responsible for the regulation of kinesin-1/mitochondrial movement within the cell.

The *in vivo* association of KLC to KHC of kinesin-1 has been shown to inhibit microtubule binding (Verhey *et al.*, 1998). The interaction of kinesin-1 with microtubules is inhibited when the 64 C-terminal amino acids of KHC are available for KLC binding. In deletion mutants without this C-terminal domain the association of KHCs with KLCs is not enough to prevent binding of kinesin-1 to the microtubules (Adio *et al.*, 2006). This indicates that the KLC may also be involved in the change in conformation to regulate microtubule binding of the KHC motor domain to microtubules.

### **1.5 Disease states associated with the malfunction of motor protein complexes in the CNS**

The defects of transport within dendrites and axons have been linked to a number of diseases. These diseases result from mutations in the motor protein or changes in the release/attachment of cargo to motor proteins. The possible member of the

TRAK/Milton protein family, HAP1 (Section 1.3), is known to transport huntington protein which is responsible for Huntington's disease. The huntington protein is known to be mutated in affected individuals and one of the causes of neuronal cell death is that of the resulting aggregates of the mutated huntington protein in cells (Borrell-Pages *et al.*, 2006).

The hereditary spastic paraplegias (HSP) are a group of neurodegenerative diseases generally characterised by progressive lower limb spasticity and weakness (Reid *et al.*, 2002). A wide variety of genetic mutations in over 46 different loci have been attributed to the HSP disease state (Salinas *et al.*, 2008). One such set of mutations is known as spastic gait type 10 (SPG10) and affects the KIF5A locus. Inheritance of mutations in SPG10 is known to be autosomal dominant and several missense mutations in KIF5A have been linked to the phenotypic effect seen in HSP. One mutation, N256S, is present in the motor domain of KIF5A and is thought to slow the movement of KIF5A when moving along the microtubule network (Ebbing *et al.*, 2008). Another mutant, R280S, is present also in the motor domain and is known to reduce the ability of KIF5A to bind the microtubules (Ebbing *et al.*, 2008).

Charcot–Marie–Tooth disease (CMT) has been classified into two types, CMT1 and CMT2. It is characterised by a progressive loss of touch sensation and muscle tissue across various extremities of the body. CMT is known to be caused by defective neuronal function, of which CMT1 is thought to be caused by the demyelination of Schwann cells and CMT2 by axonal degeneration (Garcia, 1999). CMT2 has been further subdivided into eight groups. CMT2A, a member of the CMT2 disease group, is linked to chromosome 1p35–p36 and mutation in the KIF1B gene present in 1p35–p36 has been reported in one family suffering from CMT2A (Zhao *et al.*, 2001). A Q98L missense mutation in the ATP binding region of the motor domain of KIF1B demonstrated a decreased ATPase activity and motility suggesting this KIF1B mutation is responsible for CMT2A neuropathy (Zhao *et al.*, 2001). CMT2A has also been linked to point mutations in Mfn2. In some cases CMT2A mutant forms of Mfn2 are unable to mediate mitochondrial fusion in fibroblasts, whereas others are completely competent to promote fusion. This is thought to be because in some cases Mfn1 can rescue the effects of defective Mfn2 (Kijima *et al.*, 2005; Detmer and Chan, 2007).

As discussed in Section 1.3.2, Pink1 is a serine/threonine protein kinase that localises to mitochondria and it is thought to be involved in the kinesin-1/Milton/Miro trafficking complex via an interaction with both Milton and Miro (Weihofen *et al.*, 2009). Recessive mutations in the Pink1 gene are known to cause a form of early-onset Parkinson's disease that is caused by selective degeneration of dopaminergic neurons in the substantia nigra (Gandhi *et al.*, 2006). Loss of Pink function can alter mitochondrial morphology and dynamics but exactly how the loss of Pink1 can influence mitochondrial function is unclear (Weihofen *et al.*, 2008; Weihofen *et al.*, 2009).

### **1.6 Aims of this thesis**

As described previously, transport of mitochondria and other protein complexes required for neuronal survival are regulated by several mechanisms. One such mechanism utilises the TRAK/Milton family of adaptor proteins to mediate the interaction of cargo to the molecular motor protein, kinesin-1. Therefore the overall aim of this thesis was to understand further the mode of association between kinesin-1 and the TRAK/Milton family of kinesin adaptor proteins. The first aim was to determine the structure of the cargo binding domain of the kinesin-1 sub-type KIF5A as well as the binding of KIF5A/TRAK2 in complex. The second aim was to refine further the TRAK1 and TRAK2 binding site within both KIF5A and KIF5C.

# **CHAPTER 2**

## **MATERIALS AND METHODS**

## 2.1 MATERIALS

The restriction enzymes with their buffers and DNA molecular weight markers were purchased from Fermentas (Yorkshire, U.K). Lennox B (LB) broth, SELECT agar powder, penicillin and streptomycin (10,000 units/ml), ProBond™ Ni<sup>2+</sup> chelating resin and SeeBlue® pre-stained standard molecular weight markers were from Invitrogen (Paisley, U.K). Isopropyl-β-D-thio-galactopyranoside (IPTG) and dithiothreitol (DTT) were purchased from Melford Laboratories (Suffolk, U.K). The Phusion™ high-fidelity DNA polymerase and restriction enzyme *FseI* was purchased from New England Biolabs (Hertfordshire, U.K). Shrimp alkaline phosphatase (SAP) was purchased from Promega (Southampton, U.K). Coomassie Brilliant Blue G-250 dye (Coomassie Blue), un-stained protein molecular weight markers and poly-prep chromatography columns were purchased from BioRad (Hemel Hempstead, U.K). S-Protein agarose was purchased from Novagen (Wisconsin, U.S.A). Imidazole was purchased from Acros Organics (Geel, Belgium). Protogel (30% [w/v] acrylamide: 0.8% [w/v] bis-acrylamide (37.5:1), ammonium persulphate and N,N,N',N'-tetramethylethylenediamine (TEMED) were purchased from National Diagnostics (Yorkshire, U.K). Glycerol, potassium chloride, sodium chloride, sodium hydroxide pellets, ethylenediaminetetraacetic acid (EDTA) and Tris(hydroxymethyl)aminomethane (Tris) were purchased from VWR International Ltd (Dorset, U.K). Protran® nitrocellulose membranes were purchased from Whatman (Kent, U.K). Protease inhibitor cocktail tablets were purchased from Roche (Basle, Switzerland). Protein A Sepharose and protein G Sepharose were purchased from Generon (Berkshire, U.K). HEK 293 cells were purchased from the European Collection of Cell Cultures (Wiltshire, U.K). Glycerol-free brain bovine tubulin was purchased from Cytoskeleton (Colorado, U.S.A). Paclitaxel was purchased from Calbiochem (Darmstadt, Germany). *BL21 DE3 codonplus Escherichia coli (E.coli)* cells were a kind donation from Dr Andy Wilderspin, UCL School of Pharmacy. 5-Amino-2,3-dihydro-1,4-phthalazinedione (luminol), D-sorbitol, ethylene glycol-bis(2-aminoethylether)-N,N,N',N'-tetraacetic acid (EGTA), sodium acetate anhydrous, sodium dodecyl sulphate (SDS), trans-4-hydroxycinnamic acid (p-coumaric acid), Tween-20®, ampicillin, ethidium bromide, β-mercaptoethanol (β-ME), GenElute™ HP maxiprep kit, bacitracin, benzamidine, phenylmethanesulfonyl fluoride, trypsin inhibitor-chicken egg white, sodium bicarbonate solution (7.5 % w/v), Dulbecco's modified Eagles medium nutrient mixture F-12 HAM, Hanks balanced salt solution, foetal bovine serum, 4-(2-

hydroxyethyl)piperazine-1-ethanesulphonic acid (HEPES), dimethyl sulphoxide (DMSO), Triton X-100®, protein molecular weight standards for size exclusion chromatography, oligonucleotide primers used for sequencing of recombinant DNA and oligonucleotide primers used for polymerase chain reactions (PCR) were purchased from Sigma-Aldrich (Poole, U.K). A summary of the oligonucleotide primers used for the bacterial expression of TRAK2 and KIF5A is shown in Table 2.1. A summary of the oligonucleotide primers used for the mammalian expression of KIF5A and KIF5C is shown in Table 2.2. All plasmid constructs generated were sent to either MWG-Biotech (Ebersberg, Germany) or UCL DNA Sequencing Service for nucleotide sequencing. A summary of the oligonucleotide primers used for nucleotide sequencing is shown in Table 2.3.

Oligonucleotide primer	Nucleotide sequence
pETDUETTRAK2 <sub>100-380</sub> Forward (Fwd) primer	5' AAAAGAATTCAGACAGAGTAG 3'
pETDUETTRAK2 <sub>100-380</sub> Reverse (Rev) primer	5' AAAAAAGCTTCTACCCTTCAAT 3'
pETDUETKIF5A <sub>800-1032</sub> Fwd primer	5' AAAACAATTGGCTGTTTCGTTCAA 3'
pETDUETKIF5A <sub>800-1032</sub> Rev primer	5' AAAAGGCCGCGCGCTGGCTGC 3'
pET151D-TOPOKIF5A <sub>800-1032</sub> Fwd primer	5' CACCCTGTTTCGTTCAAGACGTC 3'
pET151D-TOPOKIF5A <sub>800-1032</sub> Rev primer	5' CTAGTTCTCTGTCGTCGGTCG 3'
pETDUETKIF5A <sub>800-951</sub> Fwd primer	5' AAAAGGATCCGCTGTTTCGTTCAAGACGTC 3'
pETDUETKIF5A <sub>800-951</sub> Rev primer	5' AAAAGAATTCTTAGAAGAGGCTGTTGGTGTA 3'
pETDUETKIF5A <sub>820-1032</sub> Fwd primer	5' AAAAGGATCCGAGTGGGGGATTCACTCC 3'
pETDUETKIF5A <sub>820-1032</sub> Rev primer	5' AAAAGAATTCTTAGCTGGCTGCTGTCTCTTG 3'
pETDUETKIF5A <sub>820-951</sub> Fwd primer	5' AAAAGGATCCGAGTGGGGGATTCACTCC 3'
pETDUETKIF5A <sub>820-951</sub> Rev primer	5' AAAAGAATTCTTAGAAGAGGCTGTTGGTGTA 3'

**Table 2.1 A summary of oligonucleotide primer sequences used for the generation of bacterially expressed TRAK2 and KIF5A constructs.**

Oligonucleotide primer	Nucleotide sequence
pcDNAKIF5A Fwd primer	5' AAAAGGATCCATGGCGGAGACCAACAAC 3'
pcDNAKIF5A Rev primer	5' AAAAGAATTCTTAGCTGGCTGCTGTCTC 3'
pcDNAKIF5A <sub>1-961</sub> Rev primer	5' AAAGAATTCTTAACAATTTAGGAAGCTCACAACG 3'
pcDNAKIF5A <sub>1-942</sub> Rev primer	5' AAAAGAATTCTTACTCAGGGCTCCGGGT 3'
pcDNAKIF5A <sub>1-909</sub> Rev primer	5' AAAAGAATTCTTACGAGCTCTGTAGCGAAC 3'
pcDNAKIF5A <sub>1-885</sub> Rev primer	5' AAAAGAATTCTTAGCCCTCCTTGGCCTCCTT 3'
pcDNAKIF5A <sub>1-883</sub> Rev primer	5' AAAAGAATTCTTACTTGGCCTCCTTCAG 3'
pcDNAKIF5A <sub>1-881</sub> Rev primer	5' AAAAGAATTCTTACTCCTTCAGTGCACCCTC 3'
pcDNAKIF5A <sub>1-879</sub> Rev primer	5' AAAAGAATTCTTACAGTGCACCCTCCAGGGCCTT 3'
pcDNAKIF5A <sub>1-877</sub> Rev primer	5' AAAAGAATTCTTAACCCTCCAGGGCCTTAAC 3'
pcDNAKIF5A <sub>1-861</sub> Rev primer	5' AAAAGAATTCTTACAATTTAGGAAGCTCACAACG 3'
pcDNAKIF5A <sub>1-825</sub> Rev primer	5' AAAAGAATTCTTAGGAGTGAATCCCCCACT 3'
pcDNAKIF5A <sub>Δ877-883</sub> Primer 2	5' GTTAAGGCCCTGGAGGGTGAGGGCGCCATGAAGGAC 3'
pcDNAKIF5A <sub>Δ877-883</sub> Primer 3	5' GTCCTTCATGGCGCCCTCACCTCCAGGGCCTTAAC 3'
pcDNAKIF5C Fwd primer	5' AAAAGAATTCATGGCGGATCCAGCCGAA 3'
pcDNAKIF5C Rev primer	5' AAAAGCGGCCGCTTATTATTTCTGGTAGTGAGT 3'
pcDNAKIF5C <sub>1-889</sub> Rev primer	5' GCGGCCGCTTAGTTCTCCTTGGCCTCCTT 3'
pcDNAKIF5C <sub>1-881</sub> Rev primer	5' AAAAGCGGCCGCTTAGCTCTCCAGAGCCTTGAC 3'
pcDNAKIF5C <sub>1-828</sub> Rev primer	5' AAAAGCGGCCGCTTAAGCACTGCCCCCTCCATCAT 3'

**Table 2.2** A summary of oligonucleotide primer sequences used for the generation of mammalian expressed KIF5A and KIF5C constructs.

Oligonucleotide sequencing primer	Nucleotide sequence
pETDUET1 multiple cloning site 1 (MCS1) Fwd sequencing primer	5' ATGCGTCCGGCGTAGA 3'
pETDUET1 MCS1 Rev sequencing primer	5' GATTATGCGGCCGTGTACAA 3'
pETDUET1 MCS2 Fwd sequencing primer	5' TTGTACACGGCCGCATAATC 3'
pETDUET1 MCS2 Rev sequencing primer	5' GCTAGTTATTGCTCAGCGG 3'
pET151D-TOPO Fwd sequencing primer	5' TAATACGACTCACTATAGGGAGA 3'
pET151D-TOPO Rev sequencing primer	5' TATGCTAGTTATTGCTCAG 3'
pcDNAHisMaxC Fwd sequencing primer	5' TAATACGACTCACTATAGGG 3'
pcDNAHisMaxC Rev sequencing primer	5' TAGAAGGCACAGTCGAGG 3'

**Table 2.3** A summary of the oligonucleotide primers used for nucleotide sequencing.

### 2.1.1 Recombinant clones

The pETDUET1 and pET151D-TOPO vectors were a kind donation from Dr Carolyn Moores (Birkbeck College, London, U.K). The human clone of pBSKIF5A was purchased from Addgene (Massachusetts, U.S.A). The clones of rat pCISTRK2, rat pCMVTag4aTRAK2 and human pCMVmycTRAK1 were obtained from Dr Kieran Brickley, UCL School of Pharmacy.

### 2.1.2 Antibodies

Horseshradish peroxidase (HRP) linked anti-rabbit immunoglobulin (Ig) antibodies (Ab) and HRP linked anti-mouse Ig antibodies were purchased from GE Healthcare (Amersham, U.K). All the primary antibodies used are summarised in Table 2.4.

Antibody name	Host species	Antigen	Origin
TRAK2 <sub>8-633</sub>	Rabbit polyclonal	TRAK2 <sub>8-633</sub> (His-tagged)	In house (Beck et al., 2002)
S-protein tagged (S-tag)	Rabbit polyclonal	KETAAAKFERQHMS	Abcam (Cambridge, U.K)
Histidine tagged (His-tag)	Polyclonal	HHHHHH	Abcam (Cambridge, U.K)
His-tag (conjugated HRP)	Rabbit polyclonal	HHHHHH	Sigma-Aldrich (Poole, U.K)
Flag-tag	Rabbit polyclonal	DYKDDDDK	In house (Beck et al., 2002)
C-Myc	Mouse monoclonal	EQKLISEEDL	Thermo Fisher Scientific (Massachusetts, U.S.A)
Non-specific polyclonal	Rabbit	N/A	In house
Non-specific monoclonal	Mouse	N/A	Sigma-Aldrich (Poole, U.K)

**Table 2.4** A summary of the primary antibodies used for immunoblotting and immunoprecipitation experiments.

Protein name	Species	Nucleotide accession number	Protein accession number
KIF5A	Human	NM004984	NP004975
KIF5A	Rat	NM212523	NP997688
KIF5C	Human	NM004522	NP004513
KIF5C	Rat	NM001107730	NP001101200
TRAK1	Human	NM001042646	NP001036111
TRAK1	Rat	NM001134565	NP001128037
TRAK2	Human	NM015049	NP055864
TRAK2	Rat	NM133560	AAH88393

**Table 2.5** A summary of accession numbers of KIF5A, KIF5C and the TRAK family of proteins.

## **2.2 METHODS**

### **2.2.1 Bacterial methods**

#### **2.2.1.1 Preparation of chemically competent bacterial cells (*DH5α* or *BL21 DE3* codonplus)**

*DH5α* or *BL21 DE3* codonplus (*BL21*) *E.coli* cells were streaked from glycerol stocks onto a LB 2 % (w/v) agar plate using a sterile pipette tip. The plate was inverted and incubated for 12 - 16 h at 37°C. A 5 ml LB media pre-culture was inoculated using a single colony of cells. The culture was incubated at 37°C for 12 - 16 h at 250 rpm. A pre-culture, 0.5 ml, was added to LB media supplemented with 0.5 ml 1 M MgSO<sub>4</sub> and 0.5 ml 20% (w/v) glucose, (1 ml of this supplemented LB media was removed to serve as a re-suspension buffer). The cells were incubated at 37°C at 250 rpm until an OD<sub>λ = 600 nm</sub> of 0.6 - 0.7 was obtained (~ 2 h). The culture was removed and aliquoted into 50 ml sterile centrifuge tubes and left on ice for ~ 10 min. Cultures were then centrifuged at 4,000 x g for 10 min at 4°C. The supernatant was carefully aspirated and each pellet was re-suspended in 0.5 ml supplemented LB media (as above). Storage buffer (3.6 g polyethylene glycol [PEG], 360 μl MgSO<sub>4</sub>, 10.8 ml glycerol, made up to 30 ml with LB media and filter sterilised), 5 ml, was added. The cells were rapidly divided into 100 μl aliquots on ice and stored at -80°C until use. The competent cells were used within 6 months.

#### **2.2.1.2 Transformation of chemically competent bacterial cells**

For all routine plasmid DNA amplification and molecular cloning, *DH5α E.coli* chemically competent cells were used. Aliquots of *DH5α E.coli* chemically competent cells were removed from storage at -80°C and put immediately onto ice and subsequently defrosted for ~ 5 min. The plasmid to be transformed (~ 1 μg) was added to the cells and incubated for 30 min on ice, followed by a heat shock for 55 sec at 42°C. The cells were further incubated on ice for 10 min. The 100 μl of chemically competent cells was added to 900 μl LB media solution in a 1.5 ml sterile micro-centrifuge tube. The cells were incubated at 37°C for 1 h at 250 rpm and pelleted by centrifugation for 1 min at 16,200 x g at room temperature. The supernatant was carefully aspirated and the cell pellet gently re-suspended in 100 μl LB media solution. The cell suspension was plated onto selective LB plates, 2 % (w/v) agar (50 μg/ml

ampicillin or 50 µg/ml kanamycin, depending on the vectors antibiotic resistance), using a hockey puck spreader. The plates were inverted and incubated for 12 - 16 h at 37°C. Once colonies appeared they were selected for further study. Alternatively the plates were wrapped in Clingfilm and stored at 4°C for a maximum of one week.

### **2.2.1.3 Glycerol stocks of transformed bacterial cells**

A single colony of *E.coli* transformed with the desired plasmid was used to inoculate 5ml of LB media and grown for 12 - 16 h overnight at 37°C, 225 rpm. Culture (1 ml) was added to 0.5 ml 50 % (v/v) glycerol, thoroughly mixed by inversion and stored at -80°C until use.

## **2.2.2 Molecular cloning methods**

### **2.2.2.1 Bacterial clone design**

Expression of TRAK2 and KIF5A recombinant proteins in bacterial expression systems were cloned with the use of several bacterial expression vectors. Double expression of both TRAK2<sub>100-380</sub> and KIF5A<sub>800-1032</sub> was carried out using the bicistronic vector, pETDUET1. pETDUET1 contains two multiple cloning sites allowing for simultaneous expression in bacterial systems under the same promoter in different regions and requires 50 µg/ml ampicillin for selective growth. TRAK2<sub>100-380</sub> was inserted in-frame using the two restriction enzymes *EcoRI* and *HindIII* to facilitate directional cloning into MCS1 of pETDUET1. KIF5A<sub>800-1032</sub> was inserted in-frame using the two restriction enzymes *FseI* and *MunI* to facilitate directional cloning into MCS2 of pETDUET1. This yielded three recombinant clones; pETDUETTRAK2<sub>100-380</sub>, pETDUETKIF5A<sub>800-1032</sub> and pETDUETTRAK2<sub>100-380</sub>/KIF5A<sub>800-1032</sub>. The bacterial expression vector pETDUET1 was also used to singly express different recombinant KIF5A truncations. DNA encoding KIF5A truncations were inserted in-frame using the restriction enzymes *EcoRI* and *BamHI* to facilitate directional cloning into MCS1 to yield pETDUETKIF5A<sub>800-951</sub>, pETDUETKIF5A<sub>820-1032</sub> and pETDUETKIF5A<sub>820-951</sub>. KIF5A<sub>800-1032</sub> was cloned into the bacterial expression vector pET151D-TOPO using blunt ended PCR products to facilitate directional cloning. pET151D-TOPO requires 50 µg/ml ampicillin for selective growth. The bacterial expression constructs generated and used are summarised in Table 2.6.

Cloning vector	Description	Size (kb)
pETDUETTRAK2 <sub>100-380</sub>	Bicistronic bacterial expression vector. N-terminal His-tag. Ampicillin resistance.	6.3
pETDUETKIF5A <sub>800-1032</sub>	Bicistronic bacterial expression vector. C-terminal S-tag. Ampicillin resistance.	6.1
pETDUETTRAK2 <sub>100-380</sub> /KIF5A <sub>800-1032</sub>	Bicistronic bacterial expression vector. N-terminal His-tag on TRAK2 <sub>100-380</sub> and C-terminal S-tag on KIF5A <sub>800-1032</sub> . Ampicillin resistance.	7.0
pET151D-TOPOKIF5A <sub>800-1032</sub>	Bacterial expression vector. C-terminal His-tag. Ampicillin resistance.	6.4
pETDUETKIF5A <sub>800-951</sub>	Bacterial expression vector. C-terminal His-tag. Ampicillin resistance.	5.9
pETDUETKIF5A <sub>820-1032</sub>	Bacterial expression vector. C-terminal His-tag. Ampicillin resistance.	6.1
pETDUETKIF5A <sub>820-951</sub>	Bacterial expression vector. C-terminal His-tag. Ampicillin resistance.	5.8

**Table 2.6 A summary of the bacterial expression constructs generated and used for the expression of recombinant TRAK2 and KIF5A.**

### 2.2.2.2 Mammalian clone design

The expression of recombinant KIF5A and KIF5C truncations in mammalian expression systems were cloned with the use of the pcDNAHisMaxC (pcDNA) vector. pcDNA requires 50 µg/ml ampicillin for selective growth. DNA encoding KIF5A was inserted in-frame using the two restriction enzymes *EcoRI* and *BamHI* to facilitate directional cloning. KIF5C was inserted in-frame using the two restriction enzymes *EcoRI* and *NotI* to facilitate directional cloning. All of the KIF5A, KIF5C, TRAK1 and TRAK2 recombinant clones used are summarised in Table 2.7.

Cloning vector	Description	Size (kb)
pcDNAKIF5A	Mammalian expression vector. C-terminal His-tag. Ampicillin resistance.	8.4
pcDNAKIF5A <sub>1-961</sub>	Mammalian expression vector. C-terminal His-tag. Ampicillin resistance.	8.2
pcDNAKIF5A <sub>1-942</sub>	Mammalian expression vector. C-terminal His-tag. Ampicillin resistance.	8.1
pcDNAKIF5A <sub>1-909</sub>	Mammalian expression vector. C-terminal His-tag. Ampicillin resistance.	8.0
pcDNAKIF5A <sub>1-885</sub>	Mammalian expression vector. C-terminal His-tag. Ampicillin resistance.	8.0
pcDNAKIF5A <sub>1-883</sub>	Mammalian expression vector. C-terminal His-tag. Ampicillin resistance.	8.0
pcDNAKIF5A <sub>1-881</sub>	Mammalian expression vector. C-terminal His-tag. Ampicillin resistance.	7.9
pcDNAKIF5A <sub>1-879</sub>	Mammalian expression vector. C-terminal His-tag. Ampicillin resistance.	7.9
pcDNAKIF5A <sub>1-877</sub>	Mammalian expression vector. C-terminal His-tag. Ampicillin resistance.	7.9
pcDNAKIF5A <sub>1-861</sub>	Mammalian expression vector. C-terminal His-tag. Ampicillin resistance.	7.9
pcDNAKIF5A <sub>1-825</sub>	Mammalian expression vector. C-terminal His-tag. Ampicillin resistance.	7.8
pcDNAKIF5A <sub>Δ877-883</sub>	Mammalian expression vector. C-terminal His-tag. Ampicillin resistance.	8.4
pcDNAKIF5C	Mammalian expression vector. C-terminal His-tag. Ampicillin resistance.	8.2
pcDNAKIF5C <sub>1-889</sub>	Mammalian expression vector. C-terminal His-tag. Ampicillin resistance.	8.0
pcDNAKIF5C <sub>1-881</sub>	Mammalian expression vector. C-terminal His-tag. Ampicillin resistance.	7.9
pcDNAKIF5C <sub>1-828</sub>	Mammalian expression vector. C-terminal His-tag. Ampicillin resistance.	7.8
pCMVTag4aTRAK2	Mammalian expression vector. C-terminal Flag-tag. Kanamycin resistance.	7.0
pCMVmycTRAK1	Mammalian expression vector. N-terminal C-myc tag. Kanamycin resistance.	7.7

**Table 2.7** A summary of the mammalian expression constructs generated and used for the expression of recombinant KIF5A, KIF5C, TRAK1 and TRAK2.

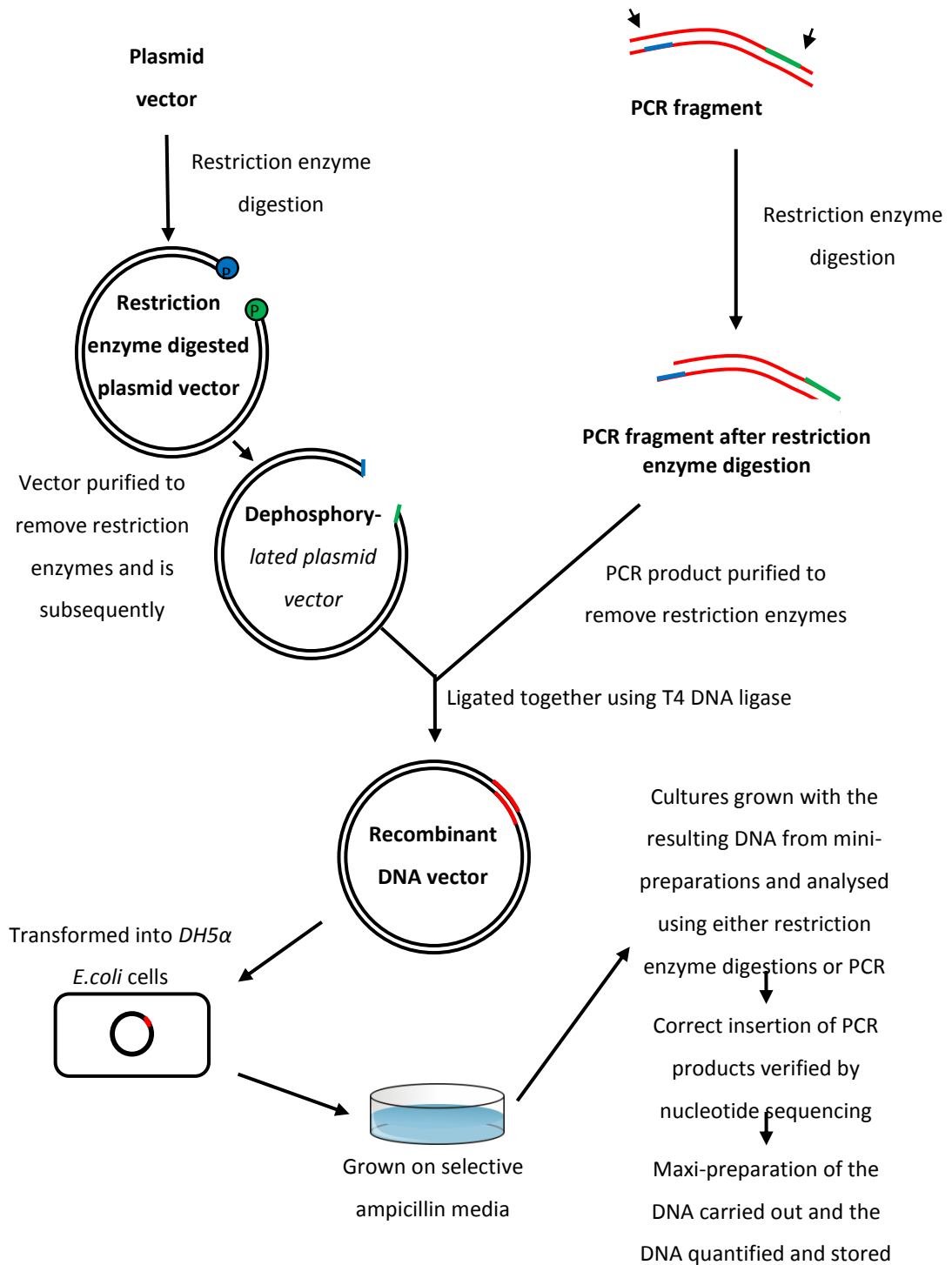


**Figure 2.1 A summary of the overall cloning strategy.**

This diagram shows all the steps necessary to successfully create a recombinant DNA vector from separate PCR fragments and a plasmid vector.

### 2.2.2.3 Design of polymerase chain reaction (PCR) and nucleotide sequencing oligonucleotide primers

The following criteria were followed when designing oligonucleotide primers for PCR amplification of DNA sequences:

- The primer must be at least 18 nucleotide bases in length.
- The optimal melting temperature of an oligonucleotide primer was in the range of 50°C - 60°C. The melting temperatures of oligonucleotide primers were calculated using the Wallace *et al.* (1979) rule:  
Melting Temperature (T<sub>m</sub>) = (4[G + C] + 2[A + T])  
[G + C] = number of guanine + cytosine bases and [A + T] = number of adenine + thymine bases.
- The melting temperature for a pair of primers must be within 10°C of each other.
- The guanine/cytosine (G/C) content should be between 40 - 60 %.
- Repeats of the same base were avoided and care was taken to ensure that the primers did not have any complementary sequence, either within the oligonucleotide or within the other primer in the pair.
- To facilitate the cloning of PCR products into cloning vectors, restriction endonuclease sites were added to the 5' end of each primer. To assist with the binding of the restriction endonuclease to the PCR product additional bases, usually AAAA, were included at the 5' end of each primer.

#### 2.2.2.3.1 PCR cycles

For the PCR amplification of DNA sequences the following reaction was mixed in a 0.5 ml sterile PCR tube; 23 µl sterile ddH<sub>2</sub>O, 1 µl of 10 mM stock of both forward and reverse PCR primers, 0.5 µg template DNA, and 25 µl Phusion<sup>TM</sup> Master Mix. Each PCR reaction had two controls carried out in parallel. These were either the absence of the template DNA or absence of the Phusion<sup>TM</sup> Master Mix. This ensured that the resulting PCR product was a specific amplification of the desired DNA sequence.

The PCR cycle used for amplification was as follows:

1. 98°C for 30 sec (once)
  2. 98°C for 10 sec
  - 55°C for 20 sec
  - 72°C for 15 sec
- } (34 cycles)
3. 72°C for 7 min
  4. 4°C hold

The PCR reactions were carried out using a G-storm GS1 thermal cycler (Gene Technologies, Essex, U.K).

#### **2.2.2.4 Flat bed agarose gel electrophoresis for DNA analysis**

Plasmid DNA or PCR products were analysed by 1 % (w/v) flat bed agarose gel electrophoresis. Electrophoresis was carried out using a Flowgen MH 1070 minigel apparatus. A 1 % (w/v) agarose solution was made in 1 x Tris-borate-EDTA buffer (TBE, 90 mM Tris-HCl, pH 8.0, 90 mM boric acid, 4 mM EDTA). The agarose was dissolved by boiling for ~ 90 sec in a microwave oven. Once the agarose had cooled to ~ 40°C, 5 µl ethidium bromide was added to the agarose solution and mixed. The agarose solution was poured between two metal bars and a comb was placed 2 cm from the top of the gel. The agarose solution was allowed to solidify for 20 min at room temperature. The metal bars and comb were removed and the agarose gel was covered in 50 ml 1 x TBE buffer. Each DNA sample was prepared by the addition of ~ 0.5 µg DNA, 2 µl 6 x DNA loading buffer and ddH<sub>2</sub>O to give a 12 µl total volume. The DNA samples were loaded and electrophoresis was carried out at 50 V for 1 h at room temperature. Gels were imaged using a Flowgen transilluminator (UV light source  $\lambda = 312$  nm) in conjunction with a Kodak DC120 206 M digital camera. Images were saved in the .tif format for storage and analysis.

#### **2.2.2.5 Extraction of DNA fragments from agarose gels**

DNA fragments were separated according to their size by flat bed electrophoresis on a 1 % agarose gel (Section 2.2.2.4). The DNA fragment of interest was excised from the gel using a scalpel and a Dark Reader Transilluminator (Clare Chemical Research, Colorado, U.S.A) and extracted using the QIAgen® gel extraction kit. The gel slice was weighed and solubilised by adding 3 x volumes of buffer QG and heated at 50°C for 10 min in a thermomixer. The solubilised gel slice was mixed with 1 volume of isopropanol, transferred to a QIAquick spin column and centrifuged for 1 min at 16,200 x g at room temperature. The DNA was washed by adding 0.5 ml buffer QG and centrifuging for 1 min at 16,200 x g at room temperature. A further wash using 0.75 ml Buffer PE was added and incubated for 5 min at room temperature, then centrifuged for 1 min at 16,200 x g. Elution buffer (EB), 30 µl, was added and incubated for 1 min, and the mixture centrifuged for 1 min at 16,200 x g at room temperature. The DNA was used immediately, and the purification efficiency was assessed qualitatively by 1 % (w/v) flat bed agarose gel electrophoresis (Section 2.2.2.4).

#### **2.2.2.6 Restriction endonuclease (R.E) digestion**

Restriction endonuclease digestions were performed for both the cloning of PCR products into the desired vector and diagnostic purposes. When digesting plasmid DNA for diagnostic purposes, restriction endonuclease digestions were carried out in sterile 0.5 ml micro-centrifuge tubes containing; 0.5 µg (~ 0.5 µl) plasmid DNA, 1 unit of each restriction endonuclease, 1 or 2 µl (1 x or 2 x concentrated) Tango™ restriction endonuclease buffer (33 mM Tris-acetate, pH 7.9, 10 mM magnesium acetate, 66 mM potassium acetate, 0.1 mg/ml bovine serum albumin [BSA]) made to a total volume of 10 µl with ddH<sub>2</sub>O. This was gently mixed and incubated for 1 h at 37°C. The reaction was terminated by the addition of 2 µl 6 x DNA loading buffer (50 % (v/v) glycerol, 20 % (w/v) EDTA, 100 mM Tris-HCl, pH 8.0, 0.1 % (w/v) bromophenol blue, 0.1 % (w/v) xylene cyanol). The digestion was verified by 1 % (w/v) flat bed agarose gel electrophoresis (Section 2.2.2.4). When digesting PCR products, the above method was followed using ~ 500 ng of PCR product, and the restriction endonuclease digestion was incubated for 2 h before being terminated by PCR purification. The digested PCR products were then ready for ligation into the cloning vector.

#### **2.2.2.7 Purification of PCR products**

The Qiagen QIAquick® PCR purification kit was used to purify PCR products from molecular cloning enzymes. To the PCR reaction mixture, 5 x volumes of PB buffer were added. The solution was transferred to a QIAquick® column and centrifuged at 16,200 x g for 1 min at room temperature and the flow-through discarded. The column was washed with 0.75 ml PE buffer and incubated for 5 min followed by centrifugation for 1 min at 16,200 x g at room temperature. The flow-through was removed and the column was again centrifuged as above to remove all traces of buffer. The column was put into a sterile 1.5 ml micro-centrifuge tube and 30 µl 10 mM Tris-HCl, pH 8.0 was added to elute the PCR product. This was incubated at room temperature for 1 min. The column was centrifuged at 16,200 x g for 1 min at room temperature. The purified PCR product was used immediately for all subsequent reactions.

#### **2.2.2.8 Dephosphorylation of vector**

Vectors were dephosphorylated to minimise the background caused by their recircularisation. The following reaction was carried out in a 0.5 ml sterile micro-centrifuge tube; 1 x shrimp alkaline phosphatase (SAP) buffer (20 mM Tris-HCl, pH 8.0, 10 mM MgCl<sub>2</sub>), 1 - 5 µg restriction endonuclease digested vector, made to a total volume of 22 µl with ddH<sub>2</sub>O, was incubated at 37°C for 30 min. SAP enzyme was then added, 1 unit, and incubated at 37°C for 1 h. The SAP reaction was terminated by heat inactivation at 65°C for 20 min. Dephosphorylated vectors were used for all subsequent cloning of PCR products.

#### **2.2.2.9 Ligation reactions**

Restriction endonuclease digested PCR products were ligated into the restriction endonuclease digested and dephosphorylated vectors by the addition of T4 DNA ligase and thermocycling. Ratios of insert:vector of 1:1, 1:3 and 1:7 were mixed with 1 unit T4 DNA ligase in 1 x ligation buffer (66 mM Tris-HCl, pH 7.5, 5 mM MgCl<sub>2</sub>, 1 mM dithiothreitol [DTT], 1 mM ATP) to a final volume of 10 µl with ddH<sub>2</sub>O. Test ligations were always carried out alongside three control reactions. These were incubation with no ligase, incubation with no insert, or incubation with no insert and ligase. The reactions were incubated for 16 h cycling between 10°C for 1 min and 30°C for 1 min.

Ligation samples were then transformed into chemically competent *DH5α E.coli* cells (Section 2.2.1.2).

#### 2.2.2.10 PCR screening of recombinants

PCR screening was used to ascertain quickly if the colonies gained from the ligation reaction had successfully incorporated the PCR product into the cloning vector. Colonies from the ligation reactions were picked using a sterile pipette tip and carefully dipped into a sterile PCR micro-centrifuge tube containing a Phusion™ enzyme amplification mixture (4.6 µl sterile ddH<sub>2</sub>O, 0.2 µl of 10 mM stocks of both forward and reverse PCR primers and 5 µl Phusion™ Master Mix). Samples with controls were carried out in parallel. These included samples with no template DNA and samples with no forward and reverse primers. The samples were gently mixed and run using the PCR cycle as described below. If the PCR screening was positive a DNA band should be seen with the same size as the original PCR product.

3. 94°C for 1 min (once)
  4. 94°C for 1 min
  - 50°C for 30 sec
  - 72°C for 1 min
- } (34 cycles)
3. 72°C for 5 min
  4. 4°C hold

#### 2.2.2.11 Mini preparation of plasmid DNA

A single colony of pre-transformed *DH5α E.coli* cells from a selective plate was picked and used to inoculate 5 ml LB media (12 - 16 h culture, 37°C at 250 rpm) containing the correct selective antibiotic, either 50 µg/ml ampicillin or 50 µg/ml kanamycin. The 16 h culture, 1.5 ml, was then transferred into a sterile 1.5 ml micro-centrifuge tube and centrifuged at 16,200 x g for 1 min at room temperature. The supernatant was aspirated and the pellet re-suspended by gentle pipetting in 200 µl re-suspension buffer (50 mM Tris-HCl, pH 8.0, containing 10 mM EDTA and 100 µg/ml RNase A). Lysis buffer, 200 µl, (200 mM NaOH, 1% [w/v] SDS) was then added. This was mixed by

gentle inversion a total of six times. Neutralisation buffer, 200  $\mu$ l, (3 M potassium acetate) was added, and the mixture was gently inverted six times until a white precipitate formed. The tubes were incubated at  $-20^{\circ}\text{C}$  for 10 min. The precipitate was removed by centrifugation at 16,200 x g for 10 min at room temperature. The supernatant was carefully transferred into a new sterile 1.5 ml micro-centrifuge tube. Isopropanol, 400  $\mu$ l, was added to the supernatant and mixed by inversion. The tubes were centrifuged at 16,200 x g for 10 min at room temperature. The supernatant was discarded and 200  $\mu$ l ice-cold 70 % (v/v) ethanol was added to the pellet. The DNA pellet was washed by a gentle flicking of the tube and centrifuged at 16,200 x g for 5 min at room temperature. The supernatant was carefully removed and the plasmid DNA pellet was air-dried at room temperature for  $\sim$  20 min. The plasmid DNA was re-suspended in TE buffer (10 mM Tris-HCl, pH 8.0 and 1 mM EDTA) and stored at  $-20^{\circ}\text{C}$  until use.

#### **2.2.2.12 Maxi preparation of plasmid DNA**

The GenElute™ HP plasmid maxiprep kit was used for all large scale plasmid DNA extractions. A single colony of pre-transformed *DH5 $\alpha$*  *E.coli* cells was picked from a selective plate and grown in 400 ml LB media containing the correct selective antibiotic, either ampicillin or kanamycin. The culture was incubated for 16 h at  $37^{\circ}\text{C}$ , 250 rpm. The culture was pelleted by centrifugation at 5,000 x g for 10 min at  $4^{\circ}\text{C}$  using a JLA 16.250 rotor in a Beckman centrifuge. The pellet was re-suspended in 12 ml re-suspension buffer by gentle pipetting. Lysis buffer, 12 ml, was added, mixed by inversion six times and incubated for 4.5 min. The lysis was terminated by the addition of 12 ml ice-cold neutralisation buffer. This was mixed by inversion six times until a white precipitate formed. Binding buffer, 9 ml, was added and the lysed cell solution was poured into a GenElute™ HP maxiprep filter syringe. Plasmid DNA was subsequently filtered by passing the lysed cell solution through the filter syringe. The GenElute™ HP maxiprep binding column was equilibrated by the addition of 12 ml column preparation buffer. This solution was passed through the binding column by centrifugation at 3,000 x g for 2 min at  $20^{\circ}\text{C}$  using a Megafuge 1.0 R centrifuge. The filtrate from the lysed cells containing the plasmid DNA was added to the equilibrated binding column and centrifuged at 3,000 x g for 2 min at  $20^{\circ}\text{C}$ . This step was repeated

until all the filtrate had passed through the binding column. Wash buffer 1, 12 ml, was added to the binding column and was centrifuged at 3,000 x g for 2 min at 20°C and the supernatant removed. Wash buffer 2, 12 ml, was added and the binding column was centrifuged at 3,000 x g for 5 min at 20°C and the supernatant removed. The plasmid DNA was eluted into 2 ml TE buffer (10 mM Tris-HCl, pH 8.0 and 1 mM EDTA) by centrifugation at 3,000 x g for 5 min at 20°C. The plasmid DNA-containing filtrate was passed through the binding column an additional time as described above. Plasmid DNA was characterised and the concentration of DNA was determined by measuring the absorbance at  $\lambda = 260$  nm, with an absorbance reading of 1 equating to 50  $\mu\text{g/ml}$  of DNA. The purity of the DNA was calculated from the absorbance ratio  $\text{OD } \lambda = 260 \text{ nm} / \text{OD } \lambda = 280 \text{ nm}$ . This ratio is equal to  $\sim 1.8 - 2.0$  for a pure DNA preparation indicative of a low protein to DNA ratio. Plasmid DNA was stored as aliquots of 200  $\mu\text{l}$  at -20°C until use.

#### **2.2.2.13 Ethanol precipitation of plasmid DNA**

Ethanol precipitation of plasmid DNA was used to concentrate plasmid DNA for DNA sequencing. To 1 x volume of plasmid DNA ( $\sim 1.5 \mu\text{g}$ ), 0.12 x volume of 3 M sodium acetate and 2.5 x volumes of ice-cold ethanol were added into a 1.5 ml sterile micro-centrifuge tube. The mixture was incubated for 2 h at -80°C. Plasmid DNA was pelleted by centrifugation at 16,200 x g for 30 min at room temperature. The supernatant was carefully discarded and 200  $\mu\text{l}$  ice-cold 70 % (v/v) ethanol was added to wash the plasmid DNA pellet. The plasmid DNA was pelleted by centrifugation at 16,200 x g for 5 min at room temperature. The supernatant was removed and the plasmid DNA pellet was allowed to air dry for  $\sim 20$  min at room temperature. The plasmid DNA pellet was either re-suspended in the appropriate volume of TE buffer (10 mM Tris-HCl, pH 8.0, 1 mM EDTA) and stored at -20°C until use or sent immediately to MWG-Biotech (Ebersberg, Germany) or UCL DNA Sequencing Service for nucleotide sequencing.

#### 2.2.2.14 Deletion mutagenesis by overlap extension PCR

Deletion mutagenesis by overlap extension PCR was used to remove a specific nucleotide sequence from a DNA sequence of interest. In this case this was the deletion of 18 nucleotides encoding for amino acid numbers 877-883 of KIF5A. To generate a PCR product with a deletion mutation a similar method to designing primers for standard sub-cloning (Section 2.2.2.3) was utilised. An overall summary of this process is shown in Figure 2.2. An initial PCR step was used to amplify the two regions of DNA either side of the deletion region (Section 2.2.2.3.1). Each DNA fragment contained an 18 nucleotide overlap specific for the region opposite to the deleted sequence. The two PCR products were analysed via flat bed agarose gel electrophoresis (Section 2.2.2.4) and subsequently extracted (Section 2.2.2.5). The extracted DNA fragments were mixed in an equal ratio to a total of 1  $\mu$ l which served as the hybrid duplex template DNA. This hybrid duplex DNA was PCR amplified to yield a recombinant PCR product and was directly cloned into the pcDNAHisMaxC vector (Section 2.2.2.4 – Section 2.2.3.11).

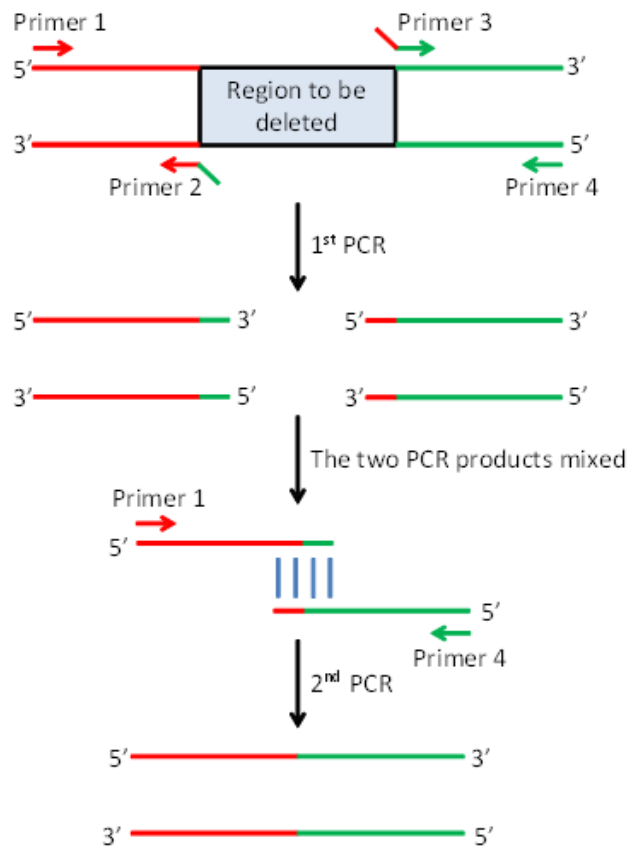


Figure 2.2 Schematic of deletion mutagenesis by overlap extension PCR.

### **2.2.3 Bacterial protein expression**

#### **2.2.3.1 Protein extraction from *BL21 DE3 codonplus E.coli* cells**

A single colony of pre-transformed *BL21 E.coli* cells from a selective plate was picked and used to inoculate 5 ml LB media (12 - 16 h culture) containing the correct selective antibiotic (50 µg/ml ampicillin). LB media cultured overnight, 1 ml, was used as a starter culture to inoculate 50 ml of LB media (1 % [w/v] glucose) containing 50 µg/ml ampicillin, and grown until OD = 600 nm reached 0.6 - 0.7. IPTG, 0.1 mM or 1 mM, was used to induce protein production for 4 h at either 18°C, 25°C or 37°C, 225 rpm. The culture was centrifuged at 4,000 x g for 15 min at 4°C, the supernatant was aspirated and the remaining pellet frozen overnight. The pellet was subsequently defrosted slowly on ice, and re-suspended in varying buffers (8 or 16 ml for 100 ml of culture) to test optimal conditions. These buffers were either (i) native buffer (250 mM NaH<sub>2</sub>PO<sub>4</sub>, pH 8.0, 1 mg/ml lysozyme) or (ii), re-suspension buffer (50 mM Tris pH 8.0, 400 mM NaCl, 10 % [w/v] glycerol, 5 mM β-ME, 20 µg/ml lysozyme and 1 protease inhibitor cocktail tablet). The re-suspended solution was incubated on ice for 30 min and then sonicated 6 x for 10 sec each with 10 sec rest in between each sonication. Solubilised samples, 1 ml, were removed and aliquoted into 1.5 ml micro-centrifuge tubes and termed the total fraction. The remaining solution was centrifuged at 3,000 x g for 15 min at 4°C. The supernatant was aliquoted into 1.5 ml micro-centrifuge tubes and termed the soluble fraction. The remaining protein pellet was carefully re-suspended and aliquoted into 1.5 ml micro-centrifuge tubes and was termed the insoluble fraction. Samples were snap frozen at -20°C until needed for future analysis.

#### **2.2.3.2 Bradford assay protein quantification**

BSA was diluted to a final concentration of 1 mg/ml using ddH<sub>2</sub>O. A series of dilutions of this stock solution were made in triplicate to give; 10 µg, 8 µg, 6 µg, 4 µg, 2 µg and 0 µg BSA each in a total volume of 800 µl. The test samples were diluted 1/10 and 1/100 with ddH<sub>2</sub>O. Coomassie Brilliant Blue G-250 dye Bio-Rad protein assay, 200 µl, was added to each sample. The samples were incubated at room temperature for 30 min. The OD λ = 595 nm was measured and a calibration curve was constructed from the protein standards. The protein concentrations of the test samples were then

determined by comparing to the standard curve.

#### **2.2.3.4 SDS-PAGE**

Sodium dodecyl sulphate - polyacrylamide gel electrophoresis (SDS-PAGE) was carried out under reducing conditions using 7 %, 12 % or 15 % (w/v) polyacrylamide mini gels. For each gel, one glass plate (8 cm x 10 cm), one aluminium plate (8 cm x 10 cm) and two 0.75 mm spacers were cleaned with 70 % (v/v) ethanol. The two spacers were put on either side of the aluminium plate with the glass plate on top, and were assembled into a Mighty Small™ dual gel caster (Hoefer, San Francisco, U.S.A).

##### **2.2.3.4.1 Preparation of running gel**

All polyacrylamide gels contained 7 %, 12 % or 15 % (w/v) acrylamide. The running gel for a 12 % solution was made with; 4.2 ml ddH<sub>2</sub>O, 3 ml running gel buffer (1.5 M Tris-HCl, pH 8.8, 8 mM EDTA, 0.4 % [w/v] SDS), 4.8 ml ProtoGel® (37.5:1 acrylamide to bisacrylamide stabilized solution) and 6 µl TEMED. The solution was de-gassed under vacuum for 30 min. The polymerisation was initiated by the addition of 60 µl 10 % (w/v) ammonium persulphate. The solution was poured gently between the glass plate and aluminium plate to reach ~ 3 cm below the top of the glass plate. To ensure an even surface on the top of the gel, ~ 250 µl 50 % (v/v) butan-1-ol was added. Gels were left to polymerise for ~ 1 h. The butan-1-ol was removed by washing 3 x with ~ 5 ml ddH<sub>2</sub>O.

##### **2.2.3.4.2 Preparation of stacking gel**

The polyacrylamide gels were transferred from the Mighty Small™ gel caster onto the Mighty Small™ electrophoresis unit. The stacking gel solution was made with; 2.3 ml ddH<sub>2</sub>O, 1 ml stacking buffer (0.5 M Tris-HCl, pH 6.8, 8 mM EDTA, and 0.4 % [w/v] SDS), 650 µl ProtoGel® and 6 µl TEMED. The stacking gel solution was degassed under vacuum for 30 min. The polymerisation reaction was initiated by the addition of 10 % (w/v) ammonium persulphate, 80 µl. The acrylamide solution was added directly to the separating gel and a comb immediately positioned. The stacking gels were polymerised for ~ 10 min. Once the stacking gels had polymerised, the buffer reservoirs were filled

with electrode buffer (50 mM Tris-HCl, pH 8.8, 384 mM glycine, 1.8 mM EDTA, 1.8 % [w/v] SDS) and the comb was gently removed. Gel lanes were then washed to remove any residual unpolymerised polyacrylamide.

#### **2.2.3.4.3 Methanol/chloroform precipitation of protein samples**

To precipitate protein samples with a volume too large for SDS-PAGE analysis, aliquots in the range of 25 – 150  $\mu$ l were mixed with four volumes of methanol (MeOH) in a 1.5 ml microcentrifuge tube. The samples were briefly vortexed and centrifuged at 5,000 x g for  $\sim$  10 sec at room temperature. One volume of chloroform was added and the resulting samples vortexed and centrifuged as above. Three volumes of ddH<sub>2</sub>O was added, vortexed and centrifuged for 1 min, 12,000 x g at room temperature. The resulting top aqueous layer was removed and one volume of MeOH added. The resulting samples were vortexed and centrifuged for 4 min at room temperature. The supernatant was carefully removed and the resulting protein pellet was dried under a vacuum for  $\sim$  20 min. The samples were then prepared and run on SDS-PAGE as described in Section 2.2.3.4.4.

#### **2.2.3.4.4 Preparation and electrophoresis of protein samples**

To each methanol/chloroform precipitated protein sample; 8.5  $\mu$ l ddH<sub>2</sub>O, 5  $\mu$ l 3 x SDS-PAGE sample buffer (30 mM NaH<sub>2</sub>PO<sub>4</sub>, pH 7, 30 % [v/v] glycerol, 0.05 % [w/v] bromophenol blue, 7.5 % [w/v] SDS) and 1.5  $\mu$ l 1 M DTT were added. The samples were briefly vortexed for  $\sim$  5 sec and centrifuged at 13,000 x g for 1 min at room temperature. The samples were heated to 75°C for 8 min whilst shaking at 500 rpm in an Eppendorf ThermoMixer. The protein samples were collected in the bottom of the micro-centrifuge tubes by another cycle of vortexing as above, and centrifuged for 10 sec. The protein samples were loaded into the gel lanes using a Hamilton syringe. Empty gel lanes were loaded with 15  $\mu$ l 1 x sample buffer. If the gels were to be analysed by immunoblotting, one lane per gel was loaded with 4  $\mu$ l of SeeBlue® pre-stained standard protein molecular weight markers. Polyacrylamide gels which were to be protein stained using Coomassie Blue were prepared and run as before except for the use of an un-stained protein molecular weight marker, in which 15  $\mu$ l 1 x sample buffer with 1  $\mu$ g of marker protein was loaded. Electrophoresis was carried out at an 8

mAmp constant current through the stacking gel then a 10 mAmp constant current through the separating gel. For protein gels which were to be used for immunoblotting, once the bromophenol blue dye front had reached the bottom of the gel the proteins were transferred onto nitrocellulose membranes (Section 2.2.3.5.1). For gels which were directly stained for proteins, once the bromophenol blue dye front had reached the bottom of the gel the gel was incubated in a Coomassie Blue stain solution overnight (per 100 ml: 60 ml ddH<sub>2</sub>O, 30 ml methanol, 10 ml acetic acid, 0.2 g Coomassie Blue G-250). The gel was subsequently washed with gentle agitation and several changes of destain solution (30% [w/v] methanol, 10% [w/v] acetic acid) until background Coomassie Blue staining had been removed. Stained gels were imaged using a HP scanjet 4570c scanner. The SeeBlue<sup>®</sup> pre-stained standard protein molecular weight markers contained the following proteins (kDa): myosin, 250; BSA, 98; glutamate dehydrogenase, 64; alcohol dehydrogenase, 50; carbonic anhydrase, 36; myoglobin, 30; lysozyme, 16; aprotinin, 6; insulin B chain, 4. The un-stained standard protein molecular weight markers contained the following proteins (kDa): myosin, 200;  $\beta$ -galactosidase, 116.25; phosphorylase b, 97.4; serum albumin, 66.2; ovalbumin, 45; carbonic anhydrase, 31; trypsin inhibitor, 21.5; lysozyme, 14.4; aprotinin, 6.5.

## **2.2.3.5 Immunoblotting**

### **2.2.3.5.1 Transfer of proteins to nitrocellulose membranes**

Once SDS-PAGE was completed, proteins were transferred onto nitrocellulose membranes using a wet transfer process. To transfer the proteins a sandwich was made of two pieces of blotting paper, pre-soaked in transfer buffer (25 mM Tris, 172 mM glycine, 20% [v/v] methanol, pH 8.5) and a piece of nitrocellulose membrane which had also been pre-soaked in transfer buffer. The polyacrylamide gel was placed onto the nitrocellulose membrane and two additional pieces of pre-soaked blotting paper were placed on top. A 2 ml pipette was rolled across the sandwich to remove any air bubbles. The sandwich was put between two pieces of sponge and into a transfer cassette. The cassette was placed into a Mighty Small<sup>™</sup> transfer tank containing transfer buffer ensuring that the cassette was fully covered, with the polyacrylamide gel facing the cathode. The transfer was conducted for 16 h at 14 V at room temperature. When removing the nitrocellulose membrane from the tank, the

size of the nitrocellulose was trimmed to exactly the same size as the gel. Nitrocellulose membranes were stored in 1 x PBS at 4°C until immunoblotting was conducted (Section 2.2.3.5.2).

#### **2.2.3.5.2 Immunoblotting**

Proteins were visualised by immunoblotting using the appropriate antibodies. The nitrocellulose membrane was blocked for 1 h in 5 % (w/v) powdered milk (Marvel, low fat powdered milk powder) and 0.05 % (w/v) polyethylene glycol sorbitan monolaurate (Tween-20®) in 1 x PBS at 37°C with gentle rotation. The primary antibodies (0.5 - 2 µg/ml in 2.5 % [w/v] powdered milk in 1 x PBS) were incubated with the nitrocellulose membrane at 37°C with gentle rotation for 1 h. The membranes were washed 4 x 10 min in 2.5 % (w/v) powdered milk and 0.05 % (w/v) Tween-20® in 1 X PBS at 37°C with gentle rotation. The secondary antibody, either horseradish peroxidase (HRP)-linked anti-rabbit IgG or HRP-linked anti-mouse IgG antibodies were prepared as a 1/2000 dilution in 2.5 % (w/v) powdered milk. In the case of the directly conjugated HRP anti-His primary antibodies incubation with secondary antibodies was not required. Immunoblots were incubated with secondary antibodies for 1 h at 37°C with gentle rotation. The membranes were washed 4 X 10 min in 2.5 % (w/v) powdered milk and 0.05 % (w/v) Tween-20® at 37°C with gentle rotation. The membranes were briefly washed in 1 x PBS. A 10 ml aliquot of 0.8 M luminol (100 mM Tris-HCl, pH 8.5 and 0.8 M luminol) and a 100 µl aliquot of 10 mg/ml hydroxycinnamic acid (p-coumaric acid) were defrosted. The 100 µl p-coumaric acid was added to the 10 ml luminol solution and mixed. The membrane was put face up into an empty tray. The blot development was initiated by the addition of 10 µl hydrogen peroxide to the luminol mixture, which was vortexed and poured over the membrane. This was incubated for 1 min and the membrane was tapped on tissue to remove the excess liquid. The membrane was then put into a plastic sleeve and tracker tape was used to mark the positions of the molecular weight markers. The immunoblots were imaged using a GeneGnome Chemiluminescence Capture and Analysis System (Syngene, Cambridge, U.K).

### **2.2.3.5.3 Quantitative immunoblot analysis**

When quantitative immunoblotting was carried out the immunoreactive bands were quantified using GeneGnome Tools software. An equal sized box was drawn around each of the resulting bands, in which the background was calculated and deducted from the resulting pixel values for each immunoblot.

## **2.2.4 Purification of bacterially expressed recombinant proteins**

### **2.2.4.1 Purification of bacterially expressed His tagged protein using ProBond™ Ni<sup>2+</sup> chelating resin**

All purification experiments were carried out at 4°C. Purification of bacterially expressed His tagged protein was carried out using two methods, these were either (i) small scale purification using 0.5 ml of settled ProBond™ Ni<sup>2+</sup> chelating resin (Ni<sup>2+</sup> affinity resin) and 6 ml of soluble protein sample, or (ii) large scale purification using 1 ml of settled resin and 40 ml of soluble protein sample. Ni<sup>2+</sup> affinity resin was prepared by washing once in 6 ml ddH<sub>2</sub>O followed by 3 x with re-suspension buffer minus the presence of β-ME (50 mM Tris pH 8.0, 400 mM NaCl, 10 % (w/v) glycerol, 20 µg/ml lysozyme, and 1 protease inhibitor cocktail tablet). Between each wash, the resin was settled via centrifugation for 1 min at 800 x g and the supernatant carefully removed using a 1 ml pipette tip. Fresh soluble protein extract gained from expression experiments in *BL21 E.coli* cells (Section 2.2.3.1) were incubated with the resin for 1 h whilst gently rocking. After incubation, the resulting mixture of resin and soluble protein was poured gently into a 5 ml poly-prep chromatography column and the unbound soluble protein allowed to run through and the resin to settle via gravity. The resulting unbound protein was snap frozen in liquid nitrogen and kept at -20°C until further analysis. The settled column was subsequently washed with a minimum of 8 x column volumes of wash solution (re-suspension buffer with 5 mM β-ME and 20 mM imidazole) or until the collected fractions O.D λ = 280 nm = 0. The column was eluted via gravity using the same method used to wash the column but using elution buffer (50 mM Tris pH 8.0, 400 mM NaCl, 10% (w/v) glycerol, 20 µg/ml lysozyme, 5 mM β-ME, 250 mM imidazole and 1 protease inhibitor cocktail tablet). All subsequent wash and elution fractions were collected as 1 ml fractions and snap frozen in liquid nitrogen and

stored at -20°C until further analysis.

#### **2.2.4.2 Purification of bacterially expressed S tagged protein using S-protein agarose resin**

All purification experiments were carried out at 4°C. Fresh soluble protein extract gained from expression experiments in *BL21 E.coli* cells (Section 2.2.3.1) was incubated with 1 ml S-protein agarose resin (50 % slurry in 50 mM Tris-HCl, pH 7.5, 150 mM NaCl, 1 mM EDTA, 0.02 % sodium azide) for 1 h whilst gently rocking. After incubation the resulting mixture of resin and soluble protein was poured gently into a 5 ml poly-prep chromatography column and the unbound soluble protein allowed to run through and the resin to settle via gravity. The resulting unbound protein was snap frozen in liquid nitrogen and kept at -20°C until further analysis. The settled column was subsequently washed with a minimum of 8 x column volumes of wash solution (20 mM Tris-HCl pH 7.5, 150 mM NaCl, 0.1% Triton X-100) or until the collected fractions O.D  $\lambda = 280 \text{ nm} = 0$ . S-tagged protein was eluted from the resin using 3 M  $\text{MgCl}_2$  via gravity. All subsequent wash and elution fractions were collected as 1 ml fractions and snap frozen in liquid nitrogen and stored at -20°C until further analysis.

#### **2.2.4.3 Buffer exchange and concentration of bacterially expressed protein samples**

Vivaspin 6 ml 10,000 Da filters were used to concentrate and buffer exchange bacterially expressed and purified protein samples in preparation for microtubule binding co-sedimentation assay experiments. Prior to use the filters were pre-washed with ~ 5 ml of re-suspension buffer (50 mM Tris pH 7.4, 150 mM NaCl and 1 protease inhibitor cocktail tablet) and centrifuged at 3,200 x g, 4°C for 10 min to remove any possible preservatives. Protein samples were subsequently loaded onto the filter and centrifuged at 3,200 x g, 4°C for 5 - 30 min depending on the time reached to obtain the desired final volume. The sample was subsequently washed 6 x with an equal volume of a new buffer and centrifuged as above. Samples were snap frozen in liquid nitrogen and stored at -20°C.

#### **2.2.4.4 Aggregation state testing**

To ensure that bacterially expressed protein remained stable after affinity tag purification, buffer exchange and snap freezing for storage, tests upon the aggregation state of the protein were carried out. Bacterial protein samples were centrifuged at 100,000 x g for 20 min at 4°C using a MLA 80 rotor in a Beckman Optima™ MAX-E ultracentrifuge. The protein supernatant was carefully removed without disturbing the pellet and placed into a micro-centrifuge tube for further analysis. The resulting pellet was re-suspended in an equal volume of appropriate buffer and also placed into a micro-centrifuge tube. Each supernatant and re-suspended pellet sample, 75 µl, was methanol/chloroform precipitated (Section 2.2.3.4.3). Resulting protein samples were mixed with SDS sample preparation buffer and analysed via SDS-PAGE and Coomassie Blue staining (Section 2.2.3.4).

#### **2.2.4.5 Size exclusion chromatography**

Size exclusion chromatography was utilised to separate proteins based on their molecular weight and native conformation in a given buffer condition. All buffers and samples were filtered using a 0.22 µm filter and degassed under a vacuum prior to use. All size exclusion chromatography experiments were carried out using a Superose™ 6 10/300 GL column on an ÄKTAprime plus chromatography system (GE Healthcare, Amersham, U.K). Before samples could be run the column was washed with 2 x column volumes (48 ml) of ddH<sub>2</sub>O followed by 2 x column volumes of re-suspension buffer (Section 2.2.3.1) minus glycerol. This process of washing the column removed any traces of 70 % ethanol, in which the column has been stored, as well as allowing the column to equilibrate to the buffer conditions. In order to calibrate the S6 column, molecular weight standards (Sigma-Aldrich, Poole, U.K) were re-suspended in re-suspension buffer minus glycerol at a concentration of ~ 1 mg/ml and run through the gel filtration system. These molecular weight standards included (kDa): blue dextran, 2,000; albumin, 158; albumin (bovine), 66; albumin (egg), 45; carbonic anhydrase, 29; chymotrypsinogen, 25; cytochrome C, 12.4. 120 µl of molecular weight protein standard was injected onto the column and allowed to run for 1.5 column volumes (36 ml) at a flow rate of 0.2 ml/min, this was repeated until all samples had been run. Elution volume peaks were noted and a calibration curve of the log of molecular

weight versus elution volume was constructed. Protein samples were injected and run as above except elution volumes were collected as 0.5 ml fractions into micro-centrifuge tubes using a fraction collector (GE Healthcare, Amersham, U.K). Elution volumes were analysed via SDS-PAGE using both immunoblotting and Coomassie Blue protein staining (Section 2.2.3.4). After use the Superose™ 6 10/300 GL column was washed with 2 x column volumes of ddH<sub>2</sub>O followed by 2 x column volumes of 70 % ethanol for long term storage.

#### **2.2.4.6 Preparation of stable and polymerised microtubules**

To prepare stable and polymerised microtubules, 5 mM GTP was mixed with 20 µl 2 x microtubule polymerisation buffer (80 mM piperazine-N,N'-bis-(2-ethanesulphonic acid) [PIPES], pH 6.8, 10 mM MgCl<sub>2</sub>). This was subsequently added to 20 µl thawed glycerol-free bovine brain tubulin and vortexed. The resulting mixture was incubated for 90 min at 37°C and afterwards 0.4 µl paclitaxel dissolved in DMSO (1 mM final) added to stabilise the microtubules. The solution was further incubated for 1 h at 37°C. The final mixture was left for 24 h at room temperature prior to use to allow complete polymerisation of the microtubules.

##### **2.2.4.6.1 Microtubule binding co-sedimentation assay**

To test the binding interaction of purified KIF5A<sub>800-951</sub> protein with microtubules a co-sedimentation assay was carried out. A range of concentrations of purified KIF5A<sub>800-951</sub> protein (6 – 78 µg) were incubated with a fixed microtubule concentration, 1.5 µM. All samples were prepared in thick walled polycarbonate tubes to a final volume of 40 µl with microtubule binding buffer (50 mM Tris, pH 7.5, 150 mM NaCl and 1 protease inhibitor cocktail tablet). Each microtubule binding co-sedimentation assay had two controls carried out in parallel. These were the absence of either the KIF5A<sub>800-951</sub> protein or the absence of microtubules. The resulting mixture was briefly vortexed and incubated at room temperature for 15 min whilst being covered with Parafilm to prevent evaporation. Tubes were centrifuged at 392,000 x g for 15 min at room temperature using a TLA 100 rotor in a Beckman Optima™ MAX-E ultracentrifuge. The supernatant was carefully removed without disturbing the pellet and placed into a

micro-centrifuge tube for further analysis. The resulting pellet was re-suspended in 40  $\mu$ l microtubule binding buffer and also placed into a micro-centrifuge tube. Each supernatant (10  $\mu$ l) and re-suspended pellet sample was mixed with 5  $\mu$ l 3 x SDS sample preparation buffer and analysed via SDS-PAGE and Coomassie Blue protein staining (Section 2.2.3.4).

## **2.2.5 Expression in mammalian cells**

### **2.2.5.1 Culturing of human embryonic kidney 293 cells**

All cell culture, Section 2.2.5.2 – Section 2.2.5.6, was carried out by Dr Cousins, Dr Brickley or Dr Lyn-Adams, UCL School of Pharmacy, U.K. For all cell culture equipment sterile techniques were employed throughout. In addition, when removing or placing an item in either the laminar flow hood or the mammalian cell incubator each item was lightly sprayed with 70 % (v/v) ethanol to maintain sterility. All solutions were sterilised either by filtration through a 0.22  $\mu$ m pore size or by autoclaving at 120°C for 20 min.

### **2.2.5.2 Preparation of cell culture media**

For routine sub-culturing of HEK 293 cells, modified Eagles medium nutrient mixture F-12 HAM (DMEM/F-12) containing L-glutamine was utilised. Media was prepared by the addition of 15.6 g powdered Dulbecco's modified Eagles medium nutrient mixture F-12 HAM (DMEM/F-12) to 500 ml sterile ddH<sub>2</sub>O, 20 ml penicillin/streptomycin (10,000 units/ml), 40 ml 7.5 % (w/v) NaHCO<sub>3</sub> and 100 ml foetal bovine serum (FBS). The total volume was made to 1 L and the pH adjusted to 7.6 using 10 M NaOH. The media was then filter sterilised through a 0.22  $\mu$ m Nalgene filter. The above described cell culture media was replaced 3 h before transfection with DMEM/F-12 L-glutamine free media. This was made by adding 100 ml FBS, 20 ml penicillin/streptomycin (10,000 units/ml) and 24 ml 7.5 % (w/v) NaHCO<sub>3</sub> to liquid DMEM/F-12 without L-glutamine to a total volume 1 L and adjusted to pH 7.6 using 10 M NaOH. The media was then filter sterilised through a 0.22  $\mu$ m Nalgene filter.

### **2.2.5.3 Storage of HEK 293 cells in liquid nitrogen**

HEK 293 cells that had reached 70 % confluence were used to make liquid nitrogen stocks. HEK 293 cells were harvested using the method described in Section 2.2.5.5. The 12 ml HEK 293 cell suspension was centrifuged at 1,000 x g for 10 min at room temperature in a sterile 15 ml centrifuge tube. The supernatant was discarded and the pellet was re-suspended in 600 µl DMSO, 600 µl FBS and 4.8 ml DMEM/F-12 media containing L-glutamine. The cell suspension was divided as 1 ml aliquots in 1.8 ml cryotubes and frozen for 24 h at -80°C. The following day the tubes were placed in liquid nitrogen until use.

### **2.2.5.4 Reviving HEK 293 cell stocks from liquid nitrogen storage**

An aliquot of HEK 293 cells was taken from liquid nitrogen storage and rapidly defrosted in a water bath at 37°C. The HEK 293 cell suspension was mixed into 50 ml DMEM/F-12 media containing L-glutamin, pre-warmed to 37°C. The cells were pelleted by centrifugation at 1,000 x g for 10 min at room temperature. The supernatant was decanted and the pellet re-suspended in 10 ml (preheated to 37°C) DMEM/F-12 media containing L-glutamine. The cell suspension was added to a 250 ml Cellstar™ sterile cell culture flask and incubated at 37°C in the presence of 5 % CO<sub>2</sub>. The following day the media was aspirated and replaced with 10 ml, pre-warmed to 37°C, DMEM/F-12 media containing L-glutamine. Once the HEK 293 cells had reached ~ 90 % confluence they were sub-cultured.

### **2.2.5.5 Sub-culturing of HEK 293 cells**

Once the HEK 293 cells had reached ~ 90 % confluency they required sub-culturing. This was approximately every 3 - 5 days. Media was aspirated from a flask of confluent cells and washed by gently passing 10 ml (preheated to 37°C) Hanks buffered salt solution (HBSS) gently over the cells. The HBSS was removed and 2 ml trypsin-EDTA (0.5 mg/ml porcine trypsin in HBSS) was added and incubated for 50 sec at room temperature. The flask was gently tapped to dislodge the cells and 10 ml DMEM/F-12 containing L-glutamine media (preheated to 37°C) was added. The cells were mixed thoroughly by repeated pipetting up and down. The 12 ml cell suspension was divided

equally between four flasks. An additional 9 ml DMEM/F-12 containing L-glutamine media (preheated to 37°C) was added to each flask. The flasks were incubated at 37°C and cultured in the presence of 5 % CO<sub>2</sub> for 24 h prior to transfection or until ~ 90 % confluent when the HEK 293 cells were sub-cultured again, as above. The HEK 293 cells were routinely used for ~ 20 passages (two months) before reviving a new aliquot of HEK 293 cells for subsequent use.

#### **2.2.5.6 Transient transfection of HEK 293 cells by the calcium phosphate method**

HEK 293 cells were sub-cultured to be ~ 40 % confluence on the day of transfection, (Section 2.2.5.5). Three hours prior to transfection the cell culture media was aspirated and replaced with 10 ml (preheated to 37°C) DMEM/F-12 L-glutamine free media. Each flask was incubated for 3 h at 37°C in the presence of 7.5 % CO<sub>2</sub>. DNA to be used for transfection at 10 µg per flask was prepared as follows:- Two sterile 1.5 ml centrifuge tubes were prepared, one containing 500 µl 2 x HEPES buffer saline (2 X HBS, 50 mM N-(2-hydroxyethyl) piperazine-N'-(2-ethanesulphonic acid) (HEPES), pH 7.12, 280 mM NaCl, 1.1 mM Na<sub>2</sub>HPO<sub>4</sub>). The second tube containing 450 µl of the required plasmid DNA and 1/10 (v/v) TE buffer (10 mM Tris-HCl, pH 8.0 and 10 mM EDTA, diluted 1/10 (v/v) with ddH<sub>2</sub>O). The solution to be transfected was started by the addition of 50 µl 2.5 M CaCl<sub>2</sub> (preheated to 37°C) to the tube containing the plasmid DNA and 1/10 (v/v) TE buffer, and the tube was shaken vigorously for 15 sec. The DNA mixture was added drop-wise to the 2 x HBS at a rate of one-drop every ~ 4 sec. This solution was mixed by gentle pipetting up and down with a 1 ml pipette tip a total of three times. The above described transfection solution was added to the HEK 293 cells by slowly pipetting the solution into a corner of the flask under the surface of the media. The flask was rotated slowly 3 times to ensure the DNA precipitate was evenly distributed over the cells. The cells were then returned to the incubator at 37°C in the presence of 5 % CO<sub>2</sub>. Transfected HEK 293 cells were cultured for either 24 or 48 h post-transfection and the cell homogenates were collected and analysed by either immunoblot analysis (Section 2.2.3.5) or immunoprecipitation experiments (Section 2.2.5.8).

### **2.2.5.7 Preparation of transfected HEK 293 cell homogenates**

Transfected HEK 293 cell homogenates were used to test expression of newly synthesised mammalian expression clones prior to immunoprecipitation experiments (Section 2.2.5.8). HEK 293 cells were harvested 24 h post-transfection. The media was aspirated and the cells were scraped using a sterile cell scraper into 8 ml ice-cold phosphate buffered saline (1 x PBS; 137 mM NaCl, 27 mM KCl, 10 mM Na<sub>2</sub>HPO<sub>4</sub>.12H<sub>2</sub>O, 1.8 mM KH<sub>2</sub>PO<sub>4</sub>, pH 7.6). The cell suspension was collected and pelleted at 1,000 x g for 10 min at 4°C. The supernatant was discarded and the pellet homogenised in 5 ml homogenisation buffer (50 mM Tris-citrate, pH 7.4, 5 mM EDTA, 5 mM EGTA) for ~ 10 strokes using a tight 7 ml Wheaton Dounce glass-glass homogeniser. Typically a 250 ml flask of transfected cells would yield ~ 1 mg protein. The homogenised protein samples were either analysed via SDS-PAGE (Section 2.2.3.4) or aliquoted and snap frozen in liquid nitrogen then stored at -20°C until analysis by immunoblotting (Section 2.2.3.5).

### **2.2.5.8 Detergent solubilisation and co-immunoprecipitation of HEK 293 cell homogenates**

Co-immunoprecipitation assays were carried out to ascertain if proteins were able to co-immunoprecipitate with each other following their co-expression in HEK 293 cells. For co-immunoprecipitations using transfected HEK 293 cells the method of Chazot *et al.* (1994) was followed. Three flasks of HEK 293 cells were harvested 48 h post-transfection and pooled together. The resulting cell homogenate was re-suspended in 8 ml solubilisation buffer (50 mM Tris-citrate, pH 7.4, 240 mM NaCl, 5 mM EDTA, 5 mM EGTA, 1 mM PMSF, bacitracin (5 g/ml), soyabean trypsin inhibitors (5 g/ml), benzamidine HCl (5 g/ml) and 1 % (v/v) Triton X-100®). The cell homogenate was thoroughly homogenised with 10 strokes using a tight 7 ml Wheaton Dounce glass-glass homogeniser followed by incubation for 1 h with gentle rotation at 4°C. Soluble fractions were collected by centrifugation at 100,000 x g for 40 min at 4°C using a MLA 80 rotor in a Beckman Optima™ MAX-E ultracentrifuge. Each detergent-solubilised sample was diluted with an equal volume of solubilisation buffer (minus Triton X-100®) to give a final volume of 12 ml and a final concentration of 0.5 % Triton X-100®. Final diluted protein samples, 300 µl, were removed and are referred to as the input sample. The remaining sample was split into two aliquots and co-

immunoprecipitations were initiated by the addition of 10  $\mu\text{g}$  of the appropriate primary antibodies to one aliquot and 10  $\mu\text{g}$  non-immune antibodies to the second aliquot. The final volumes of each assay were adjusted with 1 x PBS to ensure they were both the same final volume. The antibodies were incubated for 16 h with gentle rotation at 4°C. Antibody complexes were precipitated by the addition of 5 mg protein A Sepharose and samples were incubated for 1 h with gentle rotation at 4°C. The samples were centrifuged at 600 x g for 15 sec. The supernatants were removed and the antibody-protein A Sepharose complex was gently and rapidly washed with 1 ml solubilisation buffer followed by centrifugation at 600 x g for 15 sec at room temperature. This wash step was repeated a total of three times. On the final wash the supernatant was completely removed using a Hamilton syringe. To the pellet, 20  $\mu\text{l}$  3 x SDS-PAGE sample buffer and 5  $\mu\text{l}$  1 M DTT was added. The samples were heated to 75°C for 8 min. The proteins were collected by centrifugation at 600 x g for 15 sec at room temperature and the supernatant transferred into a fresh 1.5 ml centrifuge tube using a Hamilton syringe. The supernatants were then made up to the required volume with 1 x SDS-PAGE sample buffer and analysed by immunoblotting (Section 2.2.3.5). The supernatant collected from protein A Sepharose using antibodies specific to my protein of interest shall be referred to as the immune pellet and the supernatant from the non-immune antibodies as the non-immune pellet.

# **CHAPTER 3**

**TOWARDS THE STRUCTURAL DETERMINATION OF  
A TRAK2/KIF5A TRAFFICKING COMPLEX**

### 3.1 RATIONALE

As described in the Introduction, the kinesin-1 family are motor proteins that have many important functions including roles in cell division and the transport of various organelles and protein cargoes within cells. Kinesin-1 consists of three main structural domains; a motor domain which binds to and creates movement along microtubule tracks using ATP, a stalk domain giving flexibility and stability to the protein and a cargo binding domain to which the cargoes that are transported bind (Hirokawa and Takemura, 2005). Previous work by Kull *et al.* (1996) successfully resolved the structure of the motor domain of the human kinesin-1 sub-type KIF5B to a 1.8 Å resolution by X-ray crystallography. Kozielski *et al.* (1997) resolved the motor and stalk domains of the KIF5B KHC from rat in its native dimeric form to a resolution of 3 Å. As discussed in Section 1.2.1 the success in determining a crystal structure of the kinesin-1 motor domain, as well as a variety of other contributing data, led to the elucidation of the function and mechanism behind its ability to travel along microtubules. However, this is not the case regarding the structure and function of the cargo binding domain as a crystal structure has yet to be determined. Further, it is not known how the binding of specific cargoes to kinesin-1 is regulated. The TRAK/Milton family are kinesin-1 adaptor proteins which consist of TRAK1 and TRAK2 both of which are known to bind the cargo binding domain of conventional kinesin-1 heavy chains forming a link between the motor protein and cargo (Brickley *et al.*, 2005; Section 1.3). TRAK2 is known to interact with KIF5C via amino acids 124-283 (Brickley *et al.*, 2005). Therefore, it is reasonable to hypothesise that the TRAKs may stabilise the kinesin-1 cargo binding domain. Thus, TRAKs may help to facilitate studies directed towards the determination of the structure of the kinesin-1 cargo binding domain. In this instance it was thought that the presence of the TRAK2 protein, the *in vivo* partner of the kinesin-1 sub-type KIF5A in neurons, may help to stabilise the expression of the cargo binding domain of KIF5A to allow structural studies.

In order to gain high quantities of protein needed to carry out structural studies, most recombinant protein expression strategies involve transforming cells with a DNA expression vector which encodes the nucleotide sequence for the recombinant protein of interest. This expression vector allows the cells to transcribe and translate this protein and the cells are then subsequently lysed to allow extraction of proteins for

purification. There are several systems that can be used to express recombinant proteins for structural studies; these include yeast cells, bacterial cells, insect cells and mammalian cells. In this instance a bacterial expression system will be utilised, of which there are several advantages for the expression of recombinant proteins. Bacterial cells possess a simple physiology that is well characterised; they are capable of short generation times; they can generate high yields of protein and a simple process permits the scale-up of protein expression. Conversely, the quick turnover of protein production in the bacterial cells can lead to improper folding causing inclusion bodies. Toxicity of synthesised proteins to the bacterial cells can prevent high yields. There is also a lack of the eukaryotic post-translational enzymes that might be needed for necessary modifications to the protein.

Studies carried out by Kaan *et al.* (2011) determined the crystal structure of the motor domain of KIF5B binding to a short fragment of the tail domain, equivalent to amino acids 937-952, to a resolution of 2.2 Å. This work also highlights that the cargo binding domain peptide cross-links to the motor domain at two positions, the coiled coil and the tail interface. This cross-linking restricts the movement of the normally mobile motor domain indicating a stabilising effect of the expressed kinesin-1 protein fragment (Kaan *et al.*, 2011). Although this study utilised a synthetic peptide fragment of the cargo binding domain binding to the full dimeric motor domain, this demonstrated the ability of both KIF5B proteins to bind together *in vitro*.

There have been several examples of successful co-expression of motor proteins in bacterial systems. One such example is the co-expression of single-headed kinesin-1 heterodimers consisting of a full length *Drosophila* KHC and a mutated KHC which was devoid of the 340 amino acid motor domain. These proteins were co-expressed in *E.coli* cells and resulted in an increased level of mutated KHC protein of approximately five-fold when compared to the full length KHC (Hancock and Howard, 1998). Another example of successful co-expression was that of the myosin light and myosin heavy chain. This co-expression in bacterial cells resulted in a purified co-complex consisting of a stoichiometric relationship between the heavy and light chain (McNally *et al.*, 1988).

In this Chapter, the aim is to determine the structure of the kinesin-1 C-terminal domain. The method that will be employed is that of simultaneous co-expression of the TRAK2 and KIF5A protein fragments using a single bacterial expression vector. The pETDUET1 vector was selected because it has several advantages over other cloning vectors. It has two multiple cloning sites (MCS) to allow both the TRAK2 and KIF5A protein fragments to be expressed under the same promoter and also has the DNA encoding a His-tag in MCS1 and an S-protein recombinant tag in MCS2. These recombinant tags will help to make extraction of protein more efficient at later stages of the project. As well as co-expressing the KIF5A and TRAK2 protein fragments together each binding region will also be expressed as a single protein. This will allow the efficiency of the expression and stability of soluble KIF5A cargo binding domain protein to be compared with and without the presence of its natural binding partner TRAK2.

### 3.1.1 Aims of this chapter

- I. Generate pETDUET1 bacterial expression constructs of the known interacting domains of TRAK2 and KIF5A, the *in vivo* partner of TRAK2 in the brain i.e. TRAK2<sub>100-380</sub> and KIF5A<sub>800-1032</sub>.
- II. Verify correct TRAK2<sub>100-380</sub> and KIF5A<sub>800-1032</sub> production after transformation and induction of pETDUET1 constructs in bacterial cells.
- III. Optimise the growth and solubilisation conditions needed to maximise soluble TRAK2<sub>100-380</sub> and KIF5A<sub>800-1032</sub> protein expression.
- IV. Purify the TRAK2<sub>100-380</sub>/KIF5A<sub>800-1032</sub> protein co-complex via affinity chromatography.
- V. Resolve the three dimensional structure of the TRAK2<sub>100-380</sub>/KIF5A<sub>800-1032</sub> protein co-complex.

### 3.2 RESULTS

As discussed in Section 1.3 and Section 3.1, TRAK2 is known to interact with kinesin-1 via amino acids 124-283 (Brickley *et al.*, 2005). So to incorporate this binding region as well as the predicted coiled-coil domain (Figure 1.8), the DNA encoding amino acids 100-380 of TRAK2 were cloned into MCS1 of the bacterial expression vector pETDUET1. MCS1 consists of DNA encoding an N-terminal His-tag. To accomplish this oligonucleotide primers specific to amplify the DNA encoding TRAK2<sub>100-380</sub> were designed and used to create the pETDUETTRAK2<sub>100-380</sub> construct. The vector map for pETDUET1 is shown in Figure 3.1.

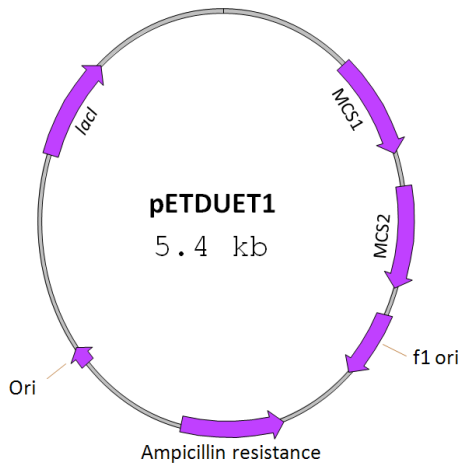


**Figure 3.1 Vector map of pETDUET1.**

To facilitate replication in *E.coli* cells the cloning vector has an ampicillin resistance marker and an origin of replication. The transcription of protein is induced by that of a T7 polymerase in turn controlled by a *lac* operon which induces protein expression in both MCS1 and MCS2. MCS1 has DNA encoding an N-terminal His-tag. MCS2 has DNA encoding a C-terminal S-tag.

All previous work that demonstrated that the kinesin-1 cargo binding domain is responsible for binding to TRAK2 was carried out using KIF5C (Smith *et al.*, 2006; Brickley *et al.*, 2011; Brickley and Stephenson, 2011). It was shown that the amino acids KIF5C 827-957 mediate association with TRAK2. However, in the brain, TRAK2 associates predominantly with the KIF5A (Brickley *et al.*, 2005). Thus KIF5A was used in this study since it most closely mimicked the *in vivo* situation. An amino acid comparison was carried out between KIF5A and KIF5C. The TRAK2 binding region of amino acids KIF5C 827-957 showed a high degree of similarity to KIF5A with an amino acid sequence identity of 84 % and amino acid similarity of 91 %. This was deemed high enough to warrant using KIF5A and still be confident of sufficient interaction. The amino acid alignment of KIF5A and KIF5C is shown in Figure 3.2. KIF5A also has a longer C-terminus than that of KIF5C as KIF5A is 1032 amino acids in length as opposed to the

957 amino acids of KIF5C. So to ensure that the entire TRAK2 binding domain was included it was decided to clone the DNA encoding KIF5A 800-1032. To accomplish this oligonucleotide primers specific to amplify the DNA encoding KIF5A<sub>800-1032</sub> were designed and used to create the pETDUETKIF5A<sub>800-1032</sub> construct. The DNA encoding amino acids KIF5A 800-1032 was cloned into MCS2 of the bacterial expression vector pETDUET1, of which MCS2 consists of DNA encoding a C-terminal S-tag.

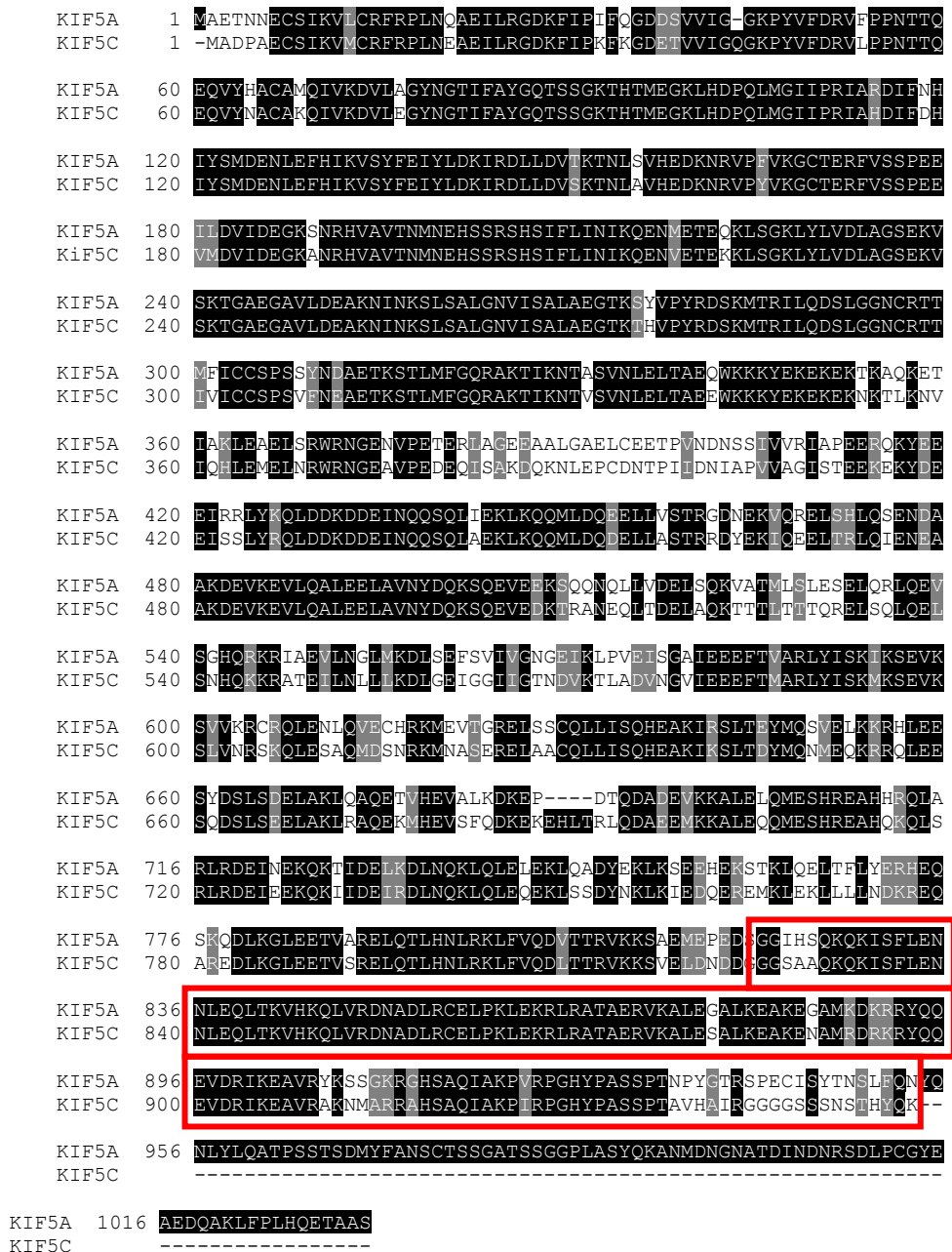


**Figure 3.2 The full amino acid sequence alignment of human KIF5A and KIF5C.**

Sequences were aligned using ClustalW. They share an overall 75 % amino acid identity and 87 % amino acid similarity. The amino acids highlighted in black are those that are identical while those in grey are similar. The known sequence of the TRAK2 binding domain is highlighted with the red boxes.

In order to express recombinant TRAK2<sub>100-380</sub> and KIF5A<sub>800-1032</sub> in a bacterial expression system the constructs pETDUETTRAK2<sub>100-380</sub>, pETDUETKIF5A<sub>800-1032</sub> and pETDUETTRAK2<sub>100-380</sub>/KIF5A<sub>800-1032</sub> were generated. In this chapter the cloning method of the recombinant TRAK2<sub>100-380</sub> and KIF5A<sub>800-1032</sub> clones are described in detail but later chapters will follow the same method presented here. These recombinant constructs were subsequently expressed in *BL21 E.coli* cells and the expressed soluble protein assessed and optimised to increase the yield (Section 2.2.3.1). Soluble protein was then purified using recombinant tag specific affinity chromatography to isolate the proteins of interest (Section 2.2.4).

### **3.2.1 Oligonucleotide primer design for the amplification of rat TRAK2<sub>100-380</sub>**

The nucleotide and amino acid sequence of rat TRAK2 was obtained from the National Centre for Biotechnology Information (NCBI) website (TRAK2 accession number: AJ288898, species: *Rattus norvegicus*, Table 2.5). The full amino acid and nucleotide sequence of TRAK2 with the sequence encoding TRAK2<sub>100-380</sub> to be cloned is highlighted in Figure 3.3. The nucleotide sequence 298-1140 of TRAK2 which corresponds to amino acids 100-380 was used to check which restriction enzymes sites could be utilised to ensure directional cloning into pETDUET1. Restriction enzyme cutting sites were evaluated using software on the bioinformatics website [www.justbio.com](http://www.justbio.com). Thus, enzymes *EcoRI* and *HindIII* were chosen because they did not cut the TRAK2<sub>100-380</sub> DNA sequence and were present in MCS1 of the pETDUET1 vector.

1 - ATGAGTCTGTCCAGAAATGCCATTTTCAAGTCACAAACAGGTGAAGAAAACCTCATGAGT - 60  
1 - M S L S Q N A I F K S Q T G E E N L M S - 20  
61 - AGCAACCATAGAGACTCGGAGAGCATCACTGATGTCTGCTCCAATGAGGATCTCCCTGAG - 120  
21 - S N H R D S E S I T D V C S N E D L P E - 40  
121 - GTCGAGCTGGTCAACTGTCTGGAAGAGCAGCTGCCACAGTATAAGCTAAGAGTGGACTCT - 180  
41 - V E L V N L L E E Q L P Q Y K L R V D S - 60  
181 - CTCTTCTCTACGAAAACCAAGACTGGTCCCAGTCATCACACCAGCAGCAGGATGCATCT - 240  
61 - L F L Y E N Q D W S Q S S H Q Q Q D A S - 80  
241 - GAGACCCTCTCTCCAGTCTGGCTGAGGAGACCTTCCGCTACATGATTCTAGGCACA **GAC** - 300  
81 - E T L S P V L A E E T F R Y M I L G T D - 100  
301 - **AGAGTAGAGCAGATGACAAAACCTACAATGACATTGACATGGTCACGCATCTCCTGGCA** - 360  
101 - R V E Q M T K T Y N D I D M V T H L L A - 120  
361 - **GAGAGGGACCGAGATCTAGAGCTGGCTGCTCGGATTGGGCAAGCCCTGCTAAAGCGGAAC** - 420  
121 - E R D R D L E L A A R I G Q A L L K R N - 140  
421 - **CATGTCTTATCTGAGCAGAATGAATCTCTGGAGGAGCAGCTGGGACAAGCCTTTGATCAA** - 480  
141 - H V L S E Q N E S L E E Q L G Q A F D Q - 160  
481 - **GTCAATCAGCTGCAGCAGGCTGTCCAAGAAAGAGGAGCTGCTCCGAATCGTCTCCATC** - 540  
161 - V N Q L Q H E L S K K E E L L R I V S I - 180  
541 - **GCCTCAGAGGAGAGTGAACGGATTCCAGCTGTCCACACCCTCCGGTTCAATGAGTCC** - 600  
181 - A S E E S E T D S S C S T P L R F N E S - 200  
601 - **TTCAGCTTATCTCAAGCCCTGCTGCAGCTGGACATGATGCACGAGAAGCTCAAGGAGCTG** - 660  
201 - F S L S Q G L L Q L D M M H E K L K E L - 220  
661 - **GAAGAAGAGAACATGGCCCTTCGGTCCAAGGCTTGTACATCAAGACAGAAAACATTTACC** - 720  
221 - E E E N M A L R S K A C H I K T E T F T - 240  
721 - **TATGAAGAGAAGGAACAAAAGCTCATCAATGACTGTGTTAATGAACTCCGTGAGACCAAT** - 780  
241 - Y E E K E Q K L I N D C V N E L R E T N - 260  
781 - **GCACAGATGTCCAGAATGACTGAAGAGCTGTCCGGAAAGAGCGATGAGCTGCTTCGGTAC** - 840  
261 - A Q M S R M T E E L S G K S D E L L R Y - 280  
841 - **CAAGAAGAGATCTCTCCCTGCTGTCTCAGATCGTAGACCTTCAGCACAACCTGAAAGAA** - 900  
281 - Q E E I S S L L S Q I V D L Q H K L K E - 300  
901 - **CATGTGATCGAGAAGGAAGAACTGAGACTTCACTGCAGGCGTCCAAGATGCCAGCGGA** - 960  
301 - H V I E K E E L R L H L Q A S K D A Q R - 320  
961 - **CAGCTGACGATGGAGCTTACAGGTTACAGGACAGAAAACATGGAGTGCCTGGGAATGTTA** - 1020  
321 - Q L T M E L H E L Q D R N M E C L G M L - 340  
1021 - **CATGAGTCTCAAGAAGAAATAAAGAGCTTCGGAACAAGCCGGCCCTTCCGCTCATCTC** - 1080  
341 - H E S Q E E I K E L R N K A G P S A H L - 360  
1081 - **TCCTTCTCCAGGCTTACGGGGTTTTTGCAGGGGAGTCACTG **GCAGCTGAGATGAAAGG**** - 1140  
361 - C F S Q A Y G V F A G E S L A A E I E G - 380  
1141 - ACCATGCGTAAAAGCTGAGTTTGGATGAGGAATCTGTCTTTAAACAAAAGGCCAGCAA - 1200  
381 - T M R K K L S L D E E S V F K Q K A Q Q - 400  
1201 - AAACGGGTGTTTGATACTGTCAAGGTTGCCAACGACACACGGGGCCGCTCTGTCCATTC - 1260  
401 - K R V F D T V K V A N D T R G R S V T F - 420  
1261 - CCAGTCTGCTGCCCATCCAGGCTCCAACCGTTCAAGTGTATCATGACAGCAAAGCCC - 1320  
421 - P V L L P I P G S N R S S V I M T A K P - 440  
1321 - TTTGAGTCCGGTGTTCAGCAAAACAGAGGACAAAACACTCCCGAACCAAGGGAGCAGACA - 1380  
441 - F E S G V Q Q T E D K T L P N Q G S S T - 460  
1381 - GAGGTTCCAGGAACTCTCATCCCAGGACCCCCAGGACTCCCTGAAGATAGTGACCTG - 1440  
461 - E V P G N S H P R D P P G L P E D S D L - 480  
1441 - GCTACAGCATTCATCGCCTTAGCCTGAGAAGACAGAACTACCTAAGTGAGAAGCAGTTC - 1500  
481 - A T A L H R L S L R R Q N Y L S E K Q F - 500  
1501 - TTCGCTGAAGAATGGGAACGGAAGCTCCAGATTCTGGCTGAGCAGGAGGAAGAAGTTAGC - 1560  
501 - F A E E W E R K L Q I L A E Q E E E V S - 520  
1561 - AGCTGTGAGGCCCTCACGGAGAACCTTGCCCTATTCTGCACTGACCAGTCAGAGACCAG - 1620  
521 - S C E A L T E N L A S F C T D Q S E T T - 540  
1621 - GAGCTCGGCAGTGCCGGCTGCCTTCGAGGCTTCATGCCAGAAAAGTTACAGATTGTCAAG - 1680  
541 - E L G S A G C L R G F M P E K L Q I V K - 560  
1681 - CCCCTAGAAGGATCACAGACGTACATCATTGGCAGCAGCTTGCTCAACCAACTTGGGA - 1740  
561 - P L E G S Q T L H H W Q Q L A Q P N L G - 580  
1741 - ACCATCCTTGATCCACGCCCAGGCGTCATCACTAAAGGCTTCACGCAGATGCCCAAGGAT - 1800  
581 - T I L D P R P G V I T K G F T Q M P K D - 600  
1801 - GCCGTCTATCACATCTCGGATTTGGAGGAGGATGAAGAAGTGGGGATCACTTTTCAGGTT - 1860  
601 - A V Y H I S D L E E D E E V G I T F Q V - 620  
1861 - CAGCAGCCTCTCAACTGGAGCAGAAGCCTGCACCACCCCGCCAGTAACGGGTATCTTC - 1920

```

621 - Q Q P L Q L E Q K P A P P P P V T G I F - 640
1921 - CTGCCGCCATGACCTCAGCAGGGGGACCAGTCTCAGTTGCAACTTCGAACCCAGGAAAG - 1980
641 - L P P M T S A G G P V S V A T S N P G K - 660
1981 - TGTCTCTCATTACGAACTCAACATTCACCTTACCACCTGCAGGATCTTACACCCCTCT - 2040
661 - C L S F T N S T F T F T T C R I L H P S - 680
2041 - GACATCACTCAGGTCACCCCTAGCTCTGGTTTCCCATCACTGTCCTGTGGAAGCAGTGG - 2100
681 - D I T Q V T P S S G F P S L S C G S S A - 700
2101 - GGCAGTGCATCCAACACGGCTGTGAACTCTCTGCTGCGTCTACAGACTGAGCATTGGT - 2160
701 - G S A S N T A V N S P A A S Y R L S I G - 720
2161 - GAATCCATCACAACCGCGCGACTCCACCATAACGTTTCAGTAGCACGAGGAGCTTAGCC - 2220
721 - E S I T N R R D S T I T F S S T R S L A - 740
2221 - AAACCTCTGCAGGAGCGAGGCATCTCCGCCAAAGTGTACCACAGCCAGCTTCAGAAAAC - 2280
741 - K L L Q E R G I S A K V Y H S P A S E N - 760
2281 - CCCCTTCTACAGCTTCGCCCAAGGCCCTGGCCACCCCTTCCACACCACCAAATTCCTCCG - 2340
761 - P L L Q L R P K A L A T P S T P P N S P - 780
2341 - TCGCAGTCACCATGTTCTCCCCCGTCCCTTTGAACCCCGTCCATGTCTCCGAGAAT - 2400
781 - S Q S P C S S P V P F E P R V H V S E N - 800
2401 - TTCTTGGCTTCCAGACCAGCTGAAACATTCCTGCAAGAAATGTATGGCTTGAGACCTTCA - 2460
801 - F L A S R P A E T F L Q E M Y G L R P S - 820
2461 - AGGGCCCTCCTGATGTTGGCCAGCTGAAGATGAACTTGGTGGACAGGCTGAAGAGGCTG - 2520
821 - R A P P D V G Q L K M N L V D R L K R L - 840
2521 - GGAATAGCCAGGGTGGTCAAGACCCCTGTTCCCGGGGAGAATGGGAAAAGCCGAGAGGCA - 2580
841 - G I A R V V K T P V P R E N G K S R E A - 860
2581 - GAAATGGTCTTCAAAAACCAGACTCTGCTGTCTATTTAAATCTGGTGGCAGTTTATTG - 2640
861 - E M G L Q K P D S A V Y L N S G G S L L - 880
2641 - GGTGGACTGAGGAGGAATCAGAGTCTCCAGTCATGATGGGTAGCTTGGAGCCCCAGTT - 2700
881 - G G L R R N Q S L P V M M G S F G A P V - 900
2701 - TGCACAACCTCGCCCAAAATGGGTATCCTGAAGGAAGACTGA - 2742
901 - C T T S P K M G I L K E D - 920

```

**Figure 3.3 Full nucleotide and amino acid sequence of rat TRAK2.**

The kinesin-1 binding site of TRAK2 is highlighted in blue. The sequences to which the oligonucleotide primers for generation of TRAK2<sub>100-380</sub> were designed are highlighted in yellow. The nucleotide sequence to be cloned is TRAK2 298-1140 (842 base pairs [bp]) encoding for the amino acid sequence TRAK2 100-380 (280).

#### Forward oligonucleotide primer design:

In order to design the forward oligonucleotide primer 18 bases were selected at the start of the desired sequence and the first enzyme cutting region was inserted (*EcoRI*).

5' **GAA TTC GAC AGA GTA GAG CAG ATG** 3'

Four **adenine** nucleotides were inserted in the start of the sequence to help with the binding of the restriction enzymes.

5' **AAAA GAA TTC GAC AGA GTA GAG CAG ATG** 3'

This sequence was checked to ensure that if inserted into the vector it would be transcribed in the correct reading frame.

**Current reading frame:** CCG AAT TCG ACA GAG TAG AGC AGA TG  
Thr Glu stop

**Desired reading frame:** GAC AGA GTA GAG CAG ATG  
Asp Arg Val Glu Gln Met

This sequence would not transcribe in the correct reading frame so an extra base was added to the start of the sequence. In this case the nucleotide **adenine** was added so that the translated amino acid will remain a serine. The inserted nucleotide sequence will now read in the correct reading frame.

5' **AAAA G AAT TCA** GAC AGA GTA GAG CAG ATG 3'

#### Reverse oligonucleotide primer design:

In order to design the reverse oligonucleotide primer a similar method to that of the forward oligonucleotide primer design was employed but with the reverse and complementary base pair sequence.

original: 5' GCA GCT GAG ATT GAA GGG 3'

complementary bases: 3' CGT CGA CTC TAA CTT CCC 5'

reversed: 5' CCC TTC AAT CTC AGC TGC 3'

A stop codon was added to the end of the sequence. In this case **TAG** (also the reverse and complementary base pair sequence). This is because the His-tag will be located at the N-terminus of the expressed TRAK2 protein fragment and the stop codon will prevent the C-terminus possessing unnecessary amino acids.

5' **CTA** CCC TTC AAT CTC AGC TGC 3'

The enzyme binding domain **HindIII** was added (**not** the reverse complementary nucleotide sequence).

5' **AAG CTT CTA** CCC TTC AAT CTC AGC TGC 3'

Four **adenine** nucleotides were inserted at the start of the sequence to help with the binding of the restriction enzymes. Two bases at the 3' end were removed to ensure it is fewer than 30 bases in length as this will help increase the efficiency in production of the oligonucleotide primer.

5' **AAAA AAG CTT CTA** CCC TTC AAT CTC AGC T 3'

The GC content and T<sub>m</sub> of each of the primers was calculated (Section 2.2.2.3) and deemed to be within the set parameters.

Forward primer GC content = 47 %

Reverse primer GC content = 50 %

Forward primer T<sub>m</sub> = 56°C

Reverse primer T<sub>m</sub> = 60°C

### 3.2.1.1 Preparation of the pETDUETTRAK2<sub>100-380</sub> construct

The DNA encoding TRAK2<sub>100-380</sub> was amplified from pCISTRAK2 using the primers designed in Section 3.2.1 and the PCR reaction conditions stated in Section 2.2.2.3.1. The resulting PCR product was analysed by 1 % (w/v) flat bed agarose gel (Section 2.2.2.4) and the results of the PCR amplification are shown in Figure 3.4.

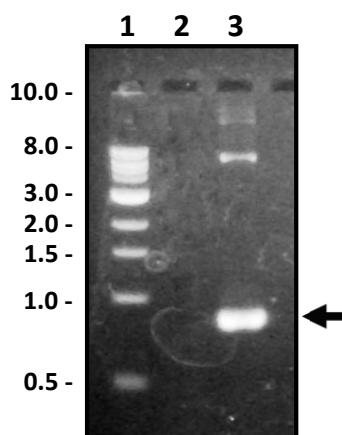


**Figure 3.4 Flat bed agarose gel electrophoresis analysis of TRAK2<sub>100-380</sub> nucleotide amplification by PCR.**

**Lane 1** = kb DNA standards. **Lane 2** = control PCR reaction; i.e. no pCISTRAK2 template DNA. **Lane 3** = PCR reaction. The band of interest is highlighted on the right by an arrow.

A band of the correct predicted size of ~ 840 bp for the TRAK2<sub>100-380</sub> nucleotide sequence was present in the reaction lane but not in the control lane. Following correct PCR amplification both the DNA encoding TRAK2<sub>100-380</sub> and the pETDUET1 vector were restriction enzyme digested to create “sticky ends” using the restriction enzymes *EcoRI* and *HindIII* (Section 2.2.2.6). The restriction enzyme digested vector sample was subsequently dephosphorylated to prevent digested vectors from annealing to one another (Section 2.2.2.8). The restriction enzyme digested TRAK2<sub>100-380</sub> nucleotide sequence was subsequently ligated into MCS1 of the pETDUET1 vector using T4 DNA ligase. The ligation reactions were carried out using vector:insert ratios of 1:1 and 1:3 (Section 2.2.2.9). The resulting ligation reactions were transformed into *DH5α E.coli* cells (Section 2.2.1.2). The results of the ligation reactions are summarised in Table 3.1.

Plate number	Restriction enzyme digested and dephosphorylated vector	Restriction enzyme digested insert	T4 DNA ligase	Number of <i>DH5α E.coli</i> colonies after transformation
1	pETDUET1 1 µl	DNA encoding TRAK2 <sub>100-380</sub> 1 µl	✓	120
2	pETDUET1 1 µl	DNA encoding TRAK2 <sub>100-380</sub> 3 µl	✓	148
3	pETDUET1 1 µl	DNA encoding TRAK2 <sub>100-380</sub> 1 µl	✗	1
4	pETDUET1 1 µl	-	✓	0
5	pETDUET1 1 µl	-	✗	18
Negative control (ddH <sub>2</sub> O)	-	-	✗	0
Positive control (pETDUET1)	-	-	✗	1,000+

**Table 3.1** Summary table of the ligation reactions used to create pETDUETTRAK2<sub>100-380</sub>.

Plate numbers one and two were the test plates and these showed the numbers of colonies to be 120 and 148 respectively. Plate numbers three, four and five were controls used to check the efficiency of both the restriction enzyme digestion and the dephosphorylation of the plasmid vector. The three control plates showed low colony numbers, which when compared to the high colony numbers seen in plates one and two indicated a successful ligation experiment. Of the resulting colonies four were selected from plate number two. These colonies were grown overnight in 5 ml of LB media and a mini preparation of plasmid DNA carried out (Section 2.2.2.11). Plasmid DNA samples were restriction enzyme digested with *EcoRI* and *HindIII* and analysed using 1 % agarose gel electrophoresis to check for the presence of the TRAK2<sub>100-380</sub> nucleotide sequence. The results of the restriction enzyme digestion are shown in Figure 3.5.

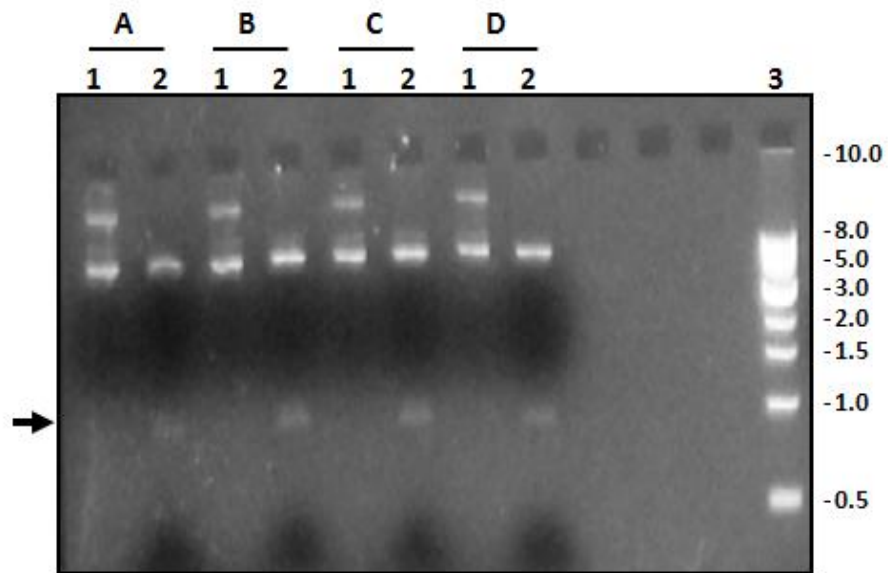


**Figure 3.5 Analysis of putative pETTRAK<sub>2100-380</sub> constructs by 1 % (w/v) flat bed agarose gel electrophoresis.**

The four potential pETDUETTRAK<sub>2100-380</sub> clones are lettered **A, B, C** and **D**. **Lanes numbered 1** = non-restriction enzyme digested controls. **Lanes numbered 2** = *EcoRI* and *HindIII* restriction enzyme digested samples. **Lane 3** = kb DNA standards. The bands of interest highlighted on the left by an arrow.

All four samples show a band of ~ 840 bp in length indicating a successful ligation of TRAK<sub>2100-380</sub> nucleotide sequence into pETDUET1. The DNA corresponding to lanes C2 and D2 was precipitated (Section 2.2.2.13) and sequenced by MWG-Biotech (Ebersberg, Germany) to confirm the correct insertion of the TRAK<sub>2100-380</sub> DNA sequence. The entire DNA sequence of the TRAK<sub>2100-380</sub> insert was sequenced and an example of the results from the sequencing reaction is shown in Figure 3.6.

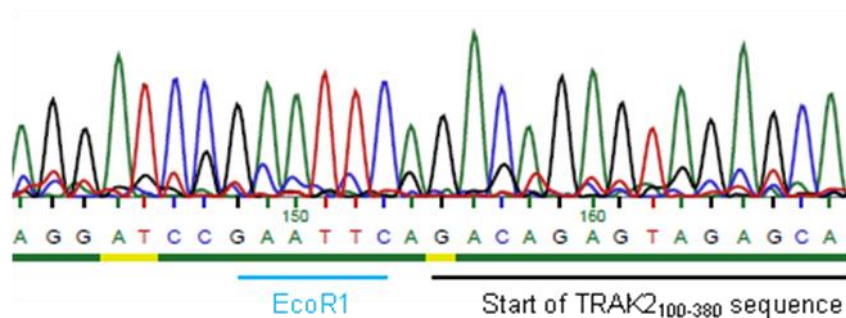


**Figure 3.6 Nucleotide sequencing results of the pETDUETTRAK<sub>2100-380</sub> clone.**

The first restriction enzyme site of *EcoRI* is underlined in blue and the sequence of the TRAK<sub>2100-380</sub> DNA insert is underlined in black.

Sequencing results showed the correct ligation of the TRAK2<sub>100-380</sub> nucleotide sequence into the pETDUET1 vector. The nucleotide sequence is in the correct reading frame with no mutations present. The pETDUETTRAK2<sub>100-380</sub> plasmid vector was subsequently transformed into *DH5α E.coli* cells and a maxi-preparation of the resulting DNA carried out (Section 2.2.2.12). The purified pETDUETTRAK2<sub>100-380</sub> clone was stored as 100 µl aliquots at -20°C until further use.

### **3.2.2 Oligonucleotide primer design for the amplification of human KIF5A<sub>800-1032</sub>**

The nucleotide and amino acid sequence of KIF5A was obtained from the NCBI website (KIF5A accession number: HSU06698, species: *Homo sapiens*, Table 2.5). The full amino acid and nucleotide sequence of KIF5A with the sequence encoding KIF5A<sub>800-1032</sub> to be cloned is highlighted in Figure 3.7. The nucleotide sequence 2398-3097 of KIF5A which corresponds to amino acids 800-1032 was used to check which restriction enzyme sites could be utilised to ensure directional cloning into the pETDUET1 vector. Restriction enzyme cutting sites were evaluated using software on the bioinformatics website [www.justbio.com](http://www.justbio.com). Thus, enzymes *MunI* and *FseI* were chosen because they did not cut the KIF5A<sub>800-1032</sub> sequence and were present in MCS2 of the pETDUET1 vector.

1 - ATGGCGGAAACCAACAACGAATGCAGCATTAAAGTGCTGTGCCGCTTTCGCCCGCTGAAC - 60  
1 - M A E T N N E C S I K V L C R F R P L N - 20  
61 - CAGGCGGAAATCTGCGCGGCGATAAATTTATCCGATTTTTTCAGGGCGATGATAGCGTG - 120  
21 - Q A E I L R G D K F I P I F Q G D D S V - 40  
121 - GTGATTGGCGCAAACCGTATGTGTTTGTATCGCGTGTTCGCCCGAACACCACCCAGGAA - 180  
41 - V I G G K P Y V F D R V F P P N T T Q E - 60  
181 - CAGGTGTATCATGCGTGCAGCAGATTGTGAAAGATGTGCTGGCGGGCTATAACGGC - 240  
61 - Q V Y H A C A M Q I V K D V L A G Y N G - 80  
241 - ACCATTTTTGCGTATGGCCAGACCAGCAGCGGCAAACCCATAACCATGGAAGGCAAACCTG - 300  
81 - T I F A Y G Q T S S G K T H T M E G K L - 100  
301 - CATGATCCGCAGCTGATGGGCATTATTCGCCGCTGCGCGCGATATTTTTAACCATATT - 360  
101 - H D P Q L M G I I P R I A R D I F N H I - 120  
361 - TATAGCATGGATGAAAACCTGGAATTTTCATATTAAGTGAGCTATTTTTGAAATTTATCTG - 420  
121 - Y S M D E N L E F H I K V S Y F E I Y L - 140  
421 - GATAAAATTCGCGATCTGCTGGATGTGACCAAAACCAACCTGAGCGTGCATGAAGATAAA - 480  
141 - D K I R D L L D V T K T N L S V H E D K - 160  
481 - AACCGCGTCCGCTTTGTGAAAGGCTGCACCGAACGCTTTGTGAGCAGCCCGGAAGAAATT - 540  
161 - N R V P F V K G C T E R F V S S P E I - 180  
541 - CTGGATGTGATTGATGAAGGCAAAGCAACCGCCATGTGGCGGTGACCAACATGAACGAA - 600  
181 - L D V I D E G K S N R H V A V T N M N E - 200  
601 - CATAGCAGCCGAGCCATAGCATTTTTCTGATTAACATTAACAGGAAAACATGGAAACC - 660  
201 - H S S R S H S I F L I N I K Q E N M E T - 220  
661 - GAACAGAACTGAGCGGCAACTGTATCTGGTGGATCTGGCGGGCAGCGAAAAGTGAAC - 720  
221 - E Q K L S G K L Y L V D L A G S E K V S - 240  
721 - AAAACCGCGCGGAAGGCGCGGTGCTGGATGAAGCGAAAACATTAACAAAAGCCTGAGC - 780  
241 - K T G A E G A V L D E A K N I N K S L S - 260  
781 - GCGCTGGCAACGTGATTAGCGCGTGGCGGAAGGCACAAAAGCTATGTGCCGTATCGC - 840  
261 - A L G N V I S A L A E G T K S Y V P Y R - 280  
841 - GATAGCAAAATGACCCGATTTCTGCAGGATAGCCTGGGCGGCAACTGCCGACCCACATG - 900  
281 - D S K M T R I L Q D S L G G N C R T T M - 300  
901 - TTTATTTGCTGCAGCCCGAGCAGCTATAACGATGCGGAAACCAAAGCACCTGATGTTT - 960  
301 - F I C C S P S S Y N D A E T K S T L M F - 320  
961 - GGCCAGCGCGGAAACCATTAAAAACACCCGCGAGCGTGAACCTGGAACCTGACCCGCGAA - 1020  
321 - G Q R A K T I K N T A S V N L E L T A E - 340  
1021 - CAGTGGAAAAAATATGAAAAAGAAAAAGAAAAACCAAAGCGCAGAAAGAAACCATT - 1080  
341 - Q W K K K Y E K E K E K T K A Q K E T I - 360  
1081 - GCGAACTGGAAGCGGAACTGAGCCGCTGGCGCAACGGCGAAAACGTCGCCGAAACCGAA - 1140  
361 - A K L E A E L S R W R N G E N V P E T E - 380  
1141 - CGCCTGGCGGGCGAAGAAGCGGCGCTGGGCGGGAAGTGTGCGAAGAAACCCGCGTGAAC - 1200  
381 - R L A G E E A A L G A E L C E E T P V N - 400  
1201 - GATAACAGCAGCATTGTTGGTGCATTCGCCCGGAAGAACGCCAGAAATATGAAGAAGAA - 1260  
401 - D N S S I V V R I A P E E R Q K Y E E E - 420  
1261 - ATTCGCCGCTGTATAAACAGCTGGATGATAAAGATGATGAAATTAACCAGCAGAGCCAG - 1320  
421 - I R R L Y K Q L D D K D D E I N Q Q S - 440  
1321 - CTGATTGAAAACTGAAACAGCAGATGCTGGATCAGGAAGAACTGCTGGTGAACCCCGC - 1380  
441 - L I E K L K Q Q M L D Q E E L L V S T R - 460  
1381 - GGCGATAACGAAAAAGTGCAGCGGCAACTGAGCCATCTGCAGAGCGAAAACGATGCGGCG - 1440  
461 - G D N E K V Q R E L S H L Q S E N D A A - 480  
1441 - AAAGATGAAGTGAAGAAGTGTGTCAGGCGCTGGAAGAACTGGCGGTGAACATGATGATG - 1500  
481 - K D E V K E V L Q A L E E L A V N D Q - 500  
1501 - AAAAGCCAGGAAGTGAAGAAGAAAGCCAGCAGAACCCAGCTGCTGGTGGATGAACTGAGC - 1560  
501 - K S Q E V E E K S Q Q N Q L L V D E L S - 520  
1561 - CAGAAAGTGGCGACCATGCTGAGCCTGGAAAGCGAAGTGCAGCGCCTGCAGGAAGTGAAC - 1620  
521 - Q K V A T M L S L E S E L Q R L Q E V S - 540  
1621 - GGCCATCAGCGCAAAACGCATTGCGGAAGTGTGAAAGCGCCTGATGAAAGATCTGAGCGAA - 1680  
541 - G H Q R K R I A E V L N G L M K D L S E - 560  
1681 - TTTAGCGTATTGTTGGCAACGGCGAAATTAACCTGCGGTTGAAATTAGCGGCGCGATT - 1740  
561 - F S V I V G N G E I K L P V E I S G A I - 580  
1741 - GAAGAAGAATTTACCGTGGCGCGCTGTATATTAGCAAAATTAAGCGAAGTGAAGG - 1800  
581 - E E E F T V A R L Y I S K I K S E V K S - 600  
1801 - GTGGTGAACGCTGCCGCCAGCTGGAACCTGCAGGTGGAATGCCATCGCAAAATGGAA - 1860  
601 - V V K R C R Q L E N L Q V E C H R K M E - 620  
1861 - GTGACCGCCGCAACTGAGCAGCTGCCAGCTGCTGATTAGCCAGCATGAAGCGAAAATT - 1920  
621 - V T G R E L S S C Q L L I S Q H E A K I - 640  
1921 - CGCAGCCTGACCGAATATATGAGAGCGTGGAACTGAAAACCGCCATCTGGAAGAAAGC - 1980  
641 - R S L T E Y M Q S V E L K K R H L E E S - 660  
1981 - TATGATAGCCTGAGCGATGAACTGGCGAAACTGCAGGCGCAGGAAACCGTGCATGAAGTG - 2040  
661 - Y D S L S D E L A K L Q A Q E T V H E V - 680  
2041 - GCGCTGAAAGATAAAGAACCGGATACCCAGGATGCGGATGAAGTGAAGAAAGCGCTGGAA - 2100  
681 - A L K D K E P D T Q D A D E V K K A L E - 700  
2101 - CTGCAGATGGAAGCCATCGCGAAGCGCATCGCCAGCTGGCGCGCTGCGCGATGAA - 2160  
701 - L Q M E S H R E A H H R Q L A R L R D E - 720  
2161 - ATTAACGAAAACAGAAAACCATTTGATGAACTGAAAGATCTGAACCGAAAACCTGCAGCTG - 2220  
721 - I N E K Q K T I D E L K D L N Q K L Q L - 740

```

2221 - GAACTGGAAAACTGCAGGCGGATTATGAAAACTGAAAAGCGAAGAACATGAAAAAGC - 2280
741 - E L E K L Q A D Y E K L K S E E H E K S - 760
2281 - ACCAACTGCAGGAAGTACCTTTCTGTATGAACGCCATGAACAGAGCAAACAGGATCTG - 2340
761 - T K L Q E L T F L Y E R H E Q S K Q D L - 780
2341 - AAGGGTCTGGAGGAGACAGTTGCCCGGAACTCCAGACCCTCCACAACCTTCGCAAGCTG - 2400
781 - K G L E E T V A R E L Q T L H N L R K L - 800
2401 - TTCGTTCAAGACGTCACGACTCGAGTCAAGAAAAGTGCAGAAATGGAGCCCGAAGACAGT - 2460
801 - F V Q D V T T R V K K S A E M E P E D S - 820
2461 - GGGGGGATTCACTCCAAAAGCAGAAGATTTCTTTCTTGAGAACAACCTGGAACAGCTT - 2520
821 - G G I H S Q K Q K I S F L E N N L E Q L - 840
2521 - ACAAAGTTTCAAAAACAGCTGGTACGTGACAATGCAGATCTGCGTTGTGAGCTTCCTAAA - 2580
841 - T K V H K Q L V R D N A D L R C E L P K - 860
2581 - TTGGAAAAACGACTTAGGGCTACGGCTGAGAGAGTTAAGGCCCTGGAGGGTGCCTGAAG - 2640
861 - L E K R L R A T A E R V K A L E G A L K - 880
2641 - GAGGCCAAGGAGGGGCCATGAAGGACAAGCGCCGGTACCAGCAGGAGGTGGACCCGATC - 2700
881 - E A K E G A M K D K R R Y Q Q E V D R I - 900
2701 - AAGGAGGCCGTTGCTACAAGAGCTCGGGCAAACGGGCGCATTTGCCAGATTGCCAAA - 2760
901 - K E A V R Y K S S G K R A H S A Q I A K - 920
2761 - CCCGTCGGCCCTGGCCACTACCAGCATCCTCACCACCAACCCCTATGGCACCCGGAGC - 2820
921 - P V R P G H Y P A S S P T N P Y G T R S - 940
2821 - CCTGAGTGCATCAGTTACACCAACAGCCTCTTCCAGAATACCAGAATCTCTACCTGCAG - 2880
941 - P E C I S Y T N S L F Q N Y Q N L Y L Q - 960
2881 - GCCACACCCAGCTCCACCTCAGATATGTACTTTGCAAACCTCCTGTACCAGCAGTGGAGCC - 2940
961 - A T P S S T S D M Y F A N S C T S S G A - 980
2941 - ACATCTTCTGGCGGCCCTTTGGCTTCTTACCAGAAGGCCAATGGACAATGGAAATGCC - 3000
981 - T S S G G P L A S Y Q K A N M D N G N A - 1000
3001 - ACAGATATCAATGACAATAGGAGTGACCTGCCGTGTGGCTATGAGGCTGAGGACCAGGCC - 3060
1001 - T D I N D N R S D L P C G Y E A E D Q A - 1020
3061 - AAGCTTTTCCCTCTCCACCAAGAGACAGCAGCCAGC - 3097
1021 - K L F P L H Q E T A A S - 1032

```

**Figure 3.7 The full nucleotide and amino acid sequence of human KIF5A.**

The predicted TRAK2 binding site of KIF5A is highlighted in blue. The sequences to which the oligonucleotide primers for generation of KIF5A<sub>800-1032</sub> were designed are highlighted in yellow. The amino acid sequence to be cloned are KIF5A 800-1032 (232) and the nucleotide sequence KIF5A 2398-3097 (696 bp).

#### Forward oligonucleotide primer design:

In order to design the forward oligonucleotide primer 18 bases were selected at the start of the desired sequence and the first enzyme cutting region was inserted (*MunI*).

5' **CAA TTG CTG TTC GTT CAA GAC GTC** 3'

Four **adenine** nucleotides were inserted in the start of the sequence to help with the binding of the restriction enzymes.

5' **AAAA CAA TTG CTG TTC GTT CAA GAC GTC** 3'

This sequence was checked to ensure that if inserted into the vector it would read in the correct frame.

**Current reading frame: C AAT TGC TGT TCG TTC AAG ACG TC**

**Cys Ser Phe Lys Thr**

**Desired reading frame:**

**CTG TTC GTT CAA GAC GTC**

**Leu Phe Val Gln Asp Val**

This sequence would not transcribe in the correct reading frame so an extra base was added to the start of the sequence. In this case the nucleotide **guanine** was added so

that the amino acid will remain a tryptophan. The inserted nucleotide sequence will read in the correct frame.

5' AAAA C AAT TGG CTG TTC GTT CAA GAC GTC 3'

#### Reverse oligonucleotide primer design:

In order to design the reverse oligonucleotide primer a similar method to that of the forward oligonucleotide primer design was employed but with the reverse complementary base pair sequence.

original: 5' CAA GAG ACA GCA GCC AGC 3'

complementary bases: 3' GTT CTC TGT CGT CGG TCG 5'

reverse: 5' GCT GGC TGC TGT CTC TTG 3'

The enzyme binding domain *FseI* was added (**not** the reverse complementary nucleotide sequence).

5' GGCCGGCC GCT GGC TGC TGT CTC TTG 3'

Four adenine nucleotides were inserted at the start of the sequence to help with the binding of the restriction enzymes.

5' AAAA GGCCGGCC GCT GGC TGC TGT CTC TTG 3'

A guanine and a cytosine nucleotide were added to make alanine; this keeps the sequence in frame for the S-tag which occurs after the KIF5A<sub>800-1032</sub> nucleotide sequence. Two bases at the 3' end were removed to ensure it is fewer 30 bases in length as this will help increase the efficiency in production of the oligonucleotide primer.

5' AAAA G GCC GGC CGC GCT GGC TGC TGT CTC T 3'

The GC and T<sub>m</sub> of each of the primers was calculated (Section 2.2.2.3) and deemed to be within the set parameters.

Forward primer GC content = 53 %

Reverse primer GC content = 67 %

Forward primer T<sub>m</sub> = 58°C

Reverse primer T<sub>m</sub> = 60°C

### 3.2.2.1 Preparation of the pETDUETKIF5A<sub>800-1032</sub> construct

The DNA encoding KIF5A<sub>800-1032</sub> was amplified from pBSKIF5A using the primers designed in Section 3.2.2 and the PCR reaction conditions stated in Section 2.2.2.3.1. The resulting PCR product was analysed by a 1 % (w/v) flat bed agarose gel (Section 2.2.2.4) and the results of the PCR amplification is shown in Figure 3.8.

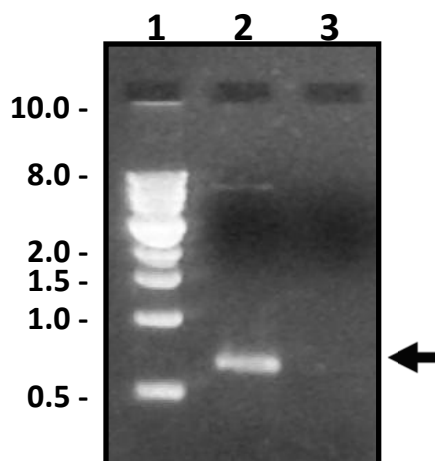


**Figure 3.8 Flat bed agarose gel electrophoresis analysis of KIF5A<sub>800-1032</sub> nucleotide amplification by PCR.**

**Lane 1** = kb DNA standards. **Lane 2** = KIF5A<sub>800-1032</sub> PCR reaction. **Lane 3** = control PCR reaction; i.e. no pBSKIF5A template DNA. The band of interest is highlighted on the right by an arrow.

A band of the correct predicted size of ~ 700 bp for the KIF5A<sub>800-1032</sub> nucleotide sequence was present in the reaction lane but not the control lane. This is as expected and demonstrates that the PCR amplification of the KIF5A<sub>800-1032</sub> sequence was successful. Following correct PCR amplification both the KIF5A<sub>800-1032</sub> nucleotide sequence and pETDUET1 vector were restriction enzyme digested to create “sticky ends” using the restriction enzymes *FseI* and *MunI*. Due to several failed attempts to ligate the KIF5A<sub>800-1032</sub> nucleotide sequence into pETDUET1 the buffer conditions for the restriction enzyme digestions were optimised. This was achieved through a series of sequential and double digestions and also a variety of different buffer conditions. It was found that the optimal conditions for that of a successful digestion was a double digestion using two units of both *FseI* and *MunI* and 1 × concentrated Tango<sup>TM</sup> restriction endonuclease buffer (of which none were the recommended conditions or buffers for the *FseI* and *MunI* enzymes). The restriction enzyme digested KIF5A<sub>800-1032</sub> nucleotide sequence was subsequently ligated into MCS2 of the pETDUET1 vector

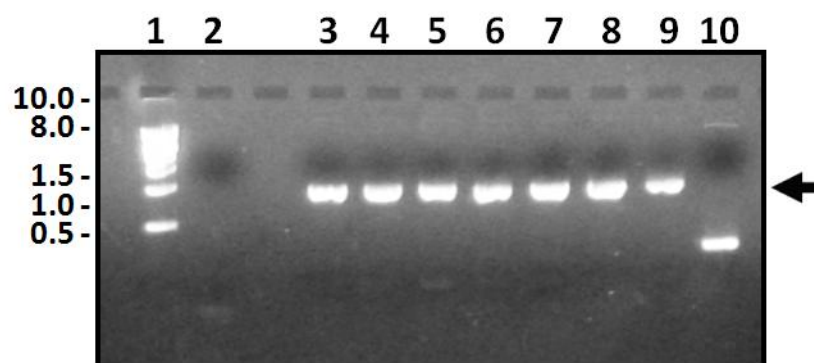
using T4 DNA ligase. The ligation reactions were carried out using vector:insert ratios of 1:4 and 1:7 as previously described in Section 2.2.2.9. The resulting ligation reactions were transformed into *DH5α E.coli* cells (Section 2.2.1.2). The results of the ligation reactions are summarised in Table 3.2.

Plate number	Restriction enzyme digested and dephosphorylated vector	Restriction enzyme digested insert	T4 DNA ligase	Number of <i>DH5α E.coli</i> colonies after transformation
1	pETDUET1 1 µl	KIF5A <sub>800-1032</sub> 4 µl	✓	0
2	pETDUET1 1 µl	KIF5A <sub>800-1032</sub> 7 µl	✓	7
3	pETDUET1 1 µl	KIF5A <sub>800-1032</sub> 1 µl	✗	0
4	pETDUET1 1 µl	-	✓	0
5	pETDUET1 1 µl	-	✗	0
Negative control (ddH <sub>2</sub> O)	-	-	✗	0
Positive control (pETDUET1)	-	-	✗	1,000+

**Table 3.2 Summary table of the ligation reactions used to create pETDUETKIF5A<sub>800-1032</sub>.**

Plate numbers one and two were the test plates and these showed the numbers of colonies to be zero and seven respectively. Plate numbers three, four and five were controls used to check the efficiency of both the restriction enzyme digestion and the dephosphorylation of the plasmid vector. The three control plates showed no colony numbers, which when compared to the seven colony numbers seen in plate two indicated a successful ligation experiment. Of the resulting colonies all seven were selected from plate number two. These colonies were grown overnight in 5 ml of LB media and a mini preparation of plasmid DNA subsequently carried out (Section 2.2.2.11). PCR screening (Section 2.2.2.10) was used to determine the presence of the

KIF5A<sub>800-1032</sub> nucleotide insert due to the previous difficulties in obtaining efficient restriction enzyme digestion with *FseI* and *MunI*. PCR screening was carried out using the sequencing oligonucleotide primers designed to the MCS2 of the pETDUET1 vector. The sequencing oligonucleotide primers were used because previous PCR screens using the KIF5A<sub>800-1032</sub> oligonucleotide primers had yielded false positive bands of ~ 700 bp. This was found to be the result of a sequence similarity between these primers and the pETDUET1 vector sequence yielding a band of the same size. If positive for the KIF5A<sub>800-1032</sub> nucleotide insert a band of ~ 900 bases in length would be produced. The results were then analysed using a 1 % (w/v) flat bed agarose gel. The results of the PCR screen are shown in Figure 3.9.



**Figure 3.9 Analysis of putative pETDUETKIF5A<sub>800-1032</sub> constructs using a PCR screen by 1 % (w/v) flat bed agarose gel electrophoresis.**

**Lane 1** contains the DNA standards in kb. **Lane 2** shows the control PCR reaction; i.e. no pBSKIF5A template DNA. **Lanes 3-9** show the ligated colonies tested for a successful KIF5A<sub>800-1032</sub> nucleotide insert. **Lane 10** shows the empty pETDUET1 vector control. The bands of interest are highlighted on the right by an arrow.

Lanes 3-9 show a band of ~ 900 bases in length indicating a successful ligation of the KIF5A<sub>800-1032</sub> nucleotide sequence into pETDUET1. The DNA corresponding to lane three was precipitated (Section 2.2.2.13) and sequenced by MWG-Biotech (Ebersberg, Germany) to confirm the correct insertion of the KIF5A<sub>800-1032</sub> sequence. The entire DNA sequence of the KIF5A<sub>800-1032</sub> insert was sequenced and an example of the results from the sequencing reaction is shown in Figure 3.10.

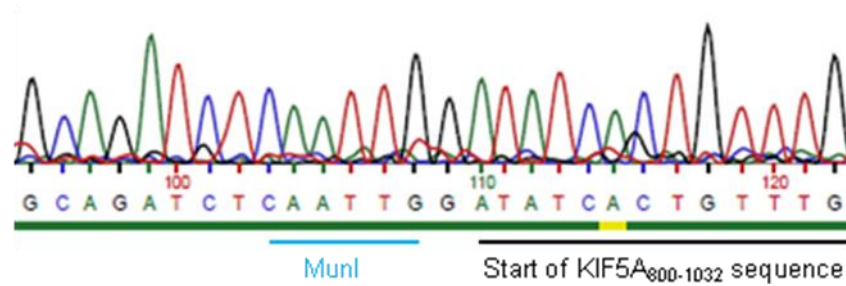


**Figure 3.10 Nucleotide sequencing results of the pETDUETKIF5A<sub>800-1032</sub> clone.**

The first restriction enzyme site of *MunI* is underlined in blue and the sequence of the KIF5A<sub>800-1032</sub> insert DNA is underlined in black.

Sequencing results show the correct ligation of the KIF5A<sub>800-1032</sub> nucleotide sequence into the pETDUET1 vector. The nucleotide sequence is in the correct reading frame and has no mutations present. The pETDUETKIF5A<sub>800-1032</sub> plasmid vector was subsequently transformed into *DH5α E.coli* cells and a maxi-preparation of the resulting DNA carried out (Section 2.2.2.12). The purified pETDUETKIF5A<sub>800-1032</sub> clone was stored as 100 µl aliquots at -20°C until further use.

### 3.2.3 Preparation of the pETDUETTRAK2<sub>100-380</sub>/KIF5A<sub>800-1032</sub> construct

Generation of pETDUETTRAK2<sub>100-380</sub>/KIF5A<sub>800-1032</sub> involved inserting the DNA encoding for KIF5A<sub>800-1032</sub> into MCS2 of pETDUETTRAK2<sub>100-380</sub>. The TRAK2<sub>100-380</sub> DNA sequence was unable to be inserted into pETDUETKIF5A<sub>800-1032</sub> due to the restriction enzymes *EcoRI* and *HindIII* both digesting within the KIF5A<sub>800-1032</sub> DNA sequence. Whereas the *FseI* and *MunI* enzymes used for KIF5A<sub>800-1032</sub> cloning did not digest anywhere in the TRAK2<sub>100-380</sub> DNA sequence and so could be inserted into pETDUETTRAK2<sub>100-380</sub>. The KIF5A<sub>800-1032</sub> DNA sequence was inserted into pETDUETTRAK2<sub>100-380</sub> as in Section 3.2.2.1. pETDUETTRAK2<sub>100-380</sub>/KIF5A<sub>800-1032</sub> was precipitated (Section 2.2.2.13) and sequenced by MWG-Biotech (Ebersberg, Germany) to confirm the correct insertion of the KIF5A<sub>800-1032</sub> sequence. Additionally MCS1 was sequenced to confirm the presence of TRAK2<sub>100-380</sub> DNA. A summary of all three pETDUET1 clones are shown in Figure 3.11.

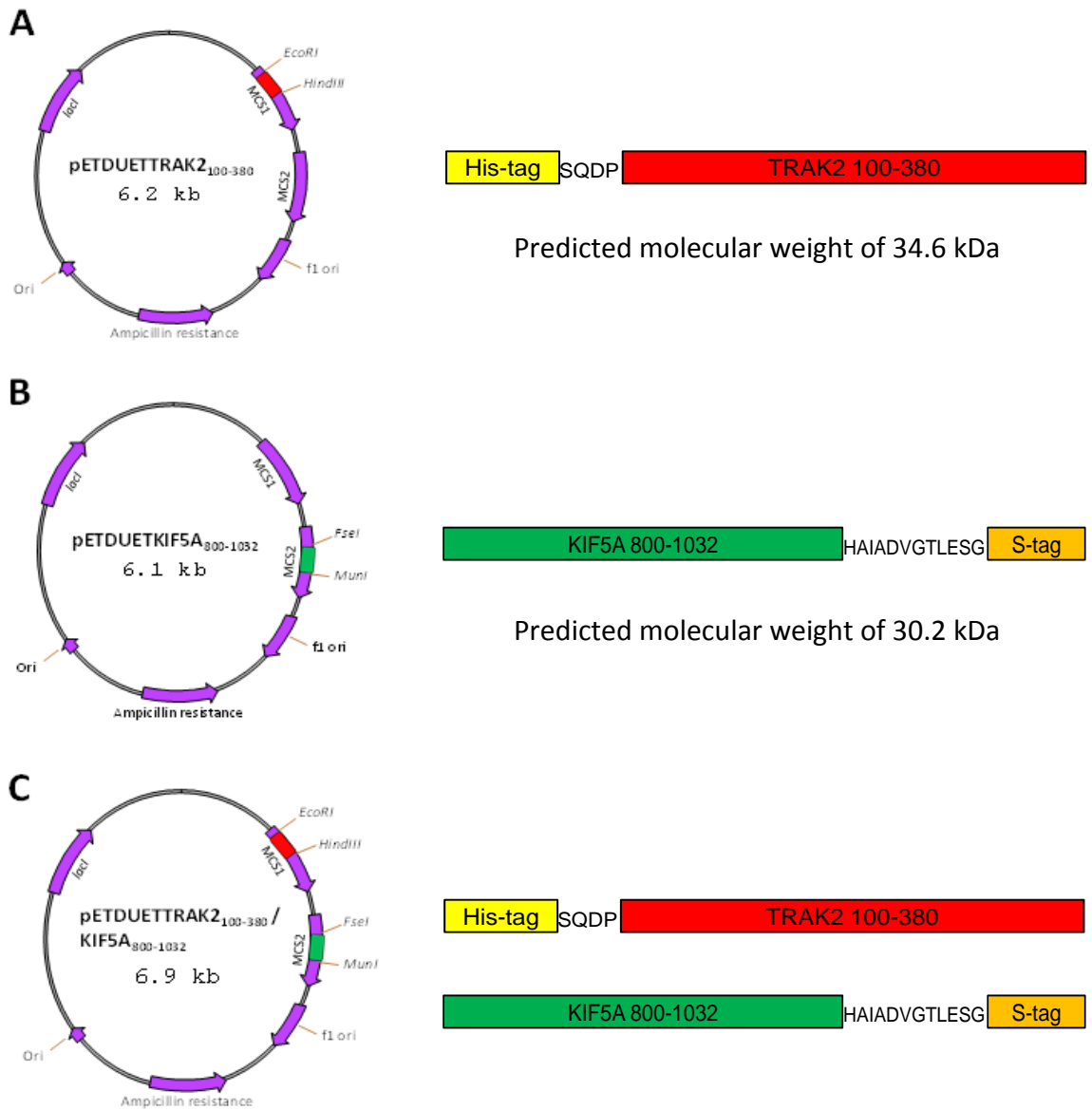


**Figure 3.11 Summary of the pETDUETTRAK2<sub>100-380</sub>, pETDUETKIF5A<sub>800-1032</sub> and pETDUETTRAK2<sub>100-380</sub>/KIF5A<sub>800-1032</sub> recombinant clones.**

The vector maps are shown on the left and a schematic of the primary structure of the resultant proteins and their predicted molecular weights are shown on the right.

**A** = pETDUETTRAK2<sub>100-380</sub> **B** = pETDUETKIF5A<sub>800-1032</sub> **C** = pETDUETTRAK2<sub>100-380</sub>/KIF5A<sub>800-1032</sub>.

### 3.2.4 Optimisation of TRAK2<sub>100-380</sub>, KIF5A<sub>800-1032</sub> and TRAK2<sub>100-380</sub>/KIF5A<sub>800-1032</sub> protein expression

Previous work in this chapter has demonstrated the successful generation of the recombinant expression constructs pETDUETTRAK2<sub>100-380</sub>, pETDUETKIF5A<sub>800-1032</sub> and pETDUETTRAK2<sub>100-380</sub>/KIF5A<sub>800-1032</sub>. To determine if these three clones can express the expected recombinant proteins, the pETDUETTRAK2<sub>100-380</sub>, pETDUETKIF5A<sub>800-1032</sub> and pETDUETTRAK2<sub>100-380</sub>/KIF5A<sub>800-1032</sub> constructs were transformed into chemically competent *BL21 E.coli* cells and protein expression induced (Section 2.2.3.1). Initial protein expression experiments utilised 1 mM IPTG to induce expression for a total of 4 h at 37°C. The resulting total expressed protein was re-suspended in 8 ml of native buffer, centrifuged to separate protein into soluble and insoluble protein fractions and ~ 1.5 µg of each protein fraction analysed via 12 % SDS-PAGE (Section 2.2.3.4). The resulting Coomassie Blue stained SDS-PAGE gels are shown in Figure 3.12. Each construct was successfully expressed as demonstrated by bands corresponding to their predicted sizes in the total and insoluble protein fractions, i.e. TRAK2<sub>100-380</sub> = 35.6 ± 2.3 kDa (n = 20, where n = number of SDS-PAGE), KIF5A<sub>800-1032</sub> = 35.4 ± 2.5 kDa (n = 20) and TRAK2<sub>100-380</sub>/KIF5A<sub>800-1032</sub> = 35.2 ± 1.9 kDa (n = 10)/35.2 ± 2.1 kDa (n = 10). In the pETDUETTRAK2<sub>100-380</sub>/KIF5A<sub>800-1032</sub> induced vector two bands are present indicating that both the TRAK2<sub>100-380</sub> and KIF5A<sub>800-1032</sub> protein fragments are able to be expressed simultaneously. No TRAK2<sub>100-380</sub> and KIF5A<sub>800-1032</sub> expressed protein could be visualised via Coomassie Blue staining in the soluble fractions derived from pETDUETTRAK2<sub>100-380</sub>, pETDUETKIF5A<sub>800-1032</sub> and pETDUETTRAK2<sub>100-380</sub>/KIF5A<sub>800-1032</sub> expression. Although the average molecular weights seen in SDS-PAGE experiments are the same for TRAK2<sub>100-380</sub> and KIF5A<sub>800-1032</sub>, KIF5A<sub>800-1032</sub> is seen to be the larger of the two bands. This is unexpected as the predicted molecular weight for KIF5A<sub>800-1032</sub> is larger than that of TRAK2<sub>100-380</sub> (Figure 3.11) and this may be due to SDS resistance of KIF5A<sub>800-1032</sub> resulting in the protein band running slightly higher than expected. Alternatively inherent differences between both KIF5A<sub>800-1032</sub> and TRAK2<sub>100-380</sub> in their charge distribution may also alter the position at which they are seen via SDS-PAGE.

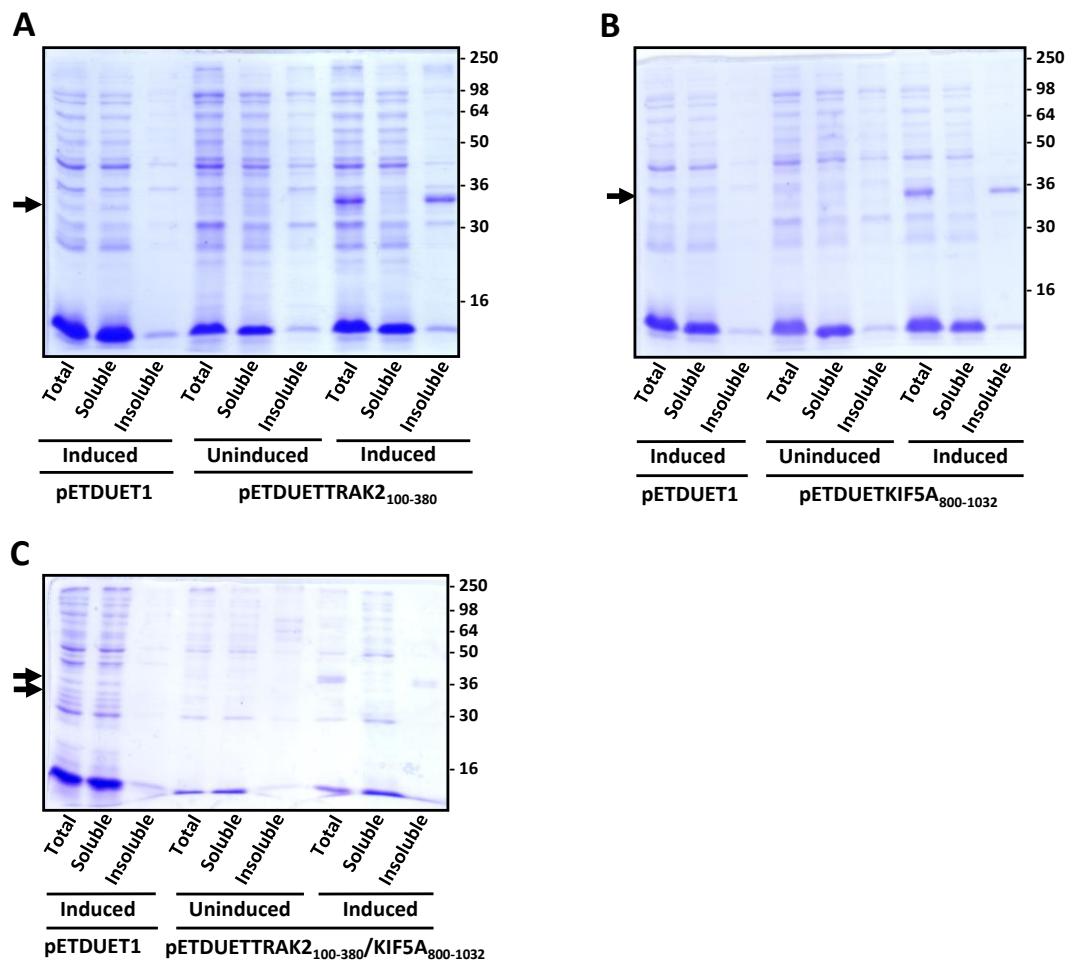


**Figure 3.12 Demonstration of the expression of TRAK2<sub>100-380</sub>, KIF5A<sub>800-1032</sub> and TRAK2<sub>100-380</sub>/KIF5A<sub>800-1032</sub> in BL21 *E.coli* cells.**

BL21 *E.coli* cells were transformed with pETDUETTRAK2<sub>100-380</sub>, pETDUETKIF5A<sub>800-1032</sub> or pETDUETTRAK2<sub>100-380</sub>/KIF5A<sub>800-1032</sub>. Cell homogenates were prepared after induction of protein expression using 1 mM IPTG for 4 hours at 37°C. In all Coomassie Blue stained gels the total, soluble and insoluble protein of the induced plasmids are shown. The induced pETDUET1 vector and uninduced controls were included. The positions of molecular weight standards (kDa) are shown on the right. Arrows indicate the positions of bands of interest.

**A** = TRAK2<sub>100-380</sub> **B** = KIF5A<sub>800-1032</sub> **C** = TRAK2<sub>100-380</sub>/KIF5A<sub>800-1032</sub>.

To verify that the pETDUETTRAK2<sub>100-380</sub>, pETDUETKIF5A<sub>800-1032</sub> and pETDUETTRAK2<sub>100-380</sub>/KIF5A<sub>800-1032</sub> constructs were the desired TRAK2<sub>100-380</sub> and KIF5A<sub>800-1032</sub> proteins, immunoblotting was carried out using anti-TRAK2<sub>8-633</sub> (TRAK2<sub>100-380</sub>) and anti-S-tag (KIF5A<sub>800-1032</sub>) antibodies (Figure 3.11). The resulting immunoblots are shown in figure 3.13.

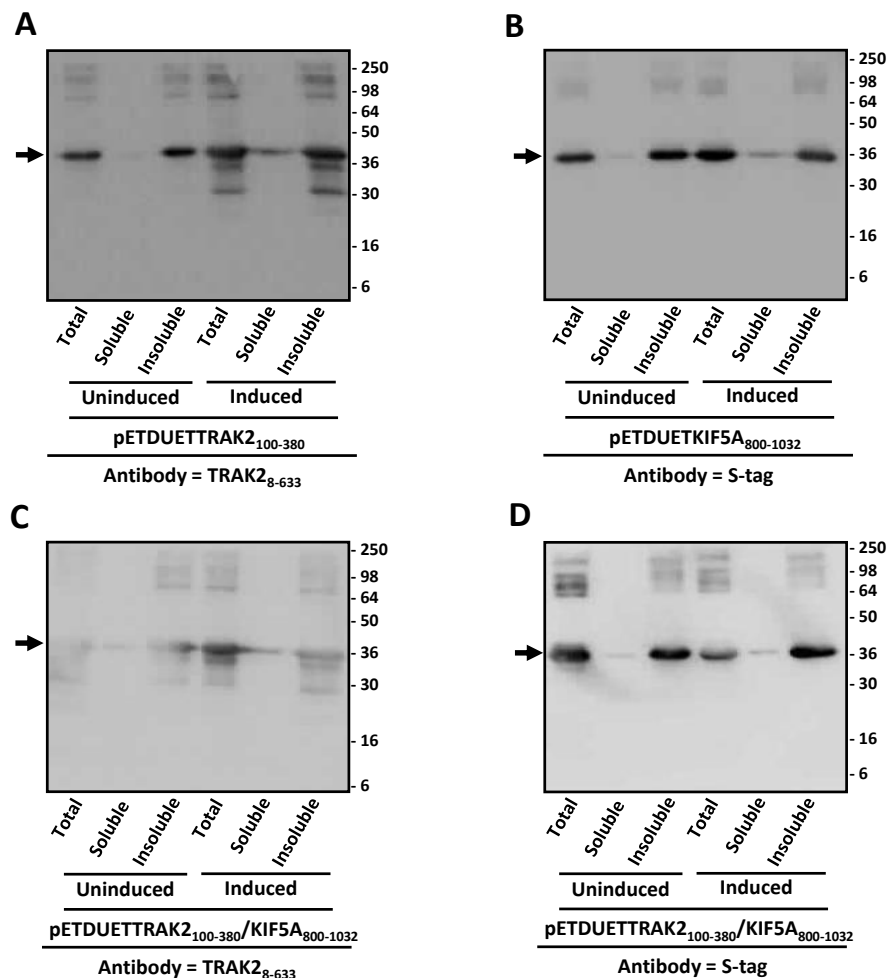


**Figure 3.13** Demonstration of the expression of TRAK2<sub>100-380</sub>, KIF5A<sub>800-1032</sub> and TRAK2<sub>100-380</sub>/KIF5A<sub>800-1032</sub> in *BL21 E.coli* cells.

*BL21 E.coli* cells were transformed with pETDUETTRAK2<sub>100-380</sub>, pETDUETKIF5A<sub>800-1032</sub> or pETDUETTRAK2<sub>100-380</sub>/KIF5A<sub>800-1032</sub>. Cell homogenates were prepared after induction of protein expression using 1 mM IPTG for 4 hours at 37°C. In all immunoblots total, soluble and insoluble protein of the induced and uninduced plasmids are shown. The positions of molecular weight standards (kDa) are shown on the right. Arrows indicate the positions of bands of interest.

**A** = TRAK2<sub>100-380</sub> probed with anti-TRAK2<sub>8-633</sub> antibodies. **B** = KIF5A<sub>800-1032</sub> probed with anti-S-tag antibodies. **C** = TRAK2<sub>100-380</sub>/KIF5A<sub>800-1032</sub> probed with anti-TRAK2<sub>8-633</sub> antibodies. **D** = TRAK2<sub>100-380</sub>/KIF5A<sub>800-1032</sub> probed with anti-S-tag antibodies.

Immunoblotting with the anti-TRAK2<sub>8-633</sub> and anti-S-tag antibodies confirms the correct transcription of TRAK2<sub>100-380</sub> and KIF5A<sub>800-1032</sub> with immunoreactive bands present in all total, soluble and insoluble fractions. Anti-TRAK2<sub>8-633</sub> as opposed to anti-His antibodies was used due to the ease of readily available in house anti-TRAK2<sub>8-633</sub> antibodies. Anti-TRAK2<sub>8-633</sub> can also detect the presence of the His-tag sequence (Table 2.4). Overall a lower concentration of TRAK2<sub>100-380</sub> and KIF5A<sub>800-1032</sub> protein is present in the soluble extract when compared to both the total and insoluble fractions. In all total and insoluble fractions the presence of several higher molecular weight bands were seen at

weights in the range of 70 - 250 kDa. These bands are most likely aggregated TRAK2<sub>100-380</sub> and KIF5A<sub>800-1032</sub> protein sample. Anti-TRAK2<sub>8-633</sub> antibodies also recognised two major immunoreactive bands lower than the predicted molecular weight of TRAK2<sub>100-380</sub> in the pETDUETTRAK2<sub>100-380</sub> and pETDUETTRAK2<sub>100-380</sub>/KIF5A<sub>800-1032</sub> induced constructs. These lower molecular weight bands may be the result of proteolytic degradation. Protein expression was also noted in the uninduced control. The presence of transcribed protein in the uninduced control is indicative of “leaky expression”. Leaky expression occurs when the *lac* operon responsible for controlling the T7 promoter is no longer being repressed due to the presence of lactose within the *E.coli* cell. *E.coli* cells prefer glucose as a carbon source but when glucose is not available then the cells use lactose, which in turn can promote this leaky expression (Alberts *et al.*, 2007). To prevent uninduced protein expression 1 % w/v glucose was added to the LB growth media. The resulting immunoblots are shown in Figure 3.14.

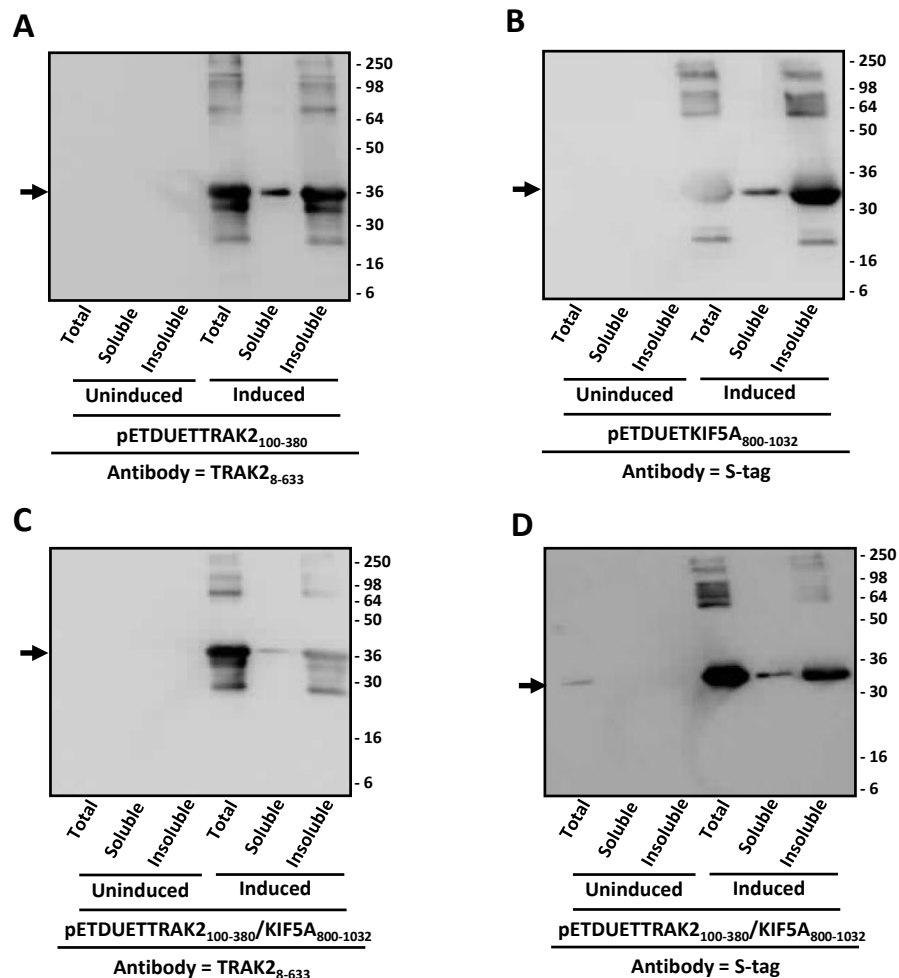


**Figure 3.14 Demonstration of the expression of TRAK2<sub>100-380</sub>, KIF5A<sub>800-1032</sub> and TRAK2<sub>100-380</sub>/KIF5A<sub>800-1032</sub> in *BL21 E.coli* cells with 1 % w/v glucose supplemented LB media.**

*BL21 E.coli* cells were transformed with pETDUETTRAK2<sub>100-380</sub>, pETDUETKIF5A<sub>800-1032</sub> or pETDUETTRAK2<sub>100-380</sub>/KIF5A<sub>800-1032</sub>. Cell homogenates were prepared after growth conditions of 1 % w/v glucose supplemented LB media, with the induction of protein expression using 1 mM IPTG for 4 hours at 37°C. In all immunoblots total, soluble and insoluble protein of the induced and uninduced plasmids are shown. The positions of molecular weight standards (kDa) are shown on the right. Arrows indicate the positions of bands of interest.

**A** = TRAK2<sub>100-380</sub> probed with anti-TRAK2<sub>8-633</sub> antibodies. **B** = KIF5A<sub>800-1032</sub> probed with anti-S-tag antibodies. **C** = TRAK2<sub>100-380</sub>/KIF5A<sub>800-1032</sub> probed with anti-TRAK2<sub>8-633</sub> antibodies. **D** = TRAK2<sub>100-380</sub>/KIF5A<sub>800-1032</sub> probed with anti-S-tag antibodies.

No immunoreactive bands are present in any of the uninduced samples after growth of *BL21 E.coli* and induction of protein expression in 1 % w/v glucose supplemented LB media, with the exception of a faint band in the total fraction of the TRAK2<sub>100-380</sub>/KIF5A<sub>800-1032</sub> anti-S-tag antibody probed immunoblot. Overall a lower concentration of TRAK2<sub>100-380</sub> and KIF5A<sub>800-1032</sub> protein present in the soluble extract compared to both the total and insoluble fractions is noted. The ratio of protein in the soluble compared to the insoluble is important because if large scale protein purification is to be efficient a high concentration of protein in the soluble fraction is required. Proteins

in the insoluble fraction aggregate into inclusion bodies which in turn require the proteins to be denatured and subsequently refolded *in vitro* to generate viable protein. This method can result in incorrect refolding of protein which is not ideal for structural studies. In order to increase the ratio of soluble:insoluble expressed protein as well as increasing protein yield different growth and re-suspension conditions were tested. These included lowering the concentration of IPTG used to induce protein expression, increasing the induction time and altering buffer re-suspension conditions. All of the immunoblots representing the differing growth and re-suspension conditions were analysed semi-quantitatively using GeneGnome Tools software (Section 2.2.3.5.3). The ratio of immunoreactivity of the soluble fraction was taken and expressed as a percentage of both the soluble and insoluble fraction combined which is 100 %. Not only was the percentage solubility of the protein used to assess the efficiency of protein expression, but also the yield of protein expression was taken into account i.e. can the expressed soluble protein band be visualised after Coomassie Blue staining? Optimisation of the expression and solubilisation conditions of TRAK2<sub>100-380</sub> is summarized in Table 3.3.

Growth conditions	Re-suspension conditions	Immunoblot analysis	Coomassie Blue staining analysis	% Solubilisation	N number
37°C, 1 mM IPTG, 4 hours induction	8 ml native buffer 250 mM NaH <sub>2</sub> PO <sub>4</sub> [pH 8.0] 1 mg/ml lysozyme	Total = Visible band Insoluble = Visible band Soluble = Visible band	Total = Visible band Insoluble = Visible band Soluble = No Visible band	18 %	1
37°C, 0.1 mM IPTG, 4 hours induction	8 ml native buffer 250 mM NaH <sub>2</sub> PO <sub>4</sub> [pH 8.0] 1 mg/ml lysozyme	Total = Visible band Insoluble = Visible band Soluble = Visible band	Total = Visible band Insoluble = Visible band Soluble = No Visible band	31 %	1
1 % glucose media, 37°C, 1 mM IPTG, 4 hours induction	8 ml native buffer 250 mM NaH <sub>2</sub> PO <sub>4</sub> [pH 8.0] 1 mg/ml lysozyme	Total = Visible band Insoluble = Visible band Soluble = Visible band	Total = Visible band Insoluble = Visible band Soluble = No Visible band	22 %	1
1 % glucose media, 25°C, 1 mM IPTG, 4 hours induction	8 ml native buffer 250 mM NaH <sub>2</sub> PO <sub>4</sub> [pH 8.0] 1 mg/ml lysozyme	Total = Visible band Insoluble = Visible band Soluble = Visible band	Total = <b>No Visible band</b> Insoluble = <b>No Visible band</b> Soluble = No Visible band	35 %	3
1 % glucose media, 25°C, 0.1 mM IPTG, 4 hours induction	8 ml native buffer 250 mM NaH <sub>2</sub> PO <sub>4</sub> [pH 8.0] 1 mg/ml lysozyme	Total = Visible band Insoluble = Visible band Soluble = Visible band	Total = <b>Faint band</b> Insoluble = <b>Faint band</b> Soluble = No Visible band	27 %	1
1 % glucose media, 25°C, 1 mM IPTG, 4 hours induction	<b>8 ml re-suspension buffer (50 mM TRIS [pH 8.0], 400 mM NaCl, 10 % w/v glycerol, 5 mM β-ME) 1 mg/ml lysozyme)</b>	Total = Visible band Insoluble = Visible band Soluble = Visible band	Total = Faint band Insoluble = Faint band Soluble = No Visible band	34 %	1
1 % glucose media, 25°C, 1 mM IPTG, 4 hours induction	8 ml re-suspension buffer (50 mM TRIS [pH 8.0], 400 mM NaCl, 10 % w/v glycerol, 5 mM β-ME, <b>protease inhibitors</b> ) 1 mg/ml lysozyme)	Total = Visible band Insoluble = Visible band Soluble = Visible band	Total = Faint band Insoluble = Faint band Soluble = No Visible band	35 %	1
1 % glucose media, 25°C, 1 mM IPTG, 4 hours induction	8 ml re-suspension buffer (50 mM TRIS [pH 8.0], 400 mM NaCl, 10 % w/v glycerol, 5 mM β-ME, protease inhibitors) <b>20 µg/ml lysozyme)</b>	Total = Visible band Insoluble = Visible band Soluble = Visible band	Total = Faint band Insoluble = Faint band Soluble = No Visible band	24 %	1
1 % glucose media, 25°C, 1 mM IPTG, <b>16 hour induction</b>	8 ml re-suspension buffer (50 mM TRIS [pH 8.0], 400 mM NaCl, 10 % w/v glycerol, 5 mM β-ME, protease inhibitors) 20 µg/ml lysozyme)	Total = Visible band Insoluble = Visible band Soluble = Visible band	Total = Faint band Insoluble = Faint band Soluble = No Visible band	16 %	1
1 % glucose media, 25°C, 1 mM IPTG, 4 hours induction	<b>1 ml re-suspension buffer (50 mM TRIS [pH 8.0], 400 mM NaCl, 10 % w/v glycerol, 5 mM β-ME, protease inhibitors) 20 µg/ml lysozyme)</b>	Total = Visible band Insoluble = Visible band Soluble = Visible band	Total = <b>Visible band</b> Insoluble = <b>Visible band</b> Soluble = No Visible band	16 %	1
1 % glucose media, 37°C, 1 mM IPTG, <b>16 hour induction</b>	8 ml re-suspension buffer (50 mM TRIS [pH 8.0], 400 mM NaCl, 10 % w/v glycerol, 5 mM β-ME, protease inhibitors) 20 µg/ml lysozyme)	Total = Visible band Insoluble = Visible band Soluble = Visible band	Total = Visible band Insoluble = Visible band Soluble = No Visible band	24 %	1
1 % glucose media, 37°C, 1 mM IPTG, 4 hours induction	<b>1 ml re-suspension buffer (50 mM TRIS [pH 8.0], 400 mM NaCl, 10 % w/v glycerol, 5 mM β-ME, protease inhibitors) 20 µg/ml lysozyme)</b>	Total = Visible band Insoluble = Visible band Soluble = Visible band	Total = Visible band Insoluble = Visible band Soluble = No Visible band	22 %	1

**Table 3.3 A summary of growth conditions to establish optimal conditions for the expression and solubilisation of TRAK2<sub>100-380</sub>.**

Text highlighted in red indicates a change from the previous condition tested.

Results from optimisation of the expressed pETDUETRAK2<sub>100-380</sub> clone found poor overall expression in all conditions tested. The growth conditions of 1 mM IPTG and 4 hours induction at 25°C show clear bands in the total and insoluble but not in the soluble fractions after staining protein with Coomassie Blue. Optimisation of the expression and solubilisation conditions of KIF5A<sub>800-1032</sub> is summarised in Table 3.4.

Growth conditions	Re-suspension conditions	Immunoblot analysis	Coomassie Blue staining analysis	% Solubilisation	N number
37°C, 1 mM IPTG, 4 hours induction	8 ml native buffer 250 mM NaH <sub>2</sub> PO <sub>4</sub> [pH 8.0] 1 mg/ml lysozyme	Total = Visible band Insoluble = Visible band Soluble = Visible band	Total = Visible band Insoluble = Visible band Soluble = No Visible band	4 %	1
37°C, 0.1 mM IPTG, 4 hours induction	8 ml native buffer 250 mM NaH <sub>2</sub> PO <sub>4</sub> [pH 8.0] 1 mg/ml lysozyme	Total = Visible band Insoluble = Visible band Soluble = Visible band	Total = Visible band Insoluble = Visible band Soluble = No Visible band	9 %	1
1 % glucose media, 37°C, 1 mM IPTG, 4 hours induction	8 ml native buffer 250 mM NaH <sub>2</sub> PO <sub>4</sub> [pH 8.0] 1 mg/ml lysozyme	Total = Visible band Insoluble = Visible band Soluble = Visible band	Total = Visible band Insoluble = Visible band Soluble = No Visible band	13 %	1
1 % glucose media, 25°C, 1 mM IPTG, 4 hours induction	8 ml native buffer 250 mM NaH <sub>2</sub> PO <sub>4</sub> [pH 8.0] 1 mg/ml lysozyme	Total = Visible band Insoluble = Visible band Soluble = Visible band	Total = Visible band Insoluble = Visible band Soluble = <b>Faint band</b>	30 %	3
1 % glucose media, 25°C, 0.1 mM IPTG, 4 hours induction	8 ml native buffer 250 mM NaH <sub>2</sub> PO <sub>4</sub> [pH 8.0] 1 mg/ml lysozyme	Total = Visible band Insoluble = Visible band Soluble = Visible band	Total = Visible band Insoluble = Visible band Soluble = Faint band	48 %	1
1 % glucose media, 25°C, 1 mM IPTG, 4 hours induction	<b>8 ml re-suspension buffer (50 mM TRIS [pH 8.0], 400 mM NaCl, 10 % w/v glycerol, 5 mM β-ME) 1 mg/ml lysozyme)</b>	Total = Visible band Insoluble = Visible band Soluble = Visible band	Total = Visible band Insoluble = Visible band Soluble = <b>No Visible band</b>	8 %	1
1 % glucose media, 25°C, 1 mM IPTG, 4 hours induction	8 ml re-suspension buffer (50 mM TRIS [pH 8.0], 400 mM NaCl, 10 % w/v glycerol, 5 mM β-ME, <b>protease inhibitors</b> ) 1 mg/ml lysozyme)	Total = Visible band Insoluble = Visible band Soluble = Visible band	Total = Visible band Insoluble = Visible band Soluble = <b>Faint band</b>	13 %	1
1 % glucose media, 25°C, 1 mM IPTG, 4 hours induction	8 ml re-suspension buffer (50 mM TRIS [pH 8.0], 400 mM NaCl, 10 % w/v glycerol, 5 mM β-ME, protease inhibitors) <b>20 µg/ml lysozyme)</b>	Total = Visible band Insoluble = Visible band Soluble = Visible band	Total = Visible band Insoluble = Visible band Soluble = Faint band	35 %	1
1 % glucose media, 25°C, 1 mM IPTG, 16 hour induction	8 ml re-suspension buffer (50 mM TRIS [pH 8.0], 400 mM NaCl, 10 % w/v glycerol, 5 mM β-ME, protease inhibitors) 20 µg/ml lysozyme)	Total = Visible band Insoluble = Visible band Soluble = Visible band	Total = Visible band Insoluble = Visible band Soluble = <b>No Visible band</b>	16 %	1
1 % glucose media, 25°C, 1 mM IPTG, 4 hours induction	<b>1 ml re-suspension buffer (50 mM TRIS [pH 8.0], 400 mM NaCl, 10 % w/v glycerol, 5 mM β-ME, protease inhibitors) 20 µg/ml lysozyme)</b>	Total = Visible band Insoluble = Visible band Soluble = Visible band	Total = Visible band Insoluble = Visible band Soluble = <b>Visible band</b>	24 %	1

**Table 3.4 A summary of growth conditions to establish optimal conditions for the expression and solubilisation of KIF5A<sub>800-1032</sub>.**

Text highlighted in red indicates a change from the previous condition tested.

Results from optimisation of the expression and solubilisation of the pETDUETKIF5A<sub>800-1032</sub> clone show good overall expression in all conditions tested. The optimal growth conditions of 1 mM IPTG and 4 hours induction at 25°C show clear bands in the total, soluble and insoluble fractions after staining protein with Coomassie Blue. Optimisation of the expression and solubilisation conditions of co-expressed TRAK2<sub>100-380</sub> and KIF5A<sub>800-1032</sub> is summarised in Table 3.5 (TRAK2<sub>100-380</sub>) and Table 3.6 (KIF5A<sub>800-1032</sub>).

Growth conditions	Re-suspension conditions	Immunoblot analysis	Coomassie Blue staining analysis	% Solubilisation	N number
37°C, 1 mM IPTG, 4 hours induction	8 ml native buffer 250 mM NaH <sub>2</sub> PO <sub>4</sub> [pH 8.0] 1 mg/ml lysozyme	Total = Visible band Insoluble = Visible band Soluble = Visible band	Total = 2 faint bands Insoluble = 2 visible bands Soluble = No visible bands	40 %	1
37°C, 0.1 mM IPTG, 4 hours induction	8 ml native buffer 250 mM NaH <sub>2</sub> PO <sub>4</sub> [pH 8.0] 1 mg/ml lysozyme	Total = Visible band Insoluble = Visible band Soluble = Visible band	Total = 2 visible bands Insoluble = 2 visible bands Soluble = No visible bands	2 %	1
1 % glucose media, 37°C, 1 mM IPTG, 4 hours induction	8 ml native buffer 250 mM NaH <sub>2</sub> PO <sub>4</sub> [pH 8.0] 1 mg/ml lysozyme	Total = Visible band Insoluble = Visible band Soluble = Visible band	Total = 2 visible bands Insoluble = 2 visible bands Soluble = No visible bands	18 %	1
1 % glucose media, 25°C, 1 mM IPTG, 4 hours induction	8 ml native buffer 250 mM NaH <sub>2</sub> PO <sub>4</sub> [pH 8.0] 1 mg/ml lysozyme	Total = Visible band Insoluble = Visible band Soluble = Visible band	Total = 2 visible bands Insoluble = 2 visible bands Soluble = No visible bands	29 %	3
1 % glucose media, 25°C, 0.1 mM IPTG, 4 hours induction	8 ml native buffer 250 mM NaH <sub>2</sub> PO <sub>4</sub> [pH 8.0] 1 mg/ml lysozyme	Total = Visible band Insoluble = Visible band Soluble = Visible band	Total = <b>2 faint bands</b> Insoluble = <b>2 faint bands</b> Soluble = No visible bands	32 %	1
1 % glucose media, 25°C, 1 mM IPTG, 4 hours induction	<b>8 ml re-suspension buffer (50 mM TRIS [pH 8.0], 400 mM NaCl, 10 % w/v glycerol, 5 mM β-ME) 1 mg/ml lysozyme)</b>	Total = Visible band Insoluble = Visible band Soluble = Visible band	Total = <b>2 faint bands</b> Insoluble = <b>2 faint bands</b> Soluble = <b>2 faint bands</b>	67 %	1
1 % glucose media, 25°C, 1 mM IPTG, 4 hours induction	8 ml re-suspension buffer (50 mM TRIS [pH 8.0], 400 mM NaCl, 10 % w/v glycerol, 5 mM β-ME, <b>protease inhibitors</b> ) 1 mg/ml lysozyme)	Total = Visible band Insoluble = Visible band Soluble = Visible band	Total = <b>2 visible bands</b> Insoluble = <b>2 visible bands</b> Soluble = <b>No visible bands</b>	33 %	1
1 % glucose media, 25°C, 1 mM IPTG, 4 hours induction	8 ml re-suspension buffer (50 mM TRIS [pH 8.0], 400 mM NaCl, 10 % w/v glycerol, 5 mM β-ME, protease inhibitors) <b>20 µg/ml lysozyme)</b>	Total = Visible band Insoluble = Visible band Soluble = Visible band	Total = 2 visible bands Insoluble = 2 visible bands Soluble = <b>2 faint bands</b>	38 %	1
1 % glucose media, 25°C, 1 mM IPTG, <b>16 hour induction</b>	8 ml re-suspension buffer (50 mM TRIS [pH 8.0], 400 mM NaCl, 10 % w/v glycerol, 5 mM β-ME, protease inhibitors) 20 µg/ml lysozyme)	Total = Visible band Insoluble = Visible band Soluble = Visible band	Total = 2 visible bands Insoluble = 2 visible bands Soluble = <b>No visible bands</b>	21 %	1
1 % glucose media, 25°C, 1 mM IPTG, 4 hours induction	<b>1 ml re-suspension buffer (50 mM TRIS [pH 8.0], 400 mM NaCl, 10 % w/v glycerol, 5 mM β-ME, protease inhibitors) 20 µg/ml lysozyme)</b>	Total = Visible band Insoluble = Visible band Soluble = Visible band	Total = 2 visible bands Insoluble = 2 visible bands Soluble = No visible bands	34 %	1

**Table 3.5 A summary of growth conditions to establish optimal conditions for the expression and solubilisation of TRAK2<sub>100-380</sub>/KIF5A<sub>800-1032</sub>.**

Immunoblot and percentage solubilisation data relates to TRAK2<sub>100-380</sub>. Text highlighted in red indicates a change from the previous condition tested.

Growth conditions	Re-suspension conditions	Immunoblot analysis	Coomassie Blue staining analysis	% Solubilisation	N number
37°C, 1 mM IPTG, 4 hours induction	8 ml native buffer 250 mM NaH <sub>2</sub> PO <sub>4</sub> [pH 8.0] 1 mg/ml lysozyme	Total = Visible band Insoluble = Visible band Soluble = Visible band	Total = 2 faint bands Insoluble = 2 visible bands Soluble = No visible bands	4 %	1
37°C, 0.1 mM IPTG, 4 hours induction	8 ml native buffer 250 mM NaH <sub>2</sub> PO <sub>4</sub> [pH 8.0] 1 mg/ml lysozyme	Total = Visible band Insoluble = Visible band Soluble = Visible band	Total = 2 visible bands Insoluble = 2 visible bands Soluble = No visible bands	5 %	1
1 % glucose media, 37°C, 1 mM IPTG, 4 hours induction	8 ml native buffer 250 mM NaH <sub>2</sub> PO <sub>4</sub> [pH 8.0] 1 mg/ml lysozyme	Total = Visible band Insoluble = Visible band Soluble = Visible band	Total = 2 visible bands Insoluble = 2 visible bands Soluble = No visible bands	21 %	1
1 % glucose media, 25°C, 1 mM IPTG, 4 hours induction	8 ml native buffer 250 mM NaH <sub>2</sub> PO <sub>4</sub> [pH 8.0] 1 mg/ml lysozyme	Total = Visible band Insoluble = Visible band Soluble = Visible band	Total = 2 visible bands Insoluble = 2 visible bands Soluble = No visible bands	21 %	3
1 % glucose media, 25°C, 0.1 mM IPTG, 4 hours induction	8 ml native buffer 250 mM NaH <sub>2</sub> PO <sub>4</sub> [pH 8.0] 1 mg/ml lysozyme	Total = Visible band Insoluble = Visible band Soluble = Visible band	Total = <b>2 faint bands</b> Insoluble = <b>2 faint bands</b> Soluble = No visible bands	26 %	1
1 % glucose media, 25°C, 1 mM IPTG, 4 hours induction	<b>8 ml re-suspension buffer (50 mM TRIS [pH 8.0], 400 mM NaCl, 10 % w/v glycerol, 5 mM β-ME) 1 mg/ml lysozyme)</b>	Total = Visible band Insoluble = Visible band Soluble = Visible band	Total = <b>2 faint bands</b> Insoluble = <b>2 faint bands</b> Soluble = <b>2 faint bands</b>	36 %	1
1 % glucose media, 25°C, 1 mM IPTG, 4 hours induction	8 ml re-suspension buffer (50 mM TRIS [pH 8.0], 400 mM NaCl, 10 % w/v glycerol, 5 mM β-ME, <b>protease inhibitors</b> ) 1 mg/ml lysozyme)	Total = Visible band Insoluble = Visible band Soluble = Visible band	Total = <b>2 visible bands</b> Insoluble = <b>2 visible bands</b> Soluble = <b>No visible bands</b>	12 %	1
1 % glucose media, 25°C, 1 mM IPTG, 4 hours induction	8 ml re-suspension buffer (50 mM TRIS [pH 8.0], 400 mM NaCl, 10 % w/v glycerol, 5 mM β-ME, protease inhibitors) <b>20 µg/ml lysozyme)</b>	Total = Visible band Insoluble = Visible band Soluble = Visible band	Total = 2 visible bands Insoluble = 2 visible bands Soluble = <b>2 faint bands</b>	24 %	1
1 % glucose media, 25°C, 1 mM IPTG, <b>16 hour induction</b>	8 ml re-suspension buffer (50 mM TRIS [pH 8.0], 400 mM NaCl, 10 % w/v glycerol, 5 mM β-ME, protease inhibitors) 20 µg/ml lysozyme)	Total = Visible band Insoluble = Visible band Soluble = Visible band	Total = 2 visible bands Insoluble = 2 visible bands Soluble = <b>No visible bands</b>	19 %	1
1 % glucose media, 25°C, 1 mM IPTG, 4 hours induction	<b>1 ml re-suspension buffer (50 mM TRIS [pH 8.0], 400 mM NaCl, 10 % w/v glycerol, 5 mM β-ME, protease inhibitors) 20 µg/ml lysozyme)</b>	Total = Visible band Insoluble = Visible band Soluble = Visible band	Total = 2 visible bands Insoluble = 2 visible bands Soluble = No visible bands	22 %	1

**Table 3.6 A summary of growth conditions to establish optimal conditions for the expression and solubilisation of TRAK2<sub>100-380</sub>/KIF5A<sub>800-1032</sub>.**

Immunoblot and percentage solubilisation data relates to KIF5A<sub>800-1032</sub>. Text highlighted in red indicates a change from the previous condition tested.

Results from the optimisation of soluble protein expression experiments for the pETDUETTRAK2<sub>100-380</sub>/KIF5A<sub>800-1032</sub> clone show an average overall expression in all conditions tested. The optimal growth conditions of 1 mM IPTG and 4 hours induction at 25°C found visible bands for both TRAK2<sub>100-380</sub> and KIF5A<sub>800-1032</sub> in the total and insoluble, with faint bands in the soluble fraction after staining protein with Coomassie Blue.

Standard growth and solubilisation conditions for all three constructs were thus established. These were the induction of construct expression with 1 mM IPTG for 4 h at 25°C. Protein was solubilised in 8 ml re-suspension buffer, 50 mM TRIS [pH 8.0], 400 mM NaCl, 10 % w/v glycerol, 5 mM  $\beta$ -ME, protease inhibitors, 20  $\mu$ g/ml lysozyme treatment for 30 min and sonication on ice with 6 bursts of 10 sec with 10 sec rest intervals. Representative Coomassie Blue stained gels and immunoblots are shown in Figure 3.15.

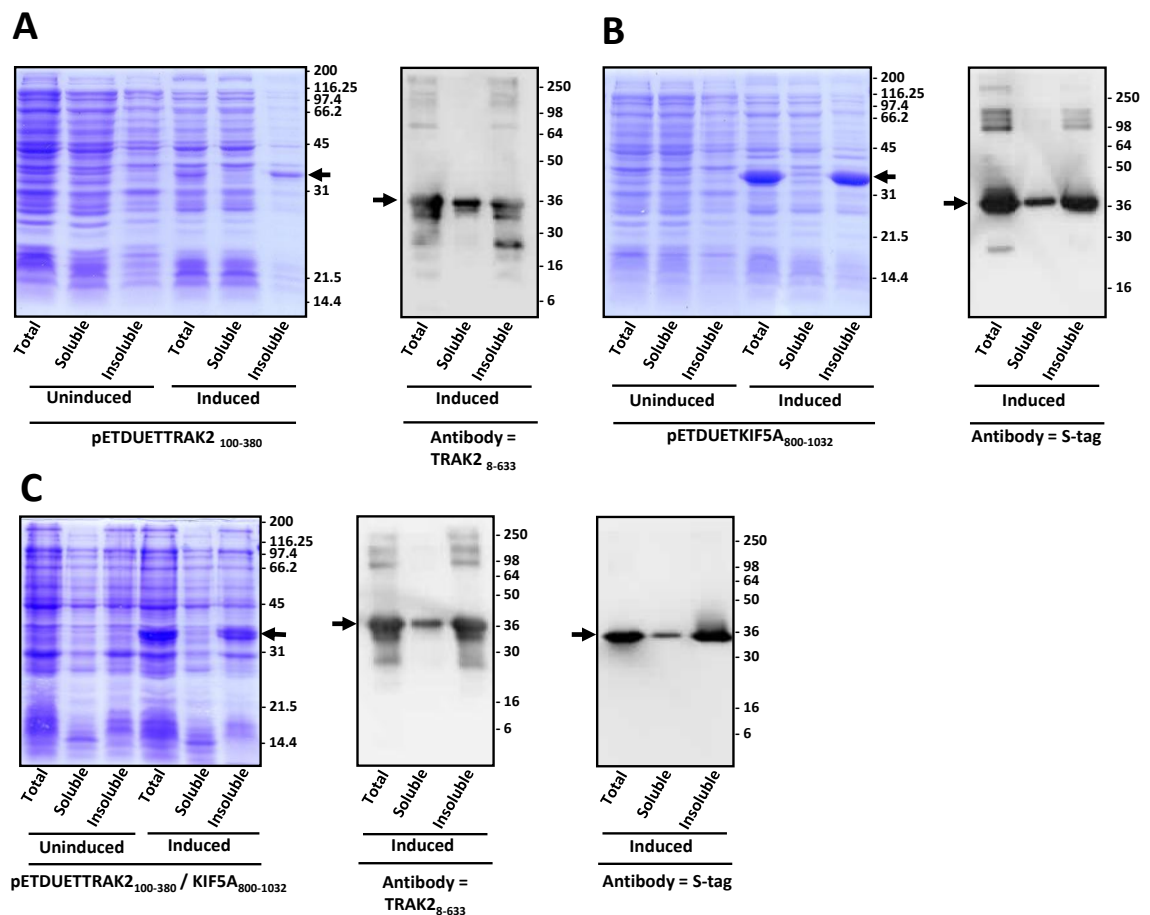


**Figure 3.15 Demonstration of the optimised expression of TRAK2<sub>100-380</sub>, KIF5A<sub>800-1032</sub> and TRAK2<sub>100-380</sub>/KIF5A<sub>800-1032</sub> in BL21 *E.coli* cells.**

BL21 *E.coli* cells were transformed with pETDUETTRAK2<sub>100-380</sub>, pETDUETKIF5A<sub>800-1032</sub> or pETDUETTRAK2<sub>100-380</sub>/KIF5A<sub>800-1032</sub>. Cell homogenates were prepared after growth conditions of 1 % w/v glucose supplemented LB media, with the induction of protein expression using 1 mM IPTG for 4 hours at 25°C. In all Coomassie Blue stained gels the total, soluble and insoluble protein of the induced and uninduced plasmids are shown. In all immunoblots the total, soluble and insoluble protein of the induced plasmids are shown. The positions of molecular weight standards (kDa) are shown on the right. Arrows indicate the positions of bands of interest.

**A** = TRAK2<sub>100-380</sub>. Immunoblot probed with anti-TRAK2<sub>8-633</sub> antibodies. **B** = KIF5A<sub>800-1032</sub>. Immunoblot probed with anti-S-tag antibodies. **C** = TRAK2<sub>100-380</sub>/KIF5A<sub>800-1032</sub>. Immunoblot probed with either anti-TRAK2<sub>8-633</sub> or anti-S-tag antibodies.

For single protein experiments, KIF5A<sub>800-1032</sub> expression and solubilisation was satisfactory but both expression and solubilisation of TRAK2<sub>100-380</sub> was inefficient. However, transformation of the double construct, pETDUETTRAK2<sub>100-380</sub>/KIF5A<sub>800-1032</sub>, resulted in expression of TRAK2<sub>100-380</sub> and KIF5A<sub>800-1032</sub> in approximately equal ratios, albeit at the expense of KIF5A<sub>800-1032</sub> expression. This result suggests stabilisation of the TRAK2<sub>100-380</sub>/KIF5A<sub>800-1032</sub> protein co-complex. A summary of the overall cloning, expression and expression optimisation of TRAK2<sub>100-380</sub>, KIF5A<sub>800-1032</sub> and TRAK2<sub>100-380</sub>/KIF5A<sub>800-1032</sub> is shown in Table 3.7.

Protein name	Generation of construct	Correct expression in <i>E.coli</i>	Analysis of soluble fraction yield via Coomassie Blue staining	% Solubilisation
TRAK2 <sub>100-380</sub>	✓	✓	No clear band in the soluble fraction	22 %
KIF5A <sub>800-1032</sub>	✓	✓	Clear band in the soluble fraction	35 %
TRAK2 <sub>100-380</sub> /KIF5A <sub>800-1032</sub>	✓	✓	Two clear bands in the soluble fraction	TRAK2 <sub>100-380</sub> = 24 % KIF5A <sub>800-1032</sub> = 35 %

**Table 3.7 Summary of the overall cloning, expression and expression optimisation for pETDUETTRAK2<sub>100-380</sub>, pETDUETKIF5A<sub>800-1032</sub> and pETDUETTRAK2<sub>100-380</sub>/KIF5A<sub>800-1032</sub>.**

### 3.2.5 Affinity tag purification of soluble TRAK2<sub>100-380</sub>/KIF5A<sub>800-1032</sub>

Experiments carried out in Section 3.2.4 demonstrated the ability of the dual construct, TRAK2<sub>100-380</sub>/KIF5A<sub>800-1032</sub>, to express in a bacterial expression system. In order to investigate if the expressed TRAK2<sub>100-380</sub>/KIF5A<sub>800-1032</sub> co-complex could be purified via affinity chromatography initial experiments using Ni<sup>2+</sup> affinity resin were carried out (Section 2.2.4.1). Ni<sup>2+</sup> affinity resin will specifically interact with the His-tag present on the N-terminus of TRAK2<sub>100-380</sub>. Hence, this method will be used to purify TRAK2<sub>100-380</sub> in the hope that KIF5A<sub>800-1032</sub> will co-purify. Soluble protein extract (20 ml) of transformed pETDUETTRAK2<sub>100-380</sub>/KIF5A<sub>800-1032</sub> bacterial cultures induced with 1 mM IPTG for 4 h at 25°C were incubated with the Ni<sup>2+</sup> affinity resin for 1 h, washed with 20 mM imidazole to remove non-specifically bound protein and eluted with 250 mM imidazole. Soluble, unbound, washed and eluted fractions were analysed by SDS-PAGE using Coomassie Blue staining and immunoblotting with anti-TRAK2<sub>8-633</sub> and anti-

S-tag antibodies. The results of the affinity purification of TRAK2<sub>100-380</sub>/KIF5A<sub>800-1032</sub> are shown in Figure 3.16.

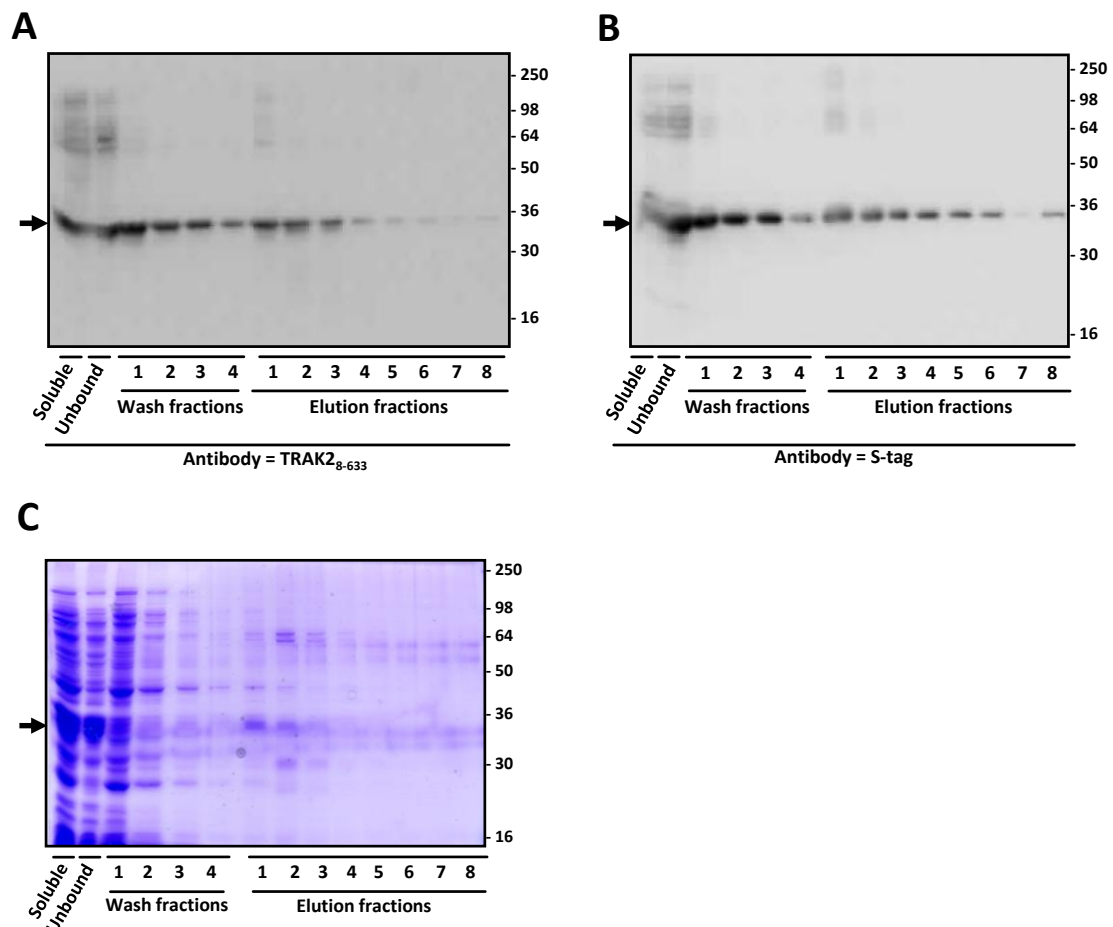


**Figure 3.16 Purification of TRAK2<sub>100-380</sub>/KIF5A<sub>800-1032</sub> under native conditions using Ni<sup>2+</sup> affinity resin.**

*BL21 E.coli* cells were transformed with pETDUETTRAK2<sub>100-380</sub>/KIF5A<sub>800-1032</sub> and the cell homogenate prepared after growth conditions of 1 % w/v glucose supplemented LB media, with the induction of protein expression using 1 mM IPTG for 4 hours at 25°C. Soluble cell homogenate was incubated with Ni<sup>2+</sup> affinity resin for 1 h and washed and eluted from the resin as 1 ml fractions. Results are representative of n = 1 co-purification experiments. The positions of molecular weight standards (kDa) are shown on the right. Arrows indicate the positions of bands of interest.

**A** = TRAK2<sub>100-380</sub>/KIF5A<sub>800-1032</sub> purification probed with anti-TRAK2<sub>8-633</sub> antibodies. **B** = TRAK2<sub>100-380</sub>/KIF5A<sub>800-1032</sub> purification probed with anti-S-tag antibodies. **C** = Coomassie Blue stained TRAK2<sub>100-380</sub>/KIF5A<sub>800-1032</sub> purification.

Initial chromatography experiments show the presence of both TRAK2<sub>100-380</sub> and KIF5A<sub>800-1032</sub> in the soluble fractions of immunoblots indicating the correct expression and solubilisation of the TRAK2<sub>100-380</sub>/KIF5A<sub>800-1032</sub> co-complex. There is no decrease in TRAK2<sub>100-380</sub> or KIF5A<sub>800-1032</sub> in the supernatant sample compared to the soluble sample indicating that the TRAK2<sub>100-380</sub>/KIF5A<sub>800-1032</sub> co-complex is not efficiently binding the Ni<sup>2+</sup> affinity resin and is hence remaining in the supernatant. Background protein is also still being eluted, albeit at lower concentrations, from the resin after 4 ml of 20

mM imidazole wash buffer. The concentration of eluted TRAK2<sub>100-380</sub>/KIF5A<sub>800-1032</sub> in both the Coomassie Blue stained gel and immunoblots appears to be low with a high concentration of background binding proteins. This purification strategy, as discussed previously, should result in the purification of TRAK2<sub>100-380</sub> and by virtue of their interaction KIF5A<sub>800-1032</sub> should also purify as a TRAK2<sub>100-380</sub>/KIF5A<sub>800-1032</sub> co-complex. Although the efficiency of the purification of the co-complex appears to be low it has remained in approximately equal ratio throughout the purification experiments indicating that TRAK2<sub>100-380</sub> and KIF5A<sub>800-1032</sub> are still remaining bound to one another.

To assess the efficiency of affinity chromatography experiments several factors need to be considered. These include the specific activity of the purified proteins and the purification factor. The specific activity gives information regarding the purity of the isolated TRAK2<sub>100-380</sub>/KIF5A<sub>800-1032</sub> co-complex, whereas the purification factor compares the concentration of TRAK2<sub>100-380</sub>/KIF5A<sub>800-1032</sub> in the purified sample to the concentration of TRAK2<sub>100-380</sub>/KIF5A<sub>800-1032</sub> in the soluble cell homogenate. It is by using the specific activity, purification factor and visually analysing the Coomassie Blue stained gels and immunoblots that a good idea of the overall affinity chromatography efficiency can be gained. In order to assess the specific activity and purification factor a Coomassie Blue stained gel comparing the soluble extract and the elution volume with varying known concentrations of standard molecular weight proteins was carried out. The resulting Coomassie Blue stained gel is shown in Figure 3.17.

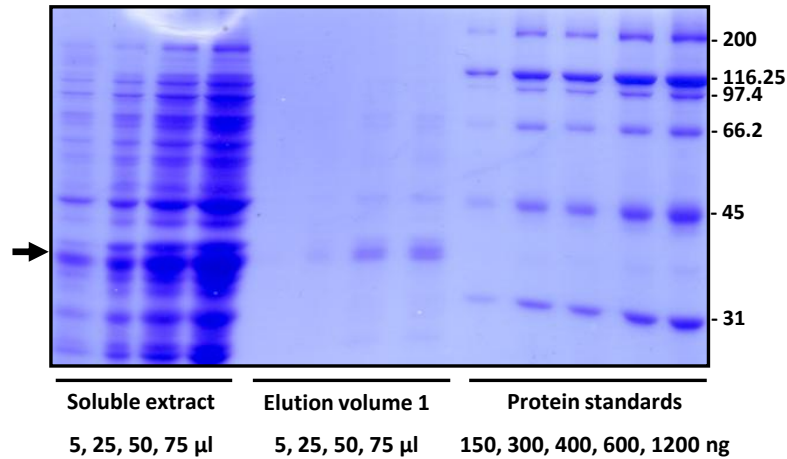


**Figure 3.17 Assessment of the specific activity and purification factor after the purification of TRAK2<sub>100-380</sub>/KIF5A<sub>800-1032</sub> under native conditions using Ni<sup>2+</sup> affinity resin.**

SDS-PAGE of varying concentrations of soluble TRAK2<sub>100-380</sub>/KIF5A<sub>800-1032</sub> co-complex, eluted purified TRAK2<sub>100-380</sub>/KIF5A<sub>800-1032</sub> co-complex and molecular weight protein standards. The positions of molecular weight standards (kDa) are shown on the right. The arrow indicates the positions of bands of interest.

**Estimating the TRAK2<sub>100-380</sub>/KIF5A<sub>800-1032</sub> content of the soluble fraction:**

- 5 μl of soluble TRAK2<sub>100-380</sub>/KIF5A<sub>800-1032</sub> looks to be approximately the same as the 300 ng standard band.
- 300 ng in 5 μl = 60 μg in 1 ml = 1.2 mg per 20 ml of soluble extract added to the resin.

**Estimating the specific activity of TRAK2<sub>100-380</sub>/KIF5A<sub>800-1032</sub> in the soluble fraction:**

The total protein of the soluble extract (20 ml) was calculated via Bradford assay (Section 2.2.3.2) was 0.19 mg protein/ml. Therefore the specific activity of TRAK2<sub>100-380</sub>/KIF5A<sub>800-1032</sub> is 0.38 mg/1 mg of soluble protein.

**Estimating the TRAK2<sub>100-380</sub>/KIF5A<sub>800-1032</sub> content of elution volume 1:**

- 75 μl of elution volume 3 looks to be approximately the same as the 300 ng standard band.
- 300 ng in 75 μl = 4 μg per 1 ml of elution volume 1.

**Estimating specific activity of TRAK2<sub>100-380</sub>/KIF5A<sub>800-1032</sub> of elution volume 1:**

The amount of soluble protein was unable to be efficiently calculated via a Bradford assay due to the low concentration. Hence the lowest measurable protein concentration was used to help estimate specific activity, which in this case was 0.1 mg

protein/ml. Therefore the specific activity of TRAK2<sub>100-380</sub>/KIF5A<sub>800-1032</sub> is 0.04 mg/1 mg of total protein from elution volume 1.

**Estimating the purification factor:**

$$\text{Purification factor} = \frac{\text{Specific activity in the purified}}{\text{Specific activity in the soluble}} = \frac{0.04 \text{ mg/1 mg purified}}{0.32 \text{ mg/1 mg soluble}} = \mathbf{0.125}$$

A purification factor value of less than one indicates that not all of the affinity tagged protein present in the soluble sample is binding the resin hence resulting in a poor yield of eluted protein sample. The purification factor value of 0.125 from the affinity purification of TRAK2<sub>100-380</sub>/KIF5A<sub>800-1032</sub>, although only an estimate, shows that the TRAK2<sub>100-380</sub>/KIF5A<sub>800-1032</sub> co-complex is not efficiently binding the column to be eluted. Combined with the low specific activity of TRAK2<sub>100-380</sub>/KIF5A<sub>800-1032</sub> in the eluted fraction, as well as the visual analysis, this indicates overall a poor yield of the purified TRAK2<sub>100-380</sub>/KIF5A<sub>800-1032</sub> co-complex. In order to increase the yield and purity of TRAK2<sub>100-380</sub>/KIF5A<sub>800-1032</sub> optimisation of the affinity purification process was carried out. The optimisation involved altering the concentration of imidazole in the wash buffer, changing the affinity resin specific for the His-tag and using S-protein affinity resin to target the S-tag present on KIF5A<sub>800-1032</sub>. The different methods and affinity resins used to purify the TRAK2<sub>100-380</sub>/KIF5A<sub>800-1032</sub> co-complex are summarised in Table 3.8.

<b>TRAK2<sub>100-380</sub>/KIF5A<sub>800-1032</sub> purification conditions</b>	<b>Visual analysis of Comma ssie Blue stained gels and immunoblots</b>	<b>Estimated specific activity of purified co-complex (mg/mg protein)</b>	<b>Estimated purification factor of the co-complex</b>
<b>Ni<sup>2+</sup> affinity resin (1 mg/ml protein binding capacity), 20 mM imidazole wash, 250 mM imidazole elution conditions</b>	No decrease in TRAK2 <sub>100-380</sub> or KIF5A <sub>800-1032</sub> in supernatant compared to soluble. No enrichment of protein being eluted from the resin. High background binding. Low yield.	0.085	0.125
<b>Ni<sup>2+</sup> affinity resin (1 mg/ml protein binding capacity), 75 mM imidazole wash, 250 mM imidazole elution conditions</b>	No decrease in TRAK2 <sub>100-380</sub> or KIF5A <sub>800-1032</sub> in supernatant compared to soluble. Enrichment of protein being eluted from the resin, with lower background binding. Low yield.	0.04	2.08
<b>Ni<sup>2+</sup> affinity resin (1 mg/ml protein binding capacity), 20 mM imidazole in re-suspension solution, 75 mM wash, 250 mM imidazole elution conditions</b>	No decrease in TRAK2 <sub>100-380</sub> or KIF5A <sub>800-1032</sub> in supernatant compared to soluble. No enrichment of protein being eluted from the resin. Slightly higher background binding than 75 mM imidazole wash. Low yield.	0.029	2.6
<b>Talon (Co<sup>3+</sup>) affinity resin (5 mg/ml protein binding capacity), 150 mM imidazole elution conditions</b>	No decrease in TRAK2 <sub>100-380</sub> or KIF5A <sub>800-1032</sub> in supernatant compared to soluble. No enrichment of protein being eluted from the resin. Very high background binding but also poor protein enrichment. Very low yield.	0.004	0.057
<b>S-tag protein resin (500 µg/ml protein binding capacity), elution with 3 M MgCl<sub>2</sub></b>	No decrease in TRAK2 <sub>100-380</sub> or KIF5A <sub>800-1032</sub> in supernatant compared to soluble. No enrichment of protein being eluted from the resin. Very low background binding but also poor protein enrichment. Low yield.	0.21	1.1

**Table 3.8 Table summarising the different conditions and affinity chromatography resins tested to purify the TRAK2<sub>100-380</sub>/KIF5A<sub>800-1032</sub> co-complex.**

Overall, purification of the TRAK2<sub>100-380</sub>/KIF5A<sub>800-1032</sub> co-complex was poor with respect to the estimated specific activity of the purified protein co-complex. Further, the purification factor indicated a low yield of purified TRAK2<sub>100-380</sub>/KIF5A<sub>800-1032</sub> co-complex in all the conditions tested. The efficiency of TRAK2<sub>100-380</sub> binding to the Ni<sup>2+</sup> and Co<sup>3+</sup> affinity resins has been poor as demonstrated by the high concentration of TRAK2<sub>100-380</sub>/KIF5A<sub>800-1032</sub> co-complex remaining in the supernatant after incubation. Therefore, this inefficient purification could be due to poor accessibility of the His-tag to the resin. Although each purification is only representative of an n = 1 experiment the results were sufficient to ascertain if the purification conditions were suitable for further consideration. A change in strategy to use the S-tag present on KIF5A<sub>800-1032</sub> to

purify the TRAK2<sub>100-380</sub>/KIF5A<sub>800-1032</sub> co-complex as opposed to the His-tag present on TRAK2<sub>100-380</sub> also did not purify the protein co-complex to a sufficient yield. Optimisation of S-tag purification conditions were also confined due to the limitations of the resin itself when compared to the relatively flexible His-tag purification system. The S-protein affinity resin system is limited because relatively harsh elution conditions of 3M MgCl<sub>2</sub> are needed to disrupt the S-tag present on KIF5A<sub>800-1032</sub> binding to the affinity resin. Hence, the elution conditions are difficult to optimise and only one purification condition could be tested. Due to the poor yield of eluted protein and the high concentration of the TRAK2<sub>100-380</sub>/KIF5A<sub>800-1032</sub> co-complex remaining in the supernatant sample after incubation with the S-tag protein affinity resin, this result indicates that the S-tag may also be being obscured either by the tertiary structure of KIF5A<sub>800-1032</sub> or the binding of TRAK2<sub>100-380</sub>.

In order to assess if either the tertiary structure or the co-complex itself is inhibiting affinity tag binding to the affinity resin, purification of the TRAK2<sub>100-380</sub>/KIF5A<sub>800-1032</sub> co-complex was carried out under denaturing conditions using Ni<sup>2+</sup> affinity resin. S-protein affinity resin could not be used as the specificity relies on a protein-protein interaction and denaturing conditions would abolish this. Soluble TRAK2<sub>100-380</sub>/KIF5A<sub>800-1032</sub> protein was incubated with 3 M urea prior to purification, in order to denature the soluble TRAK2<sub>100-380</sub>/KIF5A<sub>800-1032</sub> protein sample, using the same conditions as Figure 3.17. The results of the purification under denaturing conditions are shown in Figure 3.18.

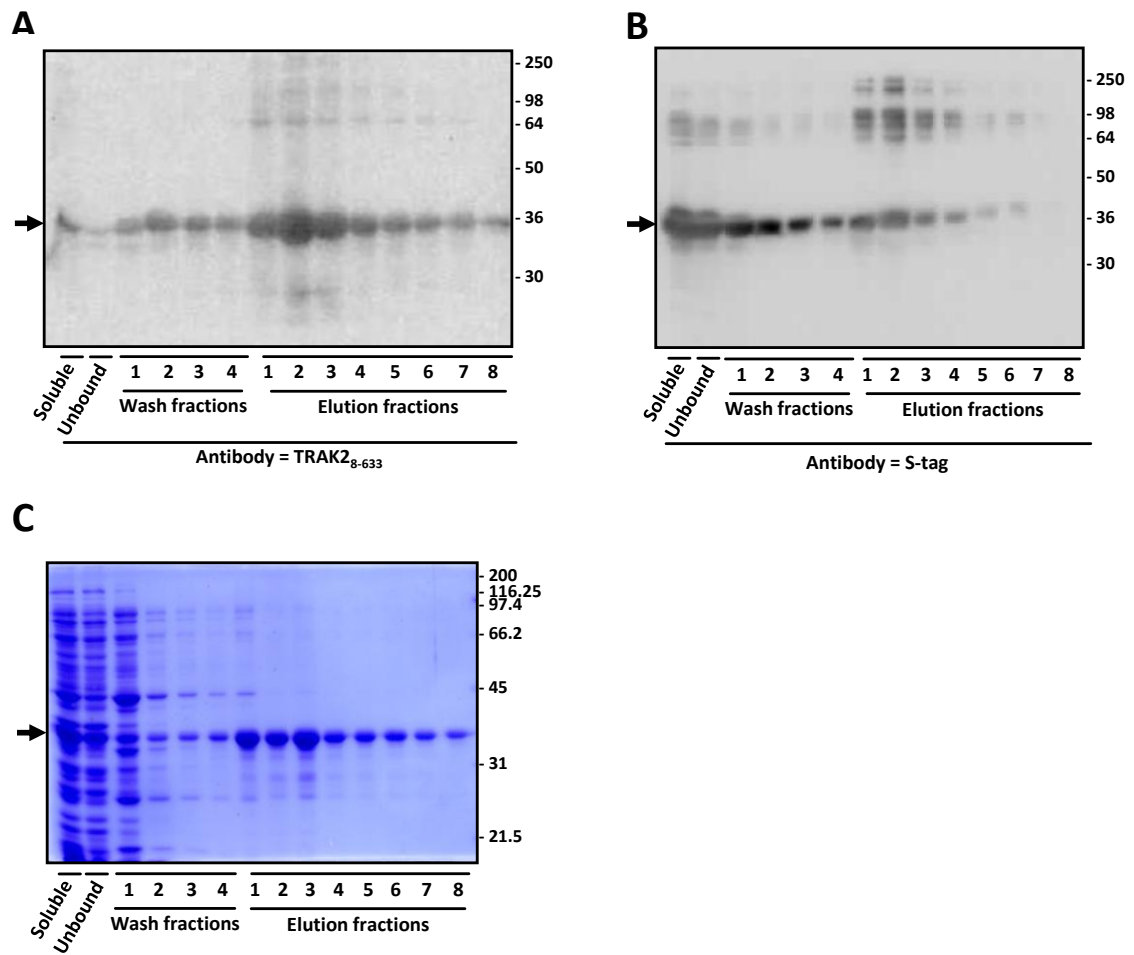


**Figure 3.18 Purification of TRAK2<sub>100-380</sub>/KIF5A<sub>800-1032</sub> under denaturing conditions using Ni<sup>2+</sup> affinity resin.**

*BL21 E.coli* cells were transformed with pETDUETTRAK2<sub>100-380</sub>/KIF5A<sub>800-1032</sub> and the cell homogenate prepared after growth conditions of 1 % w/v glucose supplemented LB media, with the induction of protein expression using 1 mM IPTG for 4 hours at 25°C. Soluble cell homogenate was denatured using 3 M urea and incubated with Ni<sup>2+</sup> affinity resin for 1 h and washed and eluted from the resin as 1 ml fractions. Results are representative of n = 1 co-purification experiments. The positions of molecular weight standards (kDa) are shown on the right. Arrows indicate the positions of bands of interest.

**A** = TRAK2<sub>100-380</sub>/KIF5A<sub>800-1032</sub> purification probed with anti-TRAK2<sub>8-633</sub> antibodies. **B** = TRAK2<sub>100-380</sub>/KIF5A<sub>800-1032</sub> purification probed with anti-S-tag antibodies. **C** = Coomassie Blue stained TRAK2<sub>100-380</sub>/KIF5A<sub>800-1032</sub> purification.

Ni<sup>2+</sup> affinity chromatography under denaturing conditions shows the presence of both TRAK2<sub>100-380</sub> and KIF5A<sub>800-1032</sub> in immunoblots indicating the co-purification of TRAK2<sub>100-380</sub>/KIF5A<sub>800-1032</sub>. In immunoblots there is a marked decrease of TRAK2<sub>100-380</sub> in the supernatant compared to the soluble sample, whereas levels of KIF5A<sub>800-1032</sub> in both the supernatant and soluble fractions remained the same. This large difference in soluble versus supernatant concentration of TRAK2<sub>100-380</sub> was not seen in any of the previous native purification conditions tested and indicates that the His-tag is now

efficiently binding to the Ni<sup>2+</sup> affinity resin. This result also indicates that TRAK2<sub>100-380</sub> but not KIF5A<sub>800-1032</sub> is binding the Ni<sup>2+</sup> affinity resin efficiently. Purification under denaturing conditions has improved the yield of eluted TRAK2<sub>100-380</sub> and also resulted in decreased levels of co-purifying KIF5A<sub>800-1032</sub> when compared to TRAK2<sub>100-380</sub>. An estimated purification factor value of 58 indicates that TRAK2<sub>100-380</sub> is efficiently binding the column and is able to be eluted from the resin with a high yield. Overall this result suggests that in the native TRAK2<sub>100-380</sub>/KIF5A<sub>800-1032</sub> co-complex the His affinity tag may not be accessible for binding to the affinity resin.

### 3.3 DISCUSSION

The aim of this chapter was to generate a functional and pure TRAK2<sub>100-380</sub>/KIF5A<sub>800-1032</sub> protein co-complex. This would allow for structural studies to be carried out upon the co-complex and valuable insight gained into how the TRAK2 kinesin adaptor protein may function. In this chapter three bacterial expression constructs, pETDUETTRAK2<sub>100-380</sub>, pETDUETKIF5A<sub>800-1032</sub> and pETDUETTRAK2<sub>100-380</sub>/KIF5A<sub>800-1032</sub> were generated. TRAK2<sub>100-380</sub> and KIF5A<sub>800-1032</sub> were successfully expressed in BL21 *E.coli* cells. TRAK2<sub>100-380</sub>/KIF5A<sub>800-1032</sub> was also shown to successfully co-express in BL21 *E.coli* cells. Optimisation of the expression of soluble protein using different induction, growth and re-suspension conditions resulted in an improvement of the yield of TRAK2<sub>100-380</sub>, KIF5A<sub>800-1032</sub> and TRAK2<sub>100-380</sub>/KIF5A<sub>800-1032</sub> compared to original test conditions. As previously discussed in Section 3.1 the expression of soluble protein at a high yield is essential for large scale purification of recombinant proteins from bacterial systems. The protein present in inclusion bodies would be required to be denatured and subsequently refolded *in vitro* to generate viable protein. There is no guarantee that protein recovered from inclusion bodies will refold correctly and hence a high yield of soluble as opposed to insoluble protein is needed for structural studies. The best condition for the overall yield and solubility of TRAK2<sub>100-380</sub> was the induction of protein expression using 1 mM IPTG for 4 hours at 25°C. TRAK2<sub>100-380</sub> was subsequently solubilised in 8 ml re-suspension buffer, 50 mM TRIS [pH 8.0], 400 mM NaCl, 10 % w/v glycerol, 5 mM β-ME, protease inhibitors, 20 µg/ml lysozyme treatment for 30 min and sonication on ice with 6 bursts of 10 sec with 10 sec rest intervals. This resulted in a 22 % solubilisation of TRAK2<sub>100-380</sub> under these conditions. However, the overall the yield of soluble TRAK2<sub>100-380</sub> was poor. Conversely, the optimisation of KIF5A<sub>800-1032</sub> using the above conditions resulted in solubilisation levels of 35 % and showed a high yield of expressed protein. Interestingly, when co-expressed together, TRAK2<sub>100-380</sub>/KIF5A<sub>800-1032</sub> was in approximately equal ratios in all growth conditions tested indicating that TRAK2<sub>100-380</sub>/KIF5A<sub>800-1032</sub> forms a co-complex.

Although the original hypothesis behind co-expressing TRAK2<sub>100-380</sub>/KIF5A<sub>800-1032</sub> together was aimed at helping to stabilise KIF5A<sub>800-1032</sub>, the presence of KIF5A<sub>800-1032</sub> appeared to rescue TRAK2<sub>100-380</sub> yield when co-expressed together. The increase in stability of TRAK2<sub>100-380</sub> solubility by KIF5A<sub>800-1032</sub> also demonstrated a decrease in the

yield of KIF5A<sub>800-1032</sub> expression, indicating that KIF5A<sub>800-1032</sub> expression is being sacrificed in order to improve the poor expression of TRAK2<sub>100-380</sub> seen when expressed alone. As previously discussed in Section 3.1, the ability of a co-expressing protein binding partner can significantly increase soluble expression. Hancock and Howard (1998) demonstrated that the co-expression of a *Drosophila* KHC mutant lacking the motor domain increased soluble expression by approximately five-fold when co-expressed with wild-type KHC in *E.coli* cells. Although not a kinesin protein, co-expression of myosin light and heavy chain was shown to result in stoichiometric expression of both proteins in *E.coli* cells (McNally *et al.*, 1998). The work presented in this chapter has shown that not only does KIF5A<sub>800-1032</sub> co-expression with TRAK2<sub>100-380</sub> increase soluble TRAK2<sub>100-380</sub>, but the TRAK2<sub>100-380</sub>/KIF5A<sub>800-1032</sub> co-complex appears to be stoichiometric.

The same conditions found to be most efficient for single TRAK2<sub>100-380</sub> and KIF5A<sub>800-1032</sub> expression, as discussed above, also resulted in an overall increase of TRAK2<sub>100-380</sub>/KIF5A<sub>800-1032</sub> yield and solubility. Several factors including temperature of growth, the temperature of protein induction and the re-suspension conditions can help to affect the solubility and yield of protein expression in bacterial cells. In the case of all three constructs it was found that a lowered induction temperature of 25°C helped to increase the expression of soluble protein. This may be due to the lowered temperature slowing the formation of expressed protein in the bacterial cell leading to less chance for the protein to aggregate into inclusion bodies.

Affinity chromatography purification targeting either the His-tag present on TRAK2<sub>100-380</sub> or the S-tag on KIF5A<sub>800-1032</sub> was designed to purify each respective protein in the hope that due to the association with their interacting protein, co-purification would occur. Both TRAK2<sub>100-380</sub> and KIF5A<sub>800-1032</sub> immunoreactivities were co-purified by Ni<sup>2+</sup> affinity resin suggesting that the two proteins associate to form a TRAK2<sub>100-380</sub>/KIF5A<sub>800-1032</sub> co-complex. Despite using different affinity resins and resin wash/elution conditions the yield of the purified co-complex remained poor. Purification under denaturing conditions to inhibit TRAK2<sub>100-380</sub>/KIF5A<sub>800-1032</sub> co-complex formation improved the yield of TRAK2<sub>100-380</sub> and also resulted in decreased amounts of co-purifying KIF5A<sub>800-1032</sub> after purification using Ni<sup>2+</sup> affinity resin. It is interesting that the co-purification of KIF5A<sub>800-1032</sub> with TRAK2<sub>100-380</sub> is not completely

abolished under denaturing conditions as theoretically KIF5A<sub>800-1032</sub> should no longer interact with TRAK2<sub>100-380</sub> due to the loss of the secondary and tertiary structures of both proteins. Although the exact mechanism behind the TRAK2<sub>100-380</sub>/KIF5A<sub>800-1032</sub> interaction is unknown, it is possible to speculate that under denaturing conditions charged regions of amino acids may be in part responsible for the remaining interaction of KIF5A<sub>800-1032</sub> with TRAK2<sub>100-380</sub>, which in turn results in the, albeit reduced, levels of co-purification. The presence of KIF5A<sub>800-1032</sub> is unlikely to be due to a specific interaction between KIF5A<sub>800-1032</sub> and the Ni<sup>2+</sup> affinity resin as there are no obvious histidine sequences within KIF5A<sub>800-1032</sub>, although any region of negatively charged amino acids present on the denatured KIF5A<sub>800-1032</sub> may weakly bind the positively charged Ni<sup>2+</sup>. The poor binding of the tagged TRAK2<sub>100-380</sub>/KIF5A<sub>800-1032</sub> co-complex to the differing affinity resins could be due to saturation of the protein binding sites, although this is unlikely due to the high binding capacity of each of the affinity resins used (Table 3.8). Overall these purification experiments suggest that in the TRAK2<sub>100-380</sub>/KIF5A<sub>800-1032</sub> co-complex the His affinity tag may not be accessible for binding to the affinity resin. Unfortunately it is difficult to deduce whether this His-tag obscurity is due to the tertiary folding of the TRAK2<sub>100-380</sub> protein or the binding of KIF5A<sub>800-1032</sub> to TRAK2<sub>100-380</sub>.

Gaining a functional purified protein for structural studies is dependent on many factors, including yield and solubility of the expressed protein as well as the yield and efficiency of purification. All of these factors need to be optimised in order to gain a protein of a high enough yield that could be considered suitable for structural studies. These factors can be influenced by a variety of subtle differences including changes in amino acid composition, protein charge, tertiary structure or type and location of affinity tag. Although work in this chapter has shown optimisation of nearly all of the above factors, ultimately TRAK2<sub>100-380</sub>/KIF5A<sub>800-1032</sub> was shown to be unsuitable for structural studies due to its inability to co-purify to a sufficient yield. Hence, work in the next chapter will focus upon the single expression and purification of KIF5A, including KIF5A<sub>800-1032</sub>, in an attempt to gain pure protein of sufficient yield to carry out structural studies.

### 3.3.1 Overall conclusions

- The bacterial expression constructs, pETDUETTRAK2<sub>100-380</sub>, pETDUETKIF5A<sub>800-1032</sub> and pETDUETTRAK2<sub>100-380</sub>/KIF5A<sub>800-1032</sub> were successfully generated. Expressed tagged proteins, TRAK2<sub>100-380</sub> and KIF5A<sub>800-1032</sub>, with the correct predicted sizes were verified by immunoblotting.
- Optimal growth and solubilisation conditions for all three constructs were established. Under these conditions, high levels of expression and solubilisation of KIF5A<sub>800-1032</sub> and the TRAK2<sub>100-380</sub>/KIF5A<sub>800-1032</sub> co-complex were obtained. Levels of TRAK2<sub>100-380</sub> when expressed alone were low suggesting that in the presence of its binding partner, KIF5A<sub>800-1032</sub>, TRAK2<sub>100-380</sub> is stabilised.
- Both TRAK2<sub>100-380</sub> and KIF5A<sub>800-1032</sub> immunoreactivities were co-purified by ProBond Ni<sup>2+</sup> resin affinity chromatography suggesting that the two proteins associate to form a TRAK2<sub>100-380</sub>/KIF5A<sub>800-1032</sub> co-complex. The yield of the purified co-complex was, however, poor. Purification under denaturing conditions to inhibit TRAK2<sub>100-380</sub>/KIF5A<sub>800-1032</sub> co-complex formation improved the yield of TRAK2<sub>100-380</sub> and also resulted in decreased amounts of co-purifying KIF5A<sub>800-1032</sub>. This result suggests that in the TRAK2<sub>100-380</sub>/KIF5A<sub>800-1032</sub> co-complex the His affinity tag may not be accessible for binding to the affinity resin.
- The yield of co-purified TRAK2<sub>100-380</sub>/KIF5A<sub>800-1032</sub> was found to be too low for further structural studies.

# **CHAPTER 4**

**TOWARDS THE STRUCTURAL  
DETERMINATION OF THE KIF5A  
CARGO BINDING DOMAIN**

#### 4.1 RATIONALE

Previous work from Chapter 3 showed that KIF5A<sub>800-1032</sub> does co-express with TRAK2<sub>100-380</sub> in a bacterial expression system. It was also demonstrated that the presence of KIF5A<sub>800-1032</sub> increased the stability of TRAK2<sub>100-380</sub> after co-expression. Unfortunately although the TRAK2<sub>100-380</sub>/KIF5A<sub>800-1032</sub> co-complex could be purified, the yield after optimization of affinity chromatography was not sufficient. This was most likely due to either the interaction of the TRAK2<sub>100-380</sub>/KIF5A<sub>800-1032</sub> co-complex or the tertiary structure of TRAK2<sub>100-380</sub> and KIF5A<sub>800-1032</sub> inhibiting the affinity tags from binding the resin. Therefore a different approach was needed in order to gain pure and stable KIF5A cargo binding domain for further structural studies. The first aim of this chapter was to gain pure and stable KIF5A cargo binding domain protein that would be suitable for structural studies, such as X-ray crystallography.

As mentioned in the Introduction (Section 1.4), there are two proposed methods of how kinesin-1 is thought to govern self regulation of movement throughout the neuron. The first of these is where the motor domain of kinesin-1 dissociates from the microtubule and interacts with Miro, an atypical Rho GTPase, present on the outer membrane of the mitochondria. This would keep the entire trafficking complex intact whilst no longer being bound to the microtubule (Wang and Schwarz, 2008). The second proposed method is that cargo dissociates from kinesin-1 and subsequently the cargo binding domain binds directly to the motor domain and microtubule simultaneously to prevent movement (Dietrich *et al.*, 2008; Hackney *et al.*, 2009; Wong *et al.*, 2009; Seeger and Rice, 2010; Kaan *et al.*, 2011). Previous work regarding the association of the cargo binding domain of kinesin-1 to microtubules has been carried out using the kinesin-1 sub-type, KIF5B (Seeger and Rice, 2010). This study showed that amino acids KIF5B 822-944 can interact with microtubules with a submicromolar affinity using electrostatic forces to bind the acidic E-hook at the C-terminal end of tubulin. However, whether this possible regulatory binding mechanism is shared by KIF5A is unknown. Therefore, the second aim of this chapter was to gain pure and stable KIF5A cargo binding domain protein to ascertain if the cargo binding domain, like KIF5B, can interact with microtubules and hence may be involved in the regulation of KIF5A movement throughout the cell.

#### **4.1.1 Aims of this chapter**

- I. Generate bacterial expression constructs of the cargo binding domain of the kinesin-1 sub-type, KIF5A.
- II. Verify correct KIF5A production after transformation and induction of constructs in bacterial cells.
- III. Optimize the growth and solubilisation conditions needed to maximise soluble KIF5A cargo binding domain protein expression.
- IV. Purify in mg quantities the expressed KIF5A protein via affinity chromatography in a form suitable for further structural studies.
- V. Assess the ability of purified KIF5A cargo binding domain to bind microtubules *in vitro*.
- VI. Resolve the three dimensional structure of the KIF5A cargo binding domain.

## 4.2 RESULTS

As described in the rationale, the aim of this chapter was to determine the structure of the cargo binding domain of KIF5A as well as to understand more fully the mechanism as to how the movement of KIF5A along microtubules is regulated. In order to do this, tagged recombinant clones of the cargo binding domain of KIF5A were expressed in *BL21 E.coli* cells and their relative expression, solubilisation, purification and aggregation state were optimized. Initially five recombinant KIF5A constructs were generated following PCR amplification from pBSKIF5A (Section 2.2.2.3.1). These were pETDUETKIF5A<sub>800-1032</sub>, pET151TOPOKIF5A<sub>800-1032</sub>, pETDUETKIF5A<sub>820-1032</sub>, pETDUETKIF5A<sub>800-951</sub> and pETDUETKIF5A<sub>820-951</sub>. pETDUETKIF5A<sub>800-1032</sub> was generated as described in Section 3.2.2 and possesses DNA encoding for a C-terminal S-tag. pET151TOPOKIF5A<sub>800-1032</sub> was sub-cloned in frame using directional cloning of a blunt ended PCR product and possesses DNA encoding an N-terminal His-tag. pETDUETKIF5A<sub>820-1032</sub>, pETDUETKIF5A<sub>800-951</sub> and pETDUETKIF5A<sub>820-951</sub> were sub-cloned in frame using the restriction sites *BamHI/EcoRI* and all possess DNA encoding a N-terminal His tag. All recombinant clones were verified via DNA sequencing (Section 2.2.2.13). Figure 4.1 shows schematics of the recombinant KIF5A proteins.

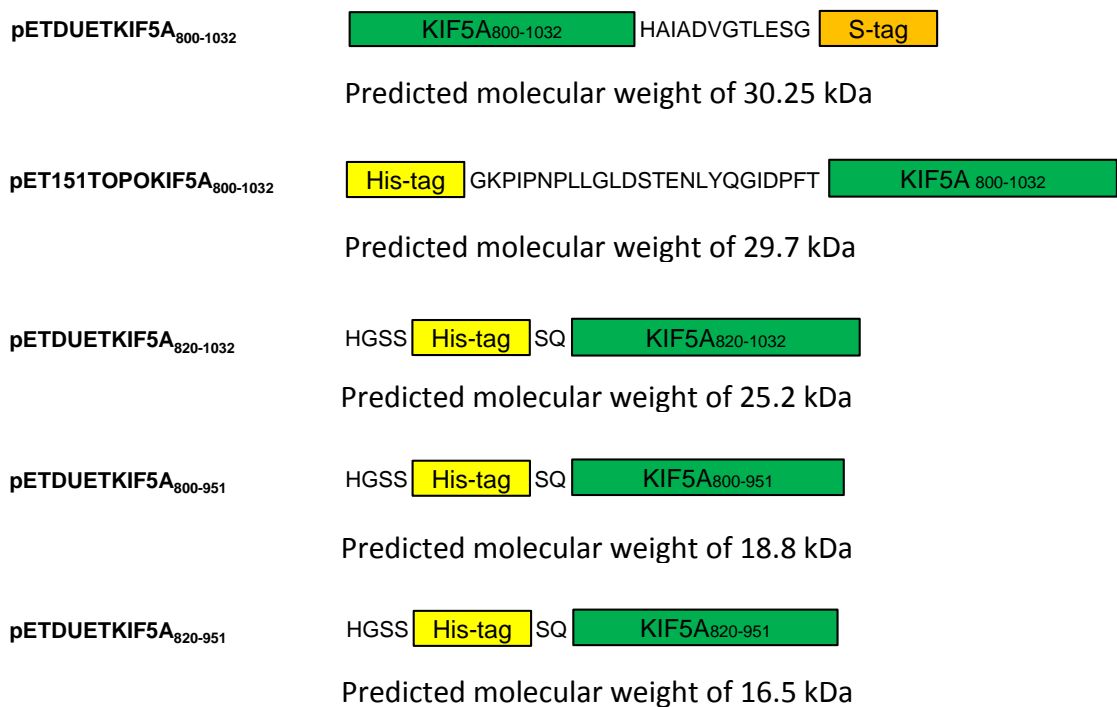


**Figure 4.1** Schematic representations of the recombinant tagged KIF5A cargo binding domain constructs.

#### 4.2.1 Assessment of KIF5A<sub>800-1032</sub> as a suitable recombinant protein for structural studies

The results in Chapter 3 demonstrated that the transformation of pETDUETKIF5A<sub>800-1032</sub> in *BL21 E.coli* cells resulted in high expression, yield and solubilisation of KIF5A<sub>800-1032</sub>. Therefore the next step was to purify soluble KIF5A<sub>800-1032</sub>. KIF5A<sub>800-1032</sub> possesses an S-tag on the C-terminus and thus it can be purified using this affinity tag. Hence, initial experiments using S-tag protein affinity resin were carried out. The same conditions used to purify TRAK2<sub>100-380</sub>/KIF5A<sub>800-1032</sub> were utilised to purify KIF5A<sub>800-1032</sub> (Table 3.8). A soluble protein extract of transformed pETDUETKIF5A<sub>800-1032</sub> bacterial cultures induced with 1 mM IPTG for 4 h at 25°C (20 ml) were incubated with the S-tag protein affinity resin for 1 h, washed to remove non-specifically bound protein and eluted with 3 M MgCl<sub>2</sub> (Section 2.2.4.2). Soluble, unbound, washed and eluted fractions were analysed by SDS-PAGE using Coomassie Blue staining and immunoblotting with anti-S-tag antibodies (Section 2.2.3.4; Section 2.2.3.5). The results of the affinity purification are shown in Figure 4.2.

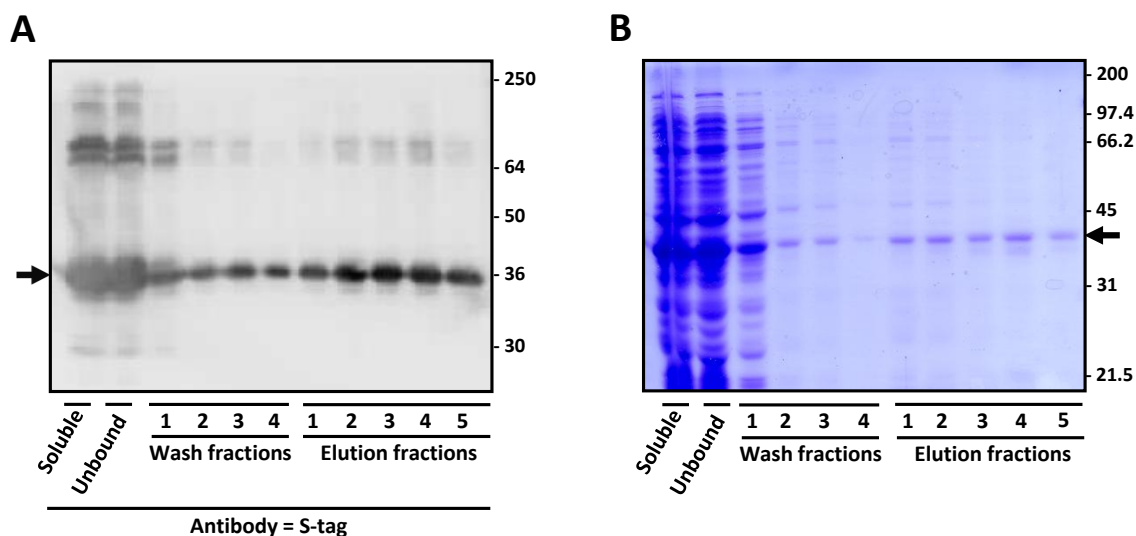


**Figure 4.2 Purification of KIF5A<sub>800-1032</sub> under native conditions using S-tag protein affinity resin.**

*BL21 E.coli* cells were transformed with pETDUETKIF5A<sub>800-1032</sub> and the cell homogenates were prepared after growth conditions of 1 % w/v glucose supplemented LB media, with the induction of protein expression using 1 mM IPTG for 4 hours at 25°C. The soluble cell homogenate was incubated with S-tag protein affinity resin for 1 h and washed and eluted from the resin as 1 ml fractions. The positions of molecular weight standards (kDa) are shown on the right. Arrows indicate the positions of bands of interest.

**A** = KIF5A<sub>800-1032</sub> purification probed with anti-S-tag antibodies. **B** = Coomassie Blue stained KIF5A<sub>800-1032</sub> purification.

Immunoblots of the samples show the presence of KIF5A<sub>800-1032</sub> (molecular weight of  $35.4 \pm 2.5$  kDa,  $n = 20$ ) in the soluble fraction indicating correct expression and solubilisation. There is no decrease in KIF5A<sub>800-1032</sub> in the supernatant compared to the soluble sample indicating that KIF5A<sub>800-1032</sub> is not efficiently binding the S-protein affinity resin. Background protein is also still being eluted, albeit at lower concentrations, from the resin after 4 ml of wash buffer. The concentration of eluted KIF5A<sub>800-1032</sub> in both the Coomassie Blue stained gel and immunoblot appears to be low with a high concentration of background binding proteins. These results combined with the results seen in Section 3.2.5, where S-tag purification of TRAK2<sub>100-380</sub>/KIF5A<sub>800-1032</sub> is inhibited by either the binding of the co-complex or the tertiary structure of KIF5A<sub>800-1032</sub>, indicate that the tertiary structure of the KIF5A<sub>800-1032</sub> protein may be preventing the binding of the S-tag to the S-tag protein affinity resin. Therefore, due to the poor yield seen after purification KIF5A<sub>800-1032</sub> was deemed to be unsuitable for further characterisation for structural studies.

#### **4.2.2 Assessment of His-tagged KIF5A<sub>800-1032</sub> as a suitable recombinant protein for structural studies**

Section 4.2.1 demonstrated that KIF5A<sub>800-1032</sub> is unable to be purified to a sufficient yield using the S-tag present on the C-terminus. This is most likely due to the location of the affinity tag and/or the tertiary structure of the KIF5A protein inhibiting binding of the affinity tag to the resin. Hence, in order to increase efficiency of binding to the affinity, the pET151TOPOKIF5A<sub>800-1032</sub> construct was generated. The pET151TOPO vector was chosen to facilitate the cloning of KIF5A<sub>800-1032</sub> due to the presence of DNA encoding an N-terminus His-tag. pET151TOPO also utilises blunt ended directional cloning, this removes the need for restriction enzyme sites and also facilitates a less complicated cloning process. The change in position of the affinity tag from the C-terminus to the N-terminus of KIF5A<sub>800-1032</sub> may help to improve the binding of KIF5A<sub>800-1032</sub> to the affinity resin.

pET151TOPOKIF5A<sub>800-1032</sub> was transformed into chemically competent *BL21 E.coli* cells and protein expression induced (Section 2.2.3.1). Initial protein expression experiments utilized 1 mM IPTG to induce expression for a total of 4 h at 37°C. The resulting expressed protein was re-suspended in 8 ml of re-suspension buffer,

centrifuged to separate protein into soluble and insoluble protein fraction and ~ 10 µg of each protein fraction analysed via 12 % SDS-PAGE (Section 2.2.3.4). The Coomassie Blue stained SDS-PAGE of the resulting fractions are shown in Figure 4.3. His-tagged KIF5A<sub>800-1032</sub> was successfully expressed as demonstrated by bands corresponding to the predicted size in the total and insoluble protein fractions, i.e. KIF5A<sub>800-1032</sub> = 35.2 ± 2.3 kDa (n = 30). No His-tagged KIF5A<sub>800-1032</sub> expressed protein could be visualized clearly via Coomassie Blue staining in the soluble fractions derived from pET151TOPOKIF5A<sub>800-1032</sub> transformations. This was a result of the large concentration of His-tagged KIF5A<sub>800-1032</sub> in the total and insoluble fractions obscuring the soluble gel lane.

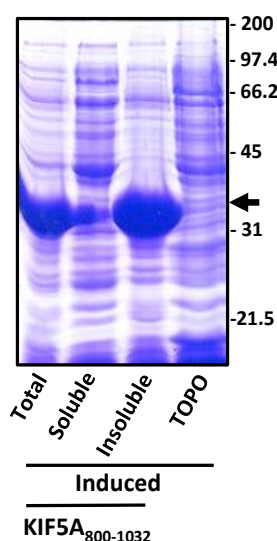


**Figure 4.3 Demonstration of the expression of KIF5A<sub>800-1032</sub> in BL21 *E.coli* cells.**

*BL21 E.coli* cells were transformed with pET151TOPOKIF5A<sub>800-1032</sub>. Cell homogenates were prepared after growth conditions of 1 % w/v glucose supplemented LB media, with the induction of protein expression using 1 mM IPTG for 4 hours at 37°C. In the Coomassie Blue stained gel the total, soluble and insoluble protein of the expressed KIF5A<sub>800-1032</sub> is shown. The induced total control was included. The positions of molecular weight standards (kDa) are shown on the right. The arrow indicates the positions of bands of interest.

To verify that the pET151TOPOKIF5A<sub>800-1032</sub> construct was the desired His-tagged KIF5A<sub>800-1032</sub> protein, immunoblotting was carried out using anti-His antibodies. Due to His-tagged KIF5A<sub>800-1032</sub> being difficult to visualize in the soluble fraction (Figure 4.3) all experiments subsequently employed the loading of ~ 0.1 µg of protein from the total and insoluble fractions for SDS-PAGE analysis. The resulting immunoblot is shown in Figure 4.4.

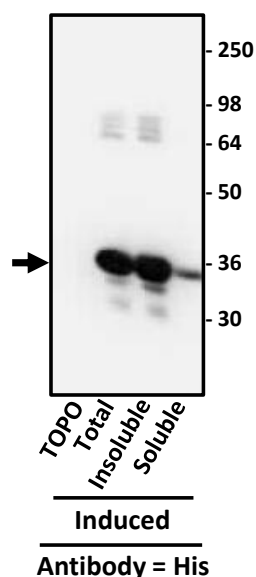


**Figure 4.4 Demonstration of the expression of KIF5A<sub>800-1032</sub> in BL21 *E. coli* cells.**

BL21 *E. coli* cells were transformed with pET151TOPOKIF5A<sub>800-1032</sub>. Cell homogenates were prepared after growth conditions of 1 % w/v glucose supplemented LB media, with the induction of protein expression using 1 mM IPTG for 4 hours at 37°C. In the immunoblot the total, soluble and insoluble protein of the expressed KIF5A<sub>800-1032</sub> is shown. The induced total control was included. The immunoblot is probed with anti-His antibodies. The positions of molecular weight standards (kDa) are shown on the right. The arrow indicates the positions of bands of interest.

Immunoblotting with anti-His antibodies confirms the correct transcription of His-tagged KIF5A<sub>800-1032</sub> with immunoreactive bands present in all total, soluble and insoluble fractions. Overall a lower concentration of His-tagged KIF5A<sub>800-1032</sub> is present in the soluble extract when compared to both the total and insoluble fractions. In both total and insoluble fractions the presence of several higher molecular weight bands were seen at weights in the range of 60-90 kDa and these bands are most likely aggregated His-tagged KIF5A<sub>800-1032</sub>. Anti-His antibodies also recognised two immunoreactive bands at a lower molecular weight than the most significant His-tagged KIF5A<sub>800-1032</sub> band in the total and insoluble fractions. These lower molecular weight bands may be the result of proteolytic degradation. In order to increase the ratio of soluble:insoluble expressed protein as well as increasing the protein yield, differing growth and re-suspension conditions were tested. These included lowering the concentration of IPTG to induce protein expression, lowering the temperature at which protein expression is induced and altering re-suspension buffer conditions. All of the immunoblots representing the differing growth and re-suspension conditions were analysed semi-quantitatively using GeneGnome Tools software (Section 2.2.3.5.3). The ratio of immunoreactivity of the soluble fraction was taken and expressed as a percentage of both the soluble and insoluble fraction combined which is 100 %. Not only was the percentage solubility of the protein used to assess the efficiency of protein expression, but also the yield of protein expression was taken into account i.e. can the expressed soluble protein band be visualised after Coomassie Blue staining?

Optimization of the expression and solubilisation conditions of His-tagged KIF5A<sub>800-1032</sub> is summarized in Table 4.1.

Growth conditions	Re-suspension conditions	Immunoblot analysis	Coomassie Blue staining analysis	% Solubilisation	N number
1 % glucose media, 37°C, 1 mM IPTG, 4 h induction	8 ml re-suspension buffer [pH 8.0] 20 µg/ml lysozyme	Total = Visible band Insoluble = Visible band Soluble = Visible band	Total = Visible band Insoluble = Visible band Soluble = Visible band	0.5 %	3
1 % glucose media, 37°C, 0.1 mM IPTG, 4 h induction	8 ml re-suspension buffer [pH 8.0] 20 µg/ml lysozyme	Total = Visible band Insoluble = Visible band Soluble = Visible band	Total = Visible band Insoluble = Visible band Soluble = Visible band	0.5 %	3
1 % glucose media, 37°C, 1 mM IPTG, 16 h induction	8 ml re-suspension buffer [pH 8.0] 20 µg/ml lysozyme	Total = Visible band Insoluble = Visible band Soluble = Visible band	Total = Visible band Insoluble = Visible band Soluble = Visible band	0.5 %	3
1 % glucose media, 25°C, 1 mM IPTG, 4 h induction	8 ml re-suspension buffer [pH 8.0] 20 µg/ml lysozyme	Total = Visible band Insoluble = Visible band Soluble = Visible band	Total = Visible band Insoluble = Visible band Soluble = Visible band	0.5 %	3
1 % glucose media, 25°C, 0.1 mM IPTG, 4 h induction	8 ml re-suspension buffer [pH 8.0] 20 µg/ml lysozyme	Total = Visible band Insoluble = Visible band Soluble = Visible band	Total = Visible band Insoluble = Visible band Soluble = Visible band	0.5 %	3
1 % glucose media, 25°C, 1 mM IPTG, 16 h induction	8 ml re-suspension buffer [pH 8.0] 20 µg/ml lysozyme	Total = Visible band Insoluble = Visible band Soluble = Visible band	Total = Visible band Insoluble = Visible band Soluble = Visible band	0.5 %	3
1 % glucose media, 18°C, 1 mM IPTG, 4 h induction	8 ml re-suspension buffer [pH 8.0] 20 µg/ml lysozyme	Total = Visible band Insoluble = Visible band Soluble = Visible band	Total = Visible band Insoluble = Visible band Soluble = Visible band	2 %	3
1 % glucose media, 18°C, 0.1 mM IPTG, 4 h induction	8 ml re-suspension buffer [pH 8.0] 20 µg/ml lysozyme	Total = Visible band Insoluble = Visible band Soluble = Visible band	Total = Visible band Insoluble = Visible band Soluble = Visible band	1 %	3
1 % glucose media, 18°C, 1 mM IPTG, 16 h induction	8 ml re-suspension buffer [pH 8.0] 20 µg/ml lysozyme	Total = Visible band Insoluble = Visible band Soluble = Visible band	Total = Visible band Insoluble = Visible band Soluble = Visible band	0.5 %	3
250 ml culture, 1 % glucose media, 18°C, 1 mM IPTG, 4 h induction	40 ml re-suspension buffer [pH 8.0] 20 µg/ml lysozyme	Total = Visible band Insoluble = Visible band Soluble = Visible band	Total = Visible band Insoluble = Visible band Soluble = Visible band	4 %	3
250 ml culture, 1 % glucose media, 18°C, 1 mM IPTG, 4 h induction	40 ml re-suspension buffer [pH 7.4] 20 µg/ml lysozyme	Total = Visible band Insoluble = Visible band Soluble = Visible band	Total = Visible band Insoluble = Visible band Soluble = Visible band	2 %	3

**Table 4.1 A summary of growth conditions to establish optimal conditions for the expression and solubilisation of His-tagged KIF5A<sub>800-1032</sub>.**

Text highlighted in red indicates a change from the previous condition tested.

Results from optimization of the expression and solubilisation of His-tagged KIF5A<sub>800-1032</sub> show good overall expression in all conditions tested. The optimal growth conditions of 1 mM IPTG and 4 h induction at 18°C show clear bands in the total, soluble and insoluble fractions after staining protein with Coomassie Blue. The percentage of soluble:insoluble His-tagged KIF5A<sub>800-1032</sub> was found to be 4 % when

induced using a 250 ml culture as opposed to 2 % with a 50 ml culture. This increase of the ratio of soluble:insoluble KIF5A<sub>800-1032</sub> could be due to greater aeration of *BL21 E.coli* cells caused by the increase in flask size used to accommodate the larger culture. The yield of expressed His-tagged KIF5A<sub>800-1032</sub> was also high enough to compensate for the low soluble:insoluble ratio and was deemed suitable for purification using affinity chromatography. Standard growth and solubilisation conditions for pET151TOPOKIF5A<sub>800-1032</sub> were thus established. This was the induction of construct expression in a 250 ml *BL21 E.coli* culture with 1 mM IPTG for 4 h at 18°C. Protein was solubilised in 40 ml re-suspension buffer, 50 mM TRIS-HCl pH 8.0, 400 mM NaCl, 10 % w/v glycerol, 5 mM β-ME, protease inhibitors and 20 µg/ml lysozyme treatment for 30 min and sonication on ice with 6 bursts of 10 sec with 10 sec rest intervals. A representative Coomassie Blue stained gel and immunoblot is shown in Figure 4.5.

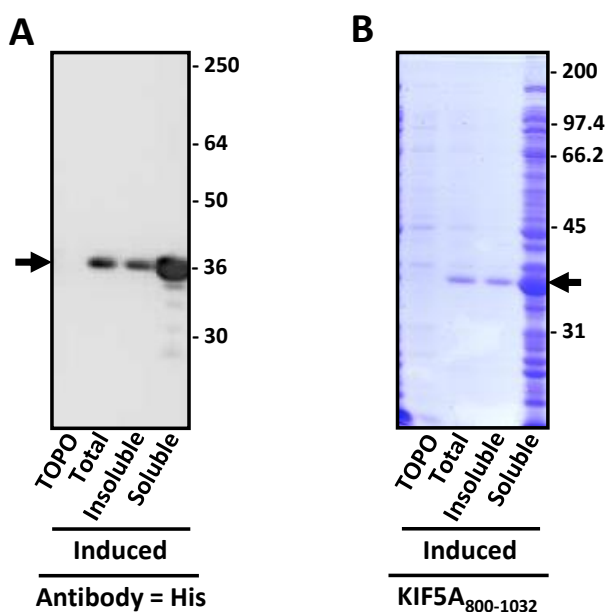


**Figure 4.5 Demonstration of the optimized expression of His-tagged KIF5A<sub>800-1032</sub> in *BL21 E.coli* cells.** *BL21 E.coli* cells were transformed with pET151TOPOKIF5A<sub>800-1032</sub>. Cell homogenates were prepared after 250 ml cultures supplemented with 1 % w/v glucose were induced with 1 mM IPTG for 4 h at 18°C. In all Coomassie Blue stained gels and immunoblots the total, soluble and insoluble protein of the expressed KIF5A<sub>800-1032</sub> is shown. The induced total control was included. The positions of molecular weight standards (kDa) are shown on the right. Arrows indicate the positions of bands of interest. **A** = KIF5A<sub>800-1032</sub>. Immunoblot probed with anti-His antibodies. **B** = KIF5A<sub>800-1032</sub>.

To investigate if the expressed His-tagged KIF5A<sub>800-1032</sub> could be purified via affinity chromatography initial experiments using Ni<sup>2+</sup> affinity resin were carried out. Ni<sup>2+</sup>

affinity resin will bind the His-tag present on the N-terminus of the KIF5A<sub>800-1032</sub> protein with micromolar affinity. A soluble protein extract (40 ml) of transformed pET151TOPOKIF5A<sub>800-1032</sub> bacterial cultures induced with 1 mM IPTG for 4 h at 18°C was incubated with the Ni<sup>2+</sup> affinity resin for 1 h, washed with 20 mM imidazole to remove non-specifically bound protein and eluted with 250 mM imidazole (Section 2.2.4.1). Soluble, unbound, washed and eluted fractions were analysed by SDS-PAGE using Coomassie Blue staining and immunoblotting with anti-His antibodies. The results of the affinity purification are shown in Figure 4.6.

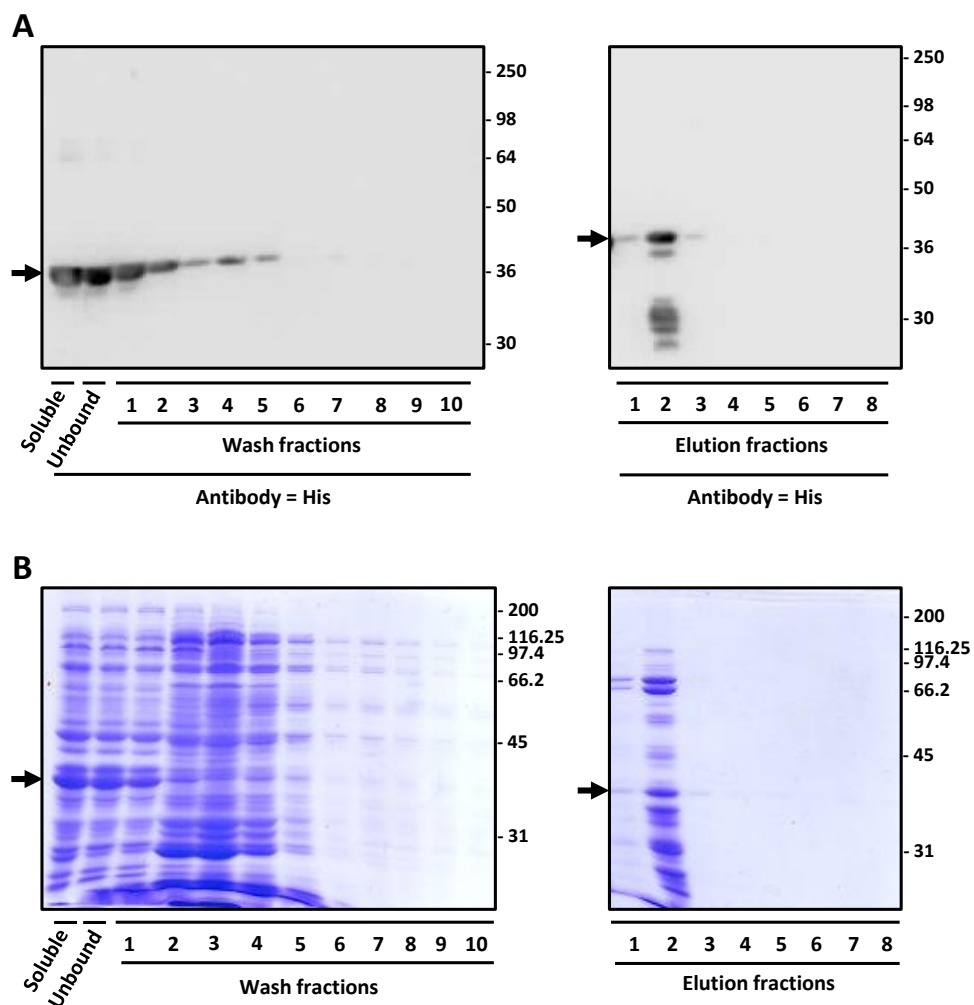


**Figure 4.6 Initial purification of His-tagged KIF5A<sub>800-1032</sub> under native conditions using Ni<sup>2+</sup> affinity resin.** *BL21 E.coli* cells were transformed with pET151TOPOKIF5A<sub>800-1032</sub> and the cell homogenates were prepared after 250 ml cultures supplemented with 1 % w/v glucose were induced with 1 mM IPTG for 4 h at 18°C. The soluble cell homogenate was incubated with Ni<sup>2+</sup> affinity resin for 1 h and washed and eluted from the resin as 1 ml fractions. Results are representative of n = 1 purification experiments. The positions of molecular weight standards (kDa) are shown on the right. Arrows indicate the positions of bands of interest.

**A** = KIF5A<sub>800-1032</sub> purification probed with anti-His antibodies. **B** = Coomassie Blue stained KIF5A<sub>800-1032</sub> purification.

Initial affinity chromatography experiments show the presence of His-tagged KIF5A<sub>800-1032</sub> in the soluble fraction indicating correct expression and solubilisation. There is no visible decrease in His-tagged KIF5A<sub>800-1032</sub> in the supernatant compared to the soluble sample indicating that His-tagged KIF5A<sub>800-1032</sub> is not efficiently binding the Ni<sup>2+</sup> affinity resin. The concentration of His-tagged KIF5A<sub>800-1032</sub> of the eluted fractions in both the Coomassie Blue stained gels and immunoblots appears to be low with a high concentration of background binding proteins. Attempts to optimize further the purification conditions included increasing the concentration of imidazole present in the wash buffer to reduce the binding of background binding of *E.coli* proteins to the resin, as well as eluting His-tagged KIF5A<sub>800-1032</sub> from the resin using a step-wise increase of imidazole concentration. However, it was not until the KIF5A<sub>800-1032</sub> bound resin was incubated with the elution buffer containing 250 mM imidazole for three h that a high yield of purified His-tagged KIF5A<sub>800-1032</sub> was recovered. Representative results of the affinity purification under these conditions are shown in Figure 4.7.

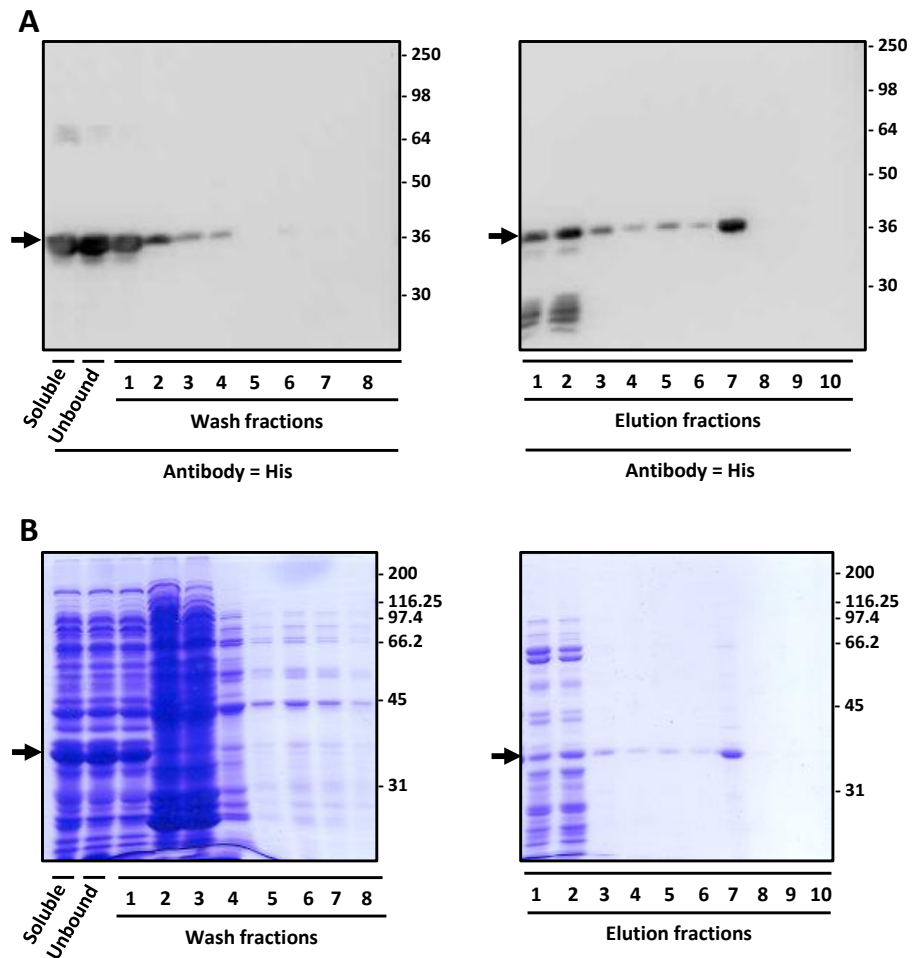


**Figure 4.7 Optimal purification of KIF5A<sub>800-1032</sub> under native conditions using Ni<sup>2+</sup> affinity resin.**

*BL21 E.coli* cells were transformed with pET151TOPOKIF5A<sub>800-1032</sub> and the cell homogenates were prepared after 250 ml cultures supplemented with 1 % w/v glucose were induced with 1 mM IPTG for 4 h at 18°C. A soluble cell homogenate was incubated with Ni<sup>2+</sup> affinity resin for 1 h and washed and eluted from the resin as 1 ml fractions. Results are representative of n = 5 purification experiments. Elution fraction numbers 7-10 represent eluted KIF5A<sub>800-1032</sub> after incubation with elution buffer for 3 h. The positions of molecular weight standards (kDa) are shown on the right. Arrows indicate the positions of bands of interest.

**A** = KIF5A<sub>800-1032</sub> purification probed with anti-His antibodies. **B** = Coomassie Blue stained KIF5A<sub>800-1032</sub> purification.

Affinity chromatography experiments show the presence of His-tagged KIF5A<sub>800-1032</sub> in the soluble fraction indicating correct expression and solubilisation. There is no visible decrease of His-tagged KIF5A<sub>800-1032</sub> in the supernatant compared to the soluble sample indicating that KIF5A<sub>800-1032</sub> is not efficiently binding the Ni<sup>2+</sup> affinity resin. This is similar to previous affinity chromatography purification results seen in Section 3.2.5, and Section 4.2.1 where both TRAK2<sub>100-380</sub>/KIF5A<sub>800-1032</sub> and KIF5A<sub>800-1032</sub> showed no visible decrease in the supernatant compared to the soluble sample. The concentration of His-tagged KIF5A<sub>800-1032</sub> from eluted fractions one to six in both immunoblots and Coomassie Blue stained gels appears to be low. A high concentration

of background binding proteins is also seen after Coomassie Blue staining. It was not until incubation of the Ni<sup>2+</sup> affinity resin with elution buffer containing 250 mM imidazole for a period of three h that a higher yield of eluted KIF5A<sub>800-1032</sub> protein with relatively low background protein was seen in elution fraction number seven. This result indicates that the strong interaction of the His-tag present on KIF5A<sub>800-1032</sub> requires a more thorough elution regime.

In an attempt to further purify as well as to assess the native state of His-tagged KIF5A<sub>800-1032</sub> an additional step of size exclusion chromatography was carried out (Section 2.2.4.5). Size exclusion chromatography involves separating a protein sample by the size of its native constituents using a specific column packed with a resin of a set pore size. In this case a Superpose™ 6 column was used which can separate proteins from 5–5,000 kDa in size. Unfortunately, results from the size exclusion chromatography proved inconclusive as no His-tagged KIF5A<sub>800-1032</sub> was detected in any eluted fractions either via immunoblotting or Coomassie Blue staining (data not shown). The most likely explanation for this result is that the purified His-tagged KIF5A<sub>800-1032</sub> from affinity chromatography experiments could be aggregating and in turn being collected on the filter before the sample enters the Superpose™ 6 column. Hence in order to test if the His-tagged KIF5A<sub>800-1032</sub> protein is in fact aggregating after affinity chromatography experiments, affinity chromatography purified His-tagged KIF5A<sub>800-1032</sub> was centrifuged at 100,000 x g for 20 min and the resulting pellet and soluble protein sample analysed. The results of the assessment of the aggregation state of His-tagged KIF5A<sub>800-1032</sub> are shown in Figure 4.8.

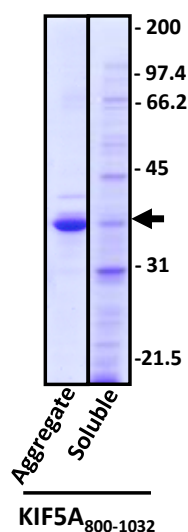


**Figure 4.8 Assessment of the aggregation state of KIF5A<sub>800-1032</sub>.**

Bacterial protein samples were centrifuged at 100,000 x g for 20 min at 4°C and the resulting protein pellet and soluble supernatant analysed via SDS-PAGE and Coomassie Blue staining.

High speed centrifugation demonstrated that the majority of the affinity chromatography purified KIF5A<sub>800-1032</sub> is in fact aggregating and hence does not make an ideal candidate to carry out further structural studies.

#### **4.2.3 Assessment of KIF5A<sub>820-1032</sub>, KIF5A<sub>800-951</sub> and KIF5A<sub>820-951</sub> as suitable recombinant proteins for structural studies**

Previous work carried out by Seeger and Rice (2010) has demonstrated the successful expression and purification of two kinesin-1 cargo binding domain protein fragments from a bacterial expression system. These were amino acids 822-963 and 822-945 of KIF5B. Both KIF5B cargo binding domain fragments possessed an N-terminal His-tag for affinity purification. Hence, it is reasonable to hypothesise that a similar region of KIF5A could be purified more efficiently than the previous KIF5A cargo binding domain proteins shown in Section 4.2.1 and Section 4.2.2. Amino acid sequence alignment analysis demonstrated that the equivalent amino acid region 822-945 of KIF5B was amino acids 820-951 of KIF5A. Thus, bacterial expression constructs pETDUETKIF5A<sub>820-1032</sub>, pETDUETKIF5A<sub>800-951</sub> and pETDUETKIF5A<sub>820-951</sub> were generated. The pETDUET1 vector was chosen because MCS1 possesses DNA encoding for an N-terminal His-tag and previous work in Section 4.2.2 has demonstrated that expressed KIF5A with an N-terminal His-tag was soluble and able to be purified via affinity chromatography to a high yield. pETDUETKIF5A<sub>820-1032</sub> possessed DNA encoding for the same start region of amino acids used in the two expressed clones from the Seeger and Rice (2010) study. pETDUETKIF5A<sub>800-951</sub> was the same as previous KIF5A cargo binding domain clones but with a shorter C-terminus in an attempt to avoid the proteolytic cleavage seen in KIF5B 822-963 (Seeger and Rice, 2010). pETDUETKIF5A<sub>800-951</sub> was the closest equivalent of the successfully expressed KIF5B construct.

pETDUETKIF5A<sub>820-1032</sub>, pETDUETKIF5A<sub>800-951</sub> and pETDUETKIF5A<sub>820-951</sub> were transformed into chemically competent *BL21 E.coli* cells and protein expression induced (Section 2.2.3). Previous work carried out in Section 4.2.2 has demonstrated the optimization of expression of the KIF5A<sub>800-1032</sub> constructs to be the induction of protein expression using 250 ml cultures and 1 mM IPTG to induce expression for a total of 4 h at 18°C. Hence, these same conditions were used for expression of pETDUETKIF5A<sub>820-1032</sub>,

pETDUETKIF5A<sub>800-951</sub> and pETDUETKIF5A<sub>820-951</sub>. The resulting expressed protein was re-suspended in 40 ml of re-suspension buffer, centrifuged to separate protein into soluble and insoluble protein pellets and ~ 10 µg of each protein fraction analysed via 15 % SDS-PAGE (Section 2.2.3.4). The resulting Coomassie Blue stained gels are shown in Figure 4.9. KIF5A<sub>820-1032</sub>, KIF5A<sub>800-951</sub> and KIF5A<sub>820-951</sub> were successfully expressed as demonstrated by bands corresponding to the predicted sizes in the total, soluble and insoluble protein fractions, i.e. KIF5A<sub>820-1032</sub> = 31.4 ± 1.1 kDa (n = 3), KIF5A<sub>800-951</sub> = 22.5 ± 1.2 kDa (n = 3) and KIF5A<sub>820-951</sub> = 19.2 ± 0.5 kDa (n = 3).

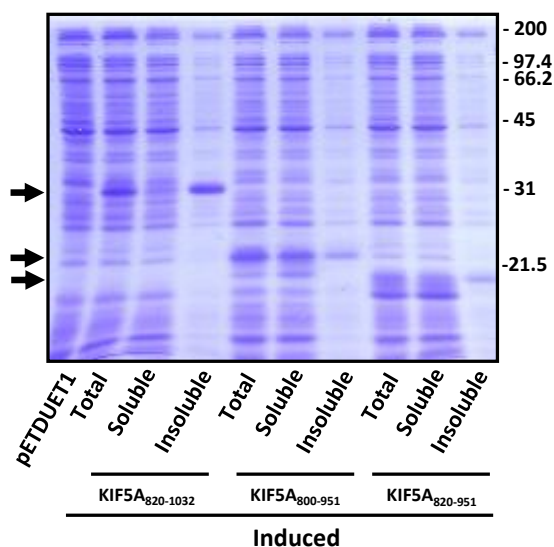


**Figure 4.9 Demonstration of the expression of KIF5A<sub>820-1032</sub>, KIF5A<sub>800-951</sub> and KIF5A<sub>820-951</sub> in *BL21 E.coli* cells.**

*BL21 E.coli* cells were transformed with pETDUETKIF5A<sub>820-1032</sub>, pETDUETKIF5A<sub>800-951</sub> or pETDUETKIF5A<sub>820-951</sub>. Cell homogenates were prepared after 250 ml cultures supplemented with 1 % w/v glucose were induced with 1 mM IPTG for 4 h at 18°C. In the Coomassie Blue stained gel the total, soluble and insoluble protein of the induced plasmid is shown. The induced total protein control was included. The positions of molecular weight standards (kDa) are shown on the right. Arrows indicate the positions of bands of interest.

To verify that the pETDUETKIF5A<sub>820-1032</sub>, pETDUETKIF5A<sub>800-951</sub> and pETDUETKIF5A<sub>820-951</sub> constructs were the desired KIF5A<sub>820-1032</sub>, KIF5A<sub>800-951</sub> and KIF5A<sub>820-951</sub> proteins, immunoblotting was carried out using anti-His antibodies. The resulting immunoblot is shown in Figure 4.10.

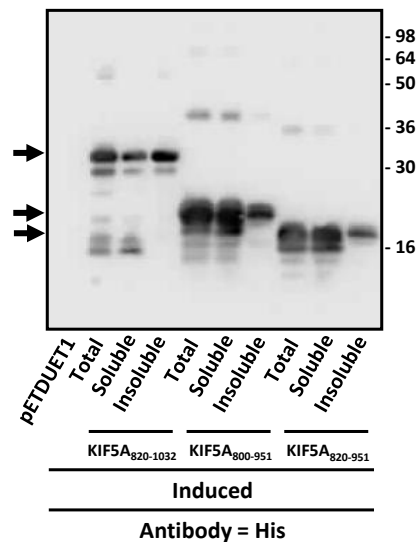


**Figure 4.10 Demonstration of the expression of KIF5A<sub>820-1032</sub>, KIF5A<sub>800-951</sub> and KIF5A<sub>820-951</sub> in BL21 *E.coli* cells.**

*BL21 E.coli* cells were transformed with pETDUETKIF5A<sub>820-1032</sub>, pETDUETKIF5A<sub>800-951</sub> or pETDUETKIF5A<sub>820-951</sub>. Cell homogenates were prepared after 250 ml cultures supplemented with 1 % w/v glucose were induced with 1 mM IPTG for 4 h at 18°C. In the immunoblot the total, soluble and insoluble protein of the induced plasmid is shown. The induced total protein control was included. The positions of molecular weight standards (kDa) are shown on the right. Arrows indicate the positions of bands of interest.

Immunoblotting with anti-His antibodies confirms the correct transcription of KIF5A<sub>820-1032</sub>, KIF5A<sub>800-951</sub> and KIF5A<sub>820-951</sub> with immunoreactive bands present in all total, soluble and insoluble fractions. Overall a lower concentration of KIF5A<sub>820-1032</sub> is present in the soluble extract when compared to both the total and insoluble fractions, resulting in a soluble:insoluble ratio of 32 %. Whereas higher concentrations of KIF5A<sub>800-951</sub> and KIF5A<sub>820-951</sub> are present in the soluble extract when compared to both the total and insoluble fractions, giving a soluble:insoluble ratio of 54 % and 57 % respectively. In the total and insoluble fractions of KIF5A<sub>820-1032</sub> the presence of a higher molecular weight band was seen at ~ 55 kDa. In the total, soluble and insoluble fractions of KIF5A<sub>800-951</sub> and KIF5A<sub>820-951</sub> the presence of several higher molecular weight bands were seen at weights in the range of 36-98 kDa for KIF5A<sub>800-951</sub> and ~ 36 kDa for KIF5A<sub>820-951</sub>. These higher molecular weight bands are most likely aggregated KIF5A<sub>820-951</sub>. Anti-His antibodies also recognised several major immunoreactive bands lower than the predicted molecular weight of KIF5A<sub>820-1032</sub>, KIF5A<sub>800-951</sub> and KIF5A<sub>820-951</sub>. These lower molecular weight bands may be the result of proteolytic degradation occurring at the C-terminus of KIF5A<sub>820-1032</sub>, KIF5A<sub>800-951</sub> and KIF5A<sub>820-951</sub>. This is because KIF5A<sub>820-1032</sub>, KIF5A<sub>800-951</sub> and KIF5A<sub>820-951</sub> are N-terminally His-tagged and the lower molecular weight band can be visualised after immunoblotting with anti-His

antibodies. Previous work in Section 3.2.4 and Section 4.2.2 has shown that KIF5A<sub>800-1032</sub> constructs are prone to proteolytic degradation at the C-terminus. As mentioned earlier, Seeger and Rice (2010) also showed that the degradation of the C-terminal amino acids 945-963 of KIF5B occurs over time in bacterially expressed constructs. However, the KIF5A<sub>800-951</sub> and KIF5A<sub>820-951</sub> constructs were designed specifically in an attempt to prevent this proteolytic degradation from occurring. Thus, it is quite likely that KIF5A and KIF5B do not share the same proteolytic cleavage sites.

Solubility was deemed sufficient after expression using conditions previously optimized for the expression of pET151TOPOKIF5A<sub>800-1032</sub> (Section 4.2.2). Thus, standard growth and solubilisation conditions for all three constructs were established. These were the induction of 250 ml cultures with 1 mM IPTG for 4 h at 18°C. Protein was solubilised in 40 ml re-suspension buffer (50 mM TRIS-HCl [pH 8.0], 400 mM NaCl, 10 % w/v glycerol, 5 mM β-ME, protease inhibitors) 20 µg/ml lysozyme for 30 min and sonicated on ice with 6 bursts of 10 sec with 10 sec rest intervals. A summary of the overall cloning, expression and optimization of expression is shown in Table 4.2.

Protein	Generation of construct	Correct expression in <i>E.coli</i>	Visual analysis of the soluble fraction using Coomassie Blue staining	% Solubilisation
KIF5A <sub>820-1032</sub>	✓	✓	Clear band in the soluble fraction	32 %
KIF5A <sub>800-951</sub>	✓	✓	Clear band in the soluble fraction	54 %
KIF5A <sub>820-951</sub>	✓	✓	Clear band in the soluble fraction	57 %

**Table 4.2 Summary of the overall cloning, expression and solubilisation optimisation for pETDUETKIF5A<sub>820-1032</sub>, pETDUETKIF5A<sub>800-951</sub> and pETDUETKIF5A<sub>820-951</sub>.**

In order to investigate if expressed KIF5A<sub>820-1032</sub>, KIF5A<sub>800-951</sub> and KIF5A<sub>820-951</sub> can be purified via affinity chromatography experiments using Ni<sup>2+</sup> affinity resin were carried out. Soluble protein extract (20 ml) of transformed pETDUETKIF5A<sub>820-1032</sub>, pETDUETKIF5A<sub>800-951</sub> or pETDUETKIF5A<sub>820-951</sub> bacterial cultures of 250 ml induced with 1 mM IPTG for 4 h at 18°C were incubated with the Ni<sup>2+</sup> affinity resin for 1 h, washed to remove non-specifically bound protein and eluted with 250 mM imidazole (Section 2.2.4.1). Soluble, unbound, washed and eluted fractions were analysed by SDS-PAGE

using Coomassie blue staining. The results of the affinity purification of KIF5A<sub>820-1032</sub>, KIF5A<sub>800-951</sub> and KIF5A<sub>820-951</sub> are shown in Figure 4.11.

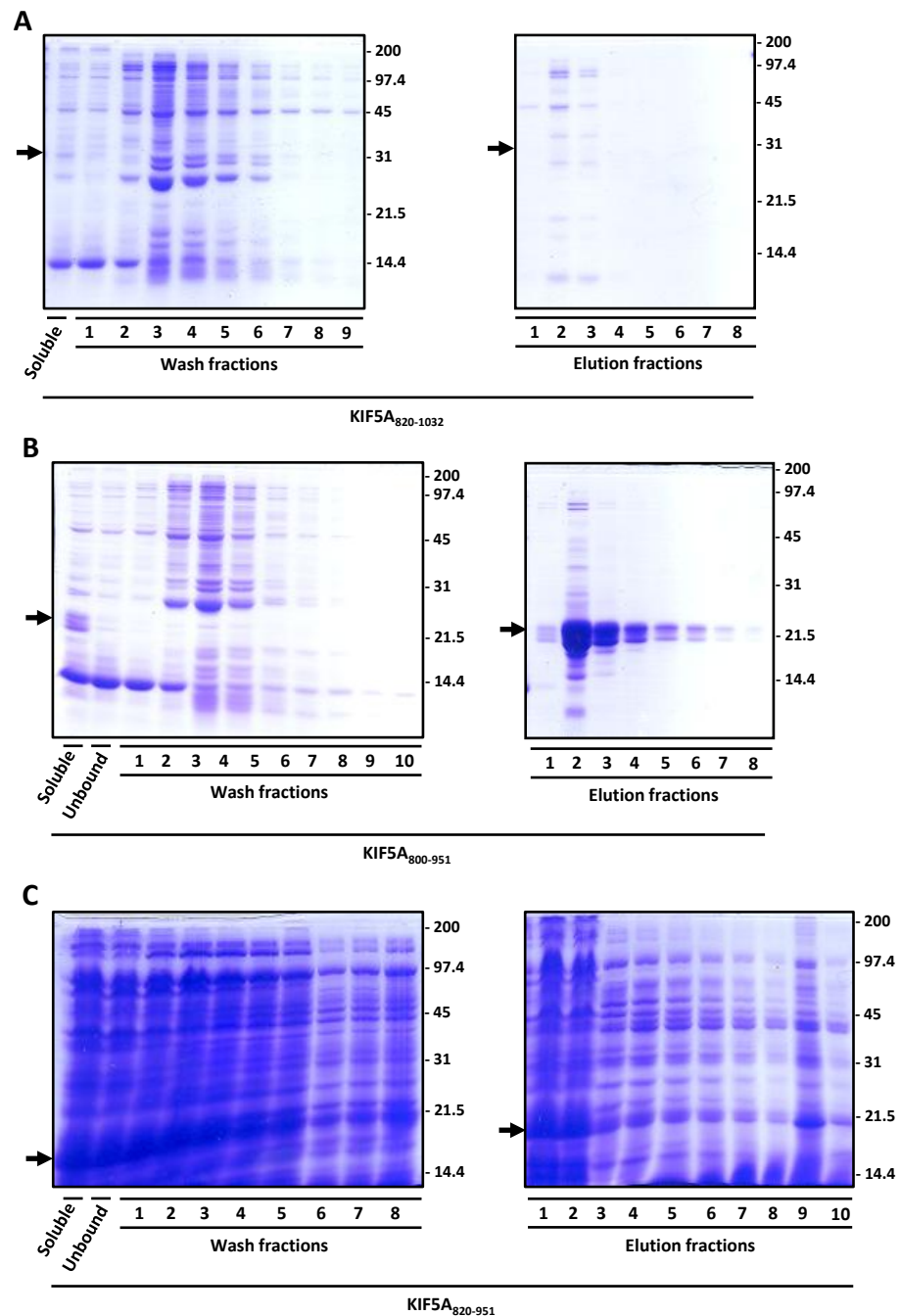


**Figure 4.11 Purification of KIF5A<sub>820-1032</sub>, KIF5A<sub>800-951</sub> and KIF5A<sub>820-951</sub> under native conditions using Ni<sup>2+</sup> affinity resin.**

*BL21 E. coli* cells were transformed with pETDUETKIF5A<sub>820-1032</sub>, pETDUETKIF5A<sub>800-951</sub> or pETDUETKIF5A<sub>820-951</sub> and the cell homogenates were prepared after 250 ml cultures supplemented with 1 % w/v glucose were induced with 1 mM IPTG for 4 h at 18°C. Soluble cell homogenate was incubated with Ni<sup>2+</sup> affinity resin for 1 h and washed and eluted from the resin as 1 ml fractions. KIF5A<sub>820-1032</sub> and KIF5A<sub>820-951</sub> are representative of n = 1 purification experiments, whereas KIF5A<sub>800-951</sub> is representative of n = 4 purification experiments. The positions of molecular weight standards (kDa) are shown on the right. Arrows indicate the positions of bands of interest.

**A** = Coomassie Blue stained KIF5A<sub>820-1032</sub> purification. **B** = Coomassie Blue stained KIF5A<sub>800-951</sub> purification. **C** = Coomassie Blue stained KIF5A<sub>820-951</sub> purification.

Affinity chromatography experiments show the presence of KIF5A<sub>820-1032</sub>, KIF5A<sub>800-951</sub> and KIF5A<sub>820-951</sub> in the soluble fraction indicating correct expression and solubilisation. Analysis of KIF5A<sub>820-1032</sub> purification does not include the supernatant sample which makes it difficult to assess how efficiently KIF5A<sub>820-1032</sub> binds the Ni<sup>2+</sup> affinity resin. KIF5A<sub>800-951</sub> shows a visible decrease in protein in the supernatant compared to the soluble sample indicating that KIF5A<sub>800-951</sub> is efficiently binding the Ni<sup>2+</sup> affinity resin. There is no visible decrease in KIF5A<sub>820-951</sub> in the supernatant compared to the soluble sample indicating that KIF5A<sub>820-951</sub> is not efficiently binding the Ni<sup>2+</sup> affinity resin. KIF5A<sub>820-1032</sub> is not visible in any of the eluted fractions after Coomassie Blue staining. Whereas a high yield of KIF5A<sub>820-951</sub> is visible in the eluted fractions after Coomassie Blue staining. KIF5A<sub>820-951</sub> purification also shows the presence of several contaminating background proteins in the elution fractions, albeit at a very low concentration in comparison to KIF5A<sub>820-951</sub>. The purification of KIF5A<sub>820-951</sub> indicates two major bands being eluted from the resin. The lower molecular weight band is most likely the product of proteolytic degradation, as noted previously in Figure 4.10, after expression in *BL21 E.coli* cells. KIF5A<sub>820-951</sub> shows poor overall elution from Ni<sup>2+</sup> affinity resin with very high concentrations of contaminating proteins detected in all elution fractions. In summary, KIF5A<sub>820-1032</sub> and KIF5A<sub>820-951</sub> showed poor purification when using Ni<sup>2+</sup> affinity resin, with the proteins either not being eluted from the resin or a high concentration of contaminating background proteins also being eluted. Whereas KIF5A<sub>800-951</sub> displayed a high yield of relatively pure protein after affinity chromatography experiments and is a good candidate for further analysis.

Due to the aggregation of KIF5A<sub>800-1032</sub> seen in Figure 4.8 the aggregation state of affinity chromatography purified KIF5A<sub>800-951</sub> was tested. Purified KIF5A<sub>800-951</sub> was centrifuged at 100,000 x g for 20 min and the resulting pellet and soluble protein sample analysed. The results are shown in Figure 4.12.

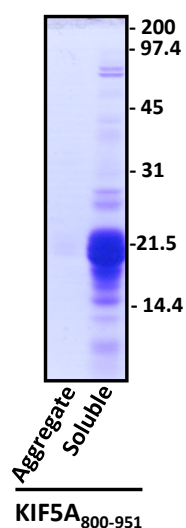


**Figure 4.12 Assessment of the aggregation state of KIF5A<sub>800-951</sub>.**

Bacterial protein samples were centrifuged at 100,000 x g for 20 min at 4°C and the resulting protein pellet and soluble supernatant analysed via SDS-PAGE using Coomassie Blue staining.

High speed centrifugation has demonstrated that the majority of the affinity chromatography purified KIF5A<sub>800-1032</sub> is soluble and hence is an ideal candidate to carry out further structural studies. A summary of the overall cloning, expression, optimization of expression, yield after purification and aggregation state testing of all single KIF5A cargo binding domain proteins is shown in Table 4.3.

Protein	Generation of construct	Correct expression in <i>E.coli</i> cells?	Visual analysis of the soluble fraction	% Solubilisation	Sufficient yield after purification?	Aggregation testing
KIF5A <sub>800-1032</sub> (S-tag)	✓	✓	Clear band in the soluble fraction	35 %	✗	✗
KIF5A <sub>800-1032</sub> (His-tag)	✓	✓	Clear band in the soluble fraction	4 %	✓	✗
KIF5A <sub>820-1032</sub> (His-tag)	✓	✓	Clear band in the soluble fraction	32 %	✗	✗
KIF5A <sub>800-951</sub> (His-tag)	✓	✓	Clear band in the soluble fraction	54 %	✓	✓
KIF5A <sub>820-951</sub> (His-tag)	✓	✓	Clear band in the soluble fraction	57 %	✗	✗

**Table 4.3 Summary of the overall cloning, expression, solubilisation optimisation, purification and aggregation testing for KIF5A<sub>800-1032</sub>, His-tagged KIF5A<sub>800-1032</sub>, KIF5A<sub>820-1032</sub>, KIF5A<sub>800-951</sub> and KIF5A<sub>820-951</sub>.**

In an attempt to further purify as well as assess the native state of KIF5A<sub>800-951</sub> an additional step of size exclusion chromatography was carried out (Section 2.2.4.5). In this case a Superpose™ 6 column was used and can separate proteins from 5–5,000

kDa in size. Prior to loading onto the Superose 6 column KIF5A<sub>800-951</sub> protein was buffer exchanged to remove glycerol and concentrated on a Vivaspin 10 kDa molecular weight cut off column to a concentration of ~ 2 mg/ml (Section 2.2.4.3). The resulting KIF5A<sub>800-951</sub> was found to remain soluble after buffer exchange and protein concentration (data not shown). The results of the size exclusion chromatography are shown in Figure 4.13.

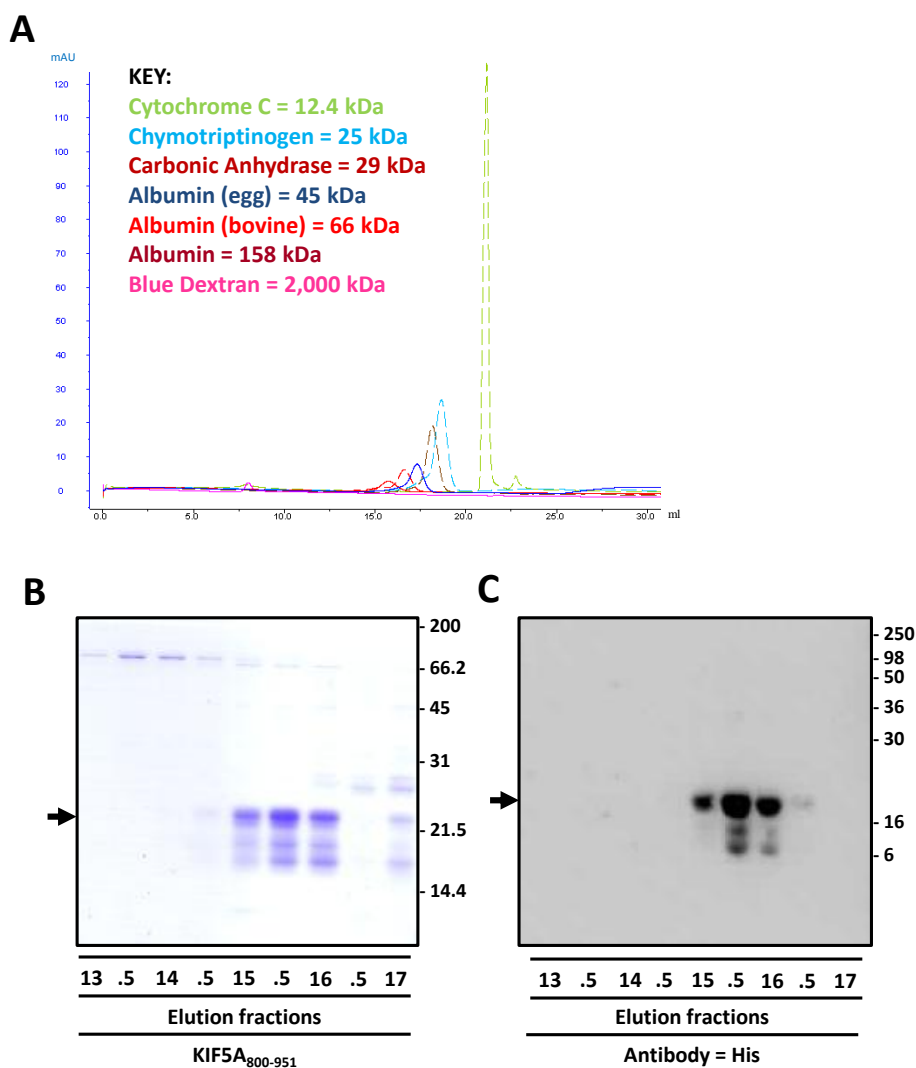


**Figure 4.13** Size exclusion chromatography analysis of affinity chromatography purified KIF5A<sub>800-951</sub>. Affinity chromatography purified KIF5A<sub>800-951</sub> was eluted from the Superose 6 column as 0.5 ml fractions. Results are representative of n = 2 size exclusion experiments. In all Coomassie Blue stained gels and immunoblots elution volumes 13 – 17 ml are shown. The positions of molecular weight standards (kDa) are shown on the right. Arrows indicate the positions of bands of interest. **A** = Molecular weight standards used to calibrate the Superose 6 column and the resulting elution profile. **B** = Coomassie Blue stained KIF5A<sub>800-951</sub> elution fractions. **C** = Immunoblot of KIF5A<sub>800-951</sub> elution fractions probed with anti-His antibodies.

The results from the size exclusion chromatography experiments indicate a good separation of molecular weight standards. KIF5A<sub>800-951</sub> was detected in immunoblot lanes corresponding to elution volumes 15–16.5 ml. The majority of KIF5A<sub>800-951</sub> is seen in elution volume 15.5 ml in both Coomassie Blue stained gels and immunoblots. Calibration of the protein standards indicate that the eluted KIF5A<sub>800-951</sub> is in the range of 66 – 158 kDa. Immunoblotting also indicates two lower molecular weight bands of approximately 16 kDa and 6 kDa in size as seen previously in Figure 4.10. Although size exclusion chromatography has yielded some limited information regarding the native state of KIF5A<sub>800-951</sub>, the yield is seen to decrease after separation and is hence not an ideal method to further purify KIF5A<sub>800-951</sub>.

In order to assess if KIF5A<sub>800-951</sub> can bind microtubules in a similar manner to KIF5B 822-944 (Seeger and Rice, 2010) a microtubule binding assay was performed (Section 2.2.4.6.1). Previous work in the same study has indicated that the interaction of KIF5B with the microtubule is largely electrostatic and can be influenced by the strength of the ionic buffer. Therefore, prior to the microtubule binding assay KIF5A<sub>800-951</sub> was buffer exchanged using a Vivispin 10 kDa molecular weight cut off column to lower the NaCl concentration from 400 mM to 150 mM. The resulting KIF5A<sub>800-951</sub> was found to remain soluble after buffer exchange and to not aggregate (data not shown). Approximately 1.8  $\mu$ M of stable and polymerised microtubules were incubated with varying concentrations of KIF5A<sub>800-951</sub> and the resulting soluble and pellet fractions analysed after high speed centrifugation via SDS-PAGE and Coomassie Blue staining. The results of the microtubule binding assay are shown in Figure 4.14.

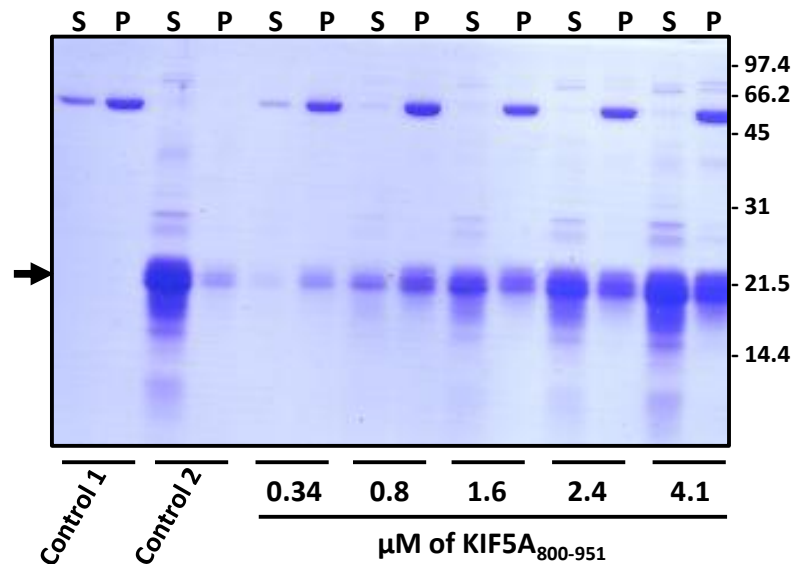


**Figure 4.14 Microtubule binding assay showing the association of microtubules with KIF5A<sub>800-951</sub>.**

Varying concentrations of affinity chromatography purified KIF5A<sub>800-951</sub> was incubated with approximately 1.8  $\mu\text{M}$  of stable and polymerised microtubules for 15 min at room temperature. The samples were subsequently centrifuged for 15 min at 392,000  $\times g$  to separate into pellet and soluble fractions. **S** = supernatant or unbound KIF5A<sub>800-951</sub> and **P** = pellet or bound KIF5A<sub>800-951</sub>. **Control 1** = microtubule only sample and **Control 2** = KIF5A<sub>800-951</sub> only sample. The positions of molecular weight standards (kDa) are shown on the right. The arrow indicates the position of KIF5A<sub>800-951</sub>.

The results from the Coomassie Blue stained gel of the microtubule binding assay indicates the presence of tubulin at approximately 50 kDa in all sample lanes except for control two. The majority of tubulin is seen in the pellet fraction indicating the successful polymerisation of tubulin subunits into microtubules. The results also indicate that the majority of KIF5A<sub>800-951</sub> incubated at a concentration of 0.34–1.6  $\mu\text{M}$  are found in the protein pellet, indicating that KIF5A<sub>800-951</sub> is binding to the microtubules. Samples incubated with 2.4  $\mu\text{M}$  and 4.1  $\mu\text{M}$  of KIF5A<sub>800-951</sub> also show the presence of KIF5A<sub>800-951</sub> in the pellet indicating a positive interaction with microtubules. Although the majority of KIF5A<sub>800-951</sub> in the 2.4  $\mu\text{M}$  and 4.1  $\mu\text{M}$  microtubule incubated samples are seen in the soluble fraction. This is most likely due to the saturation of binding domains available on the polymerised microtubules. As the incubated concentration of KIF5A<sub>800-951</sub> increases the amount of tubulin noted in the soluble sample decreases. This could be due to a “bundling effect” where soluble tubulin is pelleted in the sample despite not specifically binding KIF5A<sub>800-951</sub>. Overall the results from the microtubule binding assay have indicated that KIF5A<sub>800-951</sub> can interact with polymerised microtubules *in vitro*.

### 4.3 DISCUSSION

The structure and function of the motor domain of kinesin-1 has been well studied, with a high resolution crystal structure of the motor domain having been elucidated (Kull *et al.*, 1996; Kozielski *et al.*, 1997; Section 1.2.1). However structural information regarding the cargo binding domain of kinesin-1, vital for transportation of cargo, is relatively unknown. Attempts to gain a high yield of purified KIF5A cargo binding domain in association with its *in vitro* binding partner TRAK2 for structural studies were unsuccessful (see work in Chapter 3). Therefore the aim of this chapter was to generate a high yield of the purified cargo binding domain of KIF5A as a singly expressed protein.

In this chapter it has been demonstrated that a functional KIF5A cargo binding domain protein with a high yield after affinity chromatography can be generated in bacterial cells. Initially five constructs, pETDUETKIF5A<sub>800-1032</sub>, pET151TOPOKIF5A<sub>800-1032</sub>, pETDUETKIF5A<sub>820-1032</sub>, pETDUETKIF5A<sub>800-951</sub> and pETDUETKIF5A<sub>820-951</sub>, were generated and the successful expression of protein in a bacterial system were verified. The analysis of S-tagged KIF5A<sub>800-1032</sub> showed poor yield of purified protein after affinity chromatography using S-protein affinity resin. This result coupled with the poor yield of purified TRAK2<sub>100-380</sub>/KIF5A<sub>800-1032</sub> seen in Section 4.2.1, also using S-protein affinity resin, indicates that the S-tag is being obscured from the resin via the tertiary folding of KIF5A<sub>800-1032</sub>. Subsequently, the generation of a construct to re-locate and change the affinity tag from an S-tag present on the C-terminus to a His-tag present on the N-terminus of KIF5A<sub>800-1032</sub> resulted in an increased yield of protein after affinity chromatography purification experiments. However, the His-tagged KIF5A<sub>800-1032</sub> was unstable and the majority of His-tagged KIF5A<sub>800-1032</sub> aggregated after purification. The analysis of KIF5A<sub>820-1032</sub> and KIF5A<sub>820-951</sub> showed high solubility after protein expression but poor yield after purification via affinity chromatography. Whereas KIF5A<sub>800-951</sub> resulted in high solubility after expression, gave a high yield after affinity chromatography purification and remained stable. Therefore KIF5A<sub>800-951</sub> is an ideal candidate for further structural studies.

The analysis of KIF5A<sub>800-951</sub> using size exclusion chromatography gave some insight into the native state of the purified protein. Results indicated that the majority of KIF5A<sub>800-951</sub> elutes from the column in the region of 66–158 kDa. The predicted molecular

weight of KIF5A<sub>800-951</sub> is 18.8 kDa and hence the size exclusion chromatography data implies the affinity purified KIF5A<sub>800-951</sub> is not a single monomeric subunit. KIF5A<sub>800-951</sub> could instead be possibly interacting with more than one other KIF5A<sub>800-951</sub> molecule. Dimerisation of native kinesin-1 normally involves interaction of the two heavy chains via the stalks coiled-coil domain (Jiang *et al.*, 1997; Hackney *et al.*, 2009). However this region is not present in KIF5A<sub>800-951</sub> and so cannot explain the interaction of KIF5A<sub>800-951</sub> molecules after expression in bacterial cells. One alternative interpretation may be the presence of the two cysteine residues present at amino acids 847 and 943 of KIF5A<sub>800-951</sub>. These cysteine residues may be forming disulfide bonds resulting in the cross linking of more than one KIF5A<sub>800-951</sub> molecule. This cross linking of cysteine residues is unlikely to be occurring after solubilisation of KIF5A<sub>800-951</sub> due to the presence of the reducing agent  $\beta$ -ME in the solubilisation buffer. Disulfide bonds may be being introduced after purification via affinity chromatography due to the high concentration of KIF5A<sub>800-951</sub> without the presence of a reducing agent in the elution buffer. It is also worth noting that estimating the size of KIF5A<sub>800-951</sub> using size exclusion chromatography relies on the assumption that the protein is globular. Recent work by Seeger *et al.* (2012) has indicated that the cargo binding domain of kinesin proteins are highly disordered. More specifically this work demonstrated that KIF5B 822-963 and KIF5B 860-963 are highly disordered. However, using microtubule binding assays it was also shown that KIF5B 822-963 and KIF5B 860-963 remain functional (Seeger *et al.*, 2012). Thus, it is difficult to know if KIF5A<sub>800-951</sub> is acting as a globular protein to allow an accurate assessment of its native state after purification. The results from the size exclusion chromatography experiments indicated that the yield of KIF5A<sub>800-951</sub> decreased after separation by molecular weight using size exclusion chromatography. Overall, although size exclusion chromatography gave some insight into the native state of the affinity chromatography purified KIF5A<sub>800-951</sub>, due to the loss of protein yield it was deemed unsuitable to act as an additional purification step.

The work in this chapter has not managed to fulfil the long term aim, stated in Section 4.1.1, of gaining a solved crystal structure of the cargo binding domain of KIF5A. However, what this chapter has done is make significant steps forward to help achieve this goal. Work presented here has demonstrated that soluble KIF5A<sub>800-951</sub> is able to be expressed in a bacterial expression system and is also able to be purified to mg

quantities after affinity chromatography purification. The affinity purified KIF5A<sub>800-951</sub> is also stable and does not aggregate after buffer exchange experiments. Although the yield of KIF5A<sub>800-951</sub> is high there is the presence of His-tagged protein with a lower molecular weight. If future experiments to generate a crystal structure of KIF5A<sub>800-951</sub> are to succeed then the protein sample will need to be purified further. A homogenous sample i.e. no proteolytically cleaved species, must be present in order to create conditions to form crystals for structural analysis. This work to gain a crystal structure of the cargo binding domain of kinesin-1 still remains an important target to achieve. A solved tertiary structure of the cargo binding domain of KIF5A could lead to a better understanding of how kinesin-1 can interact with such a variety of cargo and adaptor proteins, as well as a better understanding of the mechanisms behind their regulation. However, as discussed earlier, the recent work by Seeger *et al.* (2012) has suggested that the cargo binding domain of KIF5B is highly disordered. This work suggests that gaining a protein of the kinesin-1 cargo binding domain that can crystallise is unlikely due to their unstructured nature. Hence an alternative method such as protein nuclear magnetic resonance (NMR) spectroscopy could be employed. Due to the small size of KIF5A<sub>800-951</sub> NMR spectroscopy may be used to help determine the structure of the kinesin-1 cargo binding domain.

As discussed in Section 1.4 previous studies have shown that the cargo binding domain of kinesin-1 is capable of binding to the motor domain (Cai *et al.*, 2007; Hackney *et al.*, 2009; Wong *et al.*, 2009). The binding of the cargo binding to the motor domain is thought to act as a mechanism for self-inhibition and could act as way to prevent the unnecessary movement of kinesin-1 without any cargo. Seeger and Rice, (2010) has also demonstrated the ability of KIF5B 892-914 to bind directly to microtubules. KIF5B 892-914 includes the final few turns of the predicted coiled-coil domain finishing just before the conserved QIAK region known to be important for binding of the cargo binding to the motor domain. KIF5B 892–914 and the equivalent region of KIF5A share a 70 % amino acid sequence identity. This high amino acid identity alludes to the possibility that KIF5A may also bind microtubules using a similar sequence domain. In this chapter KIF5A<sub>800-951</sub> was shown, via a microtubule binding assay, to co-sediment with microtubules. This result demonstrates that, like KIF5B, the cargo binding domain of KIF5A can interact with microtubules *in vitro*. This also indicates that the regulation

of movement of KIF5A *in vivo* may be mediated by the interaction of the cargo binding domain to the microtubules. Dietrich *et al.* (2008) has further demonstrated that the KIF5B cargo binding domain can bind both the motor domain and microtubules simultaneously. This is interesting as it alludes to the possibility that the cargo binding domain of kinesin-1 can prevent movement by binding directly the microtubule as well as the nucleotide pocket of the motor domain. The work presented in this chapter as well as the work referenced above gives a strong network of evidence to indicate that kinesin-1 will dissociate from the cargo that is being transported and remain bound to the microtubules.

#### 4.3.1 Overall conclusions

- The bacterial expression constructs pETDUETKIF5A<sub>800-1032</sub>, pET151TOPOKIF5A<sub>800-1032</sub>, pETDUETKIF5A<sub>820-1032</sub>, pETDUETKIF5A<sub>800-951</sub> and pETDUETKIF5A<sub>820-951</sub> were successfully generated.
- The expression of each tagged KIF5A cargo binding domain with the correct predicted size was verified by immunoblotting. Further, optimal growth and solubilisation conditions were established for each construct.
- His-tagged KIF5A<sub>800-1032</sub> and KIF5A<sub>800-951</sub> cargo binding domain constructs could be purified. However, the highest yield and the least aggregation were found for KIF5A<sub>800-951</sub>. Thus, KIF5A<sub>800-951</sub> is a good candidate for further structural analyses.
- Similar to KIF5B, KIF5A<sub>800-951</sub> was found to associate with microtubules *in vitro*.

# **CHAPTER 5**

**THE ASSOCIATION BETWEEN THE TRAK AND  
KINESIN-1 FAMILIES; AN INVESTIGATION USING A  
CO-IMMUNOPRECIPITATION STRATEGY**

## 5.1 RATIONALE

As discussed in the Introduction the KHC of kinesin-1 has been shown to bind several kinesin adaptor proteins including Syntabulin, GRIP-1, UNC76, Milton, SNAP23, SNAP25, FEZ1, TRAK1 and TRAK2 (Section 1.2.4). How and where on the KHC the binding occurs for each of these is as yet poorly understood. Only on the adaptor proteins UNC-76, GRIP-1, SNAP23, SNAP25, Milton, TRAK1 and TRAK2 have experiments been carried out in an attempt to map their site of binding to kinesin-1. What is not known is if the interaction between kinesin-1 and the many adaptor proteins known to bind kinesin-1 share conserved binding patterns or in fact have separate methods of association. The C-terminal tail domain of *Drosophila* UNC-76 has been shown via yeast two-hybrid and co-purification assays to bind amino acids 850-975 of *Drosophila* KHC (Gindhart *et al.*, 2003). GRIP1 will bind to amino acids 807-934 to the KHC of KIF5A, KIF5B and KIF5C (Setou *et al.*, 2002). Previous experiments to identify the binding domain of kinesin-1 to the TRAK/Milton family of adaptor proteins utilised KIF5C as a model kinesin. Initially KIF5C was divided into two main regions. These regions were amino acids 1-335 and 336-957. KIF5C 1-335 corresponded to the motor domain and KIF5C 336-957 included the non-motor domain. KIF5C 336-953 was shown using yeast two-hybrid interaction assays, co-immunoprecipitation experiments and FRET studies to interact with TRAK2. Whereas yeast two-hybrid interaction assays and co-immunoprecipitation experiments using KIF5C 1-335 showed no interaction with TRAK2 (Smith *et al.*, 2006). FRET experiments utilising TRAK1 have also concluded that the non-motor domain of KIF5C is responsible for correct interaction (Brickley *et al.*, 2011). Further work divided the KIF5C non-motor domain into three regions; these were amino acids 336-542, 593-804 and 827-957. Again using yeast two-hybrid interaction assays and co-immunoprecipitation experiments it was shown that amino acids 827-957 of KIF5 interact with TRAK2 while 336-542 and 593-804 do not. Conversely the amino acids 124-283 of TRAK2 but not TRAK1 were found to associate with the cargo binding domain of KIF5C, amino acids 827-957 (Brickley *et al.*, 2005).

The cargo binding domains of the kinesin-1 family share an overall ~ 86 % amino acid identity. KIF5A possesses an additional distal 71 C-terminal amino acids compared to KIF5B and KIF5C as shown in Figure 5.1. In the brain, TRAK2 associates predominantly with the kinesin-1, KIF5A (Brickley *et al.*, 2005). In this chapter experiments have been

designed to refine further the TRAK1 and TRAK2 binding site within the cargo domain of KIF5A and KIF5C. Initially a series of KIF5A C-terminal truncations were generated to confirm that, as for KIF5C, it is the cargo binding domain that binds to TRAK2.

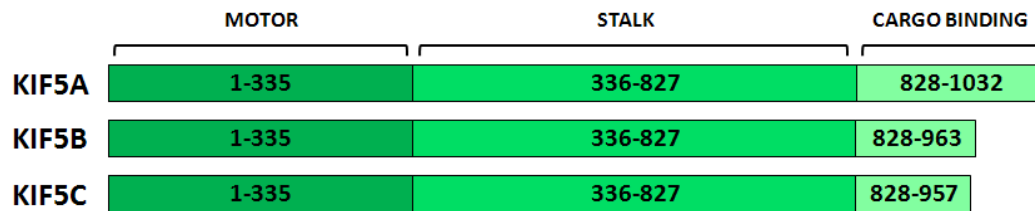


**Figure 5.1 Comparison of human KIF5A, KIF5B and KIF5C kinesin-1 sub-types.**

Structures of KIF5A, KIF5B and KIF5C showing the amino acid numbers of the motor, stalk and cargo binding domains.

In order to assess the binding relationship between kinesin-1 and the TRAK/Milton protein family, recombinant tagged clones of kinesin-1 and TRAK1 and TRAK2 need to be co-expressed in a mammalian cell line. HEK 293 cells are widely used for co-immunoprecipitation experiments because they are simple to culture and transfect. Although HEK 293 cells endogenously express KIF5B there is no endogenous expression of KIF5A, KIF5C or the TRAK/Milton family of proteins (Brickley *et al.*, 2005). Hence the HEK 293 mammalian cell line makes it ideal to assess these proteins of interest in isolation.

### 5.1.1 Aims of this chapter

- I. Ascertain if KIF5A can co-immunoprecipitate with TRAK2 after co-expression in HEK 293 cells.
- II. Using truncated KIF5A constructs refine the binding site within TRAK1 and TRAK2 via co-immunoprecipitation in HEK 293 cells.
- III. Using truncated KIF5C constructs refine the binding site within TRAK1 and TRAK2 via co-immunoprecipitation in HEK 293 cells.

## 5.2 RESULTS

The aim of this chapter was to refine the region of amino acids on kinesin-1 that bind to the TRAK family of proteins. In order to do this, tagged recombinant clones of TRAK1 or TRAK2 and either wild-type and mutated KIF5A or KIF5C were co-expressed in HEK 293 cells and their respective association determined by co-immunoprecipitation. A schematic representation of the co-immunoprecipitation experiments are shown in Figure 5.2.

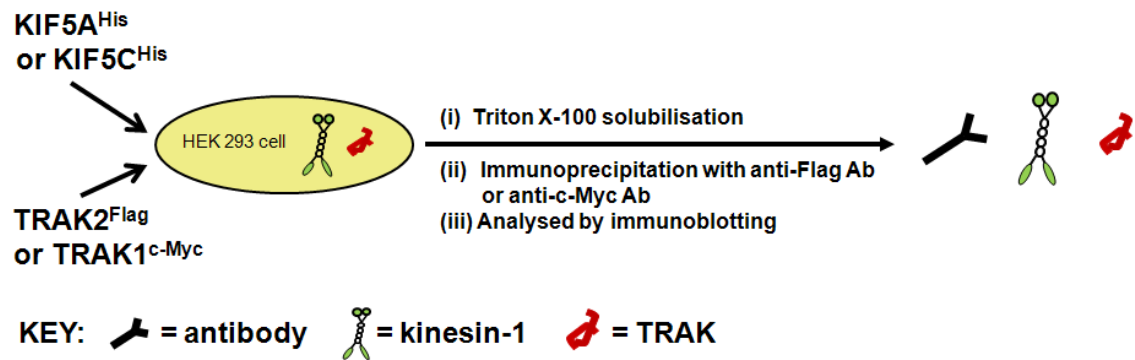
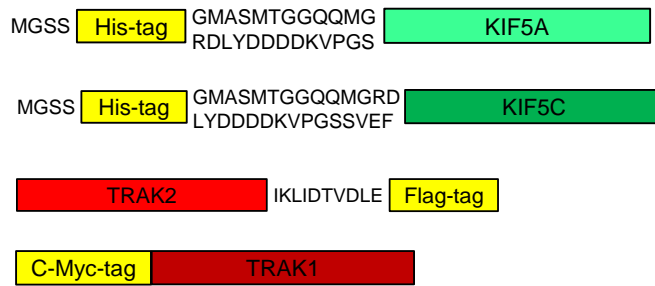


Figure 5.2 A schematic representation of the co-immunoprecipitation experiments.

Initially, wild-type and mutated KIF5A and KIF5C recombinant constructs for expression in mammalian cells were generated following PCR amplification from pBSKIF5A (human) and pN-EYFP-KIF5C (human). KIF5A PCR products were sub-cloned in frame using the restriction sites *EcoRI/BamHI* into pcDNA4HisMax (pcDNA). KIF5C PCR products were sub-cloned in frame using the restriction sites *EcoRI/NotI* into pcDNA. Recombinant KIF5A and KIF5C have an N-terminal His-tag. pCMVTRAK2 was generated as in Smith *et al.* (2006). Recombinant TRAK2 (rat) has a C-terminal Flag-tag. pCMVTRAK1 was generated as in Brickley *et al.* (2005). Recombinant TRAK1 (human) has an N-terminal c-Myc-tag. All recombinant clones were verified via DNA sequencing (Section 2.2.2.13). Figure 5.3 shows schematics of the recombinant clones after expression in HEK 293 cells.



**Figure 5.3 Schematic representations of recombinant tagged KIF5A, KIF5C, TRAK1 and TRAK2.**

HEK 293 cells were co-transfected with TRAK1 or TRAK2 and either wild-type or mutated KIF5A or KIF5C, cell homogenates were prepared, Triton X-100 solubilised and the resulting soluble fraction used for co-immunoprecipitation experiments (Section 2.2.5.8). Co-immunoprecipitation experiments involving TRAK1 were carried out using anti-c-Myc antibodies. Co-immunoprecipitation experiments involving TRAK2 were carried out using anti-Flag antibodies. Both TRAK1 and TRAK2 co-immunoprecipitation experiments were carried out simultaneously with non-immune antibodies as a negative control. The resulting immune and non-immune pellets were dissolved in 20  $\mu$ l 3 x SDS-PAGE sample buffer and 5  $\mu$ l 1 M DTT and divided into 90 % and 10 % aliquots. The 10 % samples of the immune and non-immune pellets were analysed using the precipitating antibody i.e. anti-c-Myc or anti-Flag for detection of TRAK1 or TRAK2 respectively. The 90 % samples were analysed using anti-His antibodies for detection of KIF5A or KIF5C.

### **5.2.1 Does TRAK2 associate with the cargo binding domain of KIF5A?**

To determine if TRAK2 associates with the cargo binding domain of KIF5A three recombinant KIF5A clones were generated. These were pcDNAKIF5A, pcDNAKIF5A<sub>1-825</sub> and pcDNAKIF5A<sub>1-961</sub>. pcDNAKIF5A encodes full length KIF5A which is a positive control, pcDNAKIF5A<sub>1-825</sub> was engineered to delete the KIF5A cargo binding domain and pcDNAKIF5A<sub>1-961</sub> to remove the extra C-terminal 71 amino acids not found in KIF5B and KIF5C (Figure 5.1).

Initially experiments were carried out to show that the recombinant proteins were expressed in mammalian cell lines. Thus, HEK 293 cells were transfected with pCMVTRAK2, pcDNAKIF5A, pcDNAKIF5A<sub>1-825</sub> or pcDNAKIF5A<sub>1-961</sub>, cell homogenates

were prepared (Section 2.2.5.7) and analysed by immunoblotting using either anti-Flag or anti-His antibodies as appropriate (Section 2.2.3.5). Representative immunoblots are shown in Figure 5.4. Each KIF5A construct was successfully expressed in HEK 293 cells as demonstrated by immunoreactive bands corresponding to their predicted sizes, i.e. KIF5A =  $126.5 \pm 2$  kDa ( $n = 21$ ), KIF5A<sub>1-825</sub> =  $99.5 \pm 1.3$  kDa ( $n = 11$ ) and KIF5A<sub>1-961</sub> =  $115.8 \pm 1.3$  kDa ( $n = 13$ ). For the TRAK2 construct, anti-Flag antibodies recognised two major immunoreactive bands, i.e.  $120.4 \pm 1.7$  kDa ( $n = 20$ ) and  $115.1 \pm 1.3$  kDa ( $n = 20$ ). The major band of  $\sim 120$  kDa corresponds to the predicted molecular weight of TRAK2. Previous experiments to over-express the same TRAK2-Flag construct in HEK 293 cells also resulted in the detection of a lower molecular weight immunoreactive species (Brickley *et al.*, 2005). The lower molecular weight band is most likely a product of proteolytic degradation. It is unlikely that this lower molecular weight band is caused by non-specific antibody reactivity since it is not detected in the non-transfected cell samples. It could also be theorised that the proteolytic degradation is occurring at the N-terminus of the TRAK2 protein. This is because the TRAK2 is C-terminally Flag tagged and the lower molecular weight band can be visualised after immunoblotting with anti-Flag antibodies. Another possible cause of the lower molecular weight band seen could be that the TRAK2 proteins are differentially post-translationally modified.

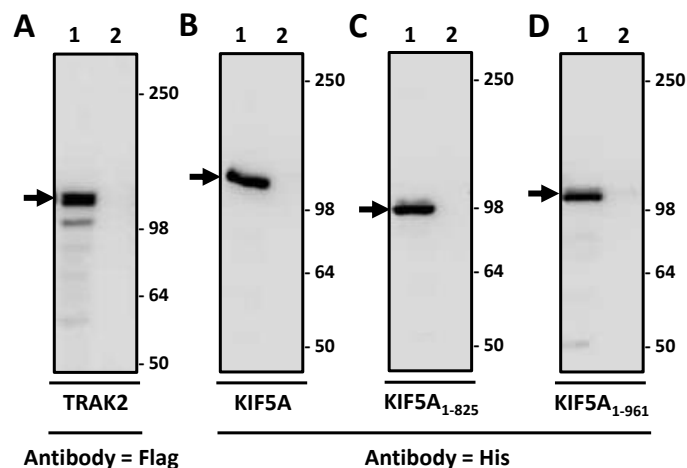


**Figure 5.4 Demonstration of the expression of TRAK2, KIF5A, KIF5A<sub>1-825</sub> and KIF5A<sub>1-961</sub> in HEK 293 cells.** HEK 293 cells were transfected with pCMVTRAK2, pcDNAKIF5A, pcDNAKIF5A<sub>1-825</sub> or pcDNAKIF5A<sub>1-961</sub>. Cell homogenates were prepared 48 h post-transfection and detergent solubilised. In all immunoblots **lane 1** = transfected cell homogenate and **lane 2** = non-transfected cell homogenate. The positions of molecular mass standards (kDa) are shown on the right. Arrows indicate the positions of immunoreactive bands.

**A** = Immunoblot probed with anti-Flag antibodies. **B, C, D** = Immunoblot probed with anti-His antibodies.

To ascertain if the cargo binding domain of KIF5A binds to TRAK2, co-immunoprecipitation assays were carried out. HEK 293 cells were co-transfected with pCMVTRAK2 and either pcDNAKIF5A, pcDNAKIF5A<sub>1-825</sub> or pcDNAKIF5A<sub>1-961</sub>. Representative immunoblots from co-immunoprecipitation experiments (Section 2.2.5.8) are shown in Figure 5.5.

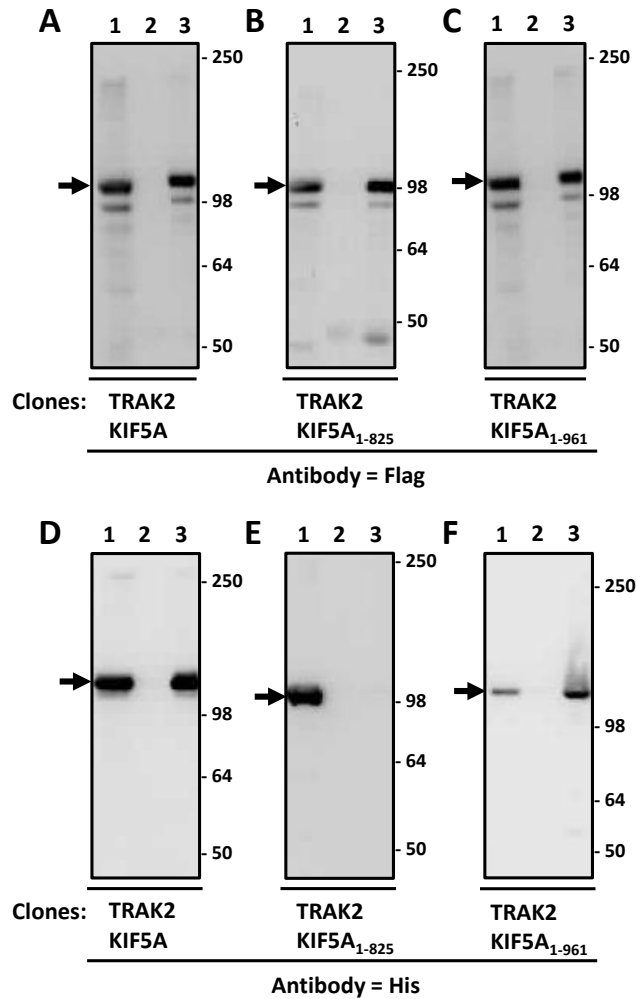


**Figure 5.5 Association of TRAK2 with KIF5A, KIF5A<sub>1-825</sub> and KIF5A<sub>1-961</sub>: demonstration by co-immunoprecipitation.**

HEK 293 cells were co-transfected with pCMVTRAK2 and either pcDNAKIF5A, pcDNAKIF5A<sub>1-825</sub> or pcDNAKIF5A<sub>1-961</sub>. Cell homogenates were prepared 48 h post-transfection, detergent solubilised and co-immunoprecipitations carried out using either anti-Flag antibodies or non-immune Ig. In all immunoblots **lane 1** = transfected HEK 293 cell homogenate, **lane 2** = non-immune pellet and **lane 3** = anti-Flag pellet. Immunoblots are representative of at least  $n = 3$  co-immunoprecipitations from at least  $n = 3$  independent transfections. The positions of molecular mass standards (kDa) are shown on the right. Arrows indicate the position of immunoreactive bands.

**A, B, C** = 10 % of the immune and non-immune pellets probed with anti-Flag antibodies. **D, E, F** = 90 % of the immune and non-immune pellets probed with anti-His antibodies.

TRAK2 was present in all immune pellets but not in the non-immune pellets. This is expected and demonstrates that the immunoprecipitation of the TRAK2 protein was successful. KIF5A and KIF5A<sub>1-961</sub> were present in the immune pellet but not the non-immune pellet. This shows that KIF5A and KIF5A<sub>1-961</sub> co-immunoprecipitate with TRAK2 following co-expression in HEK 293 cells. No signal was detected for KIF5A<sub>1-825</sub> in immune pellets. This indicates that KIF5A<sub>1-825</sub> does not co-immunoprecipitate with TRAK2 when co-expressed in HEK 293 cells.

To demonstrate that KIF5A, KIF5A<sub>1-825</sub> and KIF5A<sub>1-961</sub> recombinant proteins were expressed to a similar level when co-expressed with TRAK2, quantitative immunoblotting was performed (Section 2.2.3.5). Band densitometry of the solubilised fractions from co-expression experiments were expressed as a percentage of the full length KIF5A. Histograms summarising the relative expression of TRAK2, KIF5A, KIF5A<sub>1-825</sub> and KIF5A<sub>1-961</sub> are shown in Figure 5.6.

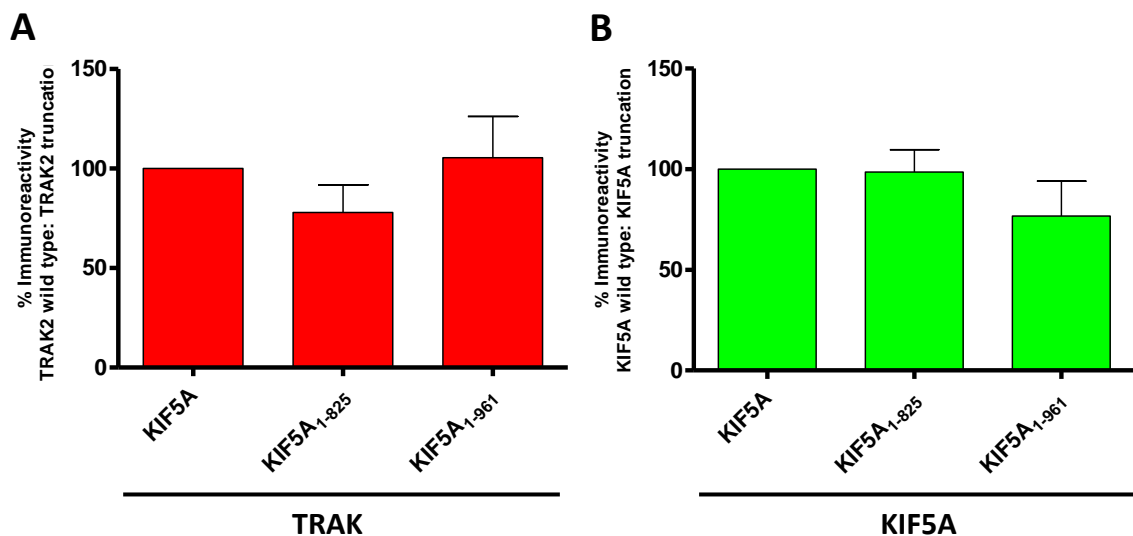


**Figure 5.6** Histograms showing the expression levels of TRAK2 and KIF5A, KIF5A<sub>1-825</sub> and KIF5A<sub>1-961</sub> following co-expression.

HEK 293 cells were co-transfected with pCMVTRAK2 and either pcDNAKIF5A, pcDNAKIF5A<sub>1-825</sub> or pcDNAKIF5A<sub>1-961</sub>. Cell homogenates were prepared 48 h post-transfection, detergent solubilised and each was analysed by immunoblotting with the appropriate antibodies. The ratio of immunoreactivity of the soluble input was taken and expressed as a percentage of the control which is 100 %. The graph shows the means  $\pm$  S.E.M for at least  $n = 3$  experiments from at least  $n = 3$  independent co-transfections. Statistical significance was measured using a student's *t*-test.

**A** = Immunoreactivity of TRAK2 wild type: TRAK2 truncation after co-expression with KIF5A.

**B** = Immunoreactivity of KIF5A wild type: KIF5A truncation after co-expression with TRAK2.

No significant change in the expression level of TRAK2 was noted when co-expressed with KIF5A, KIF5A<sub>1-825</sub> or KIF5A<sub>1-961</sub>. Also no significant change in the expression level of KIF5A<sub>1-825</sub> or KIF5A<sub>1-961</sub> recombinant proteins were seen when co-expressed together with TRAK2 compared to the full length KIF5A.

The immunoblots from co-immunoprecipitation experiments (Figure 5.4) were quantified to determine if there was a difference in the efficiency of co-immunoprecipitation of TRAK2 with KIF5A, KIF5A<sub>1-825</sub> and KIF5A<sub>1-961</sub>. Band densitometry of immune pellet bands compared to that of the input from co-immunoprecipitations were taken and expressed as a percentage of the full length KIF5A control (100 %). Representative histograms are shown in Figure 5.7.

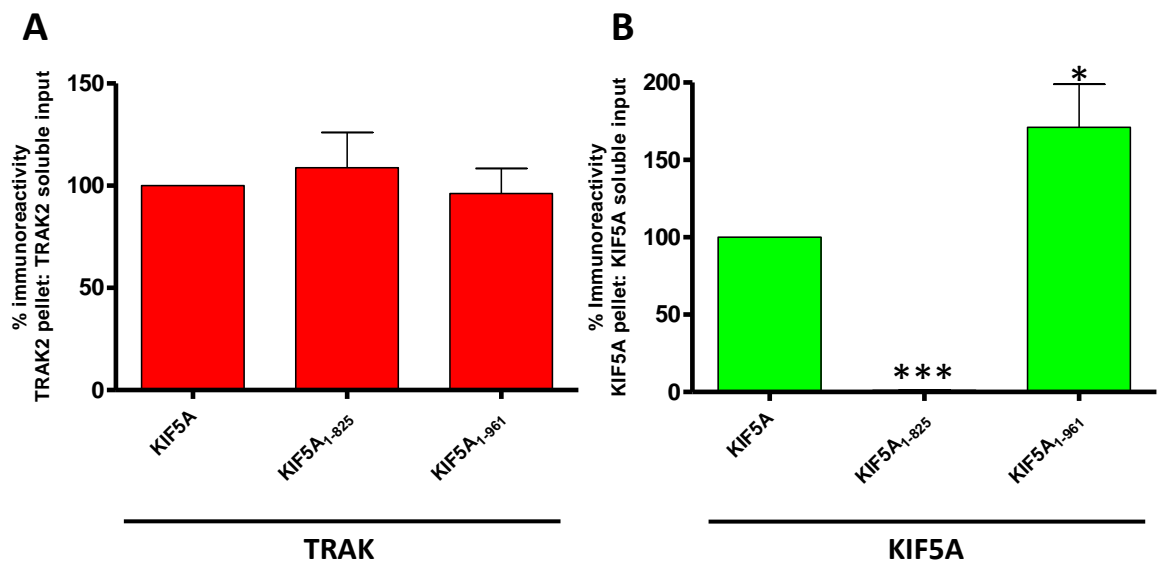


**Figure 5.7 Histograms showing the association of TRAK2 with KIF5A, KIF5A<sub>1-825</sub> and KIF5A<sub>1-961</sub> following co-immunoprecipitation.**

HEK 293 cells were co-transfected with pCMVTRAK2 and either pcDNAKIF5A, pcDNAKIF5A<sub>1-825</sub> or pcDNAKIF5A<sub>1-961</sub>. Cell homogenates were prepared 48 h post-transfection, detergent solubilised and co-immunoprecipitations carried out using either anti-Flag antibodies or non-immune Ig. The ratio of immunoreactivity of the immune pellet: soluble input was taken and expressed as a percentage of the control which is 100 %. The graph shows the means  $\pm$  S.E.M for at least  $n = 3$  co-immunoprecipitations from at least  $n = 3$  independent transfections. The statistical significance was measured using a student's  $t$ -test where  $*P < 0.05$  and  $***P < 0.001$ .

**A** = Immunoreactivity of TRAK2 pellet: TRAK2 soluble input. **B** = Immunoreactivity of KIF5A pellet: KIF5A soluble input.

Quantitative immunoblot analysis confirmed the findings demonstrated in Figure 5.4, i.e. KIF5A<sub>1-825</sub> does not co-immunoprecipitate with TRAK2 to a statistical significance of  $P < 0.001$ . In contrast, KIF5A<sub>1-961</sub> has a  $\sim 50$  % increase in interaction with TRAK2 with

respect to TRAK2/KIF5A (n = 6 independent co-immunoprecipitations from n = 6 independent transfections).

### 5.2.2 Refinement of the TRAK2 binding site within the KIF5A cargo binding domain

Experiments carried out in Section 5.2.1 demonstrated that KIF5A co-immunoprecipitates with TRAK2 via the KIF5A cargo binding domain. To investigate the specific residues in the cargo binding domain responsible for binding to TRAK2 further truncations were generated. These truncations exploited amino acid regions showing the highest degree of difference and similarity between the three kinesin-1 subtypes. These KIF5A truncations were pcDNAKIF5A<sub>1-942</sub>, pcDNAKIF5A<sub>1-909</sub>, pcDNAKIF5A<sub>1-885</sub>, pcDNAKIF5A<sub>1-877</sub> and pcDNAKIF5A<sub>1-861</sub>. KIF5A<sub>1-942</sub>, KIF5A<sub>1-909</sub>, KIF5A<sub>1-885</sub> and KIF5A<sub>1-877</sub> were chosen to exploit the amino acids of KIF5A that are different when compared to KIF5B and KIF5C. KIF5A<sub>1-861</sub> was chosen to remove some of the positively charged amino acids present between KIF5A 825-877 that may be responsible for protein-protein interactions. The amino acid locations of the KIF5A truncations are shown in Figure 5.8.

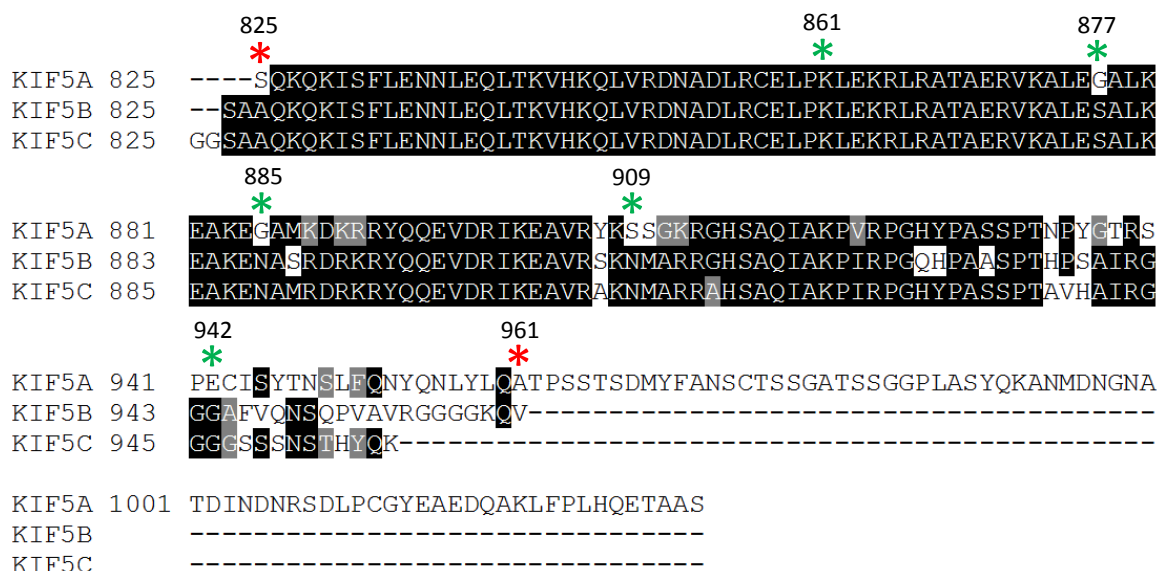


**Figure 5.8 Alignment of the kinesin-1 cargo binding domains.**

An alignment of the cargo binding domain amino acid sequences of KIF5A, KIF5B and KIF5C showing the choice of truncated amino acids. The amino acids identical between KIF5A, KIF5B and KIF5C sub-types are highlighted in black while those in grey are similar. Red stars indicate previously truncated KIF5A constructs. Green stars indicate newly truncated KIF5A constructs.

Initial experiments were carried out to show that the recombinant proteins were expressed in mammalian cell lines. Thus, HEK 293 cells were transfected with pcDNAKIF5A<sub>1-942</sub>, pcDNAKIF5A<sub>1-909</sub>, pcDNAKIF5A<sub>1-885</sub>, pcDNAKIF5A<sub>1-877</sub> and pcDNAKIF5A<sub>1-861</sub>, cell homogenates were prepared (Section 2.2.5.7) and analysed by immunoblotting using anti-His antibodies (Section 2.2.3.5). Representative immunoblots are shown in Figure 5.9. Each KIF5A construct was successfully expressed in HEK 293 cells as demonstrated by immunoreactive bands corresponding to their predicted sizes, i.e. KIF5A<sub>1-942</sub> = 117.4 ± 1.8 kDa (n = 7), KIF5A<sub>1-909</sub> = 114.7 ± 2 kDa (n = 7), KIF5A<sub>1-885</sub> = 107.1 ± 4.6 kDa (n = 5), KIF5A<sub>1-877</sub> = 105.9 ± 2.8 kDa (n = 8) and KIF5A<sub>1-861</sub> = 107.8 ± 4.6 kDa (n = 3).

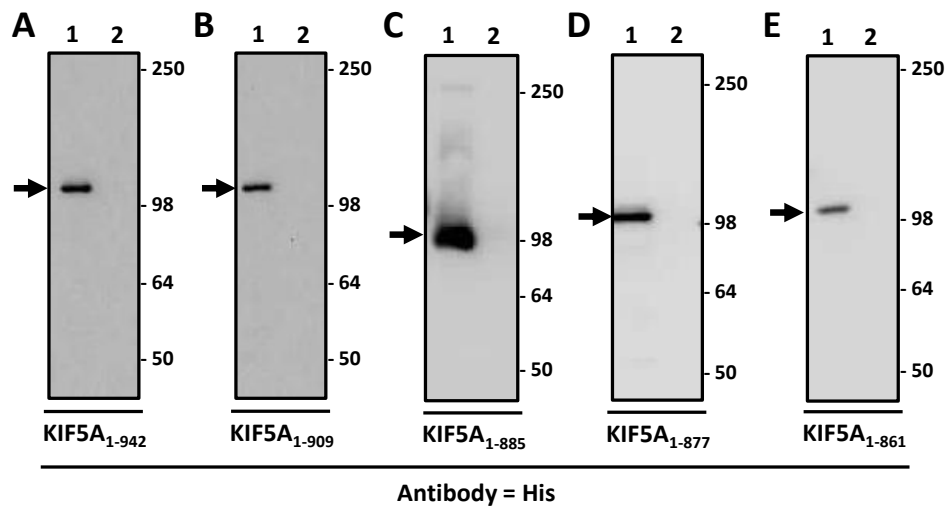


**Figure 5.9 Demonstration of the expression of KIF5A<sub>1-942</sub>, KIF5A<sub>1-909</sub>, KIF5A<sub>1-885</sub>, KIF5A<sub>1-877</sub> and KIF5A<sub>1-861</sub> in HEK 293 cells.**

HEK 293 cells were transfected with pcDNAKIF5A<sub>1-942</sub>, pcDNAKIF5A<sub>1-909</sub>, pcDNAKIF5A<sub>1-885</sub>, pcDNAKIF5A<sub>1-877</sub> or pcDNAKIF5A<sub>1-861</sub>. Cell homogenates were prepared 48 h post-transfection and detergent solubilised. In all immunoblots **lane 1** = transfected soluble sample and **lane 2** = non-transfected HEK 293 cells. The positions of molecular mass standards (kDa) are shown on the right. Arrows indicate the position of immunoreactive bands.

**A, B, C, D, E** = Immunoblot probed with anti-His antibodies.

To refine the TRAK2 binding site within the KIF5A cargo binding domain co-immunoprecipitation assays were carried out. HEK 293 cells were co-transfected with pCMVTRAK2 and either pcDNAKIF5A<sub>1-942</sub>, pcDNAKIF5A<sub>1-909</sub>, pcDNAKIF5A<sub>1-885</sub>, pcDNAKIF5A<sub>1-877</sub> or pcDNAKIF5A<sub>1-861</sub>. Full length KIF5A is known to co-immunoprecipitate with TRAK2 and KIF5A<sub>1-825</sub> does not co-immunoprecipitate with TRAK2 (Section 5.2.1). Hence, pcDNAKIF5A and pcDNAKIF5A<sub>1-825</sub> were each co-

transfected with pCMVTRAK2 to act as positive and negative controls. Representative immunoblots from co-immunoprecipitation experiments (Section 2.2.5.8) are shown in Figure 5.10.

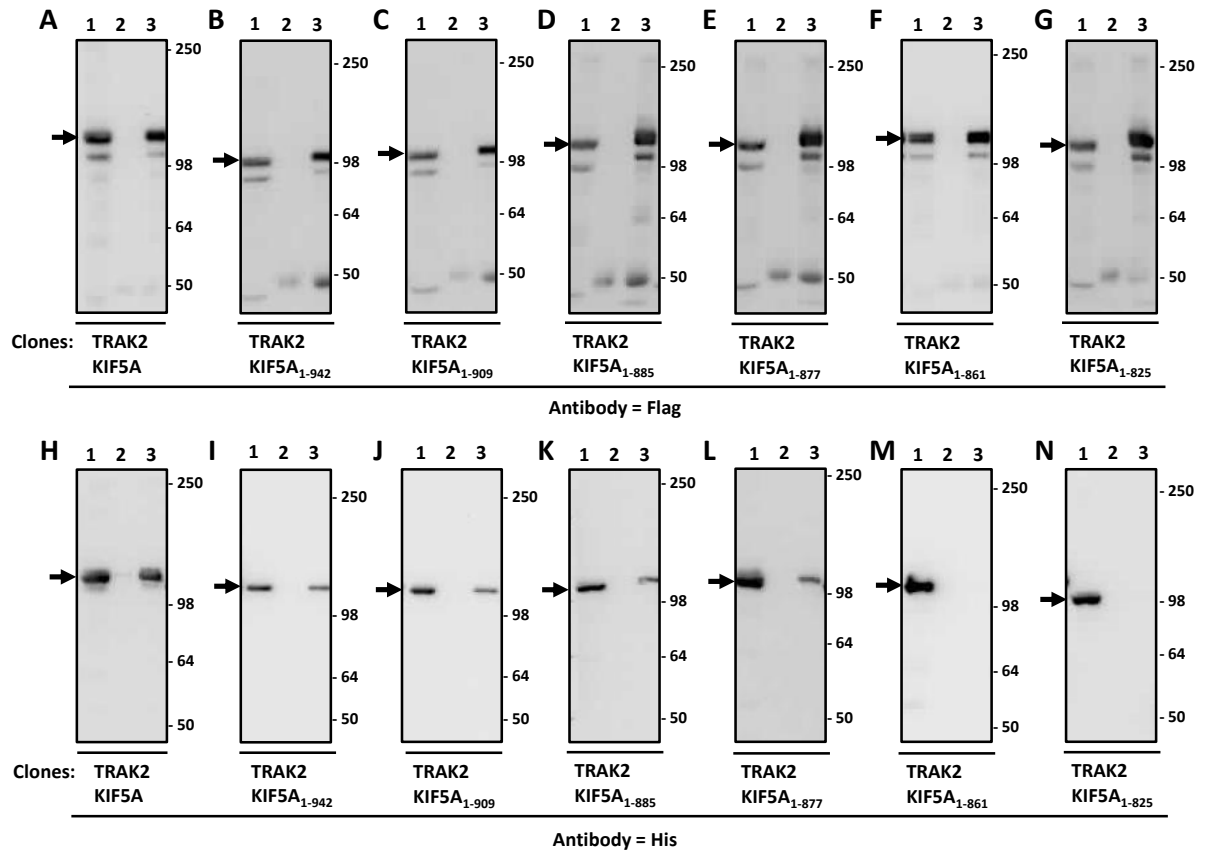


**Figure 5.10 Association of TRAK2 with KIF5A, KIF5A<sub>1-942</sub>, KIF5A<sub>1-909</sub>, KIF5A<sub>1-885</sub>, KIF5A<sub>1-877</sub>, KIF5A<sub>1-861</sub> and KIF5A<sub>1-825</sub>: demonstration by co-immunoprecipitation.**

HEK 293 cells were transfected with pCMVTRAK2 and either pcDNAKIF5A, pcDNAKIF5A<sub>1-942</sub>, pcDNAKIF5A<sub>1-909</sub>, pcDNAKIF5A<sub>1-885</sub>, pcDNAKIF5A<sub>1-877</sub>, pcDNAKIF5A<sub>1-861</sub> or pcDNAKIF5A<sub>1-825</sub>. Cell homogenates were prepared 48 h post-transfection, detergent solubilised and co-immunoprecipitations carried out using either anti-Flag antibodies or non-immune Ig. In all immunoblots **lane 1** = transfected soluble HEK 293 cell homogenate, **lane 2** = non-immune pellet and **lane 3** = anti-Flag pellet. Immunoblots are representative of at least  $n = 3$  co-immunoprecipitations from  $n = 3$  independent transfections. The positions of molecular mass standards (kDa) are shown on the right. Arrows indicate the position of immunoreactive bands.

**A, B, C, D, E, F, G** = 10 % of the immune and non-immune pellets probed with anti-Flag antibodies.

**H, I, J, K, L, M, N** = 90 % of the immune and non-immune pellets probed with anti-His antibodies.

TRAK2 was present in all immune pellets but not in the non-immune pellets. This is expected and demonstrates that the immunoprecipitation of the TRAK2 protein was successful. KIF5A, KIF5A<sub>1-942</sub>, KIF5A<sub>1-909</sub>, KIF5A<sub>1-885</sub> and KIF5A<sub>1-877</sub> were present in the immune pellet but not the non-immune pellet. This shows that KIF5A, KIF5A<sub>1-942</sub>, KIF5A<sub>1-909</sub>, KIF5A<sub>1-885</sub> and KIF5A<sub>1-877</sub> co-immunoprecipitate with TRAK2 following co-

expression in HEK 293 cells. No signal was detected for KIF5A<sub>1-861</sub> and KIF5A<sub>1-825</sub> in immune pellets. This indicates that KIF5A<sub>1-861</sub> and KIF5A<sub>1-825</sub> do not co-immunoprecipitate with TRAK2 when co-expressed in HEK 293 cells. Thus, the critical amino acids for TRAK2 binding are 861-961 of KIF5A.

To demonstrate that KIF5A, KIF5A<sub>1-942</sub>, KIF5A<sub>1-909</sub>, KIF5A<sub>1-885</sub>, KIF5A<sub>1-877</sub>, KIF5A<sub>1-861</sub> and KIF5A<sub>1-825</sub> recombinant proteins were expressed to a similar level when co-expressed with TRAK2, quantitative immunoblotting was performed (Section 2.2.3.5.3). Band densitometry of the solubilised fractions from co-expression experiments were expressed as a percentage of the full length KIF5A. Histograms summarising the relative expression of TRAK2, KIF5A, KIF5A<sub>1-942</sub>, KIF5A<sub>1-909</sub>, KIF5A<sub>1-885</sub>, KIF5A<sub>1-877</sub>, KIF5A<sub>1-861</sub> and KIF5A<sub>1-825</sub> are shown in Figure 5.11.

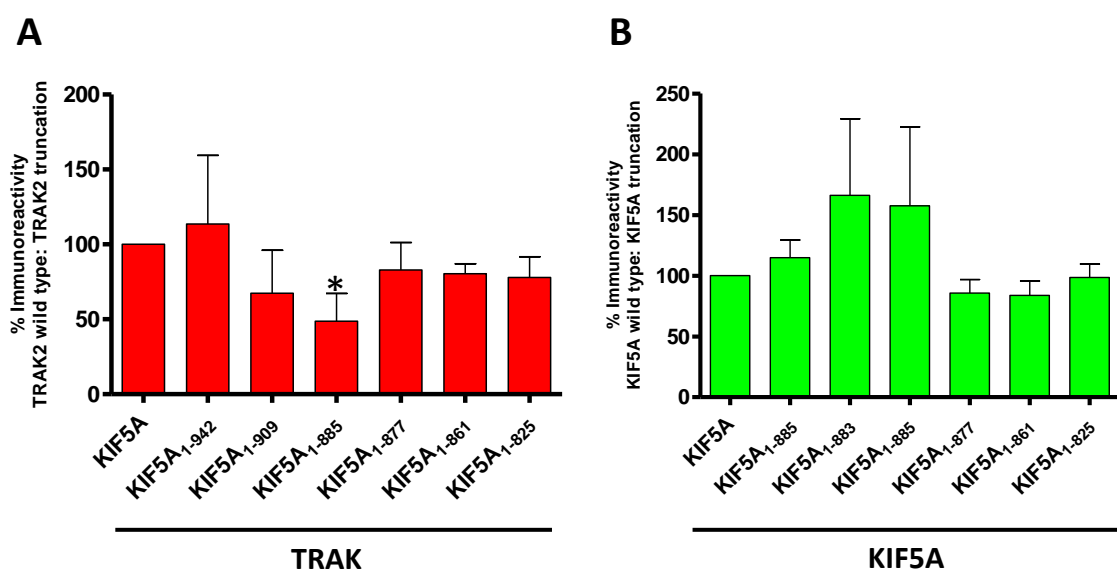


**Figure 5.11** Histograms showing the expression levels of TRAK2 and KIF5A, KIF5A<sub>1-942</sub>, KIF5A<sub>1-909</sub>, KIF5A<sub>1-885</sub>, KIF5A<sub>1-877</sub>, KIF5A<sub>1-861</sub> and KIF5A<sub>1-825</sub> following co-expression.

HEK 293 cells were transfected with pCMVTRAK2 and either pcDNAKIF5A, pcDNAKIF5A<sub>1-942</sub>, pcDNAKIF5A<sub>1-909</sub>, pcDNAKIF5A<sub>1-885</sub>, pcDNAKIF5A<sub>1-877</sub>, pcDNAKIF5A<sub>1-861</sub> or pcDNAKIF5A<sub>1-825</sub>. Cell homogenates were prepared 48 h post-transfection, detergent solubilised and each was analysed by immunoblotting with the appropriate antibody as shown above. The ratio of immunoreactivity of the soluble input was taken and expressed as a percentage of the control which is 100 %. The graph shows the means  $\pm$  S.E.M for at least  $n = 3$  experiments from at least  $n = 3$  independent co-transfections. Statistical significance was measured using a student's  $t$ -test where  $*P < 0.05$ .

**A** = Immunoreactivity of TRAK2 wild type: TRAK2 truncation after co-expression with KIF5A.

**B** = Immunoreactivity of KIF5A wild type: KIF5A truncation after co-expression with TRAK2.

No significant change in the expression level of KIF5A<sub>1-942</sub>, KIF5A<sub>1-909</sub>, KIF5A<sub>1-885</sub>, KIF5A<sub>1-877</sub>, KIF5A<sub>1-861</sub> and KIF5A<sub>1-825</sub> recombinant proteins when co-expressed together with

TRAK2 were seen when compared to the full length KIF5A. Also no significant change in the expression level of TRAK2 was noted when co-expressed with KIF5A, KIF5A<sub>1-942</sub>, KIF5A<sub>1-909</sub>, KIF5A<sub>1-877</sub>, KIF5A<sub>1-861</sub> and KIF5A<sub>1-825</sub>. However, the relative expression of TRAK2 when co-expressed with KIF5A<sub>1-885</sub> was found to be significantly lower ( $P < 0.05$ ).

The immunoblots from co-immunoprecipitation experiments (Figure 5.9) were quantified to determine if there was a difference in the efficiency of co-immunoprecipitation of TRAK2 with KIF5A, KIF5A<sub>1-942</sub>, KIF5A<sub>1-909</sub>, KIF5A<sub>1-885</sub>, KIF5A<sub>1-877</sub>, KIF5A<sub>1-861</sub> and KIF5A<sub>1-825</sub>. Band densitometry of immune pellet bands compared to that of the input from co-immunoprecipitations were taken and expressed as a percentage of the full length KIF5A control (100 %). Representative histograms are shown in Figure 5.12.

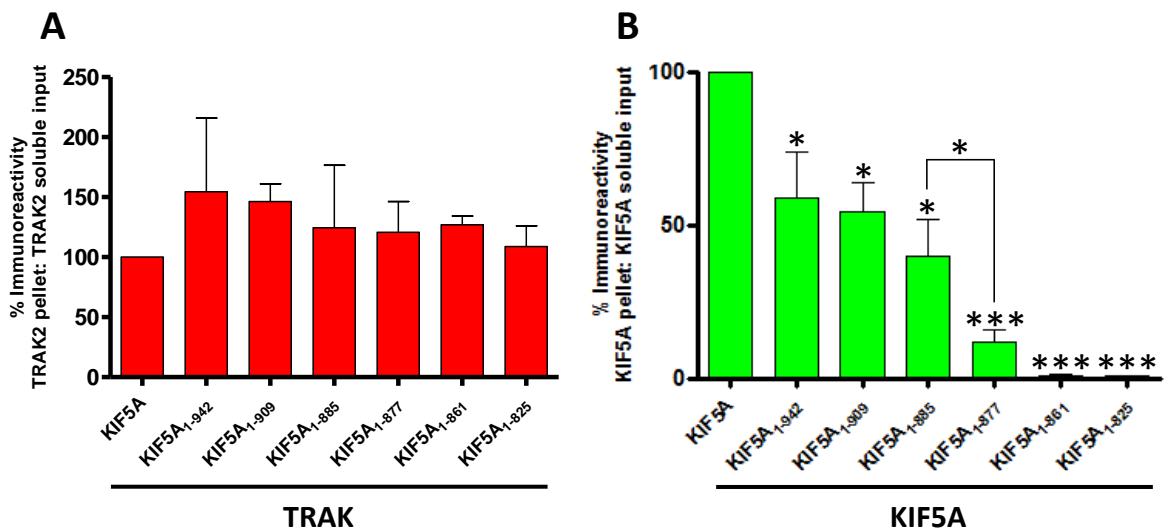


**Figure 5.12 Histograms showing the association of TRAK2 with KIF5A, KIF5A<sub>1-942</sub>, KIF5A<sub>1-909</sub>, KIF5A<sub>1-885</sub>, KIF5A<sub>1-877</sub>, KIF5A<sub>1-861</sub> and KIF5A<sub>1-825</sub> following co-immunoprecipitation.**

HEK 293 cells were transfected with pCMVTRAK2 and either pcDNAKIF5A, pcDNAKIF5A<sub>1-942</sub>, pcDNAKIF5A<sub>1-909</sub>, pcDNAKIF5A<sub>1-885</sub>, pcDNAKIF5A<sub>1-877</sub>, pcDNAKIF5A<sub>1-861</sub> and pcDNAKIF5A<sub>1-825</sub>. Cell homogenates were prepared 48 h post-transfection, detergent solubilised and co-immunoprecipitations carried out using either anti-Flag antibodies or non-immune Ig. The ratio of immunoreactivity of the immune pellet: soluble input was taken and expressed as a percentage of the control which is 100 %. The graph shows the means  $\pm$  S.E.M for at least  $n = 3$  co-immunoprecipitations from at least  $n = 3$  independent transfections. The statistical significance was measured using a student's  $t$ -test where  $*P < 0.05$  and  $***P < 0.001$ .

**A** = Immunoreactivity of TRAK2 pellet: TRAK2 soluble input. **B** = Immunoreactivity of KIF5A pellet: KIF5A soluble input.

Quantitative band analysis shows a significant decrease in the co-immunoprecipitation of the truncated KIF5A recombinant proteins with that of TRAK2. KIF5A<sub>1-942</sub>, KIF5A<sub>1-909</sub>, KIF5A<sub>1-885</sub> all appear to show a ~ 50 % decrease in co-immunoprecipitation with TRAK2. KIF5A<sub>1-877</sub> shows a ~ 90 % decrease in co-immunoprecipitation with TRAK2. KIF5A<sub>1-861</sub> does not co-immunoprecipitate with TRAK2 after co-expression in HEK 293 cells. Truncation of the eight amino acid sequence from KIF5A<sub>1-885</sub> to create KIF5A<sub>1-877</sub> has also revealed a significant reduction in co-immunoprecipitation with TRAK2 of ~ 30 %. KIF5A<sub>1-861</sub> and KIF5A<sub>1-825</sub> both demonstrate no ability to co-immunoprecipitate with TRAK2. This group of co-immunoprecipitation experiments has revealed three possible sites within the KIF5A cargo binding domain as being important for association with TRAK2. The first identified site was located between KIF5A 942-961, the second site between KIF5A 877-885 and the third between KIF5A 861-877. All three amino acid binding regions are highlighted in Figure 5.13.

```

KIF5A 825  SQKQKISFLENNLEQLTKVHKQLVRDNADLRCELPKLEKRLRATAERVKALEGALKEAKEG
KIF5A 886  AMKDKRRYQQEVDRIKEAVRYKSSGKRGHSAQIAKPVRPGHYPASSPTNPYGTRSPECISY
KIF5A 947  TNSLFQNYQNLYLQATPSSTSDMYFANSCTSSGATSSGGPLASYQKANMDNGNATDINDNR
KIF5A 1008 SDLPCGYEAEDQAKLFPLHQETAAS

```

**Figure 5.13 Amino acid regions responsible for the association of KIF5A with TRAK2.**

The first identified site is located between amino acids 942-961 and is highlighted in purple. The second identified site is located between amino acids 877-885 and is highlighted in red. The third identified site is located between amino acids 861-877 and is highlighted in blue.

### 5.2.3 Further refinement of amino acids 877-885 of KIF5A by truncation

Section 5.2.2 showed that an eight amino acid sequence between KIF5A 877-885 is responsible for ~ 30 % of KIF5A's ability to co-immunoprecipitate with TRAK2. Hence, the role of these eight amino acids was investigated. This was carried out by further truncating the amino acid region of interest resulting in three new recombinant clones, pcDNAKIF5A<sub>1-883</sub>, pcDNAKIF5A<sub>1-881</sub> and pcDNAKIF5A<sub>1-879</sub>.

As for previous recombinant KIF5A proteins, initial experiments were carried out to show that the recombinant proteins were expressed in mammalian cell lines. Thus, HEK 293 cells were transfected with pcDNAKIF5A<sub>1-883</sub>, pcDNAKIF5A<sub>1-881</sub> and pcDNAKIF5A<sub>1-879</sub>, cell homogenates were prepared (Section 2.2.5.7) and analysed by

immunoblotting using anti-His antibodies. Representative immunoblots are shown in Figure 5.14. Each KIF5A construct was successfully expressed in HEK 293 cells as demonstrated by immunoreactive bands corresponding to their predicted sizes, i.e. KIF5A<sub>1-883</sub> = 105.7 kDa ± 3.4 (n = 6), KIF5A<sub>1-881</sub> = 101 kDa ± 1.6 (n = 3) and KIF5A<sub>1-879</sub> = 107.3 kDa ± 2.2 (n = 7).

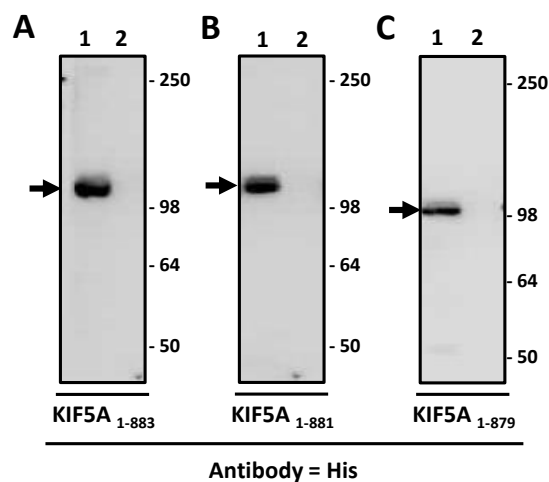


**Figure 5.14 Demonstration of the expression of KIF5A<sub>1-883</sub>, KIF5A<sub>1-881</sub> and KIF5A<sub>1-879</sub> in HEK 293 cells.** HEK 293 cells were transfected with pcDNAKIF5A<sub>1-883</sub>, pcDNAKIF5A<sub>1-881</sub> or pcDNAKIF5A<sub>1-879</sub>. Cell homogenates were prepared 48 h post-transfection and detergent solubilised. In all immunoblots **lane 1** = transfected cell homogenate and **lane 2** = non-transfected cell homogenate. The positions of molecular mass standards (kDa) are shown on the right. Arrows indicate the position of immunoreactive bands.

**A, B, C** = Immunoblot probed with anti-His antibodies.

To further refine the amino acids 877-885 of KIF5A, co-immunoprecipitation assays were carried out. HEK 293 cells were co-transfected with pCMVTRAK2 and either pcDNAKIF5A<sub>1-883</sub>, pcDNAKIF5A<sub>1-881</sub> or pcDNAKIF5A<sub>1-879</sub>. pcDNAKIF5A and pcDNAKIF5A<sub>1-825</sub> were each co-transfected with pCMVTRAK2 to act as positive and negative controls. Representative immunoblots from co-immunoprecipitation experiments (Section 2.2.5.8) are shown in Figure 5.15.

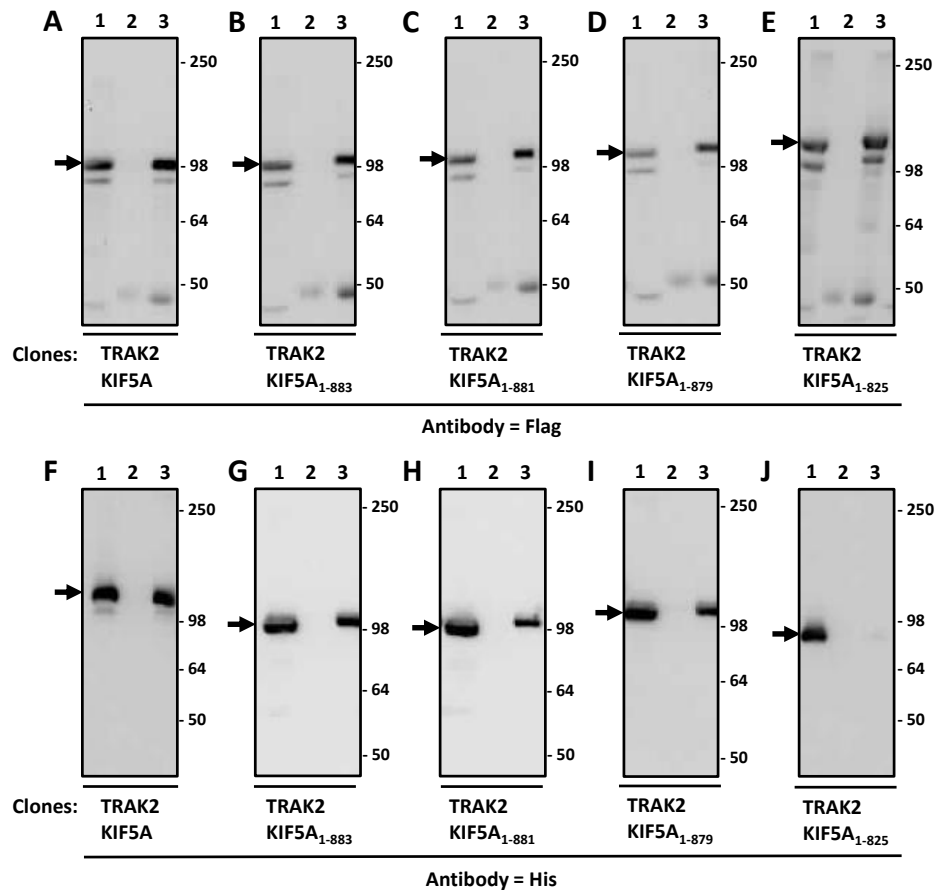


**Figure 5.15 Demonstration by immunoprecipitation the association of TRAK2 with KIF5A, KIF5A<sub>1-883</sub>, KIF5A<sub>1-881</sub>, KIF5A<sub>1-879</sub> and KIF5A<sub>1-825</sub> following their co-expression in HEK 293 cells.**

HEK 293 cells were transfected with pCMVTRAK2 and either KIF5A, KIF5A<sub>1-883</sub>, KIF5A<sub>1-881</sub>, KIF5A<sub>1-879</sub> and KIF5A<sub>1-825</sub>. Cell homogenates were prepared 48 h post-transfection, detergent solubilised and co-immunoprecipitations carried out using either anti-Flag antibodies or non-immune Ig. In all immunoblots **lane 1** = transfected soluble HEK 293 cell homogenate, **lane 2** = non-immune pellet and **lane 3** = anti-Flag pellet. Immunoblots are representative of at least n = 3 co-immunoprecipitations from n = 3 independent transfections. The positions of molecular mass standards (kDa) are shown on the right. Arrows indicate the position of immunoreactive bands.

**A, B, C, D, E** = 10 % of the immune and non-immune pellets probed with anti-Flag antibodies. **F, G, H, I, J** = 90 % of the immune and non-immune pellets probed with anti-His antibodies.

TRAK2 was present in all immune pellets but not in the non-immune pellets. This was expected and demonstrates that the immunoprecipitation of the TRAK2 protein was successful. KIF5A, KIF5A<sub>1-883</sub>, KIF5A<sub>1-881</sub> and KIF5A<sub>1-879</sub> were all found to be present in the immune pellet but not in the non-immune pellet. This indicates that KIF5A, KIF5A<sub>1-883</sub>, KIF5A<sub>1-881</sub> and KIF5A<sub>1-879</sub> co-immunoprecipitate with TRAK2 following their co-expression in HEK 293 cells. No signal was detected for KIF5A<sub>1-825</sub> in immune pellets. This indicates that KIF5A<sub>1-825</sub> does not co-immunoprecipitate with TRAK2 when co-expressed in HEK 293 cells.

To demonstrate that KIF5A, KIF5A<sub>1-883</sub>, KIF5A<sub>1-881</sub>, KIF5A<sub>1-879</sub> and KIF5A<sub>1-825</sub> recombinant proteins were expressed to a similar level when co-expressed with TRAK2, quantitative immunoblotting was performed (Section 2.2.3.5). Band densitometry of the solubilised fractions from co-expression experiments were expressed as a percentage of the full length KIF5A. Histograms summarising the relative expression of TRAK2, KIF5A, KIF5A<sub>1-883</sub>, KIF5A<sub>1-881</sub>, KIF5A<sub>1-879</sub> and KIF5A<sub>1-825</sub> are shown in Figure 5.16.

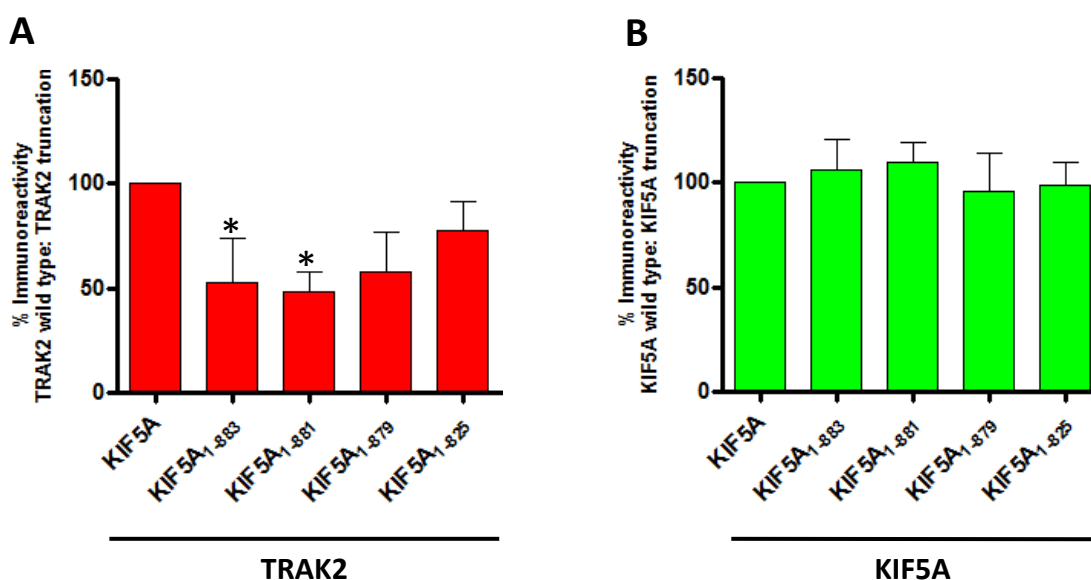


**Figure 5.16** Histograms showing the expression levels of TRAK2 and KIF5A, KIF5A<sub>1-883</sub>, KIF5A<sub>1-881</sub>, KIF5A<sub>1-879</sub> and KIF5A<sub>1-825</sub> following co-expression.

HEK 293 cells were transfected with pCMVTRAK2 and either pcDNAKIF5A, pcDNAKIF5A<sub>1-883</sub>, pcDNAKIF5A<sub>1-881</sub>, pcDNAKIF5A<sub>1-879</sub> or pcDNAKIF5A<sub>1-825</sub>. Cell homogenates were prepared 48 h post-transfection, detergent solubilised and analysed by immunoblotting with the appropriate antibody. The ratio of immunoreactivity of the soluble input was taken and expressed as a percentage of the control which is 100 %. The graph shows the means  $\pm$  S.E.M for at least  $n = 3$  experiments from at least  $n = 3$  independent co-transfections. Statistical significance was measured using a student's *t*-test where  $*P < 0.05$ .

**A** = Immunoreactivity of TRAK2 wild type: TRAK2 truncation after co-expression with KIF5A.

**B** = Immunoreactivity of KIF5A wild type: KIF5A truncation after co-expression with TRAK2.

No significant change in the expression level of TRAK2 was noted when co-expressed with KIF5A, KIF5A<sub>1-879</sub> and KIF5A<sub>1-825</sub>. However, the relative expression of TRAK2 when co-expressed with both KIF5A<sub>1-883</sub> and KIF5A<sub>1-881</sub> is significantly lower. Also no significant change in the expression level of KIF5A<sub>1-883</sub>, KIF5A<sub>1-881</sub>, KIF5A<sub>1-879</sub> and KIF5A<sub>1-825</sub> recombinant proteins when co-expressed together with TRAK2 were seen when compared to the full length KIF5A.

The immunoblots from co-immunoprecipitation experiments (Figure 5.15) were quantified to determine if there was a difference in the efficiency of co-immunoprecipitation of TRAK2 with KIF5A<sub>1-883</sub>, KIF5A<sub>1-881</sub>, KIF5A<sub>1-879</sub> and KIF5A<sub>1-825</sub>. Band densitometry of immune pellet bands compared to that of the input from co-immunoprecipitations were taken and expressed as a percentage of the full length KIF5A control (100 %). Representative histograms are shown in Figure 5.17.

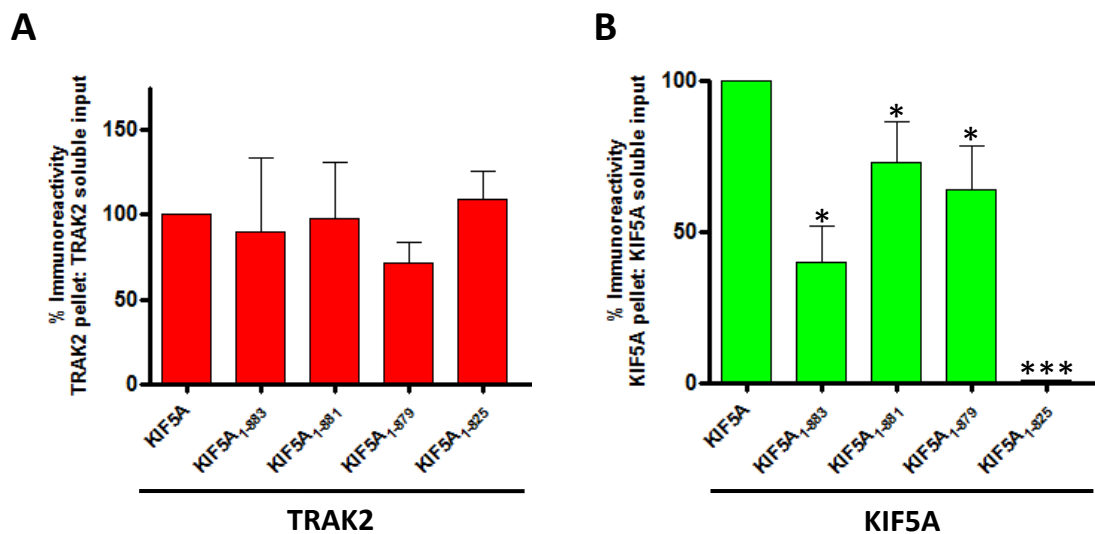


**Figure 5.17** Histograms showing the association of TRAK2 with KIF5A, KIF5A<sub>1-883</sub>, KIF5A<sub>1-881</sub>, KIF5A<sub>1-879</sub> and KIF5A<sub>1-825</sub> following co-immunoprecipitation.

HEK 293 cells were transfected with pCMVTRAK2 and either pcDNAKIF5A, pcDNAKIF5A<sub>1-883</sub>, pcDNAKIF5A<sub>1-881</sub>, pcDNAKIF5A<sub>1-879</sub> or pcDNAKIF5A<sub>1-825</sub>. Cell homogenates were prepared 48 h post-transfection, detergent solubilised and co-immunoprecipitations carried out using either anti-Flag antibodies or non-immune Ig. The ratio of immunoreactivity of the immune pellet: soluble input was taken and expressed as a percentage of the control which is 100 %. The graph shows the means  $\pm$  S.E.M for at least  $n = 3$  co-immunoprecipitations from at least  $n = 3$  independent transfections. Statistical significance was measured using a student's *t*-test where \* $P < 0.05$  and \*\*\* $P < 0.001$ .

**A** = Immunoreactivity of TRAK2 pellet: TRAK2 soluble input. **B** = Immunoreactivity of KIF5A pellet: KIF5A soluble input.

Quantitative band analysis shows a significant decrease of co-immunoprecipitation of the truncated KIF5A recombinant proteins with that of TRAK2. KIF5A<sub>1-883</sub>, KIF5A<sub>1-881</sub>, KIF5A<sub>1-885</sub> all appear to show a  $\sim 30$ -60 % decrease in co-immunoprecipitation with TRAK2.

#### 5.2.4 Further refinement of amino acids 877-883 of KIF5A by deletion

Results in Section 5.2.3 demonstrated that truncating the eight amino acid sequence 877-885 of KIF5A to yield KIF5A<sub>1-883</sub>, KIF5A<sub>1-881</sub> and KIF5A<sub>1-879</sub> had resulted in no further refinement of the TRAK2 binding site. Therefore, this region of amino acids was deleted from full length KIF5A protein to assess the impact this deletion has upon co-immunoprecipitation of KIF5A with TRAK2. Due to the truncated constructs pcDNAKIF5A<sub>1-883</sub> and pcDNAKIF5A<sub>1-885</sub> showing a similar level of interaction with TRAK2 after co-immunoprecipitation experiments, only the amino acids 877-883 of KIF5A were deleted from the full length KIF5A protein. The recombinant construct pcDNAKIF5A<sub>Δ877-883</sub> was achieved by overlap extension PCR (Section 2.2.2.14) allowing the deletion of the nucleotide sequence encoding these six amino acids.

Initial experiments were carried out to show that the recombinant protein was expressed in a mammalian cell line. Thus, HEK 293 cells were transfected with pcDNAKIF5A<sub>Δ877-883</sub>, cell homogenates were prepared (Section 2.2.5.7) and analysed by immunoblotting using anti-His antibodies (Section 2.2.3.5). The representative immunoblot is shown in Figure 5.18. The KIF5A<sub>Δ877-883</sub> construct was successfully expressed in HEK 293 cells as demonstrated by an immunoreactive band corresponding to the predicted size, i.e. KIF5A<sub>Δ877-883</sub> = 122.9 kDa ± 9 (n =5).

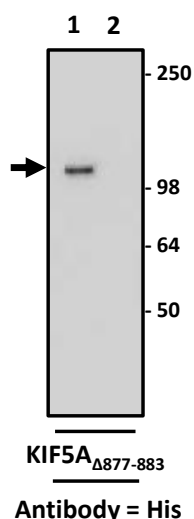


**Figure 5.18 Demonstration of the expression of KIF5A<sub>Δ877-883</sub> in HEK 293 cells.**

HEK 293 cells were transfected with KIF5A<sub>Δ877-883</sub>. Cell homogenates were prepared 48 h post-transfection and detergent solubilised. In the immunoblot **lane 1** = transfected cell homogenate and **lane 2** = non-transfected cell homogenate. The positions of molecular mass standards (kDa) are shown on the right. The arrow indicates the position of the immunoreactive band. Immunoblot probed with anti-His antibodies.

To assess the impact of deleting amino acids 877-883 from the full length KIF5A protein, co-immunoprecipitation assays were carried out. HEK 293 cells were co-transfected with pCMVTRAK2 and pcDNAKIF5A<sub>Δ877-883</sub>. pcDNAKIF5A and pcDNAKIF5A<sub>1-825</sub> were each co-transfected with pCMVTRAK2 to act as positive and negative controls.

Representative immunoblots from co-immunoprecipitation experiments (Section 2.2.5.8) are shown in Figure 5.19.

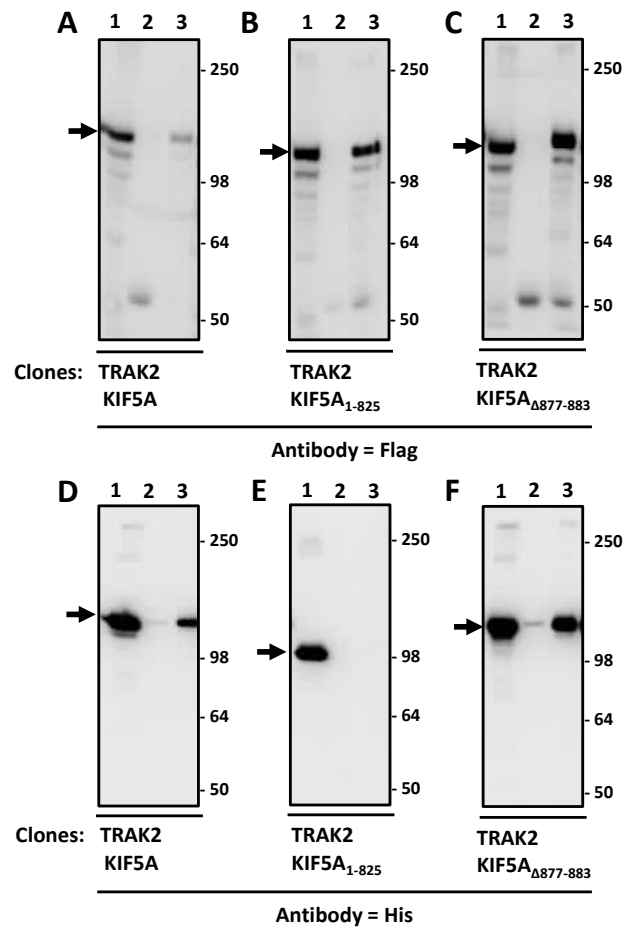


**Figure 5.19 Demonstration by immunoprecipitation the association of TRAK2 with KIF5A, KIF5A<sub>1-825</sub> and KIF5A<sub>Δ877-883</sub> following their co-expression in HEK 293 cells.**

HEK 293 cells were transfected with pCMVTRAK2 and either KIF5A, KIF5A<sub>1-825</sub> or KIF5A<sub>Δ877-883</sub>. Cell homogenates were prepared 48 h post-transfection, detergent solubilised and co-immunoprecipitations carried out using either anti-Flag antibodies or non-immune Ig. In all immunoblots **lane 1** = transfected soluble HEK 293 cell homogenate, **lane 2** = non-immune pellet and **lane 3** = anti-Flag pellet. Immunoblots are representative of at least  $n = 3$  co-immunoprecipitations from  $n = 3$  independent transfections. The positions of molecular mass standards (kDa) are shown on the right. Arrows indicate the position of immunoreactive bands.

**A, B, C** = 10 % of the immune and non-immune pellets probed with anti-Flag antibodies. **D, E, F** = 90 % of the immune and non-immune pellets probed with anti-His antibodies.

TRAK2 was present in all immune pellets but not in the non-immune pellets. This was expected and demonstrates that the immunoprecipitation of the TRAK2 protein was successful. KIF5A and KIF5A<sub>Δ877-883</sub> were found to be present in the immune pellet but some protein, albeit at a low level, is visualised in the non-immune pellet and may be a result of incomplete washing of the immune pellet. This indicates that KIF5A and KIF5A<sub>Δ877-883</sub> co-immunoprecipitates with TRAK2 following their co-expression in HEK

293 cells. No signal was detected for KIF5A<sub>1-825</sub> in immune pellets. This indicates that as observed previously KIF5A<sub>1-825</sub> does not co-immunoprecipitate with TRAK2 when co-expressed in HEK 293 cells.

To demonstrate that KIF5A, KIF5A<sub>1-825</sub> and KIF5A<sub>Δ877-883</sub> recombinant proteins were expressed to a similar level when co-expressed with TRAK2, quantitative immunoblotting was performed (Section 2.2.3.5). Band densitometry of the solubilised fractions from co-expression experiments were expressed as a percentage of the full length KIF5A. Histograms summarising the relative expression of TRAK2, KIF5A, KIF5A<sub>1-825</sub> and KIF5A<sub>Δ877-883</sub> are shown in Figure 5.20.

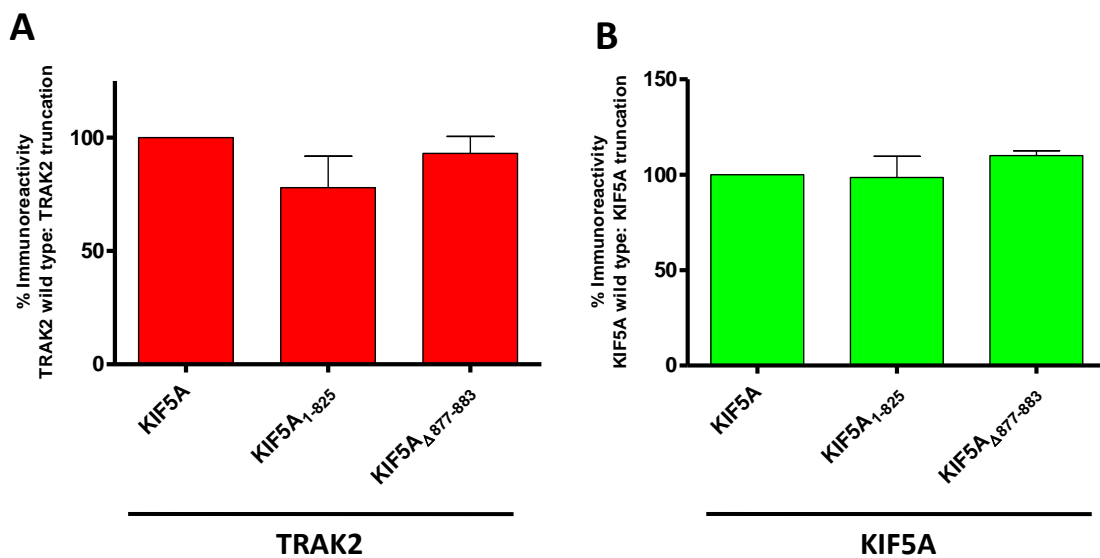


**Figure 5.20** Histograms showing the expression levels of TRAK2 and KIF5A, KIF5A<sub>1-825</sub> and KIF5A<sub>Δ877-883</sub> following co-expression.

HEK 293 cells were transfected with pCMVTRAK2 and either pcDNAKIF5A, pcDNAKIF5A<sub>1-825</sub> or pcDNA KIF5A<sub>Δ877-883</sub>. Cell homogenates were prepared 48 h post-transfection and detergent solubilised and each was analysed by immunoblotting with the appropriate antibody as shown above. The ratio of immunoreactivity of the soluble input was taken and expressed as a percentage of the control which is 100 %. The graph shows the means  $\pm$  S.E.M for at least  $n = 3$  experiments from at least  $n = 3$  independent co-transfections. Statistical significance was measured using a student's *t*-test.

**A** = Immunoreactivity of TRAK2 wild type: TRAK2 truncation after co-expression with KIF5A.

**B** = Immunoreactivity of KIF5A wild type: KIF5A truncation after co-expression with TRAK2.

No significant change in the expression level of TRAK2 was noted when co-expressed with KIF5A, KIF5A<sub>1-825</sub> and KIF5A<sub>Δ877-883</sub>. Also no significant change in the expression level of KIF5A<sub>1-825</sub> and KIF5A<sub>Δ877-883</sub> recombinant proteins when co-expressed together with TRAK2 were seen when compared to the full length KIF5A.

The immunoblots from co-immunoprecipitation experiments (Figure 5.19) were quantified to determine if there was a difference in the efficiency of co-immunoprecipitation of TRAK2 with KIF5A<sub>1-825</sub> and KIF5A<sub>Δ877-883</sub>. Band densitometry of immune pellet bands compared to that of the input from co-immunoprecipitations were taken and expressed as a percentage of the full length KIF5A control (100 %). Representative histograms are shown in Figure 5.21.

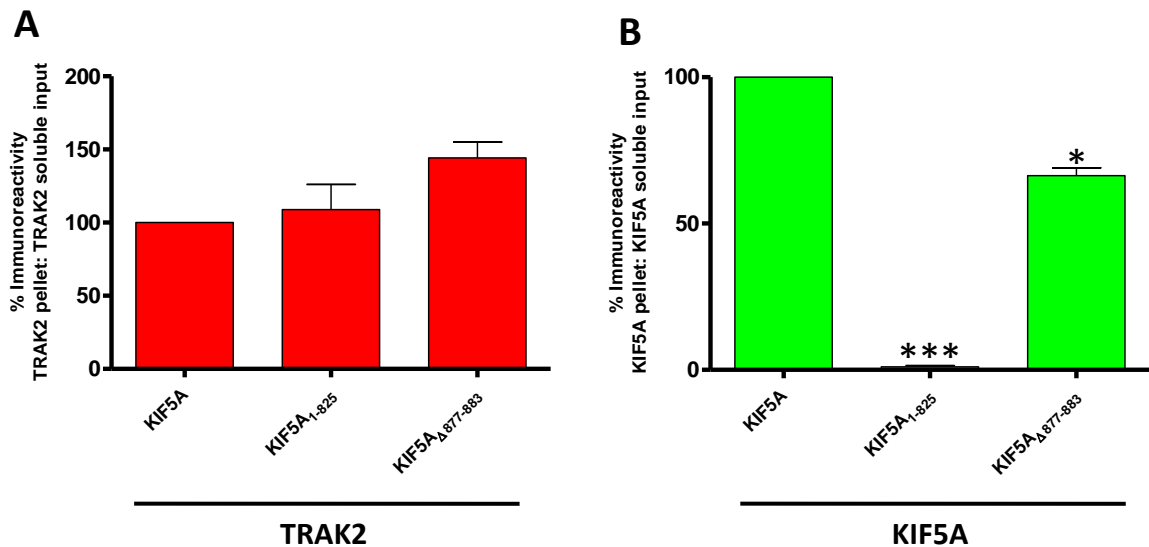


**Figure 5.21** Histograms showing the association of TRAK2 with KIF5A, KIF5A<sub>1-825</sub> and KIF5A<sub>Δ877-883</sub> following co-immunoprecipitation.

HEK 293 cells were transfected with pCMVTRAK2 and either pcDNAKIF5A, pcDNAKIF5A<sub>1-825</sub> or pcDNA KIF5A<sub>Δ877-883</sub>. Cell homogenates were prepared 48 h post-transfection, detergent solubilised and co-immunoprecipitations carried out using either anti-Flag antibodies or non-immune Ig. The ratio of immunoreactivity of the immune pellet: soluble input was taken and expressed as a percentage of the control which is 100 %. The graph shows the means  $\pm$  S.E.M for at least  $n = 3$  co-immunoprecipitations from at least  $n = 3$  independent transfections. The statistical significance was measured using a student's *t*-test where  $*P < 0.05$  and  $***P < 0.001$ .

**A** = Immunoreactivity of TRAK2 pellet: TRAK2 soluble input. **B** = Immunoreactivity of KIF5A pellet: KIF5A soluble input.

Quantitative band analysis shows a significant decrease of co-immunoprecipitation of the truncated KIF5A recombinant proteins with that of TRAK2. KIF5A<sub>Δ877-883</sub> shows a significant decrease of  $\sim 30$  % in co-immunoprecipitation with TRAK2 after co-expression in HEK 293 cells.

### 5.2.5 Does KIF5C associate with TRAK2 using the same amino acid motif as KIF5A?

Section 5.2.2 has shown that there is a step wise reduction in the co-immunoprecipitation of truncated KIF5A with TRAK2 in HEK 293 cells. As discussed previously the work undertaken to demonstrate that kinesin-1 associates with TRAK2

via the cargo binding domain had been carried out using the KIF5C sub-type (Smith *et al.*, 2006). To see if both the KIF5A and KIF5C sub-types share critical amino acid residues needed for TRAK2 binding, the KIF5C clones pcDNAKIF5A<sub>1-889</sub> and pcDNAKIF5C<sub>1-881</sub> were created. These clones contained a stop codon at identical locations to the flanking region of the eight amino acid region on KIF5A. This region has been shown in Section 5.2.2 to be responsible for approximately 30 % of the ability of KIF5A to co-immunoprecipitate with TRAK2. A positive and negative control, pcDNAKIF5C and pcDNAKIF5C<sub>1-828</sub>, were also cloned.

HEK 293 cells were transfected with pcDNAKIF5C, pcDNAKIF5C<sub>1-889</sub>, pcDNAKIF5C<sub>1-881</sub> and pcDNAKIF5C<sub>1-828</sub> and soluble cell homogenates prepared (Section 2.2.5.7). The resulting soluble cell homogenates were analysed by immunoblotting using anti-His antibodies. Representative immunoblots showing the expression of KIF5C, KIF5C<sub>1-889</sub>, KIF5C<sub>1-881</sub> and KIF5C<sub>1-828</sub> are shown in Figure 5.22. Each protein was successfully expressed in HEK 293 as demonstrated by immunoreactive bands corresponding to the predicted size. The molecular weight of KIF5C is =  $120.4 \pm 6.8$  kDa (n = 5), KIF5C<sub>1-889</sub> =  $114.4 \pm 5.2$  kDa (n = 5), KIF5C<sub>1-881</sub> =  $113.5 \pm 4.4$  kDa (n = 5) and KIF5C<sub>1-828</sub> =  $104.9 \pm 4.3$  kDa (n = 3).

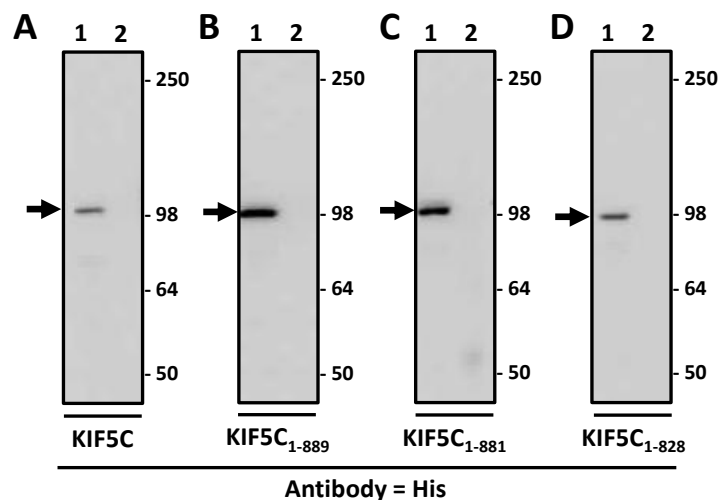


**Figure 5.22 Demonstration of the expression of KIF5C, KIF5C<sub>1-889</sub>, KIF5C<sub>1-881</sub> and KIF5C<sub>1-828</sub> in HEK 293 cells.**

HEK 293 cells were transfected with pcDNAKIF5C, pcDNAKIF5C<sub>1-889</sub>, pcDNAKIF5C<sub>1-881</sub> or pcDNAKIF5C<sub>1-828</sub>. Cell homogenates were prepared 48 h post-transfection and detergent solubilised. In all immunoblots **lane 1** = transfected soluble sample and **lane 2** = non-transfected HEK 293 cells. The positions of molecular mass standards (kDa) are shown on the right. Arrows indicate the position of immunoreactive bands.

**A, B, C, D** = Immunoblots probed with anti-His antibodies.

HEK 293 cells were co-transfected with pCMVTRAK2 and either pcDNAKIF5C, pcDNAKIF5C<sub>1-889</sub>, pcDNAKIF5C<sub>1-881</sub> or pcDNAKIF5C<sub>1-828</sub>. Representative immunoblots from co-immunoprecipitation experiments (Section 2.2.5.8) are shown in Figure 5.23.

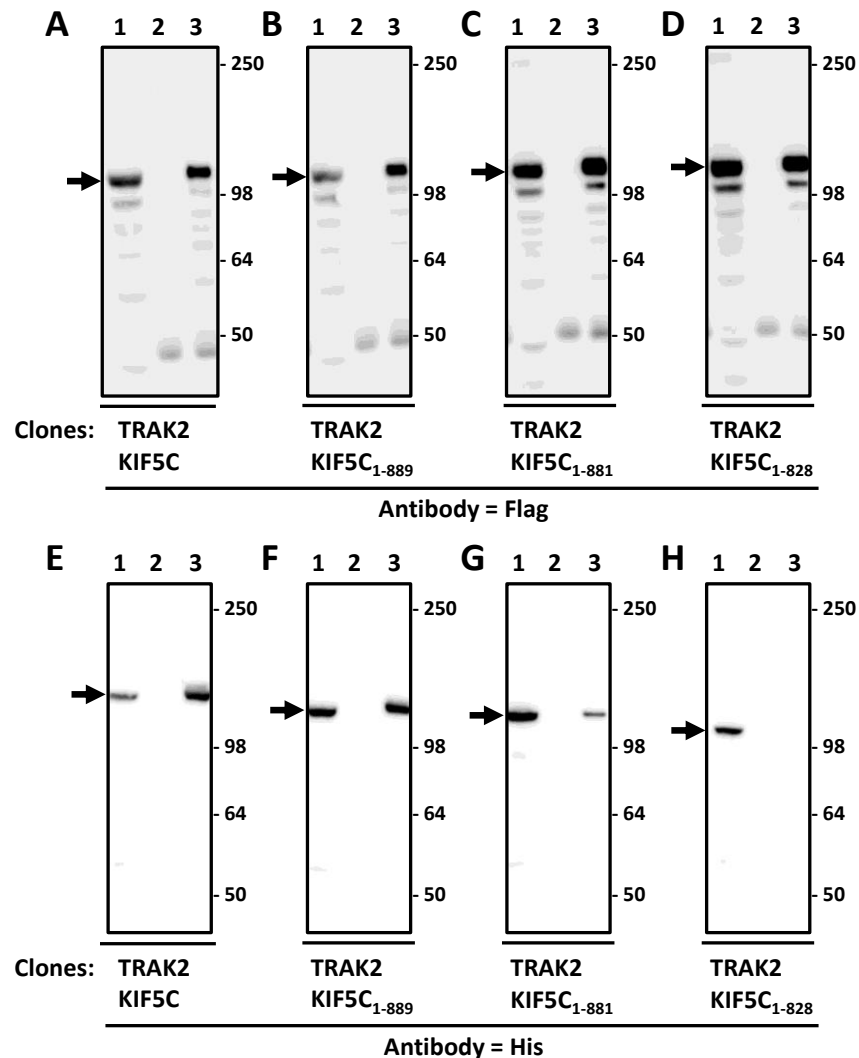


**Figure 5.23 Association of TRAK2 with KIF5C, KIF5C<sub>1-889</sub>, KIF5C<sub>1-881</sub> and KIF5C<sub>1-828</sub>: demonstration by co-immunoprecipitation.**

HEK 293 cells were co-transfected with pCMVTRAK2 and either pcDNAKIF5C, pcDNAKIF5C<sub>1-889</sub>, pcDNAKIF5C<sub>1-881</sub> or pcDNAKIF5C<sub>1-828</sub>. Cell homogenates were prepared 48 h post-transfection, detergent solubilised and immunoprecipitations carried out using either anti-Flag antibodies or non-immune Ig. In all immunoblots **lane 1** = transfected HEK 293 cell homogenate, **lane 2** = non-immune pellet and **lane 3** = anti-Flag pellet. Immunoblots are representative of at least  $n = 3$  co-immunoprecipitations from at least  $n = 3$  independent transfections. The positions of molecular mass standards (kDa) are shown on the right. Arrows indicate the position of immunoreactive bands.

**A, B, C, D** = 10 % of the immune and non-immune pellets probed with anti-Flag antibodies. **E, F, G, H** = 90 % of the immune and non-immune pellets probed with anti-His antibodies.

TRAK2 was present in all immune pellets but not in the non-immune pellets. This is expected and demonstrates that the immunoprecipitation of the TRAK2 protein was

successful. KIF5C, KIF5C<sub>1-889</sub> and KIF5C<sub>1-881</sub> were present in the immune pellet but not the non-immune pellet. This shows that KIF5C, KIF5C<sub>1-889</sub> and KIF5C<sub>1-881</sub> co-immunoprecipitate with TRAK2 following co-expression in HEK 293 cells. No signal was detected for KIF5C<sub>1-828</sub> in immune pellets. This indicates that KIF5C<sub>1-828</sub> does not co-immunoprecipitate with TRAK2 when co-expressed in HEK 293 cells.

To demonstrate that KIF5C, KIF5C<sub>1-889</sub>, KIF5C<sub>1-881</sub> and KIF5C<sub>1-828</sub> recombinant proteins were expressed to a similar level when co-expressed with TRAK2, quantitative immunoblotting was performed (Section 2.2.3.5.3). Band densitometry of the solubilised fractions from co-expression experiments were expressed as a percentage of the full length KIF5C. Histograms summarising the relative expression of TRAK2, KIF5C, KIF5C<sub>1-889</sub>, KIF5C<sub>1-881</sub> and KIF5C<sub>1-828</sub> are shown in Figure 5.24.

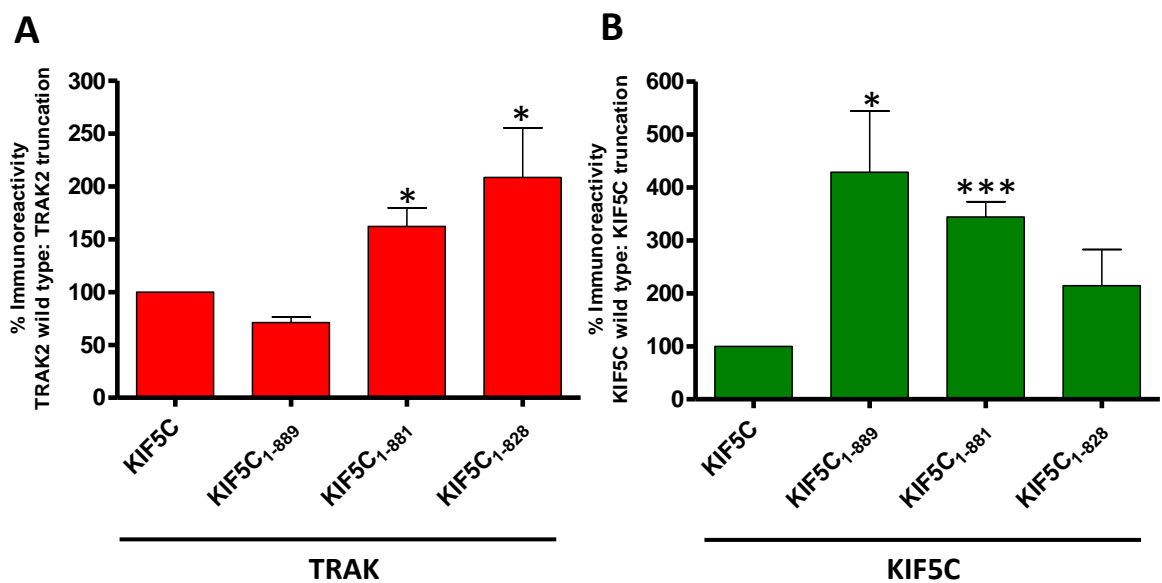


**Figure 5.24** Histograms showing the expression levels of TRAK2 and KIF5C, KIF5C<sub>1-889</sub>, KIF5C<sub>1-881</sub> and KIF5C<sub>1-828</sub> following co-expression.

HEK 293 cells were transfected with pCMVTRAK2 and either pcDNAKIF5C, pcDNAKIF5C<sub>1-889</sub>, pcDNAKIF5C<sub>1-881</sub> or pcDNAKIF5C<sub>1-828</sub>. Cell homogenates were prepared 48 h post-transfection, detergent solubilised and each was analysed by immunoblotting with the appropriate antibodies. The ratio of immunoreactivity of the soluble input was taken and expressed as a percentage of the control which is 100 %. The graph shows the means  $\pm$  S.E.M for at least  $n = 3$  experiments from at least  $n = 3$  independent co-transfections. Statistical significance was measured using a student's *t*-test where \* $P < 0.05$  and \*\*\* $P < 0.001$ .

**A** = Immunoreactivity of TRAK2 wild type: TRAK2 truncation after co-expression with KIF5C.

**B** = Immunoreactivity of KIF5C wild type: KIF5C truncation after co-expression with TRAK2.

No significant change in the expression level of TRAK2 was noted when co-expressed with KIF5C<sub>1-889</sub>. However, the relative expression of TRAK2 when co-expressed with

KIF5C<sub>1-881</sub> and KIF5C<sub>1-828</sub> was found to be significantly higher. No significant change in the expression level of KIF5C<sub>1-828</sub> recombinant proteins was seen when compared to the full length KIF5C after co-expression together with TRAK2. However, KIF5C<sub>1-889</sub> and KIF5C<sub>1-881</sub> were found to be significantly higher after co-expression with TRAK2 when compared to full length KIF5C. This difference in expression levels seen between TRAK2 and KIF5C<sub>1-889</sub> and KIF5C<sub>1-881</sub> is most likely due to differences in transfection efficiencies.

The immunoblots from co-immunoprecipitation experiments (Figure 5.23) were quantified to determine if there was a difference in the efficiency of co-immunoprecipitation of TRAK2 with KIF5C, KIF5C<sub>1-889</sub>, KIF5C<sub>1-881</sub> and KIF5C<sub>1-828</sub>. Band densitometry of immune pellet bands compared to that of the input from co-immunoprecipitations were taken and expressed as a percentage of the full length KIF5C control (100 %). Representative histograms are shown in Figure 5.25.

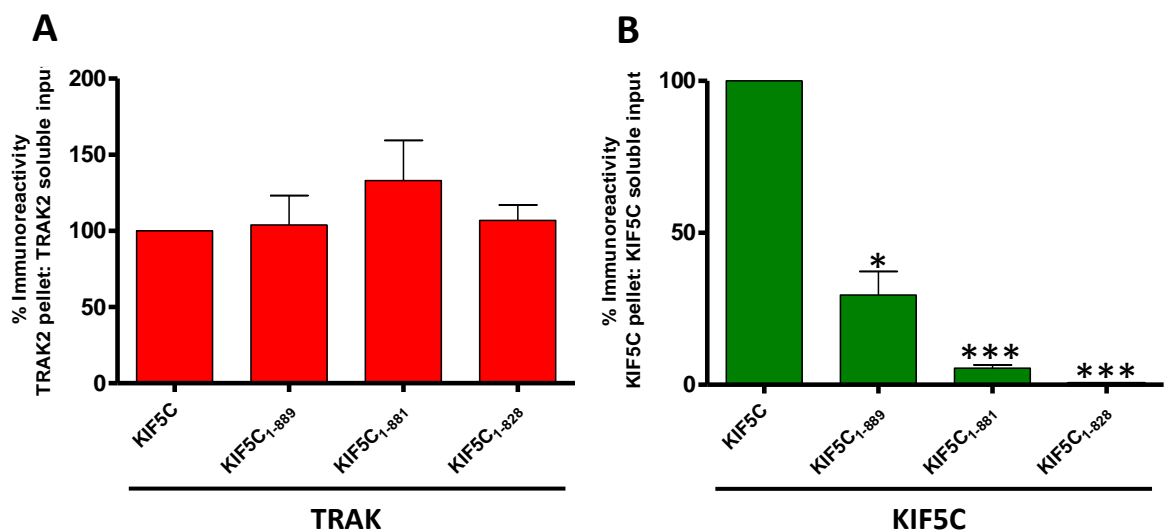


**Figure 5.25** Histograms showing the association of TRAK2 with KIF5C, KIF5C<sub>1-889</sub>, KIF5C<sub>1-881</sub> and KIF5A<sub>1-828</sub> following co-immunoprecipitation.

HEK 293 cells were transfected with pCMVTRAK2 and either pcDNAKIF5C, pcDNAKIF5C<sub>1-889</sub>, pcDNAKIF5C<sub>1-881</sub> or pcDNAKIF5A<sub>1-828</sub>. Cell homogenates were prepared 48 h post-transfection, detergent solubilised and co-immunoprecipitations carried out using either anti-Flag antibodies or non-immune Ig. The ratio of immunoreactivity of the immune pellet: soluble input was taken and expressed as a percentage of the control which is 100 %. The graph shows the means  $\pm$  S.E.M for at least  $n = 3$  co-immunoprecipitations from at least  $n = 3$  independent transfections. The statistical significance was measured using a student's  $t$ -test where  $*P < 0.05$  and  $***P < 0.001$ .

**A** = Immunoreactivity of TRAK2 pellet: TRAK2 soluble input. **B** = Immunoreactivity of KIF5C pellet: KIF5C soluble input.

Quantitative band analysis shows a significant decrease in co-immunoprecipitation of the truncated KIF5C<sub>1-889</sub>, KIF5C<sub>1-881</sub> and KIF5C<sub>1-828</sub> recombinant proteins with that of TRAK2 after co-expression in HEK 293 cells. KIF5C<sub>1-889</sub> shows a ~ 70 % decrease in co-immunoprecipitation with TRAK2 when compared to KIF5C. KIF5C<sub>1-881</sub> shows a decrease of ~ 95 % in co-immunoprecipitation with TRAK2. KIF5C<sub>1-828</sub> shows no co-immunoprecipitation with TRAK2. This result confirms that the cargo binding domain of KIF5C is needed for correct co-immunoprecipitation with TRAK2. Overall the series of KIF5C truncations revealed a similar binding profile as found for KIF5A. This is a three mode method of association; the first site was identified between amino acids KIF5C 889-957, the second between amino acids KIF5C 881-889 and the third between amino acids KIF5C 828-881.

### **5.2.6 Does TRAK1 associate with KIF5A in a similar manner to TRAK2?**

As discussed in the introduction the TRAK family consists of two family members sharing an amino acid identity of 44 %. Currently all of the experiments in this chapter have focused around the more studied rat TRAK2 protein. All three kinesin-1 sub-types have demonstrated the ability to co-immunoprecipitate with both TRAK1 and TRAK2 in HEK 293 cells (Brickley *et al.*, 2005). It is therefore interesting to assess if there are any differences in binding of the kinesin-1 family between TRAK1 and TRAK2. There is a 93 % amino acid identity between rat and human TRAK1. Due to the high amino acid sequence identity between human TRAK1 and rat TRAK1, the human TRAK1 clone was chosen to study the interaction between TRAK1 and KIF5A. Investigating the interaction between human TRAK1 and human KIF5A will also bear more physiological resemblance to the *in vivo* interaction in human neuronal cells. Recombinant clones KIF5A, KIF5A<sub>1-961</sub>, KIF5A<sub>1-879</sub>, KIF5A<sub>1-877</sub> and KIF5A<sub>1-825</sub> were selected to assess the interaction with TRAK1. These clones were used because previous work in this chapter has shown these truncations to be the most critical for interaction with TRAK2.

Initial experiments were carried out to show that recombinant TRAK1 could be expressed in a mammalian cell line. Thus, HEK 293 cells were transfected with pCMVTRAK1, cell homogenates were prepared (Section 2.2.5.7) and analysed by immunoblotting using anti-c-myc antibodies (Section 2.2.3.5). The representative immunoblot is shown in Figure 5.26. The TRAK1 construct was successfully expressed

in HEK 293 cells as demonstrated by an immunoreactive band corresponding to the predicted size, i.e. TRAK1 = 124.5 ± 2.2 kDa (n = 18).

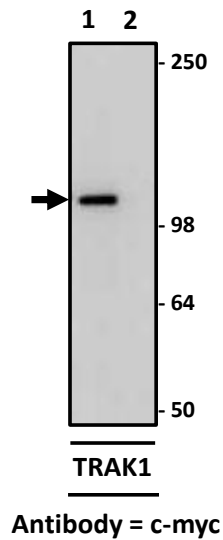


**Figure 5.26 Demonstration of the expression of TRAK1 in HEK 293 cells.**

HEK 293 cells were transfected with pCMVTRAK1. Cell homogenates were prepared 48 h post-transfection and detergent solubilised. In all immunoblots **lane 1** = transfected soluble sample and **lane 2** = non-transfected HEK 293 cells. The positions of molecular mass standards (kDa) are shown on the right. The arrow indicates the position of the immunoreactive band. Immunoblot probed with anti-c-myc antibodies.

To ascertain if the KIF5A truncated constructs bind to TRAK1 in a similar method to TRAK2, co-immunoprecipitation experiments were carried out. HEK 293 cells were co-transfected with pCMVTRAK1 and either pcDNAKIF5A<sub>1-961</sub>, pcDNAKIF5A<sub>1-879</sub>, pcDNAKIF5A<sub>1-877</sub> or pcDNAKIF5A<sub>1-825</sub>. Representative immunoblots from co-immunoprecipitation experiments (Section 2.2.5.8) are shown in Figure 5.27.

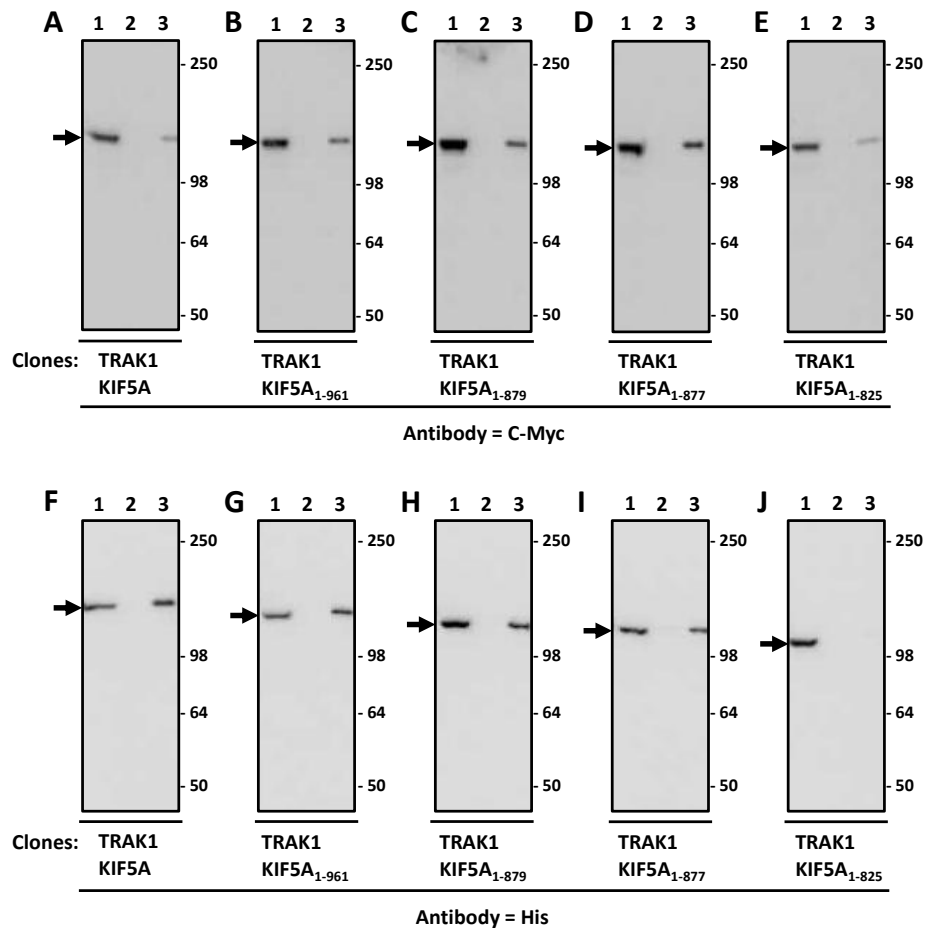


**Figure 5.27 Association of TRAK1 with KIF5A, KIF5A<sub>1-961</sub>, KIF5A<sub>1-879</sub>, KIF5A<sub>1-877</sub> and KIF5A<sub>1-825</sub>: demonstration by co-immunoprecipitation.**

HEK 293 cells were transfected with pCMVTRAK1 and either pcDNAKIF5A, pcDNAKIF5A<sub>1-961</sub>, pcDNAKIF5A<sub>1-879</sub>, pcDNAKIF5A<sub>1-877</sub> or pcDNAKIF5A<sub>1-825</sub>. Cell homogenates were prepared 48 h post-transfection, detergent solubilised and immunoprecipitations carried out using either anti-c-Myc antibodies or non-immune Ig. In all immunoblots **lane 1** = transfected HEK 293 cell homogenate, **lane 2** = non-immune pellet and **lane 3** = anti-c-myc pellet. Immunoblots are representative of at least n = 3 co-immunoprecipitations from n = 3 independent transfections. The positions of molecular mass standards (kDa) are shown on the right. Arrows indicate the position of immunoreactive bands.

**A, B, C, D, E** = 10 % of the immune and non-immune pellets probed with anti-c-myc antibodies.

**F, G, H, I, J** = 90 % of the immune and non-immune pellets probed with anti-His antibodies.

TRAK1 was present in all immune pellets but not in the non-immune pellets. This is expected and demonstrates that the immunoprecipitation of the TRAK1 protein was successful. KIF5A, KIF5A<sub>1-961</sub>, KIF5A<sub>1-879</sub>, KIF5A<sub>1-877</sub> and KIF5A<sub>1-825</sub> were present in the immune pellet but not the non-immune pellet. This shows that KIF5A, KIF5A<sub>1-961</sub>, KIF5A<sub>1-879</sub>, KIF5A<sub>1-877</sub> and KIF5A<sub>1-825</sub> co-immunoprecipitate with TRAK2 following co-expression in HEK 293 cells.

To demonstrate that KIF5A, KIF5A<sub>1-961</sub>, KIF5A<sub>1-877</sub>, KIF5A<sub>1-879</sub> and KIF5A<sub>1-825</sub> recombinant proteins were expressed to a similar level when co-expressed with TRAK1, quantitative immunoblotting was performed (Section 2.2.3.5). Band densitometry of the solubilised fractions from co-expression experiments were expressed as a percentage of the full length KIF5A. Histograms summarising the relative expression of TRAK1, KIF5A, KIF5A<sub>1-961</sub>, KIF5A<sub>1-877</sub>, KIF5A<sub>1-879</sub> and KIF5A<sub>1-825</sub> are shown in Figure 5.28.

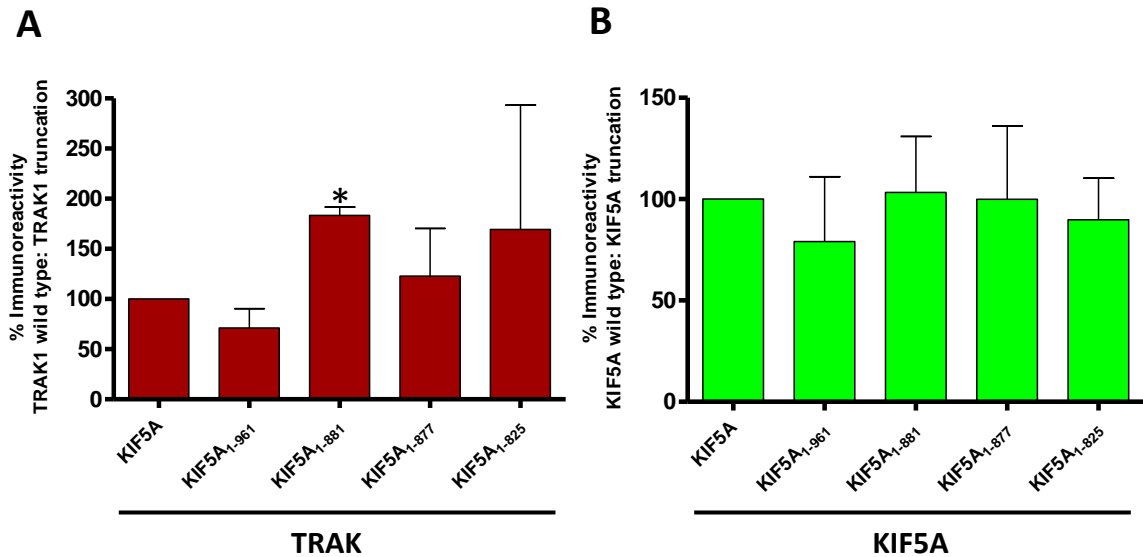


**Figure 5.28** Histograms showing the expression levels of TRAK1 and KIF5A, KIF5A<sub>1-961</sub>, KIF5A<sub>1-879</sub>, KIF5A<sub>1-877</sub> and KIF5A<sub>1-825</sub> following co-expression.

HEK 293 cells were transfected with pCMVTRAK1 and either pcDNAKIF5A, pcDNAKIF5A<sub>1-961</sub>, pcDNAKIF5A<sub>1-877</sub>, pcDNAKIF5A<sub>1-879</sub> or pcDNAKIF5A<sub>1-825</sub>. Cell homogenates were prepared 48 h post-transfection, detergent solubilised and each was analysed by immunoblotting with the appropriate antibodies. The ratio of immunoreactivity of the soluble input was taken and expressed as a percentage of the control which is 100 %. The graph shows the means  $\pm$  S.E.M for at least  $n = 3$  experiments from at least  $n = 3$  independent co-transfections. Statistical significance was measured using a student's  $t$ -test where  $*P < 0.05$ .

**A** = Immunoreactivity of TRAK1 wild type: TRAK1 truncation after co-expression with KIF5A.

**B** = Immunoreactivity of KIF5A wild type: KIF5A truncation after co-expression with TRAK1.

No significant change in the expression level of TRAK1 was noted when co-expressed with KIF5A<sub>1-961</sub>, KIF5A<sub>1-877</sub> and KIF5A<sub>1-825</sub>. However, the relative expression of TRAK1 when co-expressed with KIF5A<sub>1-879</sub> was found to be significantly higher. Also no significant change in the expression level of KIF5A<sub>1-961</sub>, KIF5A<sub>1-879</sub>, KIF5A<sub>1-877</sub> and KIF5A<sub>1-825</sub> recombinant proteins were seen when compared to the full length KIF5A after co-expression with TRAK1.

The immunoblots from co-immunoprecipitation experiments (Figure 5.27) were quantified to determine if there was a difference in the efficiency of co-immunoprecipitation of TRAK1 with KIF5A, KIF5A<sub>1-961</sub>, KIF5A<sub>1-877</sub>, KIF5A<sub>1-879</sub> and KIF5A<sub>1-825</sub>. Band densitometry of immune pellet bands compared to that of the input from co-immunoprecipitations were taken and expressed as a percentage of the full length KIF5A control (100 %). Representative histograms are shown in Figure 5.29.

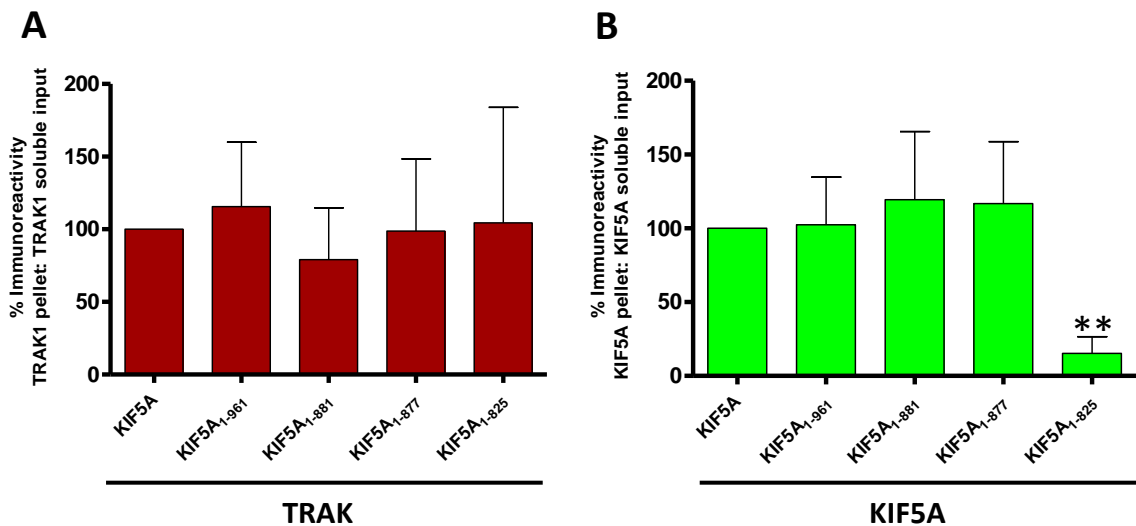


**Figure 5.29** Histograms showing the association of TRAK1 with KIF5A, KIF5A<sub>1-961</sub>, KIF5A<sub>1-879</sub>, KIF5A<sub>1-877</sub> and KIF5A<sub>1-825</sub> following co-immunoprecipitation.

HEK 293 cells were transfected with pCMVTRAK1 and either pcDNAKIF5A, pcDNAKIF5A<sub>1-961</sub>, pcDNAKIF5A<sub>1-879</sub>, pcDNAKIF5A<sub>1-877</sub> and pcDNAKIF5A<sub>1-825</sub>. Cell homogenates were prepared 48 h post-transfection, detergent solubilised and co-immunoprecipitations carried out using either anti-Flag antibodies or non-immune Ig. The ratio of immunoreactivity of the immune pellet: soluble input was taken and expressed as a percentage of the control which is 100 %. Graph shows the average values obtained ( $\pm$  S.E.M). Statistical significance was measured using a student's *t*-test where **\*\*** $P < 0.01$ .

**A** = Immunoreactivity of TRAK1 pellet: TRAK1 soluble input. **B** = Immunoreactivity of KIF5A pellet: KIF5A soluble input.

Quantitative band analysis shows no significant change in the co-immunoprecipitation of the truncated KIF5A<sub>1-961</sub>, KIF5A<sub>1-879</sub> and KIF5A<sub>1-877</sub> recombinant proteins with that of TRAK1 after co-expression in HEK 293 cells. KIF5A<sub>1-825</sub> shows a  $\sim$  85 % decrease in co-immunoprecipitation with TRAK1 when compared to full length KIF5A. Interestingly the enhancement of KIF5A<sub>1-961</sub> co-immunoprecipitation of approximately 50 % with TRAK2 seen in Figure 5.7 was not seen when KIF5A<sub>1-961</sub> was co-immunoprecipitated with TRAK1. These results imply that TRAK1/KIF5A appears to show a different pattern of binding when compared to TRAK2/KIF5A (Figure 5.7). This indicates the main region

responsible for 85 % co-immunoprecipitation with TRAK1 is amino acids 825-877 of KIF5A. A summary of all the KIF5A and KIF5C truncated constructs are shown in Figure 5.30.

```

KIF5A 825  ---S*QKQKISFLENNLEQLTKVHKQLVRDNADLRCEL*PKLEKRLRATAAERVKALE**GALK
KIF5B 825  --SAAQKQKISFLENNLEQLTKVHKQLVRDNADLRCEL*PKLEKRLRATAAERVKALE**SALK
KIF5C 825  GGSAAQKQKISFLENNLEQLTKVHKQLVRDNADLRCEL*PKLEKRLRATAAERVKALE**SALK

KIF5A 881  *EAK*EGAMKDKR*RYQQEVDRIKEAVR*YKSSGK*RGHSAQIAKPV*RP*GHYPASSP*TNFY*CTRS
KIF5B 883  *EAK*ENASRDRK*RYQQEVDRIKEAVR*SKNMARR*GHSAQIAKPI*RP*GHYPASSP*TNFY*CTRS
KIF5C 885  *EAK*ENAMRDRK*RYQQEVDRIKEAVR*AKNMARR*GHSAQIAKPI*RP*GHYPASSP*TNFY*CTRS

KIF5A 941  *PECIS*YTN*SL*E*Q*NYQ*ONLYL*CAT*PS*STSDMYFANSCT*SSGAT*SSGGPLAS*YQKANMDNGNA
KIF5B 943  GGAFVQNSQPVAVRGGGGKQV-----
KIF5C 945  GGGSSSNSTHYCK-----

KIF5A 1001 TDINDNRS*DLPCGYEAEDQAKL*FPLHQETAAS
KIF5B -----
KIF5C -----

```

**Figure 5.30 Comparison of human KIF5A, KIF5B and KIF5C kinesin-1 sub-types.**

An alignment of the cargo binding domain amino acid sequences of KIF5A, KIF5B and KIF5C. The amino acids identical between KIF5A, KIF5B and KIF5C sub-types are highlighted in black while those in grey are similar. Green stars show the position of KIF5A truncations. Blue stars show the position of KIF5C truncations. The green box shows the KIF5A amino acid sequence that was deleted.

### 5.3 DISCUSSION

Kinesin-1 is responsible for transporting many cargoes throughout the cell. It is by mapping the amino acids responsible for the binding to its wide variety of associated protein partners that a better understanding of how kinesin-1 physically interacts in a cellular environment can be gained. Previous work has demonstrated the ability of all the kinesin-1 family members to associate with TRAK2. More specifically in the case of the KIF5C sub-type it has been shown that the C-terminal tail known as the cargo binding domain interacts with TRAK2 (Smith *et al.*, 2006). In this chapter it has been demonstrated that KIF5A also co-immunoprecipitates with TRAK2 after co-expression in HEK 293 cells. It has also been established that deletion of the KIF5A cargo binding domain results in the loss of co-immunoprecipitation with TRAK2. This result suggests that TRAK2 binds to KIF5A via the cargo binding domain. Deletion of the distal 71 amino acid KIF5A C-terminal tail results in a ~ 50 % increase in co-immunoprecipitation between KIF5A/TRAK2. This indicates that this region may play a regulatory role in terms of the efficacy of binding between KIF5A and TRAK2. It is also possible to speculate that these extra 71 amino acids may also have a role in KIF5A specific cargo transport.

A series of C-terminal KIF5A truncations revealed three possible sites within the KIF5A cargo binding domain as being important for co-immunoprecipitation with TRAK2. The first identified site was located between KIF5A 942-961 and is responsible for ~ 45 % of the total ability to co-immunoprecipitation with TRAK2. The second site was between KIF5A 877-885 and is responsible for ~ 30 % of the total co-immunoprecipitation with TRAK2. The third site was between KIF5A 861-877 and is responsible for ~ 10 % of the total co-immunoprecipitation with TRAK2.

Additional analysis of the eight amino acid sequence KIF5A 877-885 by truncation or deletion did not refine the second site further. The eight amino acid region of KIF5A 877-885 consists of ALKEAKEG. When these eight amino acids are further truncated and co-expressed with TRAK2 no change in co-immunoprecipitation was revealed. This indicates that the two amino acids alanine and leucine are responsible for the ~ 30 % decrease in co-immunoprecipitation with TRAK2. This result in itself is perhaps a surprise due to the characteristics of the amino acids present in this motif. Both alanine and leucine are neutral non-polar amino acids and are rarely associated to be

necessary for protein-protein interactions. It is more likely the case that the deletion of these two alanine and leucine amino acids may alter the tertiary structure in turn inhibiting other important amino acids needed for binding.

A series of KIF5C truncations revealed a similar binding profile as found for KIF5A. This is a three mode method of association; the first site was identified between amino acids KIF5C 889-957, the second between amino acids KIF5C 881-889 and the third between amino acids KIF5C 828-881. This is not a surprising result when the 83 % amino acid identity between KIF5A and KIF5C at the cargo binding domain is taken into consideration, indicating a high probability of a shared mechanism of association with TRAK2. This also confirms the importance of the eight amino acid motif for efficient co-immunoprecipitation with the TRAK2 protein. This motif is highly conserved between KIF5A, KIF5B and KIF5C with only the very C-terminal end amino acid of the eight sequence motif differing between the three sub-types (Figure 5.30). Although the amino acid sequence identity is high between KIF5A and KIF5C, in the cargo binding domain there are subtle differences in amino acid composition. These subtle differences could allude to changes in specificities towards the kinesin-1's binding partners, as well as alternative functions within the cell. It is known that the kinesin-1 family members show marked differences in tissue distribution, with KIF5B present in nearly all tissue types and KIF5A and KIF5C found to be predominantly neuron specific (Kanai *et al.*, 2000). It is this difference in tissue specificity that could indicate roles for KIF5A and KIF5C and their binding partners that are specific only to neuronal cells.

Work in this chapter regarding the binding of TRAK1 to KIF5A has appeared to show a different pattern of association when compared to the binding of TRAK2 to KIF5A. The same KIF5A truncations that show a step-wise decrease in the ability to co-immunoprecipitate with TRAK2 in HEK 293 cells showed no reduction in the ability to co-immunoprecipitate with TRAK1. The amino acids 825-877 of KIF5A have been shown to be responsible for 85 % of the ability of KIF5A to co-immunoprecipitate with TRAK1 whereas the same region is only responsible for 10 % of the overall ability of KIF5A to co-immunoprecipitate with TRAK2. Both TRAK1 and TRAK2 share an overall amino acid identity of 44 %. Despite the low amino acid identity between the two TRAK proteins, previous research has demonstrated very similar roles for TRAK1 and TRAK2 within the cell. TRAK1 and TRAK2 will associate with kinesin-1 *in vivo* and *in vitro* (Brickley *et al.*,

2005). Furthermore, TRAK1 and TRAK2 have also demonstrated the ability to co-immunoprecipitate with both Miro1 and Miro2, atypical Rho GTPases present on the outer membrane of the mitochondria, after co-expression in HEK 293 cells (Fransson *et al.*, 2006). The work presented in Section 5.2.5 is not the first evidence to suggest that TRAK1 and TRAK2 may in fact associate with kinesin-1 via different modes of association. Previous experiments using yeast two-hybrid interaction assays and co-immunoprecipitations showed that amino acids 124-283 of TRAK2 are responsible for association with KIF5C, but this was shown to not be the case for amino acids 124-283 of TRAK1 (Brickley *et al.*, 2005). In cultured rat hippocampal neurons TRAK1 shRNAi has been shown to prevent mitochondrial movement, whereas TRAK2 shRNAi did not (Brickley and Stephenson, 2011). The role of the TRAK family has been highlighted by the number of differing cargoes known to bind either TRAK1 or TRAK2. As discussed in the introduction these cargoes include the K<sup>+</sup> channel Kir2.1 and GABA<sub>α</sub> receptor β2 subunit that are both known to bind TRAK2 (Beck *et al.*, 2002; Grishin *et al.*, 2006; Section 1.3.2). This may allude to differing roles for TRAK1 and TRAK2 within the cell as well the use of differing mechanisms to regulate the TRAK/kinesin-1 formation of trafficking complexes.

If TRAK1 and TRAK2 are to bind the kinesin-1 proteins using an independent mechanism as the data in this chapter suggests; will one TRAK protein have preferential binding to one sub-type of kinesin-1 compared to another? Macaskill *et al.* (2009a) put forward evidence suggesting that Miro proteins bind kinesin-1 independently of the TRAK family. This suggests that there is the possibility of two distinct methods of Miro-mediated mitochondrial transport within neurons; either where Miro proteins bind directly to the kinesin-1 protein, or where the association is mediated by either TRAK1 or TRAK2. This theory is given further weight when it was shown that only approximately 50 % of mitochondria co-distribute with TRAK2 in cultured neurons of which only 35 % of the mitochondrial population is mobile (MacAskill *et al.*, 2009; Brickley and Stephenson 2011). Under conditions of low ATP it is feasible to think that both TRAK1 and TRAK2 could be called into action by the cell in an attempt to increase mitochondrial distribution. This increase in mitochondrial distribution would allow the neuronal cell to maintain the high levels of ATP needed to ensure correct cellular function in locations such as the axonal processes.

Although the work in this chapter extends the understanding of the molecular interaction between kinesin-1 and the TRAK/Milton family of proteins it leaves many questions unanswered. For example kinesin-1 has always been known for its ability to transport cargo through the cellular environment, but what is less known is how this cargo transport is regulated. It has not been until relatively recently that studies into how this occurs have taken place. As explained in the introduction kinesin-1 is capable of self-regulating movement along the microtubules using the conserved QIAK motif found in the cargo binding domain (Hackney and Stock, 2000; Section 1.4). How this QIAK motif links in with the binding of adaptor proteins and cargo to the cargo binding domain has yet to be determined, but none the less asks interesting questions as to how the kinesin-1 molecule can bind cargo complexes, transport them along microtubules, stop/regulate transport to where the cargo needs to be delivered and then restart this whole process again.

### **5.3.1 Overall conclusions**

- Similarly to KIF5C, KIF5A co-immunoprecipitates with TRAK2 after co-expression in HEK 293 cells.
- Deletion of the KIF5A cargo binding domain results in the loss of co-immunoprecipitation with TRAK2. This suggests that TRAK2 binds to KIF5A via the cargo binding domain.
- Deletion of the distal 71 amino acid KIF5A C-terminal tail results in an increased co-immunoprecipitation of KIF5A with TRAK2. This demonstrates that this region may play a regulatory role in terms of the efficacy of binding between KIF5A and TRAK2.
- A series of C-terminal KIF5A truncations revealed three possible sites within the KIF5A cargo binding domain as being important for association with TRAK2. The first identified site was located between KIF5A 942-961, the second site between KIF5A 877-885 and the third between KIF5A 861-877.
- Additional analysis of the eight amino acid sequence KIF5A 877-885 by deletion or truncation did not refine the second site further.
- A series of KIF5C truncations revealed a similar binding profile as found for KIF5A. This is a three mode method of association; the first site was identified between

amino acids KIF5C 889-957, the second between amino acids KIF5C 881-889 and the third between amino acids KIF5C 828-881.

- Binding of TRAK1 to KIF5A showed a different pattern of association when compared to the binding of TRAK2 to KIF5A.

# **CHAPTER 6**

## **GENERAL CONCLUSIONS AND FUTURE DIRECTIONS**

## 6.0 GENERAL CONCLUSIONS

Kinesins are motor proteins that have roles in cell division as well as the transport of various organelles and protein complex cargoes within cells. The TRAK/Milton family of proteins are known to bind to the cargo binding domain of kinesin-1 forming a link between the motor protein and their cargoes. The main aim of this thesis was to understand the biochemical interaction of the kinesin-1/TRAK trafficking complex. This was important considering the vital role the kinesin-1/TRAK complex plays in the transport as well as the regulation of numerous cargoes, including mitochondria, throughout neuronal cells.

Previous attempts to understand further the structure of the cargo binding domain of kinesin-1 have been largely unsuccessful and a crystal structure of the cargo binding domain of kinesin-1 has yet to be determined. To determine the structure of the cargo binding domain of the kinesin-1 sub-type, KIF5A, large amounts of pure and stable protein are required. This is best achieved using expression of epitope tagged recombinant proteins in bacterial systems. In this thesis attempts were made to create a KIF5A cargo binding domain protein that could be utilised for structural analysis. Due to the known binding of TRAK2 with the kinesin-1 family it was hypothesized that TRAKs may stabilize the KIF5A cargo binding domain. Hence, the DNA encoding the KIF5A cargo binding domain, KIF5A<sub>800-1032</sub>, and the DNA encoding the kinesin interacting domain of TRAK2, TRAK2<sub>100-380</sub>, were cloned into a bicistronic expression vector to result in epitope-tagged constructs. The expression of both proteins was characterized with respect to yield and solubilisation efficiency. TRAK2<sub>100-380</sub> expression and solubilisation was found to be stabilised by the presence of the co-expressing KIF5A<sub>800-1032</sub>, contrary to the hypothesis. Affinity chromatography of soluble protein extracts found that KIF5A<sub>800-1032</sub> and TRAK2<sub>100-380</sub> did co-purify indicating that they can still associate *in vitro*. However, the yield was insufficient for further structural characterisation.

Due to the poor yield of co-expressed TRAK2<sub>100-380</sub>/KIF5A<sub>800-1032</sub> and in order to determine the structure of the cargo binding domain of KIF5A, several C-terminal constructs which varied in size and epitope tag location were generated. The bacterial growth and solubilisation conditions were optimized to maximize the yield of the various KIF5A cargo domain recombinant proteins. Each recombinant KIF5A cargo

binding domain protein was purified using an appropriate affinity chromatography resin and conditions were established to optimize the purity, yield, stability and aggregation state. One construct, KIF5A<sub>800-951</sub>, was isolated to a sufficient yield and did not aggregate. Therefore, KIF5A<sub>800-951</sub> is a good candidate for further structural analysis. However it is worth noting that, as discussed in Section 4.3, a bioinformatics survey has revealed a high magnitude of disorder in the cargo binding domain of KIF5B (Seeger *et al.*, 2012). Seeger *et al.* (2012) demonstrated that overall the KIF5B protein is predicted to be ~ 18 % disordered compared to ~ 72 % disorder in the cargo binding domain. This result indicates that the kinesin-1 cargo binding domain may not remain stable and hence may be more difficult to form a crystal needed for structural studies. It is logical to think that a certain degree of disorder/flexibility is required in order for certain domains of kinesin-1, such as the motor and stalk domain, to function correctly. For example the motor domain will regularly allow changes in the nucleotide binding region as well as the stalk domain changing conformation to allow for self-regulation. However, why the cargo binding domain needs to remain in such an unstructured conformation is unknown. It could be hypothesised that in part a disordered cargo binding domain is due to constant changes caused by post-translational modifications such as phosphorylation or O-GlcNacylation. It is known that the enzyme OGT forms part of the kinesin-1/TRAK/Miro complex (Brickley *et al.*, 2011), which could have an effect upon the cargo/kinesin complex and in turn the conformation of kinesin-1. As for KIF5B (Seeger and Rice, 2010), KIF5A<sub>800-951</sub> was found to co-sediment with microtubules *in vitro*. This result indicates that the cargo binding domain of KIF5A may be essential for the inactivation cargo transport within neuronal cells.

Previous work has demonstrated that TRAK2<sub>124-283</sub> is responsible to binding to KIF5C<sub>827-957</sub> (Brickley *et al.*, 2005; Smith *et al.*, 2006; Brickley *et al.*, 2011). In order to refine further the TRAK2 binding site within the cargo binding domain of KIF5A a series of nine rationally designed C-terminal truncations of KIF5A were generated. These constructs were co-expressed with TRAK2 in HEK 293 cells and their binding was determined by co-immunoprecipitation assays followed by quantitative immunoblotting. Results indicated that the deletion of the distal 75 C-terminal amino acids of KIF5A enhanced the co-immunoprecipitation of TRAK2 with KIF5A. Further

truncations also resulted in a reduction of KIF5A immunoreactivity in immune pellets implying a decrease in co-immunoprecipitation with KIF5A. This decrease in co-immunoprecipitation revealed three possible TRAK2 binding sites within the cargo binding domain of KIF5A. Amino acid truncations of KIF5C also revealed a three mode method of association with TRAK2 after co-immunoprecipitation from HEK 293 cells. However binding of TRAK1 to KIF5A showed a different pattern of association when compared to the binding of TRAK2 to KIF5A. This work could be the beginning of a larger effort to fully characterize the many known adaptor and cargo protein binding sites on kinesin-1. Due to the vast array of binding proteins it is feasible to think that there may be an overlap in these binding regions. Do some adaptor proteins or cargo compete for binding to kinesin-1? Previous work by Glater *et al.* (2006) has demonstrated that Milton competes with the KLCs for binding to the same KHC domain. Experiments using *Drosophila* over-expressing myc-KLC demonstrated that the co-immunoprecipitation of myc-KLC with anti-myc antibodies resulted in the presence of KHC, whereas Milton did not co-immunoprecipitate with myc-KLC. However, co-immunoprecipitation experiments utilising antibodies directed to KHC successfully co-immunoprecipitated both myc-KLC and Milton. Thus, these results indicate that the KHC of kinesin-1 may form separate complexes with either Milton or with KLC (Glater *et al.*, 2006). Hence, a better idea of where the interacting proteins of kinesin-1 bind coupled with a more detailed structural analysis may give a better picture of the overall binding mechanisms and regulation behind kinesin-1 transport.

## **6.1 FUTURE DIRECTIONS**

The results in both Chapter 3 and Chapter 4 have demonstrated that the exact design of each KIF5A cargo binding domain construct can have profound effects on the properties of each protein and the way they behave after expression in a bacterial system. So one possible future direction would be to screen a larger variety of constructs in differing combinations in order to see if a co-complex of TRAK2/KIF5A that is sufficiently soluble, able to be purified and stable after purification can be achieved.

Work in Chapter 4 has shown that it is possible to express a soluble KIF5A cargo binding domain protein that can be purified to a high yield and remains stable.

However, work still remains to be carried out in order to create a protein sample suitable for X-ray crystallographic studies. Hence it is necessary to further purify the KIF5A<sub>800-951</sub> protein sample. This could be achieved using a different purification system such as ion exchange chromatography. Seeger *et al.* (2012) has demonstrated that the cargo binding domain of kinesin-1 is disordered hence leading to the possibility that a crystal may be difficult to obtain. As mentioned in Section 4.3 protein NMR spectroscopy could also be utilised as an alternative method to learn more about the structure of the cargo binding domain of KIF5A. It would also be interesting to assess further the smaller molecular weight species of the KIF5A cargo binding domain noted after affinity tag purification. Mass spectrometry analysis of the lower molecular weight KIF5A protein could allow the possible region of proteolytic cleavage to be identified.

As demonstrated in Chapter 5 the deletion of the 75 C-terminal amino acids of KIF5A, that are not present in either KIF5B or KIF5C, have been shown to increase the co-immunoprecipitation of TRAK2 after co-expression in HEK 293 cells. This result indicates that these 75 amino acids may hinder the binding of TRAK2 to KIF5A. Therefore it would be interesting to the transfection of a deleted 75 C-terminal tail KIF5A construct in primary neuronal cells could increase the number of mitochondria that are motile. This could be achieved, as in Brickley and Stephenson (2011), by using live cell time lapse imaging of stained neuronal cells. In addition, exactly what role these extra 75 amino acids play in the binding of the cargo binding domain of KIF5A to adaptor protein/cargo is unclear. It would therefore be interesting to ascertain if these extra amino acids has a role in KIF5A specific cargo binding. This could be assessed by using a yeast two-hybrid system utilising the 75 amino acid C-terminal domain of KIF5A as bait to screen a brain cDNA library to see if any positive interactors are discovered.

Results in Chapter 4 have demonstrated that, like KIF5B, the cargo binding domain of KIF5A can interact with microtubules *in vitro* (Seeger and Rice, 2010). Work by Dietrich *et al.* (2008) has also indicated that the cargo binding domain of KIF5B can bind both the motor domain and the microtubule simultaneously. Therefore it is interesting to see if this is similar for KIF5A. A simple pull-down assay utilising the motor domain of KIF5A and KIF5A<sub>800-951</sub> would help to confirm this possible interaction. A microtubule binding assay using KIF5A<sub>800-851</sub> and a KIF5A motor domain that has been mutated to

remove its binding specificity to the microtubule (i.e. amino acids R280S of KIF5A (Ebbing *et al.*, 2008)) could also give insight into the apparent three part binding of the microtubule/motor/C-terminal tail of KIF5A complex. In addition, the complex of KIF5A<sub>800-951</sub> binding to microtubules could be assessed using cryo-electron microscopy, either with or without the presence of the motor domain. This could give some insight into the crucial binding complex.

Work in Chapter 5 as well as the previous studies summarised in Section 1.2.4 has only started to uncover the number of kinesin-1 cargo binding domain interactors. However, the way in which they coordinate and the extent of the overlap of their specific binding sites is still largely unknown. What causes a kinesin-1 protein to preferentially bind an adaptor/cargo protein over another? The affinity of these separate interactions could be individually measured by surface plasma resonance. In this experimental system the KIF5A<sub>800-951</sub> protein could be immobilized on the surface of a sensor chip, and the interacting proteins, such as GRIP1, TRAK/Milton or RanBP2 (see Section 1.2.4) introduced. The affinity of each interaction could then be measured using a BIACORE X-100 system. This could give data regarding the binding affinity of the proteins, as well as information about the kinetics and the strength of the interactions.

# REFERENCES

- Adio, S., Reth, J., Bathe, F., Woehlke, G. (2006) *J Muscle Res Cell Motil.* 27: 153-160. "Review: regulation mechanisms of Kinesin-1."
- Alberts, B., Johnson, A., Lewis, J., Raff, M., Roberts, K., Walter, P. (2007) *Molecular Biology of the Cell* 5<sup>th</sup> Edition. Garland Science. "Chapter 7 Control of gene expression."
- Asbury, C. L., Fehr, A. N., Block, S. M. (2003) *Science.* 302: 2130-2134. "Kinesin moves by an asymmetric hand-over-hand mechanism."
- Beck, M., Brickley, K., Wilkinson, H. L., Sharma, S., Smith, M., Chazot, P. L., Pollard, S., Stephenson, F. A. (2002) *J Biol Chem.* 277: 30079-30090. "Identification, molecular cloning, and characterization of a novel GABAA receptor-associated protein, GRIF-1."
- Borrell-Pages, M., Zala, D., Humbert, S., Saudou, F. (2006) *Cell Mol Life Sci.* 63: 2642-2660. "Huntington's disease: from huntingtin function and dysfunction to therapeutic strategies."
- Bowman, A. B. (2001) *Encyclopedia of Life Sciences.* John Wiley and Sons. <http://www.els.net>. "Dynein and kinesin."
- Bracale, A., Cesca, F., Neubrand, V. E., Newsome, T. P., Way, M., Schiavo, G. (2007) *Mol Biol Cell.* 18: 142-152. "Kidins220/ARMS is transported by a kinesin-1-based mechanism likely to be involved in neuronal differentiation."
- Brady, S. T. (1985) *Nature.* 317: 73-75. "A novel brain ATPase with properties expected for the fast axonal transport motor."
- Brickley, K., Smith, M. J., Beck, M., Stephenson, F. A. (2005) *J Biol Chem.* 280: 14723-14732. "GRIF-1 and OIP106, members of a novel gene family of coiled-coil domain proteins: association in vivo and in vitro with kinesin."
- Brickley, K., Pozo, K., Stephenson, F. A. (2011) *Biochim Biophys Acta.* 1813: 269-281. "N-acetylglucosamine transferase is an integral component of a kinesin-directed mitochondrial trafficking complex."
- Brickley, K., Stephenson, F. A. (2011) *J Biol Chem.* 286: 18079-18092. "Trafficking kinesin protein (TRAK)-mediated transport of mitochondria in axons of hippocampal neurons."
- Cai, D., McEwen, D. P., Martens, J. R., Meyhofer, E., Verhey, K. J. (2009) *PLoS Biol.* 7: e1000216. "Single molecule imaging reveals differences in microtubule track selection between Kinesin motors."
- Cai, Q., Gerwin, C., Sheng, Z. H. (2005) *J Cell Biol.* 170: 959-969. "Syntabulin-mediated anterograde transport of mitochondria along neuronal processes."
- Cai, Q., Pan, P. Y., Sheng, Z. H. (2007) *J Neurosci.* 27: 7284-7296. "Syntabulin-KIF-1 family member 5B-mediated axonal transport contributes to activity-dependent presynaptic assembly."
- Cai, Y., Singh, B. B., Aslanukov, A., Zhao, H., Ferreira, P. A. (2001) *J Biol Chem.* 276: 41594-41602. "The docking of kinesins, KIF5B and KIF5C, to Ran-binding protein 2 (RanBP2) is mediated via a novel RanBP2 domain."

- Case, R. B., Rice, S., Hart, C. L., Ly, B., Vale, R. D. (2000) *Curr Biol.* 10: 157-160. "Role of the kinesin neck linker and catalytic core in microtubule-based motility."
- Chazot, P. L., Coleman, S. K., Cik, M., Stephenson, F. A. (1994) *J. Biol Chem.* 269: 24403-24409. "Molecular characterisation of N-methyl-D-aspartate receptors expressed in mammalian cells yields evidence for the coexistence of three subunit types within a discrete receptor molecule."
- Chen, P., Burdette, A. J., Porter, J. C., Ricketts, J. C., Fox, S. A., Nery, F. C., Hewett, J. W., Berkowitz, L. A., Breakefield, X. O., Caldwell, K. A., Caldwell, G. A. (2010) *Hum Mol Genet.* 19: 3502-3515. "The early-onset torsion dystonia-associated protein, torsinA, is a homeostatic regulator of endoplasmic reticulum stress response."
- Cho, K. I., Cai, Y., Yi, H., Yeh, A., Aslanukov, A., Ferreira, P. A. (2007) *Traffic.* 8: 1722-1735. "Association of the kinesin-binding domain of RanBP2 to KIF5B and KIF5C determines mitochondria localization and function."
- Chua, J. J., Butkevich, E., Worseck, J. M., Kittelmann, M., Gronborg, M., Behrmann, E., Stelzl, U., Pavlos, N. J., Lalowski, M. M., Eimer, S., Wanker, E. E., Klopfenstein, D. R., Jahn, R. (2012) *Proc Natl Acad Sci U S A.* 109: 5862-5867. "Phosphorylation-regulated axonal dependent transport of syntaxin 1 is mediated by a Kinesin-1 adapter."
- Cooke, R. (2001) *Encyclopedia of Life Sciences.* John Wiley and Sons.  
*http://www.els.net.* "Motor proteins."
- Cyr, J. L., Pfister, K. K., Bloom, G. S., Slaughter, C. A., Brady, S. T. (1991) *Proc Natl Acad Sci U S A.* 88: 10114-10118. "Molecular genetics of kinesin light chains: generation of isoforms by alternative splicing."
- DeLuca, J. G., Newton, C. N., Himes, R. H., Jordan, M. A., Wilson, L. (2001) *J Biol Chem.* 276: 28014-28021. "Purification and characterization of native conventional kinesin, HSET, and CENP-E from mitotic hela cells."
- Detmer, S. A., Chan, D. C. (2007) *Nat Rev Mol Cell Biol.* 8: 870-879. "Functions and dysfunctions of mitochondrial dynamics."
- Dictenberg, J. B., Swanger, S. A., Antar, L. N., Singer, R. H., Bassell, G. J. (2008) *Dev Cell.* 14: 926-939. "A direct role for FMRP in activity-dependent dendritic mRNA transport links filopodial-spine morphogenesis to fragile X syndrome."
- Dieck, S., Sanmartí-Vila, L., Langnaese, K., Richter, K., Kindler, S., Soyke, A., Wex, H., Smalla, K. H., Kämpf, U., Fränzer, J. T., Stumm, M., Garner, C. C., Gundelfinger, E. D. (1998) *J. Cell Biol.* 142: 499-509. "Bassoon, a novel zinc-finger CAG/glutaminerepeat protein selectively localized at the active zone of presynaptic nerve terminals."
- Diefenbach, R. J., Mackay, J. P., Armati, P. J., Cunningham, A. L. (1998) *Biochemistry.* 37: 16663-16670. "The C-terminal region of the stalk domain of ubiquitous human kinesin heavy chain contains the binding site for kinesin light chain."
- Diefenbach, R. J., Diefenbach, E., Douglas, M. W., Cunningham, A. L. (2002) *Biochemistry.* 41: 14906-14915. "The heavy chain of conventional kinesin interacts with the SNARE proteins SNAP25 and SNAP23."

- Diefenbach, R. J., Diefenbach, E., Douglas, M. W., Cunningham, A. L. (2004) *Biochem Biophys Res Commun.* 319: 987-992. "The ribosome receptor, p180, interacts with kinesin heavy chain, KIF5B."
- Dietrich, K. A., Sindelar, C. V., Brewer, P. D., Downing, K. H., Cremo, C. R., Rice, S. E. (2008) *Proc Natl Acad Sci U S A.* 105: 8938-8943. "The kinesin-1 motor protein is regulated by a direct interaction of its head and tail."
- Dotti, C. G., Banker, G. (1991) *J Cell Sci Suppl.* 15: 75-84. "Intracellular organization of hippocampal neurons during the development of neuronal polarity."
- Ebbing, B., Mann, K., Starosta, A., Jaud, J., Schols, L., Schule, R., Woehlke, G. (2008) *Hum Mol Genet.* 17: 1245-1252. "Effect of spastic paraplegia mutations in KIF5A kinesin on transport activity."
- Endow, S. A. (1999) *Nat Cell Biol.* 1: E163-167. "Determinants of molecular motor directionality."
- Engelender, S., Sharp, A. H., Colomer, V., Tokito, M. K., Lanahan, A., Worley, P., Holzbaur, E. L., Ross, C. A. (1997) *Hum Mol Genet.* 6: 2205-2212. "Huntingtin-associated protein 1 (HAP1) interacts with the p150Glued subunit of dynactin."
- Fransson, S., Ruusala, A., Aspenstrom, P. (2006) *Biochem Biophys Res Commun.* 344: 500-510. "The atypical Rho GTPases Miro-1 and Miro-2 have essential roles in mitochondrial trafficking."
- Fridolfsson, H. N., Ly, N., Meyerzon, M., Starr, D. A. (2010) *Dev Biol.* 338: 237-250. "UNC-83 coordinates kinesin-1 and dynein activities at the nuclear envelope during nuclear migration."
- Friedman, D. S., Vale, R. D. (1999) *Nat Cell Biol.* 1: 293-297. "Single-molecule analysis of kinesin motility reveals regulation by the cargo-binding tail domain."
- Fujita, T., Maturana, A. D., Ikuta, J., Hamada, J., Walchli, S., Suzuki, T., Sawa, H., Wooten, M. W., Okajima, T., Tatematsu, K., Tanizawa, K., Kuroda, S. (2007) *Biochem Biophys Res Commun.* 361: 605-610. "Axonal guidance protein FEZ1 associates with tubulin and kinesin motor protein to transport mitochondria in neurites of NGF-stimulated PC12 cells."
- Gandhi, S., Muqit, M. M., Stanyer, L., Healy, D. G., Abou-Sleiman, P. M., Hargreaves, I., Heales, S., Ganguly, M., Parsons, L., Lees, A. J., Latchman, D. S., Holton, J. L., Wood, N. W., Revesz, T. (2006) *Brain.* 129: 1720-1731. "PINK1 protein in normal human brain and Parkinson's disease."
- Garcia, C. A. (1999) *Ann N Y Acad Sci.* 883: 69-76. "A clinical review of Charcot-Marie-Tooth."
- Garnham, C. P., Roll-Mecak, A. (2012) *Cytoskeleton (Hoboken).* "The chemical complexity of cellular microtubules: Tubulin post-translational modification enzymes and their roles in tuning microtubule functions."
- Gauger, A. K., Goldstein, L. S. (1993) *J Biol Chem.* 268: 13657-13666. "The Drosophila kinesin light chain. Primary structure and interaction with kinesin heavy chain."

Gilbert, S. L., Zhang, L., Forster, M. L., Iwase, T., Soliven, B., Donahue, L. R., Sweet, H. O., Bronson, R. T., Davisson, M. T., Wollmann, R. L., Lahn, B. T. (2005) *Nature Genetics*. 38: 245-250. "TRAK1 mutation disrupts GABA<sub>A</sub> receptor homeostasis in hypertonic mice."

Gindhart, J. G., Jr., Desai, C. J., Beushausen, S., Zinn, K., Goldstein, L. S. (1998) *J Cell Biol*. 141: 443-454. "Kinesin light chains are essential for axonal transport in *Drosophila*."

Gindhart, J. G., Chen, J., Faulkner, M., Gandhi, R., Doerner, K., Wisniewski, T., Nandlestadt, A. (2003) *Mol Biol Cell*. 14: 3356-3365. "The kinesin-associated protein UNC-76 is required for axonal transport in the *Drosophila* nervous system."

Gindhart, J. G. (2006) *Brief Funct Genomic Proteomic*. 5: 74-86. "Towards an understanding of kinesin-1 dependent transport pathways through the study of protein-protein interactions."

Glater, E. E., Megeath, L. J., Stowers, R. S., Schwarz, T. L. (2006) *J Cell Biol*. 173: 545-557. "Axonal transport of mitochondria requires Milton to recruit kinesin heavy chain and is light chain independent."

Goldberg, J. L. (2003) *Genes Dev*. 17: 941-958. "How does an axon grow?"

Grishin, A., Li, H., Levitan, E. S., Zaks-Makhina, E. (2006) *J Biol Chem*. 281: 30104-30111. "Identification of gamma-aminobutyric acid receptor-interacting factor 1 (TRAK2) as a trafficking factor for the K<sup>+</sup> channel Kir2.1."

Gross, S. P., Vershinin, M., Shubeita, G. T. (2007) *Curr Biol*. 17: R478-486. "Cargo transport: two motors are sometimes better than one."

Grummt, M., Pistor, S., Lottspeich, F., Schliwa, M. (1998) *FEBS Lett*. 427: 79-84. "Cloning and functional expression of a 'fast' fungal kinesin."

Guillard, L., Setou, M., Hirokawa, N. (2003) *Journal of Neuroscience*. 23: 131-140. "KIF17 dynamics and regulation of NR2B trafficking in hippocampal neurons."

Gutierrez-Medina, B., Fehr, A. N., Block, S. M. (2009) *Proc Natl Acad Sci U S A*. 106: 17007-17012. "Direct measurements of kinesin torsional properties reveal flexible domains and occasional stalk reversals during stepping."

Gyoeva, F. K., Sarkisov, D. V., Khodjakov, A. L., Minin, A. A. (2004) *Biochemistry*. 43: 13525-13531. "The tetrameric molecule of conventional Kinesin contains identical light chains."

Hackney, D. D., Levitt, J. D., Suhan, J. (1992) *J Biol Chem*. 267: 8696-8701. "Kinesin undergoes a 9 S to 6 S conformational transition."

Hackney, D. D., Stock, M. F. (2000) *Nat. Cell Biol*. 2: 257-260. "Kinesin's IAK tail domain inhibits initial microtubule-stimulated ADP release."

Hackney, D. D. (2007) *Science*. 316: 58-59. "Biochemistry. Processive motor movement."

Hackney, D. D., Stock, M. F. (2008) *Biochemistry*. 47: 7770-7778. "Kinesin tail domains and Mg<sup>2+</sup> directly inhibit release of ADP from head domains in the absence of microtubules."

Hackney, D. D., Baek, N., Snyder, A. C. (2009) *Biochemistry*. 48: 3448-3456. "Half-site inhibition of dimeric kinesin head domains by monomeric tail domains."

Hancock, W. O., Howard, J. (1998) *J Cell Biol*. 140: 1395-1405. "Processivity of the motor protein kinesin requires two heads."

Hart, G. W., Akimoto, Y. (2009) Cold Spring Harbor Laboratory Press. *Essentials of Glycobiology* 2<sup>nd</sup> Edition. Chapter 18. "The O-GlcNAc Modification."

Hartman, M. A., Spudich, J. A. (2012) *J Cell Sci*. 125: 1627-1632. "The myosin superfamily at a glance."

Helenius, J., Brouhard, G., Kalaidzidis, Y., Diez, S., Howard, J. (2006) *Nature*. 441: 115-119. "The depolymerizing kinesin MCAK uses lattice diffusion to rapidly target microtubule ends."

Hirokawa, N., Pfister, K. K., Yorifuji, H., Wagner, M. C., Brady, S. T., Bloom, G. S. (1989) *Cell*. 56: 867-878. "Submolecular domains of bovine brain kinesin identified by electron microscopy and monoclonal antibody decoration."

Hirokawa, N., Takemura, R. (2005) *Nat Rev Neurosci*. 6: 201-214. "Molecular motors and mechanisms of directional transport in neurons."

Hirokawa, N., Nitta, R., Okada, Y. (2009) *Nat Rev Mol Cell Biol*. 10:877-884. "The mechanisms of kinesin motor motility: lessons from the monomeric motor KIF1A."

Hirokawa, N., Noda, Y., Tanaka, Y., Niwa, S. (2009a) *Nat Rev Mol Cell Biol*. 10: 682-696. "Kinesin superfamily motor proteins and intracellular transport."

Hirokawa, N., Niwa, S., Tanaka, Y. (2010) *Neuron*. 68: 610-638. "Molecular motors in neurons: transport mechanisms and roles in brain function, development, and disease."

Hirokawa, N. (2011) *J Electron Microsc (Tokyo)*. 60 Suppl 1: S63-92. "From electron microscopy to molecular cell biology, molecular genetics and structural biology: intracellular transport and kinesin superfamily proteins, KIFs: genes, structure, dynamics and functions."

Homma, N., Takei, Y., Tanaka, Y., Nakata, T., Terada, S., Kikkawa, M., Noda, Y., Hirokawa, N. (2003) *Cell*. 114: 229-239. "Kinesin superfamily protein 2A (KIF2A) functions in suppression of collateral branch extension."

Horiuchi, D., Barkus, R. V., Pilling, A. D., Gassman, A., Saxton, W. M. (2005) *Curr Biol*. 15: 2137-2141. "APLIP1, a kinesin binding JIP-1/JNK scaffold protein, influences the axonal transport of both vesicles and mitochondria in *Drosophila*."

Hua, W., Young, E. C., Fleming, M. L., Gelles, J. (1997) *Nature*. 388: 390-393. "Coupling of kinesin steps to ATP hydrolysis."

Huang, J. D., Brady, S. T., Richards, B. W., Stenolen, D., Resau, J. H., Copeland, N. G., Jenkins, N. A. (1999) *Nature*. 397: 267-270. "Direct interaction of microtubule- and actin-based transport motors."

Iyer, S. P., Akimoto, Y., Hart, G. W. (2003) *J Biol Chem*. 278: 5399-5409. "Identification and cloning of a novel family of coiled-coil domain proteins that interact with O-GlcNAc transferase."

Jiang, W., Stock, M. F., Li, X., Hackney, D. D. (1997) *J Biol Chem*. 272: 7626-7632. "Influence of the kinesin neck domain on dimerization and ATPase kinetics."

Kamal, A., Stokin, G. B., Yang, Z., Xia, C. H., Goldstein, L. S. (2000) *Neuron*. 28: 449-459. "Axonal transport of amyloid precursor protein is mediated by direct binding to the kinesin light chain subunit of kinesin-I."

Kamal, A., Almenar-Queralt, A., LeBlanc, J. F., Roberts, E. A., Goldstein, L. S. (2001) *Nature*. 414: 643-648. "Kinesin-mediated axonal transport of a membrane compartment containing beta-secretase and presenilin-1 requires APP."

Kamal, A., Goldstein, L. S. (2002) *Curr Opin Cell Biol*. 14: 63-68. "Principles of cargo attachment to cytoplasmic motor proteins."

Kamm, C., Boston, H., Hewett, J., Wilbur, J., Corey, D. P., Hanson, P. I., Ramesh, V., Breakefield, X. O. (2004) *J Biol Chem*. 279: 19882-19892. "The early onset dystonia protein torsinA interacts with kinesin light chain 1."

Kanai, Y., Okada, Y., Tanaka, Y., Harada, A., Terada, S., Hirokawa, N. (2000) *J Neurosci*. 20: 6374-6384. "KIF5C, a novel neuronal kinesin enriched in motor neurons."

Kapitein, L. C., Kwok, B. H., Weinger, J. S., Schmidt, C. F., Kapoor, T. M., Peterman, E. J. (2008) *J Cell Biol*. 182: 421-428. "Microtubule cross-linking triggers the directional motility of kinesin-5."

Kawano, Y., Yoshimura, T., Tsuboi, D., Kawabata, S., Kaneko-Kawano, T., Shirataki, H., Takenawa, T., Kaibuchi, K. (2005) *Mol Cell Biol*. 25: 9920-9935. "CRMP-2 is involved in kinesin-1-dependent transport of the Sra-1/WAVE1 complex and axon formation."

Kijima, K., Numakura, C., Izumino, H., Umetsu, K., Nezu, A., Shiiki, T., Ogawa, M., Ishizaki, Y., Kitamura, T., Shozawa, Y., Hayasaka, K. (2005) *Hum Genet*. 116: 23-27. "Mitochondrial GTPase mitofusin 2 mutation in Charcot-Marie-Tooth neuropathy type 2A."

Kimura, T., Watanabe, H., Iwamatsu, A., Kaibuchi, K. (2005) *J Neurochem*. 93: 1371-1382. "Tubulin and CRMP-2 complex is transported via Kinesin-1."

Kirk, E., Chin, L. S., Li, L. (2006) *J Cell Sci*. 119: 4689-4701. "GRIF1 binds Hrs and is a new regulator of endosomal trafficking."

Kollman, M. J., Merdes, A., Mourey, L., Agard, D. A. (2011). *Nat Rev Mol Cell Biol*. 12: 709-721. "Microtubule nucleation by  $\gamma$ -tubulin complexes."

Konecna, A., Frischknecht, R., Kinter, J., Ludwig, A., Steuble, M., Meskenaite, V., Indermuhle, M., Engel, M., Cen, C., Mateos, J. M., Streit, P., Sonderegger, P. (2006) *Mol Biol Cell*. 17: 3651-3663. "Calsyntenin-1 docks vesicular cargo to kinesin-1."

Konishi, Y., Setou, M. (2009) *Nat Neurosci*. 12: 559-567. "Tubulin tyrosination navigates the kinesin-1 motor domain to axons."

Kozielski, F., Sack, S., Marx, A., Thormählen, M., Schönbrunn, E., Biou, V., Thompson, A., Mandelkow, E. M., Mandelkow, E. (1997) *Cell*. 91: 985-994. "The crystal structure of dimeric kinesin and implications for microtubule-dependent motility."

Kramer, M. F., Cook, W. J., Roth, F. P., Zhu, J., Holman, H., Knipe, D. M., Coen, D. M. (2003) *J Virol*. 77: 9533-9541. "Latent herpes simplex virus infection of sensory neurons alters neuronal gene expression."

Kull, F. J., Sablin, E. P., Lau, R., Fletterick, R. J., Vale, R. D. (1996) *Nature*. 380: 550-555. "Crystal structure of the kinesin motor domain reveals a structural similarity to myosin."

Lawrence, C. J., Dawe, R. K., Christie, K. R., Cleveland, D. W., Dawson, S. C., Endow, S. A., Goldstein, L. S., Goodson, H. V., Hirokawa, N., Howard, J., Malmberg, R. L., McIntosh, J. R., Miki, H., Mitchison, T. J., Okada, Y., Reddy, A. S., Saxton, W. M., Schliwa, M., Scholey, J. M., Vale, R. D., Walczak, C. E., Wordeman, L. (2004) *J Cell Biol*. 167: 19-22. "A standardized kinesin nomenclature."

Lazarov, O., Morfini, G. A., Lee, E. B., Farah, M. H., Szodorai, A., DeBoer, S. R., Koliatsos, V. E., Kins, S., Lee, V. M., Wong, P. C., Price, D. L., Brady, S. T., Sisodia, S. S. (2005) *J Neurosci*. 25: 2386-2395. "Axonal transport, amyloid precursor protein, kinesin-1, and the processing apparatus: revisited."

Li, X. J., Li, S. H., Sharp, A. H., Nucifora, F. C., Jr., Schilling, G., Lanahan, A., Worley, P., Snyder, S. H., Ross, C. A. (1995) *Nature*. 378: 398-402. "A huntingtin-associated protein enriched in brain with implications for pathology."

Lin, R. C., Scheller, R. H. (2000) *Annu Rev Cell Dev Biol*. 16: 19-49. "Mechanisms of synaptic vesicle exocytosis."

Ma, H., Cai, Q., Lu, W., Sheng, Z. H., Mochida, S. (2009) *J Neurosci*. 29: 13019-13029. "KIF5B motor adaptor syntabulin maintains synaptic transmission in sympathetic neurons."

Ma, B., Savas, J. N., Yu, M-S., Culver, B. P., Chao, M. V., Tanese, N. (2011) *Sci Rep*. 1: 140. "Huntingtin mediates dendritic transport of  $\beta$ -actin mRNA in rat neurons."

MacAskill, A. F., Brickley, K., Stephenson, F. A., Kittler, J. T. (2009) *Mol Cell Neurosci*. 40: 301-312. "GTPase dependent recruitment of Grif-1 by Miro1 regulates mitochondrial trafficking in hippocampal neurons."

Macaskill, A. F., Rinholm, J. E., Twelvetrees, A. E., Arancibia-Carcamo, I. L., Muir, J., Fransson, A., Aspenstrom, P., Attwell, D., Kittler, J. T. (2009a) *Neuron*. 61: 541-555. "Miro1 is a calcium sensor for glutamate receptor-dependent localization of mitochondria at synapses."

- Marx, A., Muller, J., Mandelkow, E. (2005) *Adv Protein Chem.* 71: 299-344. "The structure of microtubule motor proteins."
- Marx, A., Muller, J., Mandelkow, E. M., Hoenger, A., Mandelkow, E. (2006) *J Muscle Res Cell Motil.* 27: 125-137. "Interaction of kinesin motors, microtubules, and MAPs."
- McCart, A. E., Mahony, D., Rothnagel, J. A. (2003) *Traffic.* 4: 576-580. "Alternatively spliced products of the human kinesin light chain 1 (KNS2) gene."
- McGuire, J. R., Rong, J., Li, S. H., Li, X. J. (2006) *J Biol Chem.* 281: 3552-3559. "Interaction of Huntingtin-associated protein-1 with kinesin light chain: implications in intracellular trafficking in neurons."
- McNally, E. M., Goodwin, E. B., Spudich, J.A., Leinwand, L.A. (1988) *Proc Natl Acad Sci U S A.* 85: 7270-7273. "Coexpression and assembly of myosin heavy chain and myosin light chain in *Escherichia coli*."
- Meyer, D., Liu, A., Margolis, B. (1999) *J Biol Chem.* 274: 35113-35118. "Interaction of c-Jun amino-terminal kinase interacting protein-1 with p190 rhoGEF and its localization in differentiated neurons."
- Meyerzon, M., Fridolfsson, H. N., Ly, N., McNally, F. J., Starr, D. A. (2009) *Development.* 136: 2725-2733. "UNC-83 is a nuclear-specific cargo adaptor for kinesin-1-mediated nuclear migration."
- Miki, H., Okada, Y., Hirokawa, N. (2005) *Trends Cell Biol.* 15: 467-476. "Analysis of the kinesin superfamily: insights into structure and function."
- Misko, A., Jiang, S., Wegorzewska, I., Milbrandt, J., Baloh, R. H. (2010) *J Neurosci.* 30: 4232-4240. "Mitofusin 2 is necessary for transport of axonal mitochondria and interacts with the Miro/Milton complex."
- Moores, C. A., Cooper, J., Wagenbach, M., Ovechkina, Y., Wordeman, L., Milligan, R. A. (2006) *Cell Cycle.* 5: 1812-1815. "The role of the kinesin-13 neck in microtubule depolymerization."
- Mueller, J., Perrone, C. A., Bower, R., Cole, D. G., Porter, M. E. (2005) *Mol Biol Cell.* 16: 1341-1354. "The FLA3 KAP subunit is required for localization of kinesin-2 to the site of flagellar assembly and processive anterograde intraflagellar transport."
- Nakagawa, T., Setou, M., Seog, D., Ogasawara, K., Dohmae, N., Takio, K., Hirokawa, N. (2000) *Cell.* 103: 569-581. "A novel motor, KIF13A, transports mannose-6-phosphate receptor to plasma membrane through direct interaction with AP-1 complex."
- Nelson, M. R., Chazin, W. J. (1998) *Biometals.* 11: 297-318. "Structures of EF-hand Ca(2+)-binding proteins: diversity in the organization, packing and response to Ca2+ binding."
- O'Brien, R.J., Wong, P, C. (2011) 34: 185-204. "Amyloid precursor protein processing and Alzheimer's disease."

- Okada, Y., Yamazaki, H., Sekine-Aizawa, Y., Hirokawa, N. (1995) *Cell*. 81: 769-780. "The neuron-specific kinesin superfamily protein KIF1A is a unique monomeric motor for anterograde axonal transport of synaptic vesicle precursors."
- Okada, Y., Hirokawa, N. (1999) *Science*. 283: 1152-1157. "A processive single-headed motor: kinesin superfamily protein KIF1A."
- Okada, Y., Hirokawa, N. (2000) *Proc Natl Acad Sci U S A*. 97: 640-645. "Mechanism of the single-headed processivity: diffusional anchoring between the K-loop of kinesin and the C terminus of tubulin."
- Ovechkina, Y., Wordeman, L. (2003) *Traffic*. 4: 367-375. "Unconventional motoring: an overview of the Kin C and Kin I kinesins."
- Palacios, I. M., St Johnston, D. (2002) *Development*. 129: 5473-5485. "Kinesin light chain-independent function of the Kinesin heavy chain in cytoplasmic streaming and posterior localisation in the *Drosophila* oocyte."
- Pasinelli, P., Belford, M. E., Lennon, N., Bacskai, B. J., Hyman, B. T., Trotti, D., Brown, R. H., Jr. (2004) *Neuron*. 43: 19-30. "Amyotrophic lateral sclerosis-associated SOD1 mutant proteins bind and aggregate with Bcl-2 in spinal cord mitochondria."
- Rahman, A., Friedman, D. S., Goldstein, L. S. (1998) *J Biol Chem*. 273: 15395-15403. "Two kinesin light chain genes in mice. Identification and characterization of the encoded proteins."
- Rahman, A., Kamal, A., Roberts, E. A., Goldstein, L. S. (1999) *J Cell Biol*. 146: 1277-1288. "Defective kinesin heavy chain behavior in mouse kinesin light chain mutants."
- Reed, N. A., Cai, D., Blasius, T. L., Jih, G. T., Meyhofer, E., Gaertig, J., Verhey, K. J. (2006) *Curr Biol*. 16: 2166-2172. "Microtubule acetylation promotes kinesin-1 binding and transport."
- Reid, E., Kloos, M., Ashley-Koch, A., Hughes, L., Bevan, S., Svenson, I. K., Graham, F. L., Gaskell, P. C., Dearlove, A., Pericak-Vance, M. A., Rubinsztein, D. C., Marchuk, D. A. (2002) *Am J Hum Genet*. 71: 1189-1194. "A kinesin heavy chain (KIF5A) mutation in hereditary spastic paraplegia (SPG10)."
- Rice, S., Lin, A. W., Safer, D., Hart, C. L., Naber, N., Carragher, B. O., Cain, S. M., Pechatnikova, E., Wilson-Kubalek, E. M., Whittaker, M., Pate, E., Cooke, R., Taylor, E. W., Milligan, R. A., Vale, R. D. (1999) *Nature*. 402: 778-784. "A structural change in the kinesin motor protein that drives motility."
- Rong, J., McGuire, J. R., Fang, Z. H., Sheng, G., Shin, J. Y., Li, S. H., Li, X. J. (2006) *J Neurosci*. 26: 6019-6030. "Regulation of intracellular trafficking of huntingtin-associated protein-1 is critical for TrkA protein levels and neurite outgrowth."
- Roy, S., Winton, M. J., Black, M. M., Trojanowski, J. Q., Lee, V. M. (2008) *J Neurosci*. 28: 5248-5256. "Cytoskeletal requirements in axonal transport of slow component-b."
- Salinas, S., Proukakis, C., Crosby, A., Warner, T. T. (2008) *Lancet Neurol*. 7: 1127-1138. "Hereditary spastic paraplegia: clinical features and pathogenetic mechanisms."

- Santel, A., Fuller, M. T. (2001) *J Cell Sci.* 114: 867-874. "Control of mitochondrial morphology by a human mitofusin."
- Schroer, T, A. (2004). *Annu Rev Cell Dev Biol.* 20: 759-779. "Dynactin."
- Schaeffer, C., Beaulande, M., Ehresmann, C., Ehresmann, B., Moine, H. (2003) *Biol Cell.* 95: 221-228. "The RNA binding protein FMRP: new connections and missing links."
- Schafer, B., Gotz, C., Dudek, J., Hessenauer, A., Matti, U., Montenarh, M. (2009) *Cell Mol Life Sci.* 66: 339-349. "KIF5C: a new binding partner for protein kinase CK2 with a preference for the CK2alpha' subunit."
- Schnapp, B. J. (2003) *J Cell Sci.* 116: 2125-2135. "Trafficking of signaling modules by kinesin motors."
- Seeberger, C., Mandelkow, E., Meyer, B. (2000) *Biochemistry.* 39: 12558-12567. "Conformational preferences of a synthetic 30mer peptide from the interface between the neck and stalk regions of kinesin."
- Seeger, M, A., Rice, S, E. (2010) *J. Biol. Chem.* 285: 8155-8162. "Microtubule-associated protein-like binding of the kinesin-1 tail to microtubules."
- Seeger, M, A., Zhang, Y., Rice, S, E. (2012) *Proteins.* 80: 2437-2446. "Kinesin tail domains are intrinsically disordered."
- Setou, M., Nakagawa, T., Seog, D. H., Hirokawa, N. (2000) *Science.* 288: 1796-1802. "Kinesin superfamily motor protein KIF17 and mLin-10 in NMDA receptor-containing vesicle transport."
- Setou, M., Seog, D. H., Tanaka, Y., Kanai, Y., Takei, Y., Kawagishi, M., Hirokawa, N. (2002) *Nature.* 417: 83-87. "Glutamate-receptor-interacting protein GRIP1 directly steers kinesin to dendrites."
- Shao, Q., Gao, Y, Q. (2005) *PNAS.* 103: 8072-8077. "On the hand-over-hand mechanism of kinesin."
- Siegel, G, J., Agranoff, B, W., Albers, R, W., Fisher, S, K., Uhler, M, D. (1999) Lippincott-Raven. 6th Edition. "Basic Neurochemistry: Molecular, Cellular and Medical Aspects."
- Smith, M. J., Pozo, K., Brickley, K., Stephenson, F. A. (2006) *J Biol Chem.* 281: 27216-27228. "Mapping the GRIF-1 binding domain of the kinesin, KIF5C, substantiates a role for GRIF-1 as an adaptor protein in the anterograde trafficking of cargoes."
- Song, Y. H., Mandelkow, E. (1993) *Proc Natl Acad Sci U S A.* 90: 1671-1675. "Recombinant kinesin motor domain binds to beta-tubulin and decorates microtubules with a B surface lattice."
- Stockinger, W., Brandes, C., Fasching, D., Hermann, M., Gotthardt, M., Herz, J., Schneider, W. J., Nimpf, J. (2000) *J Biol Chem.* 275: 25625-25632. "The reelin receptor ApoER2 recruits JNK-interacting proteins-1 and -2."

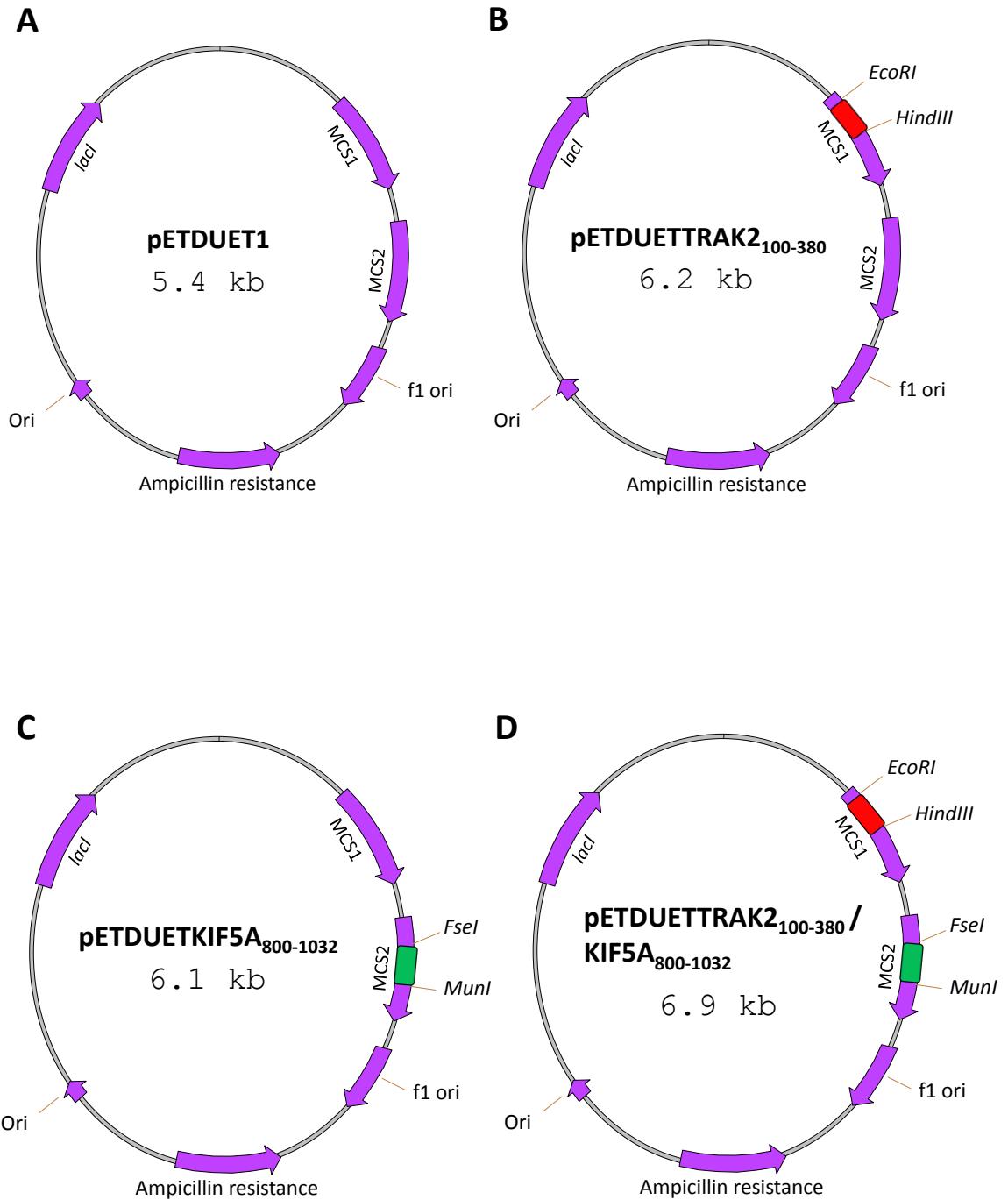
- Stowers, R. S., Megeath, L. J., Gorska-Andrzejak, J., Meinertzhagen, I. A., Schwarz, T. L. (2002) *Neuron*. 36: 1063-1077. "Axonal transport of mitochondria to synapses depends on milton, a novel *Drosophila* protein."
- Su, Q., Cai, Q., Gerwin, C., Smith, C. L., Sheng, Z. H. (2004) *Nat Cell Biol*. 6: 941-953. "Syntabulin is a microtubule-associated protein implicated in syntaxin transport in neurons."
- Sun, F., Zhu, C., Dixit, R., Cavalli, V. (2011) *EMBO J*. 30: 3416-3429. "Sunday Driver/JIP3 binds kinesin heavy chain directly and enhances its motility."
- Takeda, S., Yonekawa, Y., Tanaka, Y., Okada, Y., Nonaka, S., Hirokawa, N. (1999) *J Cell Biol*. 145: 825-836. "Left-right asymmetry and kinesin superfamily protein KIF3A: new insights in determination of laterality and mesoderm induction by *kif3A*<sup>-/-</sup> mice analysis."
- Tanaka, Y., Kanai, Y., Okada, Y., Nonaka, S., Takeda, S., Harada, A., Hirokawa, N. (1998). *Cell* 93: 1147–1158. "Targeted disruption of mouse conventional kinesin heavy chain, KIF5B, results in abnormal perinuclear clustering of mitochondria."
- Tanenbaum, M. E., Medema, R. H. (2010) *Dev Cell*. 19: 797-806. "Mechanisms of centrosome separation and bipolar spindle assembly."
- Terada, S., Kinjo, M., Aihara, M., Takei, Y., Hirokawa, N. (2010) *EMBO J*. 29: 843-854. "Kinesin-1/Hsc70-dependent mechanism of slow axonal transport and its relation to fast axonal transport."
- Theriot, J. A. (1994) *Adv Exp Med Biol*. 358: 133-145. "Actin filament dynamics in cell motility."
- Tsai, M. Y., Morfini, G., Szebenyi, G., Brady, S. T. (2000) *Mol Biol Cell*. 11: 2161-2173. "Release of kinesin from vesicles by hsc70 and regulation of fast axonal transport."
- Ueno, H., Huang, X., Tanaka, Y., Hirokawa, N. (2010) *Dev Cell*. 20: 60-71. "KIF16B/Rab14 molecular motor complex is critical for early embryonic development by transporting FGF receptor."
- Ungewickell, E., Ungewickell, H., Holstein, S. E., Lindner, R., Prasad, K., Barouch, W., Martin, B., Greene, L. E., Eisenberg, E. (1995) *Nature*. 378: 632-635. "Role of auxilin in uncoating clathrin-coated vesicles."
- Vagnoni, A., Rodriguez, L., Manser, C., De Vos, K. J., Miller, C. C. (2011) *J Cell Sci*. 124: 1032-1042. "Phosphorylation of kinesin light chain 1 at serine 460 modulates binding and trafficking of calyculin-1."
- Vale, R. D., Reese, T. S., Sheetz, M. P. (1985) *Cell*. 42: 39-50. "Identification of a novel force-generating protein, kinesin, involved in microtubule-based motility."
- Vale, R. D., Fletterick, R. J. (1997) *Annu Rev Cell Dev Biol*. 13: 745-777. "The design plan of kinesin motors."

- Verhey, K. J., Lizotte, D. L., Abramson, T., Barenboim, L., Schnapp, B. J., Rapoport, T. A. (1998) *J Cell Biol.* 143: 1053-1066. "Light chain-dependent regulation of Kinesin's interaction with microtubules."
- Verhey, K. J., Meyer, D., Deehan, R., Blenis, J., Schnapp, B. J., Rapoport, T. A., Margolis, B. (2001) *J Cell Biol.* 152: 959-970. "Cargo of kinesin identified as JIP scaffolding proteins and associated signaling molecules."
- Verhey, K. J., Hammond, J. W. (2009) *Nat Rev Mol Cell Biol.* 10: 765-777. "Traffic control: regulation of kinesin motors."
- Vershinin, M., Carter, B. C., Razafsky, D. S., King, S. J., Gross, S. P. (2007) *Proc Natl Acad Sci U S A.* 104: 87-92. "Multiple-motor based transport and its regulation by Tau."
- Wallace, R. B., Shaffer, J., Murphy, R. F., Bonner, J., Hirose, T., Itakura, K. (1979) *Nucleic Acids Res.* 6: 3543-6357. "Hybridization of synthetic oligonucleotides to Pi Chi 174 DNA: the effect of single base pair mismatch."
- Wang, X., Schwarz, T. L. (2009) *Cell.* 136: 163-174. "The mechanism of Ca<sup>2+</sup> - dependent regulation of kinesin-mediated mitochondrial motility."
- Wang, X., Winter, D., Ashrafi, G., Schlehe, J., Wong, Y. L., Selkoe, D., Rice, S., Steen, J., LaVoie, M. J., Schwarz, T. L. (2011) *Cell.* 147: 893-906. "PINK1 and Parkin target Miro for phosphorylation and degradation to arrest mitochondrial motility."
- Webber, E., Li, L., Chin, L. S. (2008) *J Mol Biol.* 382: 638-651. "Hypertonia-associated protein Trak1 is a novel regulator of endosome-to-lysosome trafficking."
- Weihofen, A., Thomas, K. J., Ostaszewski, B. L., Cookson, M. R., Selkoe, D. J. (2009) *Biochemistry.* 48: 2045-2052. "Pink1 forms a multiprotein complex with Miro and Milton, linking Pink1 function to mitochondrial trafficking."
- Wozniak, M. J., Allan, V. J. (2006) *EMBO J.* 25: 5457-5468. "Cargo selection by specific kinesin light chain 1 isoforms."
- Wu, L. L., Fan, Y., Li, S., Li, X. J., Zhou, X. F. (2010) *J Biol Chem.* 285: 5614-5623. "Huntingtin-associated protein-1 interacts with pro-brain-derived neurotrophic factor and mediates its transport and release."
- Xia, C. H., Roberts, E. A., Her, L. S., Liu, X., Williams, D. S., Cleveland, D. W., Goldstein, L. S. (2003) *J Cell Biol.* 161: 55-66. "Abnormal neurofilament transport caused by targeted disruption of neuronal kinesin heavy chain KIF5A."
- Yang, J. T., Laymon, R. A., Goldstein, L. S. B. (1989) *Cell.* 56: 879-889. "A three-domain structure of kinesin heavy chain revealed by DNA sequence and microtubule binding analyses."
- Yang, Z., Roberts, E. A., Goldstein, L. S. (2001) *Mol Cell Biol.* 21: 2463-2466. "Functional analysis of mouse C-terminal kinesin motor KifC2."
- Yildiz, A., Tomishige, M., Vale, R. D., Selvin, P. R. (2004) *Science.* 303: 676-678. "Kinesin walks hand-over-hand."

Zhao, C., Takita, J., Tanaka, Y., Setou, M., Nakagawa, T., Takeda, S., Yang, H. W., Terada, S., Nakata, T., Takei, Y., Saito, M., Tsuji, S., Hayashi, Y., Hirokawa, N. (2001) *Cell*. 105: 587-597. "Charcot-Marie-Tooth disease type 2A caused by mutation in a microtubule motor KIF1Bbeta."

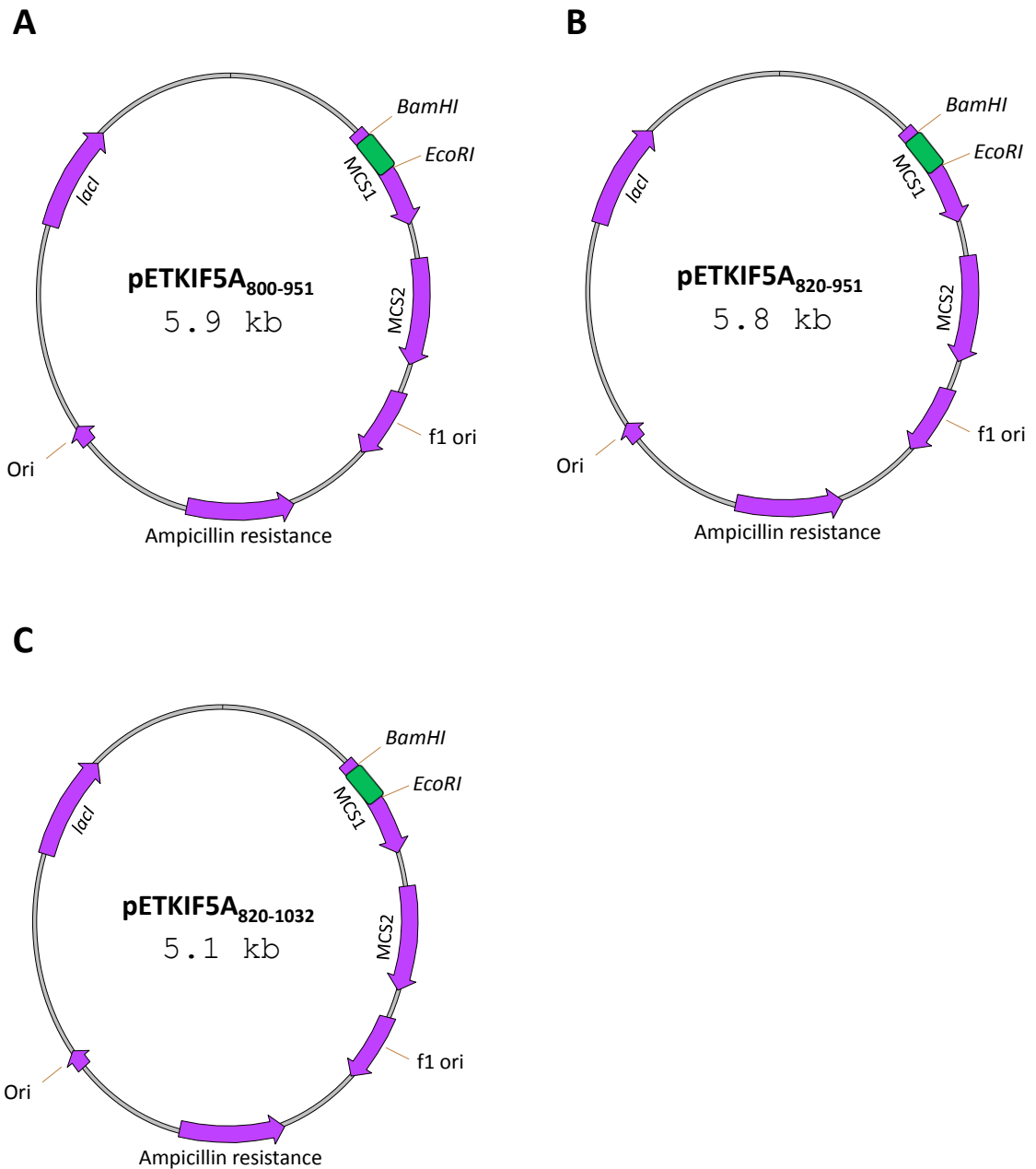
Zhu, H., Lee, H. Y., Tong, Y., Hong, B. S., Kim, K. P., Shen, Y., Lim, K. J., Mackenzie, F., Tempel, W., Park, H. W. (2012) *PLoS One*. 7: e33943. "Crystal structures of the tetratricopeptide repeat domains of kinesin light chains: insight into cargo recognition mechanisms."

# APPENDICES



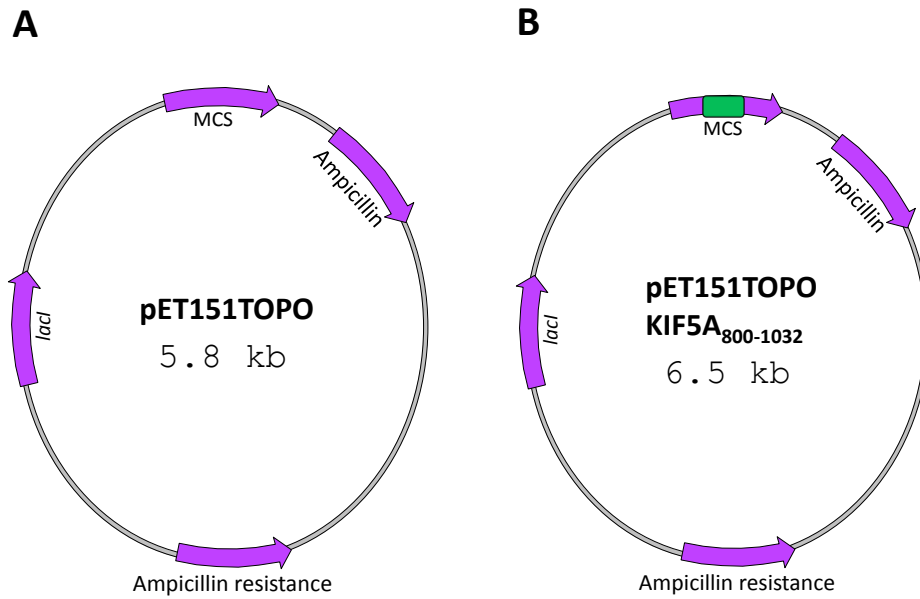
**Appendix 3.1 The vector maps for pETDUET1, pETTRAK2<sub>100-380</sub>, pETKIF5A<sub>800-1032</sub> and pETTRAK2<sub>100-380</sub>/KIF5A<sub>800-1032</sub>.**

To facilitate replication in *E. coli* cells, the cloning vector has an ampicillin resistance marker, and an origin of replication. The transcription of protein in *E. coli* cells is induced by that of a T7 polymerase, in turn controlled by a *lac* operon. **A.** Shows the vector map for pETDUET1. **B.** Shows the vector map for pETTRAK2<sub>100-380</sub>. This clone used the restriction sites *EcoRI*/*HindIII* to insert TRAK2<sub>100-380</sub> into MCS1. **C.** Shows the vector map for pETKIF5A<sub>800-1032</sub>. This clone used the restriction sites *FseI*/*MunI* to insert KIF5A<sub>800-1032</sub> into MCS2. **D.** Shows the vector map for pETTRAK2<sub>100-380</sub>/KIF5A<sub>800-1032</sub>. This clone used the restriction sites *EcoRI*/*HindIII* to insert TRAK2<sub>100-380</sub> into MCS1 and the restriction sites *FseI*/*MunI* to insert KIF5A<sub>800-1032</sub> into MCS2.



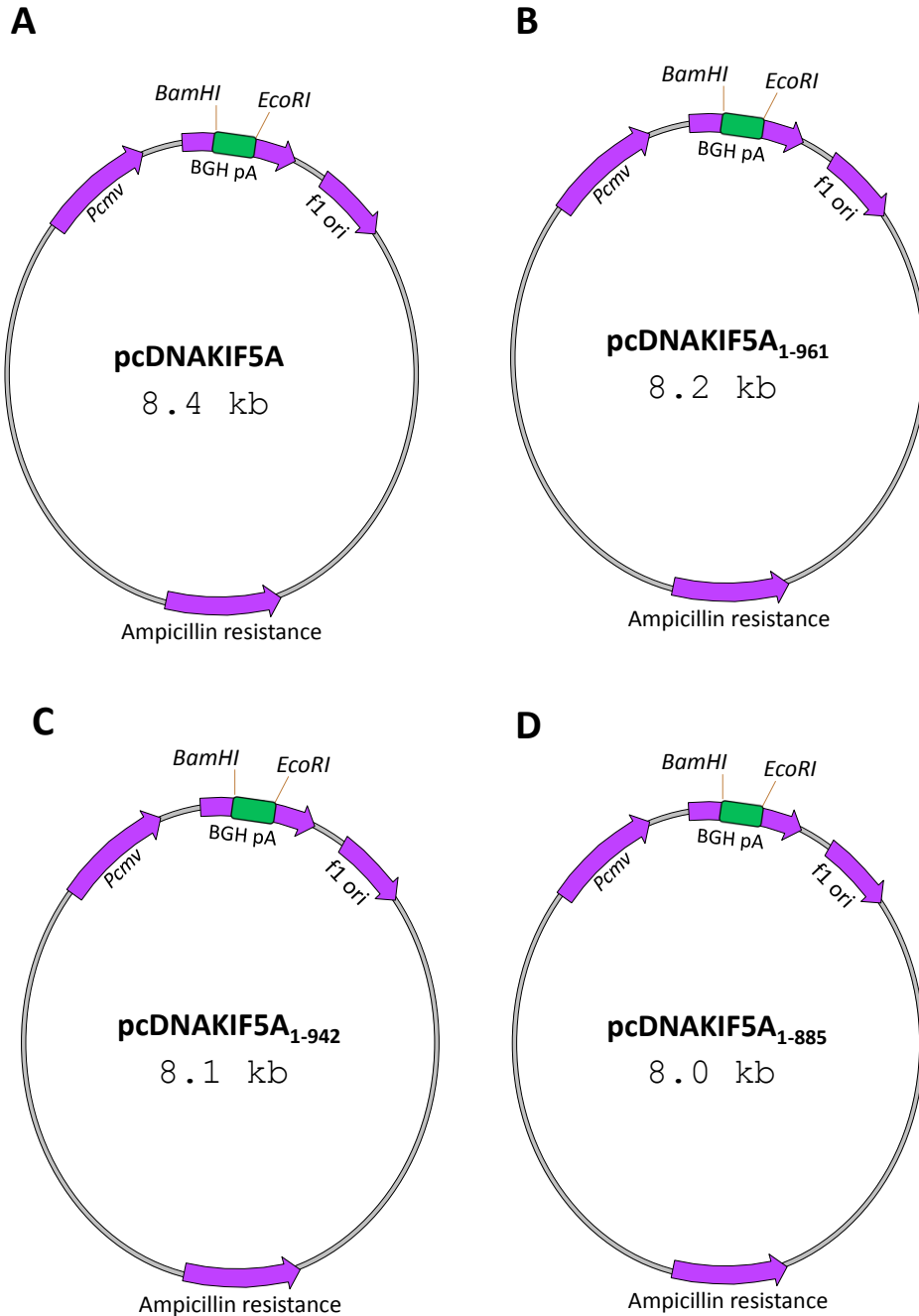
**Appendix 4.1 The vector maps for pETKIF5A<sub>800-951</sub>, pETKIF5A<sub>820-951</sub> and pETKIF5A<sub>820-1032</sub>.**

To facilitate replication in *E.coli* cells, the cloning vector has an ampicillin resistance marker, and an origin of replication. The transcription of protein in *E.coli* cells is induced by that of a T7 polymerase, in turn controlled by a *lac* operon. **A.** Shows the vector map for pETKIF5A<sub>100-280</sub>. This clone used the restriction sites *BamHI/EcoRI* to insert KIF5A<sub>800-951</sub> into MCS1. **B.** Shows the vector map for pETKIF5A<sub>820-951</sub>. This clone used the restriction sites *BamHI/EcoRI* to insert KIF5A<sub>820-951</sub> into MCS1. **C.** Shows the vector map for pETKIF5A<sub>820-1032</sub>. This clone used the restriction sites *BamHI/EcoRI* to insert KIF5A<sub>820-1032</sub> into MCS1.



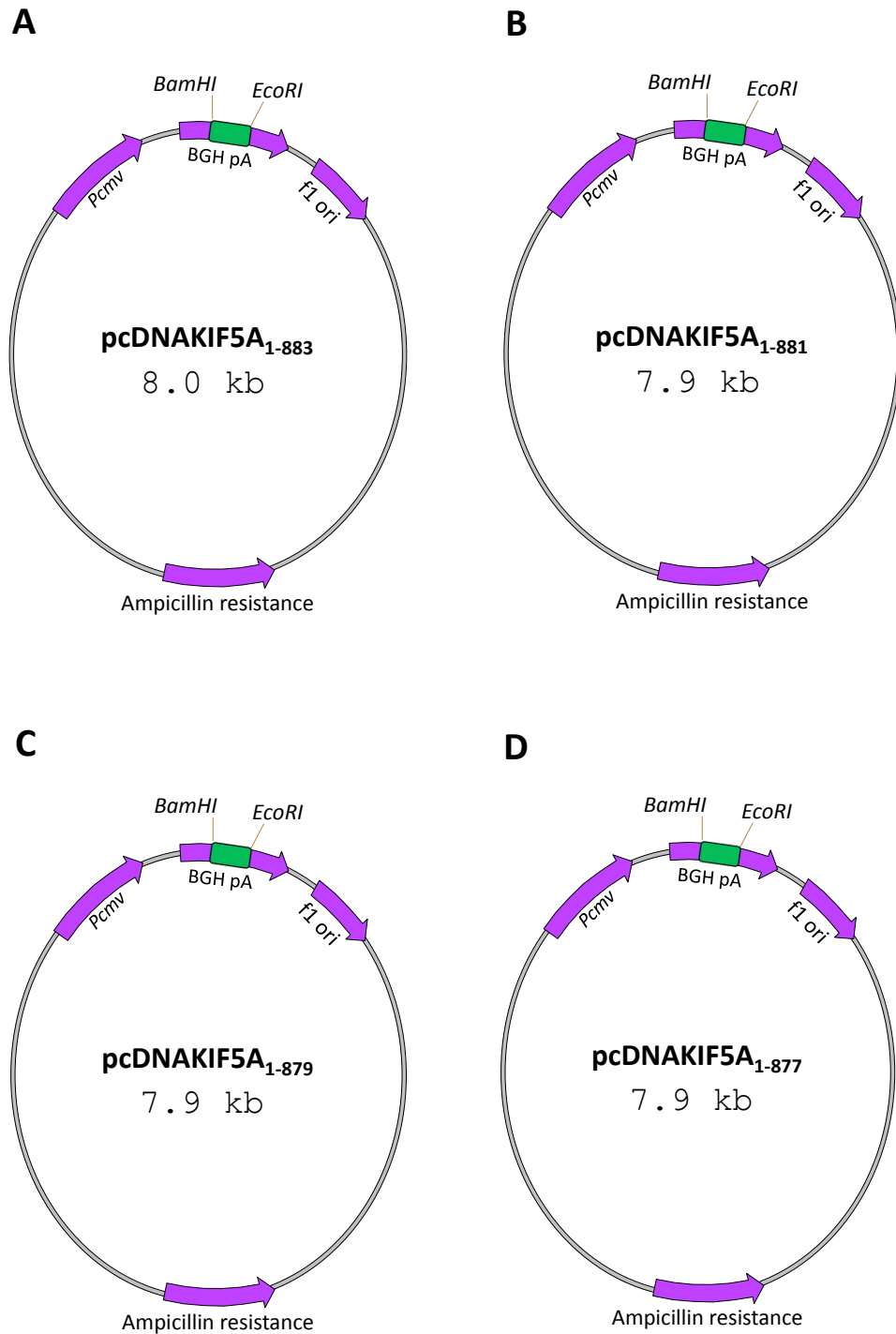
**Appendix 4.2 The vector maps for pET151D-TOPO and pET151D-TOPOKIF5A<sub>800-1032</sub>.**

To facilitate replication in *E.coli* cells, the cloning vector has an ampicillin resistance marker, and an origin of replication. The transcription of protein in *E.coli* cells is induced by that of a T7 polymerase, in turn controlled by a *lac* operon. **A.** Shows the vector map for pET151D-TOPO. **B.** Shows the vector map for pET151D-TOPOKIF5A<sub>800-1032</sub>. This clone used the blunt ended PCR product to insert KIF5A<sub>800-1032</sub> into the MCS.



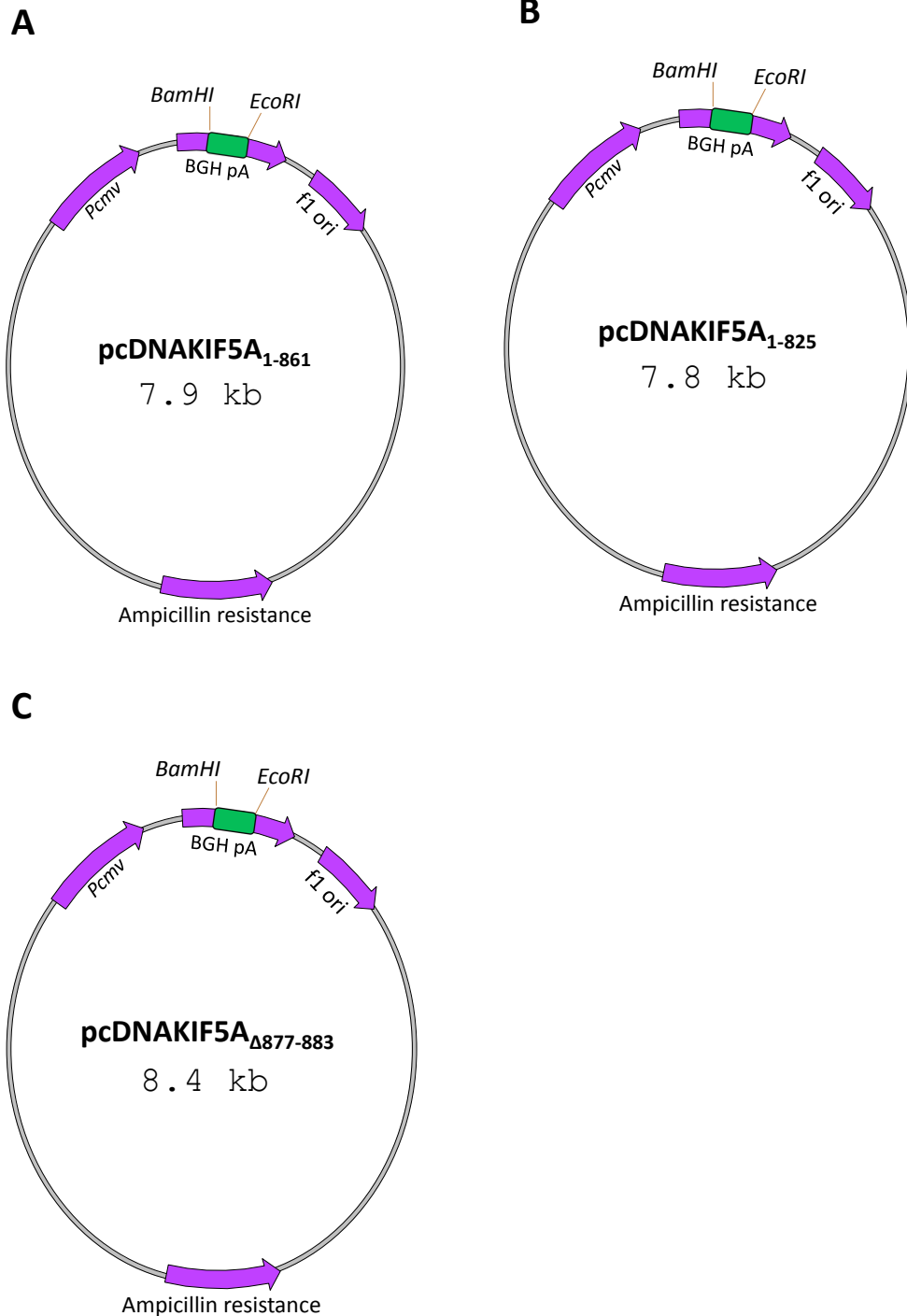
**Appendix 5.1 The vector maps for pcDNAKIF5A, pcDNAKIF5A<sub>1-961</sub>, pcDNAKIF5A<sub>1-942</sub> and pcDNAKIF5A<sub>1-885</sub>.**

To facilitate replication in *E.coli* cells, the cloning vector has an ampicillin resistance marker, and an origin of replication. The transcription of protein in mammalian cells is induced by that of a *Pcmv* promoter. **A.** Shows the vector map for pcDNAKIF5A. This clone used the restriction sites *Bam*HI/*Eco*RI to insert KIF5A into the MCS. **B.** Shows the vector map for pcDNAKIF5A<sub>1-961</sub>. This clone used the restriction sites *Bam*HI/*Eco*RI to insert KIF5A<sub>1-961</sub> into the MCS. **C.** Shows the vector map for pcDNAKIF5A<sub>1-942</sub>. This clone used the restriction sites *Bam*HI/*Eco*RI to insert KIF5A<sub>1-942</sub> into the MCS. **D.** Shows the vector map for pcDNAKIF5A<sub>1-885</sub>. This clone used the restriction sites *Bam*HI/*Eco*RI to insert KIF5A<sub>1-885</sub> into the MCS.



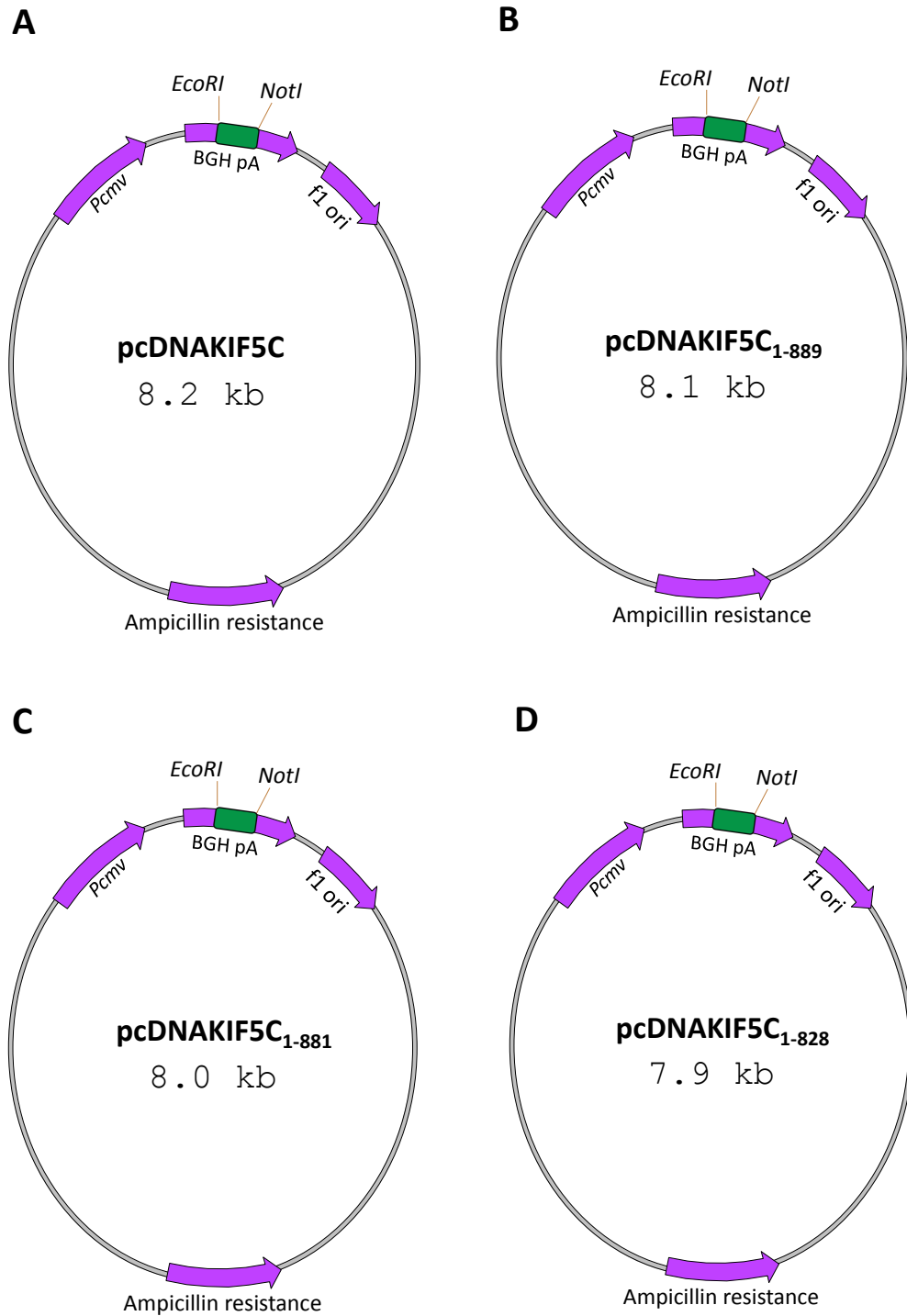
**Appendix 5.2 The vector maps for pcDNAKIF5A<sub>1-883</sub>, pcDNAKIF5A<sub>1-881</sub>, pcDNAKIF5A<sub>1-879</sub> and pcDNAKIF5A<sub>1-877</sub>.**

To facilitate replication in *E.coli* cells, the cloning vector has an ampicillin resistance marker, and an origin of replication. The transcription of protein in mammalian cells is induced by that of a *Pcmv* promoter. **A.** Shows the vector map for pcDNAKIF5A<sub>1-883</sub>. This clone used the restriction sites *Bam*HI/*Eco*RI to insert KIF5A<sub>1-883</sub> into the MCS. **B.** Shows the vector map for pcDNAKIF5A<sub>1-881</sub>. This clone used the restriction sites *Bam*HI/*Eco*RI to insert KIF5A<sub>1-881</sub> into the MCS. **C.** Shows the vector map for pcDNAKIF5A<sub>1-879</sub>. This clone used the restriction sites *Bam*HI/*Eco*RI to insert KIF5A<sub>1-879</sub> into the MCS. **D.** Shows the vector map for pcDNAKIF5A<sub>1-877</sub>. This clone used the restriction sites *Bam*HI/*Eco*RI to insert KIF5A<sub>1-877</sub> into the MCS.



**Appendix 5.3 The vector maps for pcDNAKIF5A<sub>1-861</sub>, pcDNAKIF5A<sub>1-825</sub> and pcDNAKIF5A<sub>Δ877-883</sub>**

To facilitate replication in *E.coli* cells, the cloning vector has an ampicillin resistance marker, and an origin of replication. The transcription of protein in mammalian cells is induced by that of a *Pcmv* promoter. **A.** Shows the vector map for pcDNAKIF5A<sub>1-861</sub>. This clone used the restriction sites *BamHI*/*EcoRI* to insert KIF5A<sub>1-861</sub> into the MCS. **B.** Shows the vector map for pcDNAKIF5A<sub>1-825</sub>. This clone used the restriction sites *BamHI*/*EcoRI* to insert KIF5A<sub>1-825</sub> into the MCS. **C.** Shows the vector map for pcDNAKIF5A<sub>Δ877-883</sub>. This clone used the restriction sites *BamHI*/*EcoRI* to insert KIF5A<sub>Δ877-883</sub> into the MCS.



**Appendix 5.4 The vector maps for pcDNAKIF5C, pcDNAKIF5C<sub>1-889</sub>, pcDNAKIF5C<sub>1-881</sub> and pcDNAKIF5A<sub>1-828</sub>**

To facilitate replication in *E.coli* cells, the cloning vector has an ampicillin resistance marker, and an origin of replication. The transcription of protein in mammalian cells is induced by that of a *Pcmv* promoter. **A.** Shows the vector map for pcDNAKIF5C. This clone used the restriction sites *EcoRI/NotI* to insert KIF5C into the MCS. **B.** Shows the vector map for pcDNAKIF5A<sub>1-889</sub>. This clone used the restriction sites *EcoRI/NotI* to insert KIF5A<sub>1-889</sub> into the MCS. **C.** Shows the vector map for pcDNAKIF5C<sub>1-881</sub>. This clone used the restriction sites *EcoRI/NotI* to insert KIF5C<sub>1-881</sub> into the MCS. **D.** Shows the vector map for pcDNAKIF5C<sub>1-828</sub>. This clone used the restriction sites *EcoRI/NotI* to insert KIF5C<sub>1-828</sub> into the MCS.